DECODING ASTROCYTIC IDENTITY SHIFTS POST-INJURY: IMPLICATIONS FOR NEURONAL REPROGRAMMING

Priya Maddhesiya

Graduate School of
Systemic Neurosciences
LMU Munich

Dissertation der

Graduate School of Systemic Neurosciences der

Ludwig-Maximilians-Universität München

17th April 2024

Supervisor
Prof. Dr. Jovica Ninkovic
Institute for Cell Biology and Anatomy
Biomedical Center (BMC)
Faculty of Medicine
LMU Munich

First Reviewer: Prof. Dr. Jovica Ninkovic
Second Reviewer: Dr. Nicolas Battich
External Reviewer: Prof. Dr. Maria Colomé-Tatché
Date of Submission: 17th April 2024
Date of Defense: 17th December 2024

Abstract

The regenerative capacity of the central nervous system (CNS) in the adult mammalian brain is severely limited, often leading to irreversible neuronal loss and functional decline following injury or disease. Astrocytes, the predominant glial cells in the CNS, play crucial roles in maintaining neural homeostasis, supporting the blood-brain barrier, and facilitating neuronal and synaptic functions. Upon injury or disease, these cells undergo reactive astrogliosis, significantly altering their function and phenotype. Notably, following invasive injuries, a subset of astrocytes has been observed to acquire proliferative capacity, express markers characteristic of neural stem cells (NSCs), and demonstrate the ability to self-renew and form multipotent neurospheres *in vitro*. This discovery adds a new dimension to our understanding of the neurogenic potential in the adult brain, which was previously thought to be limited and confined to specialized neurogenic niches such as the subventricular zone (SVZ) and the hippocampal dentate gyrus. However, the scarcity of these plastic astrocytes (occurring in low frequency) and the lack of distinct molecular markers have hindered their study and subsequent application in CNS repair strategies. Therefore, the thesis aims to 1) identify specific marker genes of this plastic astrocytic subset following stab wound injuries in the mouse cortex and 2) explore their potential in regenerative strategies, such as direct neuronal reprogramming.

To identify putative markers for plastic astrocytes post-injury, a trans-species approach was adopted, leveraging regenerative insights from zebrafish ependymoglia, and integrating them with astrocyte populations in a mouse stab wound model through single-cell transcriptomic integration analysis. This method enabled the identification of key marker genes, such as Hmgb2 (High Mobility Group Box 2) and others, characterizing this distinct plastic astrocytic subset. These markers are expressed in a small subset of astrocytes emerging post-injury, demonstrating proliferation and capability of forming neurospheres *in vitro*. Subsequent investigation revealed that these plastic astrocytic subsets exhibit transcriptional similarities to transient amplifying progenitors (TAPs) in the SVZ. They display a partial trajectory towards neurogenic lineages while retaining gliogenic potentials due to distinct signalling pathways, compared to bonafide TAPs.

The identification of Hmgb2, a chromatin-associated protein, through this comparative analysis, underscores its potential role in the reprogramming process, likely due to its involvement in chromatin remodelling—a critical step in activating neurogenic programs.

Overexpressing Hmgb2 alongside the pioneer transcription factor Neurog2 *in vitro*, under culture conditions mimicking the *in vivo* injury microenvironment, significantly enhances the efficiency of neuronal conversion of astrocytes to induced neurons (iNs). This improvement is attributed to the chromatin remodelling effects of Hmgb2, which facilitate accessibility and expression of neurogenic or reprogramming relevant genes, as evidenced by analysis of chromatin (ATAC-Seq) and transcriptome (RNA-Seq) data, along with the promoting maturation of iNs.

In summary, this study illuminates astrocyte plasticity following CNS injury, identifies crucial marker genes, and lays the groundwork for exploring their stem cell potential. Additionally, it underscores their significance in strategies for neuronal replacement, such as direct neuronal reprogramming. Together, these findings pave the way for advancing astrocyte research in regenerative medicine and repair approaches.

Index

1. Introduction

Brain injuries, affecting millions globally each year, pose a serious concern with significant mortality and disability rates. These injuries, arising from incidents like accidents, falls, sports-related events, or violence, vary in severity from slight concussions to extreme traumatic brain injuries (TBIs) (Dewan et al., 2019; Hyder et al., 2007; Maas et al., 2008). While some individuals fully recover, others experience long-term disabilities affecting daily life functions. TBI ranks high in terms of global death and impairment, contributing to nearly 30% of injury-related deaths annually (Demlie et al., 2023). Germany records over 300,000 TBI-related emergency room visits yearly as of 2021 (Younsi et al., 2023) and brain disorders in the European Union incur an estimated annual financial impact exceeding €800 billion (*Brain Research - European Commission*, n.d.), emphasizing the socioeconomic burden of neurological conditions in the region. Existing TBI treatments face challenges in promoting effective tissue repair and regeneration (Stein et al., 2015). To address this gap, urgent and targeted research efforts are required to deepen our understanding of the complex biological responses to TBI at various levels, spanning from molecular mechanisms to systemic interactions (Berwick et al., 2022; Maas et al., 2022).

One of the most notable responses of the brain to injury is reactive astrogliosis, a complex and multifaceted cellular response in the CNS (Burda et al., 2016). This intricate process involves morphological, molecular, and functional changes in astrocytes. These changes include phenotypic alterations like hypertrophy, functional shifts such as increased proliferation in subsets of astrocytes (juxtavascular astrocytes), and changes in gene expression such as the upregulation of glial fibrillary acidic protein (GFAP) and vimentin (Bardehle et al., 2013; Hol & Pekny, 2015; Pekny & Nilsson, 2005; Sofroniew, 2009, 2020). The extent of these modifications depends on factors such as the type of injury, severity (ranging from mild to severe), and location of the injury sites (Burda & Sofroniew, 2014; Sofroniew, 2009; Sofroniew & Vinters, 2010). However, this response is not only limited to a specific injury type; it is observed in conditions such as stroke, tumour growth, infection, inflammation, or neurodegenerative diseases (Burda & Sofroniew, 2014; Haim et al., 2015).

The understanding of astrocytic reactivity has significantly deepened in recent years, acknowledging that astrocytes can adopt various states and perform diverse functions with dual impacts on CNS repair and recovery (Matusova et al., 2023; Michinaga & Koyama, 2019; Pekny et al., 2014; Sofroniew, 2020; Yang et al., 2020). The formation of

glial borders by proliferative border-forming astrocytes, which demarcate and segregate injured tissue from healthy regions, was once predominantly viewed as an impediment to axonal regeneration (Fawcett & Asher, 1999; Fitch & Silver, 2008; Rhodes et al., 2003; Sypecka et al., 2023; Wanner et al., 2013). This was notably through the secretion of extracellular matrix (ECM) components like chondroitin sulfate proteoglycans (CSPGs) and as a contributor to inflammation (Busch & Silver, 2007; McKeon et al., 1999; Silver & Miller, 2004). However, recent studies indicate that the astrocytic border not only serves as a physical barrier to protect the lesion area from further damage but also contributes positively by supporting axonal regeneration and restoring the integrity of the CNS (Anderson et al., 2016; Buffo et al., 2010; Bush et al., 1999; Faulkner et al., 2004; Herrmann et al., 2008; Myer et al., 2006; O'Shea et al., 2023; Sofroniew, 2015).

Furthermore, recent studies have highlighted a subset of reactive astrocytes in the adult cerebral cortex that exhibit significant plasticity following acute invasive injuries. These astrocytes not only resume proliferation but also demonstrate the ability to form neurospheres *in vitro* (Buffo et al., 2008; M. Götz et al., 2015; Robel et al., 2011; Sirko et al., 2013, 2023). This plasticity emphasizes their potential for neural repair. However, the challenge lies in pinpointing this rare population without specific markers, impeding a thorough understanding and utilization of their regenerative capabilities.

The primary focus of my PhD centres on identifying the key marker genes for these rare plastic astrocytic subsets through a trans-species approach and single-cell transcriptomics. Additionally, the work explores strategies for neuronal replacement strategies, such as direct neuronal reprogramming, using one of the identified markers to assess their impact on reprogramming efficiency.

To provide context, I will briefly overview brain injury and reactive astrogliosis, emphasizing the heterogeneity of reactive astrocytes and their dual roles in repair processes—both beneficial and detrimental. Subsequently, I will introduce innovative repair approaches, such as exploring adult mammalian neurogenesis and leveraging zebrafish regenerative properties to identify injury-induced plastic astrocytic subsets in mice using single-cell transcriptomes. Furthermore, I will introduce neuronal replacement approaches, focusing on direct neuronal reprogramming. I will discuss the discrepancies between the *in vivo* injury microenvironment and the *in vitro* reprogramming culture conditions. Lastly, I will introduce the potential strategy of overcoming lineage barriers by

overexpressing chromatin architectural protein Hmgb2 to enhance astrocyte-to-neuronal conversion rates and promote the maturation of generated neurons.

1.1 Reactive Astrogliosis: A Universal Response to CNS Injury

The brain, an organ of remarkable complexity, is composed of billions of neurons that govern a wide range of functions, including cognition, memory, and motor control, all vital for everyday life (Maldonado & Alsayouri, 2023). However, the intricate neural network is not solely reliant on neurons; it also involves a collaborative effort with non-neuronal cells known as glial cells, which are dispersed throughout the CNS (Kettenmann & Verkhratsky, 2022).

Previously, glial cells were considered merely as structural components of the nervous system, providing support and "glue" for neurons (Virchow, 1856, 1858). However, advancements in histological techniques in the early 20th century allowed for the clear differentiation and classification of glia from neurons, leading to the identification of the primary glial cell types: astrocytes, oligodendrocytes, and microglia (Ramón y Cajal, 1920; del Rio-Hortega, 1920, 1921). Subsequent research revealed that beyond their traditional roles as support cells, glial cells are integral participants in synaptic plasticity, learning, and memory (Allen & Lyons, 2018; Jäkel & Dimou, 2017; Nedergaard et al., 2003). For instance, astrocytes play vital roles in maintaining homeostasis, contributing to the blood-brain barrier, regulating neurotransmitter levels, and providing metabolic support to neurons (Abbott et al., 2006; Kim et al., 2019; Nedergaard et al., 2003; Ransom et al., 2003). Microglia, immune cells in the CNS, play a crucial role in regulating neuronal activity, synaptic plasticity, maintaining brain homeostasis, and engulfing and clearing damaged cellular debris (Augusto-Oliveira et al., 2019; Kreutzberg, 1996; Szepesi et al., 2018; Wu et al., 2015); and oligodendrocytes act as the myelin producers of the CNS, supporting axonal function (Bradl & Lassmann, 2010; Stadelmann et al., 2019; Waly et al., 2014). This indicates that the nervous system relies on glial cells for the proper functioning and health of neurons and the overall performance of the brain. However, this complex network of neurons and glial cells is vulnerable to various types of injuries, including trauma, ischemia, and neurodegeneration, that can disrupt its structure and function.

Among glial cells, astrocytes remain the most abundant and diverse celltypes, outnumbering neurons by approximately 5:1 (Sofroniew & Vinters, 2010). They have a

star-shaped morphology and show regional variations, with protoplasmic astrocytes prevailing in gray matter, where they have extensive branched processes near neuronal synapses, and fibrous astrocytes dominating in white matter, where they have elongated, linear processes (Miller & Raff, 1984; Oberheim et al., 2012; D. D. Wang & Bordey, 2008). However, this traditional classification does not fully capture the complexity and diversity of astrocytes. Recent advances in single-cell sequencing have revealed additional astrocyte subtypes beyond these two categories (Batiuk et al., 2020; Bayraktar et al., 2020; Llorens-Bobadilla et al., 2015; Verkhratsky et al., 2021; Verkhratsky & Nedergaard, 2018). These subtypes are distinguished based on molecular signatures (expression profiles), anatomical locations, functional roles, and morphological criteria, suggesting a more nuanced and specialized involvement in the CNS physiology and pathology (Endo et al., 2022; Hasel et al., 2021; Khakh & Deneen, 2019; Lanjakornsiripan et al., 2018; Ohlig et al., 2021; Qian et al., 2023).

When the CNS is injured or diseased, astrocytes undergo reactive astrogliosis, which involves context-dependent changes in their phenotype, molecular expression, and function (Burda et al., 2016; Burda & Sofroniew, 2014; Escartin et al., 2021; Matusova et al., 2023; Pekny & Pekna, 2004; Sofroniew, 2005, 2009, 2020; Sofroniew & Vinters, 2010). One common hallmark of reactive astrogliosis is astrocyte hypertrophy, evidenced by enlarged cell bodies and less branched processes, along with the upregulated expression of intermediate filament proteins such as glial fibrillary acidic protein (GFAP), vimentin, and nestin. While astrocytes in healthy CNS tissue rarely divide, they can become proliferative following an injury (Bardehle et al., 2013; Frik et al., 2018; Sirko et al., 2013). A good example of this is juxtavascular astrocytes, which have their cell bodies directly adjacent to blood vessels, are more prone to proliferate in the cerebral cortex following stab wound brain injury (Bardehle et al., 2013; S. Götz et al., 2021). However, not all reactive astrocytes undergo proliferation, and some may become reactive without dividing (Escartin et al., 2021; Sofroniew, 2020).

One of the outcomes of astrocyte reactivity is the formation of a border around the lesion site, composed of boarder-forming astrocyte processes and extracellular matrix components (O'Shea et al., 2023; H. Wang et al., 2018). This border formation was previously thought to hinder CNS healing by inhibiting axon regeneration, as it expresses CSPGs and other molecules that block axonal growth (K. L. Adams & Gallo, 2018; Bovolenta et al., 1993; Fawcett & Asher, 1999; Fitch & Silver, 2008; McKeon et al., 1999; Silver & Miller, 2004). However, contrary to this, recent studies have shown that borders

aids rather than hinders CNS axon regeneration, demonstrated through genetic manipulations in adult mice with severe spinal cord injuries (Anderson et al., 2016; Bush et al., 1999). Furthermore, these border-forming astrocytes act as a physical barrier that isolates the damaged area, limits lesion expansion, reduces neurotoxic inflammation, restricts monocyte invasion, and aids in the restoration of the blood-brain barrier, highlighting their dual role in both supporting and inhibiting CNS repair processes (Buffo et al., 2010; Bush et al., 1999; Frik et al., 2018; Sofroniew, 2015). Nevertheless, it is also important to note that the prolonged effects of reactive gliosis tend to be less beneficial, as they foster an environment characterized by sustained inflammation and neurotoxicity, which can contribute to further damage to neurons (Burda & Sofroniew, 2014).

Astrocytes reactivity is not specific to a particular type of injury; it manifests across various conditions, including stroke, tumour growth, infection, inflammation, and neurodegenerative diseases (Brandao et al., 2019; Clarke et al., 2018; Escartin et al., 2021; Han et al., 2021; Hasel et al., 2021; Herrmann et al., 2008; Liddelow & Barres, 2017; Patabendige et al., 2021; Zamanian et al., 2012; Zhu et al., 2017). This response extends beyond astrocytes, encompassing microglia, meningeal fibroblasts, extracellular matrix proteins, oligodendrocytes, and their precursors (Sofroniew, 2009, 2020). Following injury or disease conditions, astrocytes activate diverse pathways, involving cytokines (e.g., interleukin-1β, tumor necrosis factor-α), chemokines (such as C-C motif chemokine ligand 2, CCL2, and C-X-C motif chemokine ligand 10, CXCL10), growth factors (transforming growth factor-β, TGF-β, and fibroblast growth factor-2, FGF-2), neurotransmitters (glutamate, ATP), and injury-related factors (reactive oxygen species, ROS, and damage-associated molecular patterns, DAMPs) (Pekny & Nilsson, 2005; Pekny & Pekna, 2004; Sofroniew, 2009, 2020; Sofroniew & Vinters, 2010). These components collectively form the intricate cellular and molecular framework that defines the CNS's reaction to injury and disease.

In conclusion, reactive astrocytes exhibit a diverse range of responses to CNS injuries and diseases, with their phenotype and function being highly context dependent. This diversity highlights the need for thorough research into astrocyte heterogeneity to better understand their impact on CNS health and disease.

1.2 Heterogeneity of reactive astrocytes: Navigating from Health to Insult

In a healthy CNS, astrocytes play diverse roles, including the regulation of blood flow, preserving the integrity of the blood–brain barrier (BBB), provision of energy molecules to neurons, contribution to synaptic activity and adaptation, and regulation of the extracellular environment in terms of ions, fluids, and transmitters (Sofroniew, 2005). This functional diversity aligns with the intricate cytoarchitecture, and diversity found throughout the CNS, indicating an expected heterogeneity among astrocytes (Chaboub & Deneen, 2013). The complexity of their functions further translates into region-specific phenotypes influenced by factors such as age, brain region, and proximity to vasculature or synapses (Westergard & Rothstein, 2020; Zhang & Barres, 2010). A myriad of studies has scrutinized the gene expression and morphology of astrocytes across different brain regions and under various conditions to explore their heterogeneity or diversity (Makarava et al., 2023). For example, the study by Zeisel *et al*., employed single-cell RNA sequencing (scRNA-seq) and spatial transcriptomics, revealing that astrocytes in different brain regions of mice have seven distinct subtypes that are determined by their developmental origins (Zeisel et al., 2018).

The heterogeneity and diversity of astrocytes have become focal points of extensive research, especially in the context of diseases and brain injuries. As the field advances, our understanding of the dual function of reactive astrocytes—both beneficial and detrimental—grows. Exploring single-cell techniques becomes crucial in unveiling the intricacies of this heterogeneity. Studies reveal that post CNS injury or disease onset, reactive astrocytes exhibit additional heterogeneity in gene expression, morphology, and secreted factor profiles, contingent upon the type, location, and stage of the pathology (Makarava et al., 2023; Sofroniew, 2015; Sofroniew & Vinters, 2010; Zamanian et al., 2012). For instance, a recent study by Makarava *et al.* explored astrocytes in the cortex, hippocampus, thalamus, and hypothalamus, revealing diverse reactive phenotypes linked to regional identity rather than the type of injury. They examined astrocytes in various pathological conditions, including prion disease, traumatic brain injury, brain ischemia, the 5XFAD Alzheimer's disease model, and normal aging, using targeted NanoString technology (Makarava et al., 2023). However, this approach limited their ability to obtain a global overview of astrocyte heterogeneity. On the other hand, Liddelow *et al.*, suggested that the nature of the insult could influence the reactive state of astrocytes and proposed a classification into A1 and A2 subtypes. According to their model, A1 astrocytes induced by neuroinflammation are neurotoxic, while A2 astrocytes induced by ischemia

are neuroprotective (Liddelow & Barres, 2017). However, this binary classification has been challenged by recent evidence, which supports a continuum of phenotypes regulated by context-specific molecular pathways rather than a simplified good-bad or neuroprotective-neurotoxic or A1-A2 categorization (Escartin et al., 2021; Lawrence et al., 2023). In fact, recent cutting-edge single-cell comparative transcriptomic analyses have illuminated the heterogeneous responses of astrocytes to different CNS insults, identifying both common and specific markers across various neurological disorders in murine models and human post-mortem tissues (Fig 1). This variation underscores the tailored nature of astrocytic reactions to different types of CNS damage (Matusova et al., 2023).

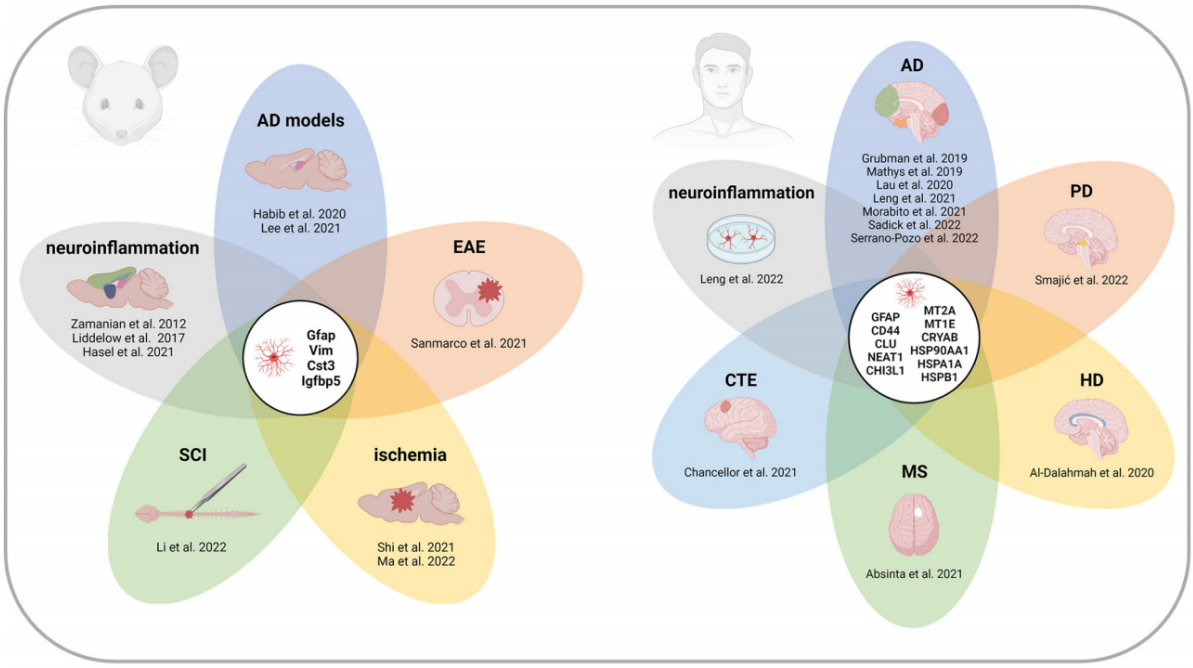

Figure 1: *Recurrent marker genes of reactive astrocytes across CNS regions and pathologies in mice and humans (Matusova et al., 2023. Reactive astrogliosis in the era of single-cell transcriptomics. Frontiers in Cellular Neuroscience, 17, Article 1173200. https://doi.org/10.3389/fncel.2023.1173200. CC BY license).*

Reactive astrocytes have different genes and functions depending on the pathology and the brain region. They can be inhibitory or supportive of CNS repair, and some can become stem cell-like under certain conditions (Buffo et al., 2008; M. Götz et al., 2015; Lang et al., 2004; Robel et al., 2011; Shimada et al., 2012; Sirko et al., 2013; Zamboni et al., 2020). Therefore, the spectrum of astrocyte heterogeneity observed in various pathological states is shaped by the interplay between injury factors (type, location, severity, and duration) and regional astrocyte identity.

1.3 Reactive astrocytes: a source of neural stem cells in CNS injury

In the adult mammalian brain, certain specialized astrocytes function similarly to neural stem cells (NSCs), typically residing within designated neurogenic niches such as the subventricular zone (SVZ) of the lateral ventricles and the subgranular zone (SGZ) of the hippocampal dentate gyrus (DG) (D. K. Ma et al., 2009; Taupin & Gage, 2002). These astrocytes are capable of self-renewal and can generate neurons and glia. Astrocytes outside these niches show little to no proliferation under normal physiological conditions. However, following invasive injuries like stab wounds or cerebral ischemia (occlusion of the middle cerebral artery, MCAo), a specific subset of cortical astrocytes begins to proliferate and exhibit stem cell-like properties, including the activation of genes typically associated with NSCs (M. Götz et al., 2015; Sirko et al., 2013). These astrocytes are capable of forming multipotent neurospheres *in vitro*, akin to NSCs; however, their behaviour *in vivo* exhibits distinct characteristics (M. Götz et al., 2015).

The reversion of reactive astrocytes to a more primitive, stem cell-like state, known as dedifferentiation, and their neurogenic potential can be influenced by several factors. For example, Notch signalling, which regulates the maintenance and differentiation of neural stem cells, is downregulated in reactive astrocytes after injury, allowing them to initiate a neurogenic program and generate neurons that express Dcx, Ascl1, and NeuN in the mouse striatum (Magnusson et al., 2014; Santopolo et al., 2020). A study by Zamboni et al. similarly demonstrated that blocking Notch signalling in the mouse cortex induces astrocyte dedifferentiation and neurogenesis (Zamboni et al., 2020). Another factor influencing astrocyte stemness is Sonic Hedgehog (SHH), a morphogen that controls cell fate and patterning in the developing nervous system. SHH is upregulated by invasive injuries such as stab wounds or cerebral ischemia, reactivates their stem cell potential of astrocytes. This allows astrocytes to proliferate and generate neurospheres, which are clusters of self-renewing and multipotent cells, *in vitro* (Sirko et al., 2013). Additionally, Loss of p53, a tumour suppressor that is commonly mutated or inactivated in glioma, destabilizes the identity of astrocytes, and primes them to dedifferentiate in response to injury, resulting in increased proliferation and multipotency (Simpson Ragdale et al., 2023). Moreover, Ischemia-induced up-regulation of Wnt2 protein activates Wnt signalling triggering astrocyte dedifferentiation (Fan et al., 2022). Also, Inflammation, driven by tumour necrosis factor-alpha (TNF-α) and the NF-κB pathway, triggers the reversion of differentiated astrocytes into neural progenitors. This is marked by a decrease in specific astrocyte markers like GFAP and glycogen metabolism genes in some cells, alongside an

increase in immature markers such as CD44, Musashi-1, and Oct4 (Ding et al., 2021; Gabel et al., 2016).

This transformation of reactive astrocytes to more plastic stem cell like state is of particular interest as it opens new avenues for research and potential regenerative mechanisms to promote tissue repair and regeneration. Yet, identifying these plastic subset remains challenging due to their occurrence as low frequency and the absence of specific markers. This limitation hinders the comprehensive understanding of the therapeutic potential and the precise role of this subset in CNS recovery. Therefore, innovative approaches are needed to identify this population.

1.4 Neurogenesis in the Adult Mammalian Brain: Limited neurogenic niches

In the adult mammalian brain, only a few regions, such as the SGZ of the hippocampal dentate gyrus and the SVZ lining the lateral ventricles, harbor NSCs that can generate new neurons (Figure 2). These regions are known as neurogenic niches and have limited capacity to replace lost neurons and restore damaged tissue and function after injury or disease (D. K. Ma et al., 2009). Within these neurogenic niches, neural stem cells (NSCs) reside in a quiescent state expressing markers Gfap and Prominin 1/CD133, capable of either self-renewal or differentiation into other cell types (Codega et al., 2014; Dulken et al., 2017; Fischer et al., 2011). Upon activation by specific stimuli, NSCs give rise to transit-amplifying progenitors (TAPs) expressing Egfr, Mash1 and Dlx2, which undergo rapid division to generate neuroblasts (NBs) (Codega et al., 2014; Doetsch et al., 2002; Kim et al., 2009). NBs express Doublecortin (DCX) as a marker for immature neurons and migrate from the neurogenic niches to their final destination, where they mature into neurons that express markers such as DCX, NeuN, and Tuj1 and integrate into existing neural networks (K. V. Adams & Morshead, 2018; Couillard-Despres et al., 2005; Dellarole & Grilli, 2008; Dulken et al., 2017). The functionality and characteristics of the newly formed neurons are contingent on the specific neurogenic niche of origin. In the SVZ niche, NBs migrate in chains along the rostral migratory stream (RMS) to the olfactory bulb (OB), where they differentiate into interneurons that modulate olfactory processing (Doetsch et al., 1999; Lim & Alvarez-Buylla, 2016; Ming & Song, 2011; Pencea et al., 2001). In the SGZ niche, NBs differentiate into granule neurons within the dentate gyrus, playing a role in hippocampal functions related to learning and memory (Ming & Song, 2011).

1.5 Zebrafish an Intriguing Model for Regeneration

In contrast to mammals, certain vertebrates like fish and amphibians possess the extraordinary ability to regenerate substantial portions of their brains post-injury (Lust & Tanaka, 2019). A prime example is the zebrafish, which can regenerate almost all organs, including the brain and spinal cord (Alunni & Bally-Cuif, 2016; Cacialli & Lucini, 2019; Diotel et al., 2020; Poss et al., 2003; Zambusi & Ninkovic, 2020). This regenerative capacity is underpinned by the presence of abundant stem cell niches across various brain regions, such as the telencephalon, optic tectum, cerebellum, and hypothalamus, and other areas, as illustrated in Figure 2 (Kizil, Kaslin, et al., 2012). These niches harbor ependymoglia or radial glial cells (RGCs)—a subtype of glial cells covering the ventricles with characteristics of both ependymal and astroglia cells, serving as neural stem cells that continuously generate new neurons through the proliferation, differentiation or direct conversion of these cells depending on the region and the stimulus (Barbosa & Ninkovic, 2016; Ganz & Brand, 2016; Kizil, Kaslin, et al., 2012; Than-Trong & Bally-Cuif, 2015). In addition, zebrafish also induce injury-specific expression of transcription regulators, such as GATA binding protein 3 (Gata3), in proliferating RGCs within the injured adult zebrafish telencephalon (as well as other tissues, like the heart and fin), which is essential for neuronal repair and regeneration (Kizil, Kyritsis, et al., 2012). This highlights that zebrafish activate specific and distinct neurogenic programs in response to inflammation or injury, which are different from those involved in constitutive neurogenesis.

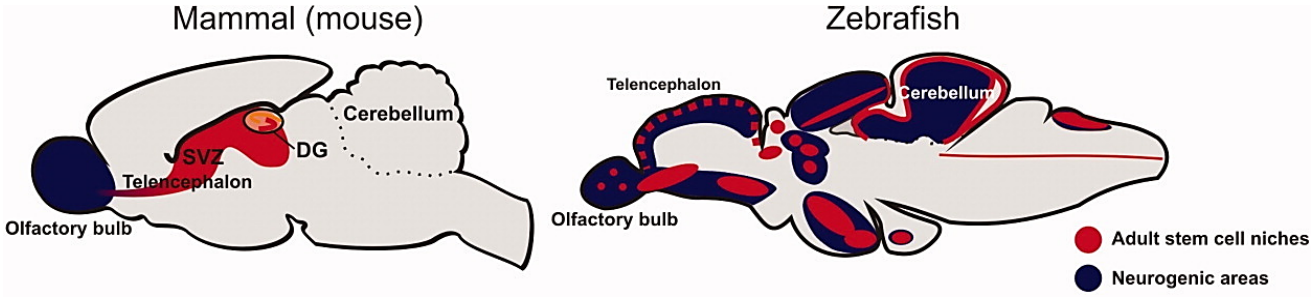

Figure 2: *Neurogenic regions of the zebrafish brain in comparison to mammals (Kizil et al. 2012. Adult neurogenesis and brain regeneration in zebrafish. Adapted by copyright permission from John Willey and Sons and Copyright Clearance Center: Developmental Neurobiology 72 (3): 429–61, 2012.* License No: *5759490306855. https://doi.org/10.1002/dneu.20918).*

RGCs in the zebrafish brain can re-initiate cell proliferation and generate neural precursors to rebuild the lost neural circuit after injury (Jurisch-Yaksi et al., 2020). For example, a stab injury in the optic tectum activates plastic RGCs, showcasing their capability to differentiate into neurons and oligodendrocytes (Yu & He, 2019). Similarly, an injury to the telencephalon in adult zebrafish triggers an immediate glial response, which typically resolves within 7 days post-injury (Sanchez-Gonzalez et al., 2022). The rapid glial response resolution in zebrafish, post-telencephalon injury, contrasts with the sustained response in mammalian brains.

Zebrafish and mammalian brains share some common features of adult neurogenesis in telencephalon, despite their divergent evolutionary histories and regenerative capacities. Studies have reported that the telencephalic ventricular zone (VZ) in the adult zebrafish brain generates neural progenitor cells (NPCs) that are similar to those found in the mammalian SVZ niche. These NPCs migrate tangentially into the OB via a pathway reminiscent of the RMS, and subsequently differentiate into mature neurons (Adolf et al., 2006; Kishimoto et al., 2011). Furthermore, RGCs display characteristics similar to mammalian astrocytes, such as complex bushy morphology and the expression of typical astrocyte markers, such as Glast, Gfap, S100b, and glutamine synthetase (GS) (Diotel et al., 2020). Also, certain populations of RGCs at early larval stages show close proximity to synapses, tiling behavior, and dynamic Ca2+ transients at both global and microdomain levels, reminiscent of mammalian astrocytes (J. Chen et al., 2020). This indicate, while ependymoglia cells and mouse astrocytes are not identical, they do share some conserved properties. This similarity could provide valuable insights into identifying common mechanisms or pathways, shedding light on the potential for identifying plastic astrocytes that acquire a more neurogenic phenotype following injury or disease in mammals by cross-comparison approach.

1.6 Cross-species analysis of single-cell transcriptomes with zebrafish: advantages and tools

Single-cell transcriptomics is a rapidly evolving field that enables the characterization of gene expression patterns at the resolution of individual cells. By comparing scRNA-seq data from different species, researchers can unveil both evolutionarily conserved and divergent biological processes, as well as unique adaptations specific to each species (Diotel et al., 2020).

As previously mentioned, Zebrafish are particularly noteworthy for their exceptional regenerative capabilities, offering valuable insights that contrast with mammals' limited brain regenerative capacities (Jurisch-Yaksi et al., 2020; Kozol et al., 2016). Emerging studies have begun to leverage the zebrafish model to dissect conserved and distinct processes in regenerative biology. For instance, Hoang *et al.* utilized integrative transcriptomic and epigenomic analysis to compare the gene expression and chromatin accessibility of Müller glia cells in zebrafish, mice, and chicks. Their study, conducted under both resting and tissue injury conditions, found that zebrafish and chick Müller glia possess a greater neurogenic potential post-injury compared to mice (Hoang et al., 2020). This potential is regulated by specific gene networks related to the cell cycle, glial quiescence, reactivity, neurogenesis, and the activation of transcription factors like nuclear factor I. By interfering with these factors, it's possible to induce Müller glia in adult mice to proliferate and generate neurons following an injury. Another example is a study where they compared single-cell/nucleus transcriptomes between zebrafish and human brains (Cosacak et al., 2022). This comparison has uncovered both shared and unique molecular pathways implicated in Alzheimer's Disease (AD), thereby enriching our comprehension of the disease's mechanisms. Moreover, integrating with zebrafish also plays a crucial role in identifying cell type markers. Pandey et al. demonstrated this by combining zebrafish and mouse forebrain single-cell transcriptome data to identify zebrafish telencephalic neuronal cell types. Their study unveiled both conserved and unique types, along with marker genes, thus illuminating the intricacies of neuronal diversity (Pandey et al., 2023). These studies underscore the importance of zebrafish in unraveling biological mechanisms and the benefits of integrating scRNA-seq data across species to explore cellular and molecular complexities.

To integrate scRNA-seq data across various dimensions, such as cell types, technologies, sources, and species, a range of specialized tools have been developed, each addressing specific aspects of data heterogeneity and complexity. Some of the commonly used tools are : (1) LIGER (Linked Inference of Genomic Experimental Relationships) that utilizes integrative nonnegative matrix factorization to jointly define cell types from multiple single-cell datasets (J. Liu et al., 2020; Welch et al., 2019); (2) Harmony that uses an iterative clustering method to adjust the cell embeddings in a low-dimensional space until the batch effect is minimized (Korsunsky et al., 2019); (3) SAMap leverages the self-assembling manifold (SAM) algorithm to align cell atlas manifolds from different species, enabling cross-species comparisons (Tarashansky et al., 2021); (4) scPoli, which focuses on

integrating population-level single-cell data (De Donno et al., 2023); (5) Seurat v4, which offers versatile data alignment tools through canonical correlation analysis (CCA) or mutual nearest neighbors (MNN), effectively removing unwanted variations (using FindIntegrationAnchors and IntegrateData functions) (Butler et al., 2018); (6) Conos (Clustering On Network Of Samples), which constructs a global graph of cells from various samples, enabling robust clustering based on multiple inter-sample mappings; (7) FastMNN and mnnCorrect provide efficient MNN-based integration solutions, addressing batch effects in large-scale datasets (Barkas et al., 2019); (8) scMerge employs factor analysis of single-cell stably expressed genes (scSEGs) and identifies pseudoreplicates across different datasets to facilitate integration (Y. Lin et al., 2019); and (9) scGen is a generative model designed to predict how single cells respond to perturbations across different cell types, studies, and species (Lotfollahi et al., 2019).

In addition to these integration tools, resources such as OrthoDB (Kuznetsov et al., 2023), OrthoFinder (Emms & Kelly, 2019), SonicParanoid (Cosentino & Iwasaki, 2019), Ensembl Compara (Herrero et al., 2016), NCBI HomoloGene (Agarwala et al., 2016), orthogene (*Bioconductor - Orthogene*, n.d.), and eggnog (Hernández-Plaza et al., 2023) are pivotal for multi-species scRNA-seq integration analysis. These resources contribute homologs and orthologs that are essential for cross-species comparative studies. They facilitate the identification of genes that are evolutionarily conserved, with orthologs indicating genes that have maintained similar functions across different species, and homologs identifying genes that share a common ancestry, enhancing our understanding of genetic evolution and function across species.

1.7 Neuronal replacement approaches for Repair

Recent advancements in neuronal replacement methods have broadened the scope for restoring lost or damaged neurons in the brain, surpassing the traditionally limited regenerative capacity of the adult brain. Neuronal replacement therapy, which encompasses exogenous and endogenous approaches, holds promise for improving brain function post-injury or disease (Grade & Götz, 2017). Exogenous approaches involve transplanting external cells, like neuronal stem cells or progenitor cells, into the damaged or diseased brain to effectively replace lost neurons. However, this method faces challenges such as low cell survival, poor migration and integration, and immune rejection (Liao et al., 2019). On the other hand, endogenous approaches aim to spur the spontaneous generation of new neurons from existing cells in the adult brain. One of the

most promising endogenous approaches is direct neuronal reprogramming, also known as transdifferentiation, which converts one mature cell type in the brain into induced neurons (iNs) by overexpressing lineage-specific transcription factors, without going through an intermediate or pluripotent stem cell state. This avoids the need for exogenous cell transplantation and exploits the potential of endogenous cells to regenerate brain tissue (Bocchi et al., 2022; Gascón et al., 2017; Grade & Götz, 2017). This is an alternative to indirect reprogramming, which reprograms somatic cells into induced pluripotent stem cells (iPSCs) by overexpressing Yamanaka factors (Pou5f1, Sox2, Myc, and Klf4) (Takahashi & Yamanaka, 2006), and then differentiates them into neurons. Recent advances have improved the efficiency and specificity of direct neuronal reprogramming, both *in vitro* and *in vivo*, by understanding the molecular and metabolic constraints of this process (Berninger et al., 2007; Gascón et al., 2016, 2017; Heinrich et al., 2010; Masserdotti et al., 2015; Mattugini et al., 2019; Wan & Ding, 2023). The following sections will discuss the details of direct astrocyte-to-neuron conversion, the reprogramming hurdles encountered within the injured brain milieu, and the role of chromatin proteins in generating efficient iNs.

1.7.1 Direct neuronal conversions

Direct neuronal reprogramming can be achieved by various methods that modulate the epigenetic and transcriptional landscape of the original cell type, enabling the activation of neuronal-specific genes while suppressing those of the cell's prior identity. This transformation is commonly facilitated by introducing transcription factors (TFs) that serve as master regulators of neuronal identity, such as Ascl1, Brn2, Dlx2, Myt1l, NeuroD4, NeuroD1, Neurog2, Nurr1, Pax6, Sox2, and Sox11 (Amamoto & Arlotta, 2014; Bergsland et al., 2006; Berninger et al., 2007; Blum et al., 2011; Brulet et al., 2017; Buffo et al., 2005; Grande et al., 2013; Heinrich et al., 2010, 2014; Mall et al., 2017; Masserdotti et al., 2015; Mattugini et al., 2019; Ninkovic & Götz, 2013; Niu et al., n.d.; Smith et al., 2016). These TFs alone or in combinations drive the conversion of non-neuronal cells into functional neurons and are commonly delivered through viral vectors, such as lentiviruses, adenoviruses, or retroviruses (Bocchi et al., 2022; M. Götz & Bocchi, 2021; Wan & Ding, 2023). This integration results in the expression of TFs and kickstart reprogramming. Some of these TFs are pioneer factors, which can bind and open closed chromatin, enabling the expression of target genes (Morris, 2016). For example, Ascl1 and Neurog2, two well-studied neurogenic transcription factors, that are widely used and studied for direct reprogramming (Smith et al., 2016; Wapinski et al., 2013).

Another method involves using small molecules or epigenetic modifiers to alter chromatin structure and conversion rate (M. L. Liu et al., 2013; N. X. Ma et al., 2019; Smith et al., 2016). This has also been shown to enhance reprogramming efficiency when combined with transcription factors. These molecules can activate neuronal genes and modify epigenetic marks, influencing the reprogramming process and improving the accessibility of target cells for efficient cell fate changes. For instance, Valproic acid inhibits histone deacetylases (HDACs); Vitamin C facilitates DNA demethylation; Forskolin activates cyclic AMP signaling, collectively bolstering reprogramming efficiency (Duan et al., 2019; Hsieh et al., 2004; Lee Chong et al., 2019; Smith et al., 2016). Moreover, microRNAs (miRNAs) are another strategy that can regulate post-transcriptional expression of multiple genes related to neuronal development and function, thereby creating a permissive chromatin environment for efficient reprogramming (Cates et al., 2021; Pascale et al., 2022). For example, miR-9/9* and miR-124 have been identified as potent neurogenic molecules that can drive the conversion of human fibroblasts into specific subtypes of neurons (Lu & Yoo, 2018; Yoo et al., 2011). MicroRNA-375 overexpression improves NeuroD1-mediated reprogramming efficiency by promoting cell survival at early stages of reprogramming (X. Chen et al., 2023).

The choice of factors and methods depends on the desired neuronal subtypes and cell source, as different combinations of TFs, small molecules, and miRNAs can induce the generation of specific types of neurons, such as glutamatergic, GABAergic, dopaminergic, or cholinergic neurons, from various cell types, including fibroblasts, astrocytes, hepatocytes, or pericytes (Amamoto & Arlotta, 2014; Bocchi et al., 2022). For instance, Ascl1 is known for generating GABAergic neurons, while Neurog2 specializes in promoting the formation of glutamatergic neurons upon overexpression of these factors in astrocytes (Masserdotti et al., 2015). Astrocytes, the most abundant type of glial cells in the brain, serve as a readily available source for reprogramming into neurons. Several research groups have successfully converted astrocytes into functional neurons *in vitro* and *in vivo*, demonstrating the feasibility and potential of this approach (Berninger et al., 2007; Chouchane et al., 2017; Gascón et al., 2016; Guo et al., 2014; Heinrich et al., 2010, 2012; F. Liu et al., 2021; Masserdotti et al., 2015; Mattugini et al., 2019; Rao et al., 2021)

1.7.2 Astrocyte-to-Neuron Conversion *in vivo*: Challenges in the Injured CNS

While direct neuronal reprogramming holds promise, translating this approach *in vivo* faces challenges, notably in delivering reprogramming factors. Current protocols relying on viral vectors pose risks, including immunogenic responses, insertional mutagenesis, lack of specificity, and limited packaging capacity (Bulcha et al., 2021; Gantner et al., 2020; Shchaslyvyi et al., 2023). Alternative non-viral delivery methods, such as plasmids, nanoparticles, or recombinant proteins, have lower efficiencies and stability (Tasset et al., 2022). The harsh, inflammatory environment following CNS injury may further inhibit viral transduction, exogenous factor expression, and iNs survival, maturation, and integration. Apart from this, another challenge lies in the discrepancy between *in vitro* and *in vivo* reprogramming conditions. *In vitro* reprogramming protocols typically utilize sustained exposure to mitogens, such as epidermal growth factor (EGF) and fibroblast growth factor 2 (FGF2), to promote iNs generation. However, the injury microenvironment exhibits dynamic and transient mitogen expression. For instance, following TBI, EGF levels spike within 24 hours but rapidly decrease to basal levels after 3 days, while FGF2 levels begin to rise 4 hours post-damage and remain elevated for at least 14 days (Addington et al., 2015). Notably, FGF2 administration after post-traumatic brain injury has been reported to enhance cognitive performance and neurogenesis (Sun et al., 2009), while EGF infusion expands the neurogenic precursor pool in the neurogenic niche after ischemic injury (Ninomiya et al., 2006) These findings suggest that the temporal dynamics of mitogen signaling play a crucial role in modulating the reprogramming outcome. Therefore, to better replicate the endogenous injury response, regulated *in vitro* reprogramming models are essential, mimicking the transient EGF and sustained FGF signaling reported *in vivo*.

1.7.3 Pioneer Factors and Chromatin Remodeling

Neuronal reprogramming involves overcoming the chromatin barriers of starter cells like astrocytes or fibroblasts, wherein essential neuronal genes are typically sequestered within inaccessible chromatin areas. Pioneer transcription factors have a unique capability to access these regions and instigate chromatin remodeling (Morris, 2016).

Ascl1, a well-known pioneer factor, exhibits “on-target” pioneering activity during neuronal reprogramming (Chanda et al., 2014; Iwafuchi-Doi & Zaret, 2014; Wapinski et al., 2013). Studies using ATAC-seq have shown that Ascl1 can rapidly open closed chromatin at its target sites within 12 hours of reprogramming initiation in mouse embryonic fibroblasts

(MEFs) into induced iNs. However, the majority of the accessibility changes occur between days 2 and 5 (Wapinski et al., 2017). This biphasic pattern suggests an initial targeting of specific regulatory elements by Ascl1, followed by broader chromatin remodeling mediated by additional factors. Rao *et al.* demonstrated a significant shift in gene expression profiles during the early stages of Ascl1-mediated reprogramming of mouse astrocytes, based on RNA-seq and ChIP-seq (Rao et al., 2021). They found that ASCL1 directly targets the regulatory regions of numerous genes critical for neuronal development and function, such as Klf10 (involved in neuritogenesis), Myt1 and Myt1l (required for the electrophysiological maturation of iN cells), and Neurod4 and Chd7 (crucial for the efficient conversion of astrocytes to iNs). The ability of ASCL1 to orchestrate such a broad transcriptional overhaul highlights the critical role of chromatin remodeling in facilitating the direct reprogramming process.

Neurog2, another pioneer factor, similarly engages with closed chromatin to activate neuronal gene expression. It has the capability to transform astrocytes into glutamatergic neurons, the primary excitatory neurons in the brain (Berninger et al., 2007; Heinrich et al., 2010; Masserdotti et al., 2015). Neurog2's bHLH domain facilitates sequence-specific DNA binding, promoting chromatin remodeling (Aydin et al., 2019). However, Neurog2 alone is not sufficient to reprogram fibroblasts, and requires additional molecules such as forskolin (FK) and dorsomorphin (DM) to enhance chromatin accessibility at its target sites (M. L. Liu et al., 2013; Smith et al., 2016). These small molecules (FK+DM) activate cooperative transcriptional activities of Neurog2 and CRE binding protein 1 (CREB1), increase H3K27 acetylation (a mark of open chromatin), elevate Sox4 (an HMG box transcription factor) expression, and subsequent Sox4-dependent chromatin remodeling, thereby synergizing with Neurog2 to augment the expression of a broad spectrum of pro-neural transcription factors and firmly establish neuronal identity in a variety of fibroblast and glioblastoma cells.

Further elucidating the significance of chromatin changes in neuronal reprogramming, the study by Rivetti di Val Cervo *et al.* employed a combination of transcription factors—Neurod1, Ascl1, and Lmx1a, along with miR218, to induce the conversion of human and mouse astrocytes into induced dopamine neurons (iDANs) and this process is notably enhanced by chromatin remodeling agents (Rivetti Di Val Cervo et al., 2017). Furthermore, Hsieh et al. showed that histone deacetylase inhibitors, such as valproic acid (VPA), drive neuronal differentiation in adult hippocampal progenitors by upregulating neurogenic

transcription factors like NeuroD, underscoring the critical role of chromatin remodeling in neuronal reprogramming (Hsieh et al., 2004).

Effective reprogramming to neurons entails not just triggering the neuronal program but also silencing the inherent identity of the original cells, particularly by overcoming key repressors such as RE-1 transcription repressor complex (REST). REST expressed in non-neuronal cells and known to suppress neuronal genes in non-neuronal cells (Jørgensen et al., 2009). Reducing REST levels significantly boosts Neurog2's ability to reprogram astrocytes into neurons, achieving up to 90% efficiency (Masserdotti et al., 2015). Similarly, repressing the RNA binding protein PTB (polypyrimidine tract binding) in MEFs, promotes neuronal reprogramming by lifting the repression on neuronal genes, facilitated by microRNA (e.g. miR-124) mediated reduction of REST activity (Xue et al., 2013). The interplay between activating desired neuronal pathways and inhibiting the original cell programming is essential for successful neuronal reprogramming.

1.7.4 Chromatin architectural Hmgb2 proteins: expression and prospective role in Neuronal Reprogramming

High Mobility Group Box 2 (Hmgb2) proteins, belonging to the non-histone chromatin-binding protein family, are instrumental in altering chromatin architecture, thereby facilitating the interaction of transcription factors and chromatin modifiers (Thomas & Travers, 2001). These proteins are characterized by two HMG-box domains and bind to the minor groove of DNA, inducing bending, looping, and unwinding. Their interaction with nucleosomes and histone tails influences histone modifications and nucleosome positioning, playing a crucial role in transcription, replication, recombination, and DNA repair.

Hmgb2 proteins have been extensively studied in cancer biology for their roles in cell proliferation, metastasis, drug resistance, and cellular senescence (Starkova et al., 2023). Beyond these aspects, Hmgb2 has also been investigated for its involvement in brain development and neurogenesis. For instance, a study by Ronfani et al. demonstrated that Hmgb2 expression is widespread in early embryonic stages (E10.5), notably in regions undergoing rapid cell division, using in situ hybridization (Ronfani et al., 2001). By E12.5, Hmgb2's distribution begins to specialize, concentrating in the ventricular zones of the brain, where it supports the proliferation of neuroepithelial cells, and extending into the

spinal cord. As development progresses to E17, Hmgb2 expression persists in the VZ but also expands to encompass the differentiated cortex and mesencephalon. Postnatally (at P4 and P17), Hmgb2 expression narrows further to specific brain regions, such as the external granular layer of the cerebellum and the hippocampus. However, this study suggests that Hmgb2 expression is low or absent in the adult brain, a finding that contrasts with other reports of Hmgb2 expression in specific adult brain regions (Abraham, Bronstein, Reddy, et al., 2013; Kimura et al., 2018). The study conducted by Kimura et al. investigated the expression and function of Hmgb2 in the dentate gyrus of the adult mouse brain, revealing that Hmgb2 is expressed in a subset of NSCs and progenitor cells, but not in mature neurons. This expression is notably associated with the transition from the quiescent to the proliferative state of NSCs, leading to the proposition of Hmgb2 as a novel marker for activated NSCs in the adult hippocampus (Kimura et al., 2018). In another study, it has also been reported that Hmgb2 potentially regulates neural stem cell proliferation in the SVZ, another adult neurogenic niche (Abraham, Bronstein, Chen, et al., 2013).

Furthermore, Bronstein et al. compared perinatal neural progenitor cell (NPC) cultures from normal and HMGB2-null mice. They found that HMGB2 regulates polycomb group (PcG) proteins, key epigenetic modifiers controlling NSC fate. HMGB2 deficiency reduces PcG proteins and H3K27 trimethylation, altering the balance between neurogenesis and gliogenesis. This identifies HMGB2 as a crucial factor in NSC epigenetic regulation (Bronstein et al., 2017).

Given these findings, Hmgb2 demonstrates an ability to influence chromatin accessibility and gene expression, marks it as a promising candidate for astrocyte-to-neuron conversion in direct reprogramming. More studies on HMGB2's mechanisms and roles in neuronal reprogramming could advance regenerative therapies for CNS injuries.

2. Results

2.1 Aim of study I

This study aimed to identify marker genes for rare plastic astrocytic subsets that exhibit proliferative and neurosphere-forming abilities in response to stab wound injuries in mice. It introduces an innovative trans-species approach that leverages the regenerative capabilities of zebrafish radial glia, employing single-cell integration analysis to achieve this goal.

Stab wound injury induces transit amplifying progenitor-like phenotype in parenchymal astrocyte

Priya Maddhesiya, Finja Berger, Christina Koupourtidou, Alessandro Zambusi, Klara Tereza Novoselc, Judith Fischer-Sternjak, Tatiana Simon, Sebastian Jessberger, Jovica Ninkovic.

My contribution to this manuscript in detail:

I was responsible for all the bioinformatic analyses presented in the manuscript. This included conducting single-cell transcriptomic (scRNA-seq) analysis, integrating data from both mouse and zebrafish species, and correlating these findings with the neurogenic niches in the subventricular zone (SVZ). I used various tools and pipelines to process, integrate, and visualize the integrated datasets. Additionally, I actively participated in the writing and editing process of the manuscript.

Currently, the manuscript is being reviewed by the co-authors and will be submitted next month.

Please note that due to an increased number of pages, supplementary tables are not included in the PDF versions of the dissertation and are available as separate excel files via the following link: https://syncandshare.lrz.de/getlink/fiHcckVbuzT8E3p6PgfrF7/

Stab wound injury induces transit amplifying progenitor-like phenotype in parenchymal astrocytes

Priya Maddhesiya[1,2,3], Finja Berger[1,2,3], Christina Koupourtidou[1,2, 3], Alessandro Zambusi[1,2,3], Klara Tereza Novoselc[1,2,3], Judith Fischer-Sternjak[4,5], Tatiana Simon[4], Sebastian Jessberger[6], Jovica Ninkovic[1,3,7,8]

Affiliations

1 Biomedical Center Munich (BMC), Department of Cell Biology and Anatomy, Medical Faculty, LMU, Munich, Germany

2 Graduate School of Systemic Neurosciences, LMU, Munich, Germany.

3 Research Unit Central Nervous System Regeneration, Helmholtz Zentrum Munich, Munich, Germany.

4 Biomedical Center Munich (BMC), Institute of Physiological Genomics, Medical Faculty, LMU, Munich, Germany

5 Institute of Stem Cell Research, Helmholtz Zentrum Munich, Munich, Germany.

6 Faculties of Medicine and Science, Laboratory of Neural Plasticity, Brain Research Institute, University of Zurich, Zurich, Switzerland

7 Munich Cluster for Systems Neurology SYNERGY, LMU, Munich, Germany

8 Corresponding author at: jovica.ninkovic@helmholtz-munich.de

Highlights

- Single-cell transcriptome and trans-species comparisons identify post-CNS injury plastic astrocytes with proliferative and de-differentiated characteristics.
- These plastic astrocytes display *in vitro* self-renewal and neurosphere-forming capabilities but exhibit gliogenic differentiation.
- Originating from reactive astrocytes, they share transcriptional traits with TAPs rather than NSCs.
- Differing from endogenous TAPs, these plastic astrocytes offer the potential for enhancing CNS repair post-injury.

Abstract

Astrocytes, as prevalent brain glial cells, have beneficial and detrimental effects on CNS recovery. Post-CNS injury, a small astrocyte subset becomes proliferative, de-differentiated, and acquires self-renewal and neurosphere capabilities in vitro. Presenting a promising target for initiating repair processes after brain injury and their potential role in neural repair. Studying these rare plastic astrocytes is challenging due to a lack of distinct markers. In our study, we identified these subsets of the astrocytic population using single-cell transcriptome and trans-species comparisons. Leveraging the regenerative properties of radial glia of zebrafish, we characterized injury-induced plastic astrocytes in mice. These injury-induced astrocytic subpopulations were predominantly proliferative and showed self-renewing and neurosphere-forming capacity, differentiating only into astrocytes. By integrating these populations with neuronal lineages in the adult mouse subependymal zones (SEZ), we traced the origins of identified injury-induced plastic astrocytic subpopulations. This revealed that a subset of these injury-induced astrocyte cells shows transcriptional similarities to endogenous transient amplifying progenitors (TAPs) of SEZ rather than neural stem cells (NSCs). These injury-induced TAP-like cells diverge from endogenous bona fide TAPs in their differentiation trajectories, adopting a gliogenic fate rather than a neurogenic one. Taken together, we identified a rare subset of injury-induced, proliferative, plastic astrocytes with neurosphere-forming capacities originating from reactive astrocytes resembling TAPs.

Introduction

Brain injuries, including traumatic brain injuries (TBIs) and strokes, pose significant challenges to human health by causing long-term damage and functional impairments (Bramlett & Dietrich, 2015; Griesbach et al., 2018). This is mainly due to restricted ability of the mammalian brain to regenerate damaged neural circuitry (Grade & Götz, 2017; Sun, 2014). Brain injuries do not only disturb the functional neural circuits, but also trigger the complex pathophysiological processes that form the glial border (Sofroniew, 2009). The glial border is a physical barrier that isolates the damaged tissue and prevents the expansion of inflammation and damage (Fawcett & Asher, 1999; Sofroniew, 2009). Astrocytes, microglia, and oligodendrocyte lineage cells undergo a complex and dynamic changes in their morphology, gene expression, and function (Liddelow & Barres, 2017; Matusova et al., 2023) to build the glial border. Recent advances showed that some components of the glial border, such as a subset of reactive astrocytes, promote the axonal regeneration after spinal cord injury (Anderson et al., 2016). However, the long-lasting neuroinflammation associated with glial border leads to the alternation of the extracellular milieu and impairment of regeneration (Li et al., 2020; Sanchez-Gonzalez et al., 2022; Zambusi et al., 2022). Therefore, the revolutionary approach to transform the glial border cells into neurons would simultaneously limit the negative impact of prolonged glial reactivity and provide new neurons for the repair purpose in the areas that require them, such as injured tissue (Grade & Götz, 2017). Indeed, the pioneering in vitro studies demonstrated that it is possible to directly convert glial cell to neurons of a specific neurotransmitter identity using overexpression of neurogenic fate determinants (Berninger et al., 2007; Bocchi et al., 2022; Heinrich et al., 2010). Following these pioneering studies, the conversion of both astrocytes and NG-2 cells has been achieved with remarkable efficiency in vivo (Liu et al., 2021; Mattugini et al., 2019; Pereira et al., 2017; Torper et al., 2015). Importantly, the stab wound injury significantly increased neurogenic fated determinants mediated conversion rate of parenchymal astrocytes compared to the intact brain (Mattugini et al., 2019). This is in line with recent studies demonstrating that astrocyte subsets change their identity and become more stem-like after

brain injury (Behrendt et al., 2012; Buffo et al., 2008; Dimou & Gotz, 2014; Gotz et al., 2015; Mori et al., 2005; Shimada et al., 2012; Simpson Ragdale et al., 2023; Sirko et al., 2023; Torper & Götz, 2017; Zamboni et al., 2020). These originally post-mitotic cells start to proliferate and acquire capacity to form multipotent neurospheres in vitro (Buffo et al., 2008; Gotz et al., 2015; Sirko et al., 2013). The mechanisms underlying such dedifferentiation of astrocytes into neurosphere-forming cells following brain injury still need to be fully understood. However, several factors have been implicated in this process. For example, Sonic hedgehog (SHH) signaling was reported to trigger stem cell responses in reactive astrocytes following invasive injuries both in vivo and in vitro (Sirko et al., 2013). Injury induces the neurogenic potential of Notch signaling-deficient cortical astrocytes (Zamboni et al., 2020). Blocking Notch signaling increases the number and diversity of neurons generated from astrocytes in the striatum after stroke and improves mouse motor function (Magnusson et al., 2014; Santopolo et al., 2020), in line with Notch signaling maintaining the glial fate. Moreover, p53 mutation-bearing astrocytes generate more neurospheres compared to wild-type astrocytes after stab wound injury (Schmid et al., 2016; Simpson Ragdale et al., 2023). This sparse experimental evidence supports the hypothesis that injury induces temporal de-differentiation of astrocytes with active mechanisms to prevent their differentiation towards the neuronal lineage. Such lineage barriers could, however, been efficiently overcome by neurogenic fate determinants overexpression following injury (Gascon et al., 2015, 2017; Heinrich et al., 2014; Mattugini et al., 2019). Therefore, these astrocytes could represent a promising target population for direct neuronal conversion. The potential use of plastic astrocytes as source for new neurons rises an important concern regarding the endogenous role of these cells within the glial border. For example, it has been recently shown that proliferating astrocytes regulate monocyte trafficking following the injury and interference with their function leads to the prolonged neuroinflammation (Frik et al., 2018). Similarly, astrocytes have also been implicated in the blood-brain-barrier recovery and neuroprotection following the mild TBI (George et al., 2022). Thus, it is crucial to prospectively identify these cells analyze their lineage barriers and suitability as targets population for direct conversion. So far, the prospective identification of plastic astrocytes has been elusive. This is largely due to the absence of distinct markers to identify them. Therefore, exploring effective ways to identify these rare injury-induced plastic astrocytes is crucial for harnessing their potential in brain injury repair.

In contrast to mammalian brain, the ependymoglia, the astrocytic counterparts in zebrafish brain, acquire plastic properties and differentiate into postmitotic neurons mediating endogenous repair after injury (Diotel et al., 2020; Zambusi & Ninkovic, 2020). Therefore, we hypothesized that the plastic mouse astrocytes should be the most similar population of astrocytes to the zebrafish ependymoglia. To test this hypothesis, we integrated cells from the zebrafish and mouse intact and injured brains based on their single cell transcriptomes. Indeed, we identified a subset of reactive astrocytes clustering together with ependymoglial cells. We further identified the unique transcriptional signature of these cells, including the high expression of Ascl1 transcription factor. Using the Ascl1:CreERT2 based genetic fate mapping we could show that these cells generate neurospheres after brain injury. Finally, the pseudotime based developmental trajectory demonstrated that these plastic cells following injury only transiently go through the state resembling neural stem cell state and end up in the gliogenic transit amplifying progenitor state. Thus, our analysis provides the cellular and molecular basis for the absence of endogenous generation of new neurons in the injured mammalian brain. Taken together, we prospectively isolated plastic, astrocyte-derived progenitors; described their specific transcriptome and identified the lineage barriers preventing them to spontaneously differentiate into neurons. This work sets the basis for further functional manipulations of plastic

astrocytes to address their endogenous role within the glial border and test their suitability for the repair.

Results

Integration of single cell transcriptomes reveals shared cellular states in zebrafish and mouse brain

To identify rare injury-induced plastic astrocytic populations, we employed a trans-species approach. We hypothesized that the plastic astrocyte population should be similar to the zebrafish ependymoglia. Therefore, we performed integration of single-cell transcriptomes-based cellular states isolated from intact and injured mouse cerebral cortex and zebrafish telencephalon (Fig. 1A) (Koupourtidou et al., 2024; Zambusi et al., 2022). We chose to integrate cells isolated from zebrafish brain 3- and 7-days post-injury (dpi) corresponding to the onset of ependymoglial reaction (3 dpi) and the peak of injury induced ependymoglial proliferation (7 dpi) (Baumgart et al., 2012; Sanchez-Gonzalez et al., 2022). Similarly, cells were isolated from the injured mouse cerebral cortex at 3 and 5 dpi, corresponding to the onset of parenchymal astrocytic proliferation (3 dpi) and the maximal neurosphere forming capacity of astrocytes after injury (5 dpi) (Buffo et al., 2008; Sirko et al., 2013). We integrated zebrafish and mouse transcriptomes using Seurat v4 (Butler et al., 2018) following standard preprocessing and employing a self-compiled function (see Methods). After integration, zebrafish and mouse cells were intermingled regardless of their origin (zebrafish or mouse) and condition (injured or intact brain) (Fig. 1B, Suppl. 1A). Unsupervised clustering was performed using PCA (1:10) at a resolution of 0.7, revealing 25 distinct cell clusters (Fig. 1C). Using cell type-specific markers, we annotated the identity of these clusters, identifying various neuronal populations, glial and microglial cell types (Fig. 1C; Suppl. Table 1). This also included clusters that expressed both astrocyte and radial glia (RG) identity markers and therefore defined them as Astrocyte/RG clusters (Fig. 1C). These annotated clusters displayed a heterogeneous distribution of cells from both mouse and zebrafish, indicating successful cross-species data integration (Fig. 1D-E).

To validate the data integration with independent integration method, we employed the Harmony algorithm, relaying on iterative integration and batch correction approach (Korsunsky et al., 2019). Similar to the Seurat analysis, after the integration using Harmony almost every cluster contained cells from both species (Suppl. Fig 1B). Utilizing unsupervised clustering, we identified 26 distinct cell clusters following PCA (1:10) at a resolution of 0.7 (Suppl. Fig. 1E). We inferred cell type relationships between clusters obtained through Harmony and Seurat using the deduced relationship function from ELeFHAnt, assessing relative cluster similarities (Thorner et al., 2021). Importantly, each cluster identified with Harmony showed a one-to-one correspondence for with unique cell clusters within the Seurat integration (Suppl. Fig. 1C-E). Furthermore, we extended our analysis to assess similarities at the gene level. As we are interested in astrocytes, we examined the top 10 marker genes from Seurat cluster 2 Astro/RG and corresponding Harmony cluster 3 Astro/RG, which showed the highest relative similarity in the heatmap (Suppl. Fig. 1D). Encouragingly, 9 out of 10 top enriched genes characterizing these clusters were identical with similar enrichment (Suppl. Fig. 1F-I). These results suggest that cell clusters identified in the integrated dataset are defined by intrinsic biological factors rather than the choice of integration algorithm. Moreover, we integrated intact and injured samples from both mouse and zebrafish, along with mouse peripheral blood mononuclear cells (PBMCs) using the Seurat (Suppl. Fig. 2A). This allowed us to scrutinize if the integration process coerced distinct cell types into a unified representation. Our analysis indicated that PBMCs clustered with brain immune cells (microglia and infiltrating monocytes), distinct from

astrocyte/radial glia or neuronal clusters (Suppl. Fig. 2B-F; Suppl. Table 2), excluding the possibility that the integration method enforces a uniform clustering of cells regardless of their transcriptional features. Additionally, to ensure that transcriptional information was not lost during integration, we assessed the relative similarity between clusters identified in unintegrated mouse and zebrafish datasets and clusters defined in the integrated seurat mouse+zebrafish datasets using ELeFHAnt SVM classifier tools (Thorner et al., 2021) (Fig.1F, G). Our analysis revealed a robust concordance between the integrated dataset clusters and the cell types present in the unintegrated mouse or zebrafish datasets. This outcome further supports maintenance of specific cellular identities and essential transcriptional profiles during the integration process. Noticeably, several clusters were identified that exhibited no correspondence with the integrated clusters. This observation implies the existence of species-specific cell type clusters within the unintegrated mouse or zebrafish datasets, highlighting the inherent biological diversity across species. Importantly, these cell clusters do not include astrocyte clusters and therefore do not compromise our downstream analysis.

A specific population of reactive astrocytes clusters with zebrafish ependymoglia

After integration, we were prompted to identify injury-induced plastic astrocytes as according to our hypothesis they would share the transcriptomic signature with zebrafish stem cells. Therefore, we focused our analysis on integrated clusters 2, 3, 9, 11, 12, 17, and 21 of Astrocytes/Radial glia (Astro/RG) and sub-cluster them further into a total of 10 Astro/RG sub-clusters using PCA (1:10) at 0.3 resolution (Fig. 2A, C). Indeed, the newly defined sub-clusters contained a different proportion of cells originating from a specific condition (Fig. 2D, F). For example, the cluster 0 is enriched in cells originating from the intact mouse cerebral cortex (Fig. 2F). These cells also express the typical homeostatic astrocyte markers (Koupourtidou et al., 2024) in line with their origin (Fig. 2B, E). Interestingly, this cluster contained some zebrafish cells as well (Fig. 2D, F), suggesting that some of ependymoglial cells could be more specialized to have a protoplasmic astrocyte function. On the other hand, we identified the clusters 3 and 6 that contain largely cells originating from zebrafish (Fig. 2D, F). The expression of typical proliferation genes (Fig. 2E) along with astroglial identity suggests that these cells belong to the actively cycling Type I radial glia (März et al., 2010). These clusters also contain cells from the injured but lack cells originating from the intact mouse cerebral cortex (Fig. 2D, F). Importantly, a fraction of mouse cluster 3 and 6 cells also expressed the typical markers identifying this cluster as zebrafish Type I stem cells (März et al., 2010) (Fig. 2G), further highlighting the similarity of these mouse cells with the zebrafish stem cells.

We further aimed at visualization of the cluster 3/6 cells in the injured tissue using the expression of cluster 3/6 enriched genes. Our analysis revealed high expression of Hmgb2, Uhrf1, Ascl1, and Rpa2 in the cluster 3/6 cells (Fig. 3A-B). These genes are significantly upregulated in cells originating from the inured mouse cerebral cortex (both 3 and 5 dpi) compared to the intact sample (Fig.3C). Furthermore, we observed the increase in both the number of cells expressing these genes and the expression level per cell at 5 dpi compared to 3 dpi (Fig. 3C). This increase in expression corresponds with the peak of astrocytes proliferation and neurosphere forming capacity (Sirko et al., 2013). The immunohistochemical analysis, showed that the subset of reactive astrocytes upregulates these genes in response to injury (Fig. 3 D-K; Suppl. Fig. 3 A-J). Importantly, a fraction of cells expressing HMGB2 also expressed the Uhrf1 (Fig. 3I) or Ascl1 (Suppl. Fig. 3C) in line with our single cell analysis suggesting that expression of these genes mark cluster 3/6 cells. Notably, we also observe reactive, GFAP-positive astrocytes expressing only single marker genes (Hmgb2 or Uhrf1) (Fig.3K and Suppl. Fig. 3J) in line the hypothesis

that 3/6 cells upregulate the specific genes sequentially as they emerge from the homeostatic astrocytes in response to brain injury.

We next asked the question if the cluster 3/6 cells could be identified without the integration with zebrafish dataset (unintegrated analysis). Therefore, we clustered only astrocytes from the intact and injured mouse cerebral cortex and identified 7 distinct clusters at 0.5 resolution using PCA (1:15) (Suppl. Fig. 4A, B). We then identified cells from the cluster 3/6 in this unintegrated analysis. Indeed, we observed the distribution of the cluster 3/6 cells from the integrated analysis to over 5 different clusters in the unintegrated analysis at resolution 0.5 (Suppl. Fig. 4E). Moreover, the different resolutions (0.3-0.8) of clustering also failed to isolate cluster 3/6 cells to the specific cluster in unintegrated analysis (Suppl. Fig. 4 C-H), suggesting that this cellular state could only be isolated in integrative analysis.

Cell proliferation is a hallmark of the injury-induced Astro/RG 3 and 6 clusters

The analysis of cluster enriched genes in different astrocyte populations revealed a notable enrichment of cell proliferation-related genes within cluster 3/6 cells, including Tuba8, Dut, Mcm2, Mcm5, Hmgb2, Mcm6, Nusap1, Ube2c, Top2a, Pcna (Chen et al., 2021; G. Han et al., 2018; Kamino et al., 2011; Kimura et al., 2018; Nicolau-Neto et al., 2018; Ohtani et al., 1999; Ramos et al., 2020; Strzalka & Ziemienowicz, 2011; Wang et al., 2022; Xu et al., 2022; Yuan et al., 2022; Zeng et al., 2021) (Fig. 2E). Subsequent cell cycle analysis further revealed enrichment of distinct cell cycle phases across astrocytic sub-clusters (Fig. 4A). Notably, cluster 3 exhibited a significant proportion of cells in the S phase (36.9% of all cluster 3 cells), while cluster 6 cells predominantly resided in the G2M phase (93.3% of all cluster 6 cells) (Fig. 4B). Conversely, cells from homeostatic astrocyte clusters were largely in G1(G0) phase (Fig. 4B). Gene Ontology (GO) analysis underscored enrichment of processes associated with the cell division, including translation, ribosome assembly, ribonuclear protein assembly, mitochondrial translation, and regulation of different phases of the cell cycle in both clusters 3/6 (Fig. 4C). Furthermore, examination of genes positively regulating the cell cycle (GO:0045787) revealed highest enrichment in these clusters (Fig. 4D, Suppl. Table 3). These finding suggests that cluster 3/6 contain astrocytes resuming the proliferation in response to injury. To test this hypothesis, we labelled all cells undergoing cell division within the first 5 days after injury using the BrdU incorporation (Fig.4E). Reactive astrocytes were identified using the GFAP immunoreactivity and cluster 3/6 astrocytes using their immunoreactivity for HMGB2 (Fig. 4F). Indeed, we observed that virtually all GFAP+ and HMGB2+ cluster 3/6 reactive astrocytes incorporated BrdU during the labelling period and only a few HMGB2+ and BrdU- cells were identified (Fig. 4G-J). Moreover, HMGB2+ cluster 3/6 astrocytes comprised about 50% of all reactive astrocytes that incorporated BrdU with the labelling period (Fig.4K), in line with previous finding that injury induced astrocytes undergo only one division after injury and after that enter the dormancy (Lange Canhos et al., 2021), also losing the cluster 3/6 identity.

Injury-induced cluster 3/6 astrocytes generate neurospheres

As proliferative cluster 3/6 astrocytes emerge only after injury, we sought to understand their emergence by employing Monocle3 (Cao et al., 2019). Monocle 3 enables the inference of temporal progression and cell fate decisions from scRNA-seq data. Pseudo-temporal ordering revealed the emergence of Astro/RG clusters 3 and 6 as continuum from the homeostatic astrocytes (Fig. 5A). The homeostatic astrocyte clusters 0 gives rise to the cluster 3/6 via

intermediate clusters 2, 4 and 5. Interestingly, these clusters show the features of astrocyte reactivity, such as Gfap upregulation (Fig. 5B), but still do not have the proliferative features (Fig. 4C-D). The cluster 3 cells precede the cluster 6 cells (Fig. 5A), in line with cell cycle analysis, with larger fraction of cluster 3 cells being in S-phase and almost all cluster 6 cells undergoing G2M transition (Fig. 4A-B). This temporal analysis, therefore, suggests that the emergence of proliferative astrocytes after brain injury is a sequential continuum of transcriptional changes. This prompted us to analyze the expression of genes changing along the pseudotemporal trajectory. The typical astrocyte genes (Aldoc, Gja1, S100b, Slc1a2, Slc1a3, Slc7a10) decrease along the trajectory (Fig. 5B). The Gfap first increases, reaches the maximum in cluster 5 and then decreases as the trajectory approaches clusters 3 and 6 (Fig. 5B). In contrast we observed an increasing expression of genes associated with neural progenitors (Ascl1, Dlx2, Olig2, Pcna, Hmgb2, Uhrf1) (Fig. 5C). This data therefore suggests the gradual de-differentiation of protoplasmic astrocytes to reach the plastic, proliferative state. To test this hypothesis, we compared the transcriptomic profile of cluster 3, 6 (proliferative clusters) and cluster 0 (homeostatic cluster, (Suppl. Fig 5A)) to recently published transcriptomes of differentiated (AC1_RNA and AC2_RNA) and dedifferentiated (TRP1_RNA and TRP2_RNA) astrocytes in vitro (Schmid et al., 2016). The gene set enriched in the cluster 3/6 astrocytes was also enriched in the de-differentiated TRP astrocytes, while gene set identifying the homeostatic cluster 0 astrocytes shows enrichment in the homeostatic AC astrocytes (Suppl. Fig.5B). In addition, we compared the transcriptome of Astro/RG clustres with less mature cycling glial progenitors and astrocytes isolated from the postnatal (P4) mouse cerebral cortex (Di Bella et al., 2021). The similarity is assessed using the gene expression scores, defining cycling glial progenitors (cRGs cluster) and two astrocytic clusters (Astro_clust_1 and 2) in the P4 cortex (Suppl. Fig. 5C, Suppl. Table 4). Astrocytic clusters from the postnatal cortex shared similarities with homeostatic Astro/RG clusters, whereas Astro/RG clusters 3 and 6 exhibited resemblances to cycling glial cells (Suppl. Fig.5A, C). This finding further substantiates the hypothesis that astrocytes undergo dedifferentiation towards a less mature state (clusters 3/6) in response to injury.

As the immature neural progenitors and neural stem cells have the capacity to form neurospheres in vitro, we sought to test the capacity of cluster 3/6 cells to generate neurospheres. As Ascl1 marks these astrocytic clusters (Fig. 3B,C; Suppl. Fig. 3), we opted for Ascl1-based genetic fate mapping. Off note, Ascl1 is also expressed in oligodendrocyte progenitors (OPCs) in the mouse cerebral cortex regardless of brain injury. However, as OPCs do not form neurospheres (Buffo et al., 2008), we reasoned that any reporter positive neurospheres would be generated by Ascl1 positive cluster 3/6 astrocyte. For the genetic fate mapping we made use of a Ascl1CreERT2 knock in mouse crossed to the tdTomato reporter mouse line, which expresses the red fluorescent protein tdTomato in Ascl1-expressing cells following tamoxifen treatment (Bottes et al., 2021; Madisen et al., 2010). The cre-mediated recombination was induced 3 and 5 dpi based on the Ascl1 expression in pseudo temporal analysis (Fig. 3C, Fig. 5C), cells were collected at 5dpi and used for the neurospheres assay (Fig. 5D). As expected, we observed neurospheres formation only after brain injury. Importantly, about 60% of all generated neurospheres expressed the tdTomato reporter (Fig. 5 E-H), suggesting that these neurospheres originate from the Ascl1-positive cluster 3/6 astrocytes. Interestingly, all reporter positive neurospheres were unipotent and in the differentiation assay generated only astrocytes. In contrast, reporter negative neurospheres were both uni- and tri-potent in the differentiation assay (Fig. 5G, H). Taken together, we identified the injury-induced de-differentiated population of astrocytes with capacity to form unipotent neurospheres.

Cluster 3/6 astrocytes display transcriptional features of several types of neural progenitors

The cluster 3/6 astrocytes appear to be unipotent in the neurospheres assay but still cluster with zebrafish neural stem cells possessing the capacity to generate neurons. Therefore, we reasoned that comparing their transcriptomes would identify the processes leading to unipotency. We identified 1123 (385 enriched in zebrafish and 738 enriched in mouse) differentially expressed genes (DEG) between zebrafish and mouse cluster 3 (Suppl. Fig. 5D, Suppl. Table 5) and 1089 DEGs (340 enriched in zebrafish and 749 enriched in mouse) in cluster 6 (Suppl. Fig. 5E, Suppl. Table 5). Collectively, zebrafish cells from Astro/RG 3 and 6 clusters exhibited enrichment in Wnt signaling, Notch signaling, G1 to S cell cycle control, ID-signaling and BMP signaling, all signaling pathways that have been implicated in regulation of neurogenesis in both zebrafish and mouse (Suppl. Fig. 5F, G) Conversely, cells from mouse Astro/RG 3 and 6 clusters showed enrichment in metabolic pathways, including oxidative stress, redox pathways, electron transport chain, glycolysis, and gluconeogenesis (Suppl. Fig. 5 F,G), suggesting that mouse cluster 3/6 astrocytes might fail to adopt their metabolic switch from astrocytes relaying on glycolysis to neural progenitors utilizing oxidative phosphorylation. As the specific metabolic programs appear to control the neuronal differentiation and neural stem cell maintenance in the adult mouse neurogenesis (Adusumilli et al., 2021; Beckervordersandforth et al., 2010; Wani et al., 2022), we hypothesized that incomplete transition of cluster 3/6 cells to neural stem cells might be the reason for the observed lack of potency and neurogenesis from cluster 3/6 astrocytes following injury. Therefore, we decided to compare the transcriptome of cluster 3/6 astrocytes and neural progenitors from the sub-ependymal zone in the adult mouse brain. We conducted an integrated analysis by combining single-cell transcriptome data from the SEZ of adult mice with previously collected data from both injured (3 + 5 dpi) and intact cerebral cortex (Fig. 6A). This approach allowed us to identify major cell types, including astrocytes, oligodendrocytes, microglia, transient amplifying progenitors (TAPs), neuroblasts (NBs), and neurons (Suppl. Table 6, Fig. 6B, D). However, the aNSCs share many markers with astrocytes, making it impossible to delineate these two cell types in the integrated analysis (Fig. 6C, D). Therefore, we performed separate analysis focused exclusively on the SEZ condition (Suppl. Fig. 6A). Within this analysis, we identified distinct populations, including quiescent NSCs (qNSCs), activated NSCs (aNSCs), TAPs, and NBs (Suppl. Fig. 6B-D) based on known markers. Additionally, we observed continuous pseudotime trajectories from quiescent NSCs to NBs, reflecting the inherent differentiation process of NSCs (Suppl. Fig. 6E). Furthermore, when we mapped SEZ NSC cells (qNSCs and aNSCs) back to the integrated astrocyte clusters alongside TAPs and NBs (Suppl. Fig. 6F), we confirmed the presence of quiescent NSCs and activated NSCs within the integrated astrocyte clusters, validating their coexistence and affirming the robustness of our analysis.

Furthermore, this allows us to assess the congruence among dedifferentiated Astro/RG 3 and 6 clusters cells, TAPs, and NBs within the integrated SEZ+cortex analysis. In line with absence of restorative neurogenesis in the cortex following injury (Buffo et al., 2008), we did not observe any cells from the cerebral cortex in the cluster containing SEZ neuroblasts, while clusters containing stem cells and TAPs contained cells from SEZ, intact and injured cortex (Fig. 6E). Furthermore, cross-referencing identities confirmed presence of cluster 3/6 cells in several clusters of with astrocyte identity Ast_4, Ast_6 and Ast_7 (Fig. 6F). To our surprise, we observed that of 20 % of cluster 6 cells cluster with SEZ derived TAPs_1 (Fig. 6F, G). Importantly, the TAPs_1 cluster did not contain any cells from the intact cerebral cortex (Fig. 6F), suggesting that this cellular state is injury induced. This prompted us to compare the transcriptome of the cluster 3/6 cells and neurogenic lineage cells identified in the SEZ only analysis following cell

cycle gene regression. Indeed, we observed that cluster 3/6 cells show the highest transcriptional similarity to the clusters of TAPs (Fig. 6H, I). Taken together, our analysis suggests that the injury induced, de-differentiated cluster 3/6 astrocytes spread along neurogenic lineage acquiring features of several progenitor types.

Injury-induced, plastic astrocytes differentiate to TAPs-like state

The distribution of cluster 3/6 cells along the neurogenic lineage, prompted us to delineate their differentiation path using pseudotime trajectory and diffusion map analyses (Figure 7A and Suppl. Fig. 7A, B). To differentiate between cortex and SEZ cells in the integrated object, the pseudotime was performed within the integrated object but considering either only SEZ or only cortical cells (Fig. 7A-C). As expected, the differentiation trajectory for SEZ cells started at cluster containing qNSCs, went via aNSCs-containing cluster to TAP containing clusters and ended up in the neuroblasts-containing cluster (Fig. 7B). Interestingly, we do not observe the heterogeneity represented by different clusters only in NSCs, but also in the TAP population. The TAPs_3 cluster transitioned to NBs, while TAPs_2 and TAPs_1 showed higher enrichment for proliferation markers (Figure 7B, Suppl. Fig. 7F). In the cortex, pseudotime trajectory, analysis unveiled a shift from homeostatic astrocytes to reactive astrocytes and subsequently to the TAPs_1 cluster (Fig. 7C). Remarkably, based on trajectory analysis, TAPs_1 cortical cells were not found to contribute to the trajectory of neuroblasts clusters (Fig. 7A-C). To confirm these state transitions by independent method, we performed diffusion map analysis (Suppl. Fig. 7A, B). In the SEZ, we found three distinct states corresponding to NSCs (q/a), TAPs and NBs with transitions identical to the pseudotime analysis (Suppl. Fig. 7A). In the cortex, we also identified three clusters of cells corresponding to homeostatic astrocytes, reactive astrocytes, and TAPs (Suppl. Fig. 7B), further supporting an emergence of TAP-like state from the homeostatic astrocytes via reactive astrocyte cluster that is similar but not identical to aNSCs following brain injury.

The SEZ and cortical trajectories diverged at the level of astrocytic cluster Ast_4 (Fig. 7A). DEG analysis of SEZ and cortical cells contributing to Ast_4 showed an enrichment of GO terms related to cilium movement, pattern specification processes, epithelial cilium movement, and protein refolding in the SEZ cells (Fig.7D). These processes are known to be associated with stem cell differentiation and renewal (Moore et al., 2015; Yanardag & Pugacheva, 2021). Conversely, Ast_4 cells from the injured cortex exhibited enrichment in GO terms such as inflammatory response, response to virus, innate immune response, and interferon beta response (Fig.7D). As these are the terms linked to the astrocyte reactivity (Koupourtidou et al., 2024), this suggests that the cells from the injured cortex did not completely downregulate inflammatory, injury-induced program and fail to establish neural stem cell maintenance network. This is in line with the observation that injury induced astrocyte plasticity diminishes after 7 days (Buffo et al., 2005, 2008). Moreover, the SEZ trajectory transits from the Ast_4 directly to the TAP clusters, while the cortical trajectory contains one additional astrocytic cluster, the cluster Ast_6 (Fig. 7A-C). The direct comparison of cortical cells from the Ast_4 and Ast_6 clusters revealed an enrichment of GO terms related to inflammatory response (interferon-beta response, defense response to virus) in the Ast_4 cells (Fig.7E). These findings suggest that the additional astrocytic state detected in the cortical trajectory could be due to longer time that these cells need to downregulate the inflammatory processes. Once the inflammatory processes are downregulated, they could proceed further to the TAP state (TAPs_1).

Injury-induced TAPs fail to upregulate neurogenic fate determinants

The progression towards TAP states was associated with the expression of typical TAP markers such as Ascl1, Dcx, Olig1, Olig2, and Mki67 (Suppl. Fig.7F, G) in both pseudotime trajectories. Additionally, we observed a decline in the expression of astrocytic markers (e.g., Sox9 and Slc1a2; Suppl. Fig.7 F, G) within these clusters as they transit into TAP-like state. The GO term analysis revealed that TAP clusters (TAPs_1 and TAPs_3) activate processes linked to metabolism, replication, post-translational gene expression regulation, and translation (Fig. 7F), in line with reported need for metabolic changes and translation regulation along the neurogenic lineage (Adusumilli et al., 2021; Baser et al., 2017, 2019; Beckervordersandforth et al., 2017; Knobloch et al., 2017; Wani et al., 2022). However, the cortical cells from the TAPs cluster were not observed to continue along the neurogenic lineage towards neuroblasts (Fig. 7C). Therefore, we conducted the DEG analysis between the neurogenic TAP_3 from the SEZ and cortical TAP_1 cells (TAPs without the transition to the neuroblasts) (Fig.7G, Suppl. Table 7). Our analysis revealed that injury-induced TAP-like clusters still expressed glial-associated genes (e.g., Gfap, S100a1, S100a6, Olig1, Lgals1, Igfbp2,) as well as NSCs markers (HopX) (Fig. 7H), implicating that they fail to completely erase their previous states. Moreover, we observed that they did not upregulate typical neurogenic genes (Sox4, Sox11, Nfib, Dlx1, Meis2, Ascl1, Pou3f2) that are however upregulated in the SEZ TAP trajectory (Fig.7H). Moreover, the cortical TAP_1/TAP_2 cluster cells express the high levels of genes indicative of Notch pathway activation (Suppl. Fig. 7 C-E, Suppl. Table 8). Importantly, these levels are comparable with the Notch activity levels in the bona fide neural stem cell clusters (Suppl. Fig. 7 D, E). This is line with findings that Notch activity inhibit progression of neural stem cells towards neurogenic progenitors (Imayoshi et al., 2010)and reports that inhibition of Notch in the astrocyte-derived cells after brain injury allows their differentiation to neurons (Zamboni et al., 2020). The analysis of expression of specific lineage genes was further confirmed by the unbiased GO term analysis. Genes specifically expressed in the TAPs_3 cluster were enriched in the processes related to neurogenesis, while genes specifically enriched in the TAPs_1 cluster were related to inflammatory response, monosaccharide catabolic process, chromosome segregation, and metal ion transport (Fig. 7G). Taken together, our analysis proposes that injury induces the de-differentiation of post-mitotic astrocytes towards the state similar to aNSC-like state. However, these cells fail to generate properly specified TAP lacking the expression of critical neurogenic genes and, therefore, hindering further lineage progression towards neuroblasts.

Discussion

Multi-species data integration

Cell linage barriers largely define the cellular reaction to the different brain pathologies, including the stab wound injury (Gascon et al., 2017; Ninkovic & Götz, 2018). Pathology induced crunching of these cellular barriers is the basis for the glial cell reactivity following brain pathology as well as their experimental trans-differentiation for the repair purposes. Importantly, glial cells show different level of the barrier plasticity with astrocytes showing the most drastic change. Namely, a subset of originally post-mitotic astrocytes re-enter the cell cycle, express NSCs markers, gain capacity to self-renew and generate multipotent neurospheres in vitro (Sirko et al., 2013). Such a dramatic change in cell and molecular biology of astrocytes in response to insult brings and important question about the functional importance of this astrocytic population. The main caveat in addressing this question is the prospective isolation of these cells. Indeed, several studies identified the plastic, proliferative astrocytes

retrospectively in both animal model organisms (Bardehle et al., 2013; Lange Canhos et al., 2021; Sirko et al., 2015) and postmortem human brain (Sirko et al., 2023), making it difficult to specifically modify their reaction after injury and address their function. The recent advances in the single cell profiling technologies did not really resolve this problem despite the identification of enormous astrocytes heterogeneity in both healthy and pathological conditions (Batiuk et al., 2020; Bugiani et al., 2022; Clarke et al., 2018; D'Elia et al., 2023; R. T. Han et al., 2021; Holt, 2023; Liddelow et al., 2017; Matias et al., 2019; Schober et al., 2022), even including the identification of proliferative astrocytes with stem cell characteristics in the intact diencephalon (Ohlig et al., 2021). One possible explanation for this could be that the currently available methods to prepare the single cell suspension specifically miss this astrocytic population, as the retrospective characterization of de-differentiated, proliferative astrocytes revealed the particular localization of these cells to the juxtavascular compartment (Bardehle et al., 2013). In addition, the proliferative astrocytes are the small cellular population that could be missed due to the lack of the power of currently available datasets (R. T. Han et al., 2021). To overcome these limitations, we have recently developed the cell isolation method for single cell transcriptome analysis (Koupourtidou et al., 2024) that recovers most of the glial cells and reveals more glial heterogeneity compared to so far available datasets (Koupourtidou et al., 2024). Moreover, we paired this analysis with the trans-species data integration to increase the power of our analysis. Indeed, this approach led to the identification of the specific cluster composed largely of zebrafish ependymoglia with stem cell properties. In addition, this cluster contained a small fraction of astrocytes from the injured tissue in line with the hypothesis that the de-differentiated astrocytes could in the cerebral cortex could be observed only after brain injury (Sirko et al., 2013). Importantly, a separate cellular cluster of proliferating plastic astrocytes could not be identified using only the dataset from the mouse brain as the cells were distributed amongst different cellular clusters (Suppl. Fig. 4), supporting the versatility of our approach. Importantly, the trans-species data integration relays on a set of genes with uniquely identified orthologues in zebrafish and mouse genome that contains about a half of all genes identified in these two species. However, this rudimentary gene set does not compromise the identification of the cellular clusters and their similarities as we identify the same basic cell types containing mouse cells in both integrated and original datasets. Moreover, the set of most variable genes identifying the cell types in two datasets do not differ significantly. This makes our approach very promising for the evolutionary comparisons and we expect it to be even more versatile by comparing more closely related species such as different mammalian species. Although, the basic analysis and the identification of different cellular states is not compromised in our analysis, we cannot exclude that a particular and cell type specific signaling pathways and regulatory mechanisms are not affected. Therefore, we trace back cells from the integrated data set to the original dataset and use the original gene-set containing all detected genes to address the regulatory pathways in representative populations.

Molecular features of de-differentiated astrocytes

The de-differentiated astrocytes are the rare population appearing exclusively after a particular type of insult including the TBI, bleeding, stroke or epilepsy (Sirko et al., 2013, 2023). Importantly the astrocyte proliferation is the most prominent feature of the plastic astrocytes (Dimou & Gotz, 2014). The gain of plasticity in this set of astrocytes is associated with changes in their cytoarchitecture and up-regulation of intermediate filament GFAP (Escartin et al., 2021; Patani et al., 2023). However, these morphological changes are shared with a number of astrocytic populations that do not gain the proliferation capacity (Sirko et al., 2013). Moreover, a specific manipulation of the innate immunity pathways reduced the astrocytes proliferation after barin injury without the change in their morphology or GFAP levels (Koupourtidou et al., 2024). This

brings an interesting concept that the different aspects of the astrocyte reactivity are controlled by the different regulatory networks. Our analysis revealed an enrichment of a number of cell specific determinants (Hmgb2, Uhrf1, Ascl1, and Rpa2) in the de-differentiated astrocytic cluster known for their roles in neural stem cell dynamics, neurogenesis, DNA methylation regulation, and DNA replication/repair (Bostick et al., 2007; Kimura et al., 2018; Păun et al., 2023; Ramesh et al., 2016; Shi et al., 2010; Zhou & Luo, 2013). These molecular features allowed the de-differentiated astrocytes to cluster with zebrafish neural stem cells. However, in stark contrast to zebrafish ependymoglia (neural stem cells), the de-differentiated astrocytes never give rise to any neurons despite up-regulation of these neurogenic genes. Our integration now allowed us to directly compare cells from zebrafish and mouse within the same cluster. This analysis revealed a differential enrichment of known neurogenic signaling pathways: the Notch, IL-6 and Wnt signaling both playing an important role in controlling neurogenesis in both zebtrafish and mouse developing and adult brain (Arredondo et al., 2020; Dray et al., 2021; Kageyama et al., 2009; Storer et al., 2018; Westphal et al., 2022). Indeed, the Wnt pathway activation in radial glia after optic tectum injury, leading to RG proliferation and neurogenesis in adult zebrafish has already been described (Shimizu et al., 2018). These findings are very well in line with the capacity of different ECM components to induce the de-differentiation of astrocytes isolated from the intact brain in vitro, supporting a concept that inductive signal in the injured environment is missing in the mouse brain. Moreover, the de-differentiated astrocytes were still enriched in the glycolytic processes and processes involved in the oxidative stress. The oxidative stress has been associated with the trans-differentiation of astrocytes to neurons (Gascon et al., 2015, 2017). The fate conversion of astrocyte to neurons requires the metabolic switch to oxidative phosphorylation and the mouse de-differentiated astrocytes might fail do so and as consequence die. In contrast, the zebrafish stem cells could change their metabolism and generate new neurons in response to injury. This is in line with the transplantation experiments of reactive astrocyte-derived neurospheres into the SEZ that failed to yield neurons (Shimada et al., 2012), suggesting a cell intrinsic block in the lineage.

A subset of astrocytes goes through incomplete neurogenic lineage in response to injury

As the comparison of zebrafish and mouse cells from the de-differentiated clusters 3/6 suggests the intrinsic barrier for the neurogenesis from de-differentiated astrocytes, we integrated these de-differentiated astrocytes to the bone fide neurogenic linage from the subependymal zone. To our surprise, at least a proportion of the de-differentiated cells clustered with TAPs. Importantly, these progenitors have been up-regulating transcription factors such as Olig2 involved in the gliogenesis (Nishiyama et al., 2021), suggesting their glial identity. Indeed, such gliogenic TAPs have been reported in the neurogenic zone as well (Colak et al., 2008; Hack et al., 2005; Malatesta et al., 2003; Ortega et al., 2013). These data are in line with our fate mapping experiments using Ascl1:CerERT2 mouse line. According to these experiments, the Ascl1-positive de-differentiated astrocytes generate unipotent, gliogenic neurospheres. The analysis of the de-differentiation trajectory of reactive astrocytes along with neurogenic lineage revealed that they go through the activated stem cell-like state in order to generate the TAP-like state. This stem cell like state could then be the possible source of multipotent neurospheres generated from the de-differentiated astrocytes (Buffo et al., 2008; Sirko et al., 2013). Interestingly, the comparison between the stem cell like astrocytes and bona fide astrocytes revealed an enrichment of the inflammatory genes in the stem cell like astrocytes suggesting that these could be interfering with the neurogenic trajectory. Indeed the TAP-like cells generated from these inflammatory signature enriched astrocytes failed to up-regulate the typical neurogenic fate determinants such as Sox4 and Sox11. The upregulation of these factors downstream of the chromatin remodeling factors such as Brg1 is necessary for the completion

of the neurogenic cascade and generation of neuroblasts (Ninkovic et al., 2013). Instead, the Brg1-deficient cells generate gliogenic oligodendrocyte progenitors similar to the de-differentiated astrocytes. One possibility is that the neurogenic fate is not fully induced or maintained due to increased level of Notch seen in these TAP-like cells of injured cortex (Santopolo et al., 2020; Zamboni et al., 2020). Notch signaling depletion in cortical astrocytes following TBI has been demonstrated to trigger a neurogenic response (Zamboni et al., 2020), possibly linking the intrinsic fate barriers with the inductive signals from the injured environment.

Methodology

Source of transcriptome data

We harnessed single-cell transcriptome datasets from our prior investigations, specifically Zebrafish data by Zambusi et al., (GSE179134: Telencephalon, Wt Intact; Telencephalon, Wt 3 dpi; Telencephalon, Wt 7 dpi), Mouse data by Koupourtidou et al., (GSE226207: Intact, bio rep 1; Intact, bio rep 2; 3dpi_CTRL, bio rep 1; 3dpi_CTRL, bio rep 2; 5dpi_CTRL, bio rep 1; 5dpi_CTRL, bio rep 2; 5dpi_CTRL, bio rep 3), Mouse adult Subependymal Zone (SEZ) data from [#GSE], and RNA-seq data pertaining to astrocyte dedifferentiation from the study conducted by Schmid et al. in 2016 (GSE75589: AC1-RNA; AC2-RNA; TRP1-RNA; TRP2-RNA). Additionally, we incorporated mouse postnatal day 4 cortex data from Di Bella et al. in 2021 (GSE153164: RNA-seq P4). For comparison of integration analysis with different mouse lineages scRNA-seq data of PBMCs (Peripheral Blood Mononuclear Cells) was sourced PBMCs from C57BL/6 mice (v1), Single Cell Immune Profiling Dataset by Cell Ranger 3.1.0, 10x Genomics, (2019, July 24).

Transcriptome data analysis

Datasets from both Mouse and Zebrafish under both injured and intact conditions were subjected to initial processing using Seurat package in R. A Seurat object was constructed using the unique molecular identifier (UMI) count matrix with minimum cells 3 and min genes 200 as cutoff. In both species datasets, cells exceeding 20% mitochondrial reads, featuring RNA counts beyond 6000 or below 200, or having RNA counts less than 40000 were systematically excluded to filter low-quality cells and potential outliers, ensuring the reliability of subsequent analyses. The potential doublets were removed using DoubletFinder (version 2.0.3) package. Normalization and identification of highly variable features were carried out using Seurat default parameters. The heterogeneity associated with the cell cycle genes, mitochondria and ribosomal percentage were regressed out using the ScaleData function taking features as all the genes. Subsequently, a Principal Component Analysis (PCA) was conducted on the resulting matrix. This PCA output was then utilized for Louvain cell clustering and Uniform Manifold Approximation and Projection (UMAP) visualization, providing a comprehensive view of the cellular landscape at 0.6 resolution and dimension 1:15. To identify the differentially expressed genes (DEGs) that serve as cluster biomarkers, we used the FindAllMarkers function of the Seurat package. The DEGs specific clusters between mouse and zebrafish was visualized using function do_VolcanoPlot of SCpubr package. In addition, we scored the known cell-type-specific markers using the Seurat AddModuleScore function and visualized the results using the FeaturePlot function of Seurat and the EnrichHeatmap function of the ScPurb package. The unintegrated mouse and zebrafish species datasets were annotated based on published studies by Zambusi et al. and Koupourtidou et al., respectively. Similarly, the mouse SEZ scRNA seq (at resolution 0.8 and dimensions 1:20), postnatal day 4 cortex (at resolution 0.7 and dimensions 1:10) and PBMCs data (at resolution 0.8 and dimensions 1:20), was analyzed and visualized.

The RNA seq data of astrocyte dedifferentiation was procured from iDEP 0.96 tool (http://149.165.154.220/idep/) to get log normalized transcript which was further visualized by scaling using pheatmap (version 1.0.12) R package.

scRNA-seq Integration analysis

We conducted trans-species integration of single-cell RNA sequencing data from both mouse and zebrafish using the Seurat package. Seurat v4 uses canonical correlation analysis (CCA) to identify correlated variables between datasets, with mutual nearest neighbors (MNN) serving as anchor points for integration. Homologous genes between mouse and zebrafish were identified using homologene R packages (version 1.4.68.19.3.27), and a custom 'RenameMyGene' function was created to ensure consistent gene nomenclature, taking mouse as a reference. To perform integration, we identified common anchors between the datasets of both species using Seurat's FindIntegrationAnchors. These anchors were used to integrate the two datasets with the IntegrateData function. Subsequently, the integrated dataset underwent dimensionality reduction PCA, clustering with the Louvain algorithm (at resolution 0.7 and dimensions 1:10), and visualization via UMAP. Differentially expressed features (cluster biomarkers) were identified using the FindAllMarkers function. Similarly, the PBMCs data from mouse integrated using Seurat with Intact and injured cortex of mouse and telencephalon of zebrafish. Furthermore, to enable comparative integrated analysis, we utilized the Harmony package (version 1.1.0) in R, which employs an iterative method for integration, following the guidelines outlined at https://portals.broadinstitute.org/harmony/articles/quickstart.html using similar parameter as Seurat dimension (at resolution 0.7 and dimensions 1:10). The Integration of the cortex and the SEZ regions of mouse was also performed and analyzed in similar way (at resolution 0.8 and dimension 1:30) in order to access the similarities of identified dedifferentiated astrocytic cluster with bonafide neuronal stem/progenitor cells of SEZ.

Cell distribution plots

To visualize the cell distribution between/within conditions or species or samples, we used various plots like bar plots, alluvial plots, chord diagram plots, and pie charts; generated in Rstudio (version 4.2.3) using ggplot2 (version 3.4.2), DittoSeq using dittoBarPlot function (version 1.8.1) and SCpubr (do_ChordDiagramPlot function) (version 1.1.2) from Seurat object in R. The color palette used in these plots was generated by the Rcolorbrewer (version 1.1-3) package in R.

Relative similarities heatmap

We assessed the relative similarity between two scRNA-seq datasets using ELeFHAnt (https://github.com/praneet1988/ELeFHAnt) in R. We used the DeduceRelationship function, which predicts the relationship between the datasets based on their gene expression profiles. We used the following default parameters: varfeatures = 2000 (most variable features to use for dimensionality reduction and clustering), classifier = SVM (algorithm to train a classifier on a subset of the data and test it on another subset; shown ~85% accuracy), and downsample = 200 (randomly samples 200 cells from each dataset to balance the class sizes and reduce the computational cost). The DeduceRelationship function returns a score that indicates how similar the two datasets are, ranging from 0 (no similarity) to 1 (high similarity). These scores can be used to identify cell types that are similar between the two datasets and to compare gene expression patterns across different cell types.

Pseudotime trajectory and diffusion map analysis

The pseudotime trajectory analysis was performed using monocle3 as described https://cole-trapnell-lab.github.io/monocle3/ in Rstudio. For the analysis we first imported the Seurat object clusters into Monocle3 as cds object. The cells were then ordered along a pseudotime trajectory using the orderCells function, taking homeostatic clusters (in context to integrated astrocytic clusters) and qNSC (in context to integrated SEZ clusters). We visualized the pseudotime trajectory of cells using plot cells function and color pallet by RColorBreweR package. Additionally, we utilized the plot_gene_in_pseudotime function to discern patterns in gene expression along the trajectory for a specific set of genes. To identify the major cell types or states in different conditions, we performed a diffusion map analysis on the Seurat clusters using the "DiffusionMap" function from the destiny package (version 3.1.1) in R with default parameters. We visualized the diffusion map using a scatter plot against the first diffusion component, which captures the main variation of the data. This allowed us to show how cells transition between different states in different conditions, where each point represents a cell and the color indicates the clusters.

Tracing back cell identity

To trace back the origin of cells from clusters from one object to an integrated object, we extracted the cells of clusters using the WhichCells function of Seurat. These cells were preprocessed using the substring function of R to match the UMI of cells. To visualize the cross-referenced cells, we utilized the highlight.cells function from DimPlot of Seurat. We used DittoBarPlot from Dittoseq to quantify and plot the number of cross-referenced cells with respect to clusters.

Biological Processes and WIKI Pathway Analysis

We used Metascape 3.5 (https://metascape.org), an online tool, to perform biological processes and WIKI pathway analysis on our gene list. We uploaded our gene list using the mouse species and opted for custom analysis, where we specified the following parameters: 1) The annotation was performed using the default databases, including the Gene Ontology (GO) Biological Process and the WIKI Pathway, 2) The enrichment analysis was performed using a hypergeometric test with a p-value cut-off of 0.01, a minimum overlap of 3 genes, and a minimum enrichment of 1.5 for GO biological process and WIKI pathway, and 3) visualization was opted using heatmaps, which showed the expression levels of the genes in each term or pathway across conditions or clusters.

Animals

All surgeries were performed on 8-12 week old male mice (Mus musculus), housed, and handled under the German and European guidelines for the use of animals for research purposes. Room temperature was maintained within the range of 20–22 °C, while the relative humidity ranged between 45–55%. The light cycle was adjusted to 12 h light:12 h dark period. Room air was exchanged 11 times per hour and filtered with HEPA-systems. All mice were housed in individually ventilated cages (2-5 individuals per cage) under specified-pathogen-free conditions with food (standard chow diet) and water ad libitum. The cages were equipped with nesting material, a red corner house and a rodent play tunnel. Soiled bedding was removed every 7 days. For ICH experiments wild-type C57BL/6J animals (strain #000664) were used, while neurospheres assay was performed in the Ascl1CreERT2 knock in mouse crossed to the tdTomato reporter mouse line (Bottes et al., 2020; Madisen et al., 2010). All animal work was performed in accordance with the German and European Union regulations and approved by the Institutional Animal Care and Use Committee (IACUC) and the Government of Upper Bavaria (AZ: ROB-55.2-2532.Vet_02-20-158). Anesthetized animals received a stab wound

lesion in the cerebral cortex by inserting a thin knife (19G, Alcon #8065911901) into the grey matter using the following coordinates from Bregma: RC: -1.2; ML: 1-1.2 and from Dura: DV: -0.6 mm. To produce stab lesions, the knife was moved over 1mm back and forth along the anteroposterior axis from -1.2 to -2.2 mm as described before32. Animals were euthanized 3 and 5 days after the injury (dpi) by transcardial perfusion (for more details see section tissue preparation). For the induction of Cre-mediated recombination in Ascl1CreERT2x tdTomato reporter mice, tamoxifen (40 mg/ml, Sigma #T5648) was administered orally (20G, Merck #CAD9921). Animals received tamoxifen twice (400 mg/kg per treatment).

BrdU labelling

Proliferating cells were labeled in vivo via water administration of the thymidine analog 5-bromo-2'-deocyuridine (BrdU). To this end, BrdU (1 mg/mL) and sucrose (1 %) were added to the animals' drinking water starting from 24h after injury.

Tissue preparation

Mice were deeply anesthetized and transcardially perfused with phosphate-buffered saline (PBS) followed by 4% paraformaldehyde (PFA) (wt/vol) dissolved in PBS. Brains were postfixed in 4% PFA overnight at 4 °C, washed with PBS and cryoprotected in 30% sucrose (Carl Roth #4621.2) at 4 °C for ICH. For RNAscope® in situ hybridization (ISH), brains were incubated in gradually concentrated sucrose solutions at 4 °C,starting with 10 % sucrose in 1X PBS, followed by 20 % and finally 30 % sucrose in 1XPBS. brains were embedded in frozen section medium Neg-50 (Epredia #6502), frozen and subsequently sectioned using a cryostat (Thermo Scientific CryoStar NX50). Coronal sections were collected either at a thickness of 20 µm on slides for RNAscope (Epredia #J1800AMNZ) or 40 µm for free-floating immunohistochemistry.

Tissue preparation

For immunohistochemistry, sections were blocked and permeabilized with 10% normal goat serum (NGS, vol/vol, Biozol #S-1000)/donkey serum (NDS, vol/vol, Sigma-Aldrich #566460) and 0.5% Triton X-100 (vol/vol, Sigma-Aldrich #T9284) dissolved in 1xPBS. The same solution was used to dilute the primary antibodies. Primary antibodies were incubated with sections overnight at 4 °C. Following primary antibodies were used: anti-RPA32/RPA2 (rabbit IgG, 1:250, Abcam, ab76420), anti-HMGB2 (rabbit IgG, 1:1000, Abcam, ab67282), anti-RFP (rabbit IgG, 1:1000, Rockland/Biomol, 600-401-379), anti-BrdU (rat IgG2a, 1:500, Abcam, ab6326), anti-GFAP (goat IgG, 1:250, Abcam, ab53554); anti-DCX (guinea pig, 1:1000, Merck/Millipore, AB2253), anti-O4 (mouse IgM, 1:50, Sigma, O7139). Sections were washed with PBS and incubated with secondary antibodies dissolved in 1xPBS solution containing 0.5% Triton X-100 for 2 h at room temperature. Following secondary antibodies were used: goat anti-mouse IgG1 Alexa Fluor™ 488 (1:1000, Thermo Fisher Scientific A21121), goat anti-rabbit IgG Alexa Fluor™ 546 (1:1000, Thermo Fisher Scientific A11035), goat anti-rat IgG Alexa Fluor™ 647 (1:1000, Thermo Fisher Scientific A21247), donkey anti-goat IgG Alexa Fluor™ 488 (1:1000, Thermo Fisher Scientific A11055), donkey anti-rabbit IgG Alexa Fluor™ 594 (1:1000, Thermo Fisher Scientific A21207), Donkey anti-Rabbit IgG Alexa Fluor™ 647 (1:1000, Thermo Fisher Scientific A31573), goat anti-mouse IgG2a A488 (1:1000, Thermofisher A-21131). For nuclear labelling, sections were incubated with DAPI (final concentration of 4 µg/mL, Sigma #D9542) for 10 min at room temperature. Stained sections were mounted on glass slides (Epredia #AG00000112E01MNZ10) with Aqua-Poly/Mount (Polysciences #18606). For BrdU detection, sections were pre-treated with HCl (4 N), followed by three washes using borate buffer (0.1 M) and another three washes with 1XPBS before incubation with primary antibody solution. For RPA2 staining, antigen retrieval using Dako TRS (Agilent, Dako S1699) was performed prior to

primary antibody incubation. Dako solution was first diluted 1:10 in distilled water (diH2O) and then prewarmed at 65 °C for 15-20 minutes. Sections were incubated in the diluted DAKO solution at 95 °C for 20 minutes followed by another 15 minutes at 65 °C to slowly cool down. After cooling-down to room temperature, sections were washed three times in 1X PBS and incubated in primary antibody solution.

In situ hybridization

RNA in situ hybridization was performed using RNAscope® Multiplex Fluorescent Reagent Kit (ACD, 323110) according to the manufacturer's instructions. Briefly, brain sections were ethanol-dehydrated (Carl Roth #9065.4), treated with H2O2 (ACD, 322381) and protease-permeabilized for 20 min at 40 °C. Brain sections were then incubated for 2 h at 40 °C using the following probes: RNAscope® Probe –Mm-Uhrf1 (Bio-Techne 559891) and RNAscope® Probe –Mm-Ascl1-CDS-C3 (Bio-Techne 476321-C3). Signal was amplified according to the manufacturer's instructions (User manual Cat.Nr: 320293, Fluorophore Opal 520: Akoya Biosciences FP1488001KT). Following washings steps with 1xPBS, sections were fixed for 15 min in 4% PFA at 4 °C and subjected to immunohistochemistry analysis as described above.

Neurosphere assay

Neurosphere cultures were prepared as previously described (Buffo et al., 2008) using a volume of tissue punched (B0.35 cm) from the lesioned areas of the somatosensory cerebral cortex obtained from the injured brains 5 days after injury. After removal of meninges and white matter, grey matter cells were plated at a density of one cell/ 10 microliters (clonal density) in 500 microliters of neurosphere medium with FGF2 and EGF (both at 20 ng/ml, Invitrogen). The number of neurospheres and the expression of the reporter was assessed after 14 days. The individual neurospheres were assessed differentiation capacity by plating individual neuroshpares on the PDL-coated coverslips as described previously (Buffo et al., 2008).

Image acquisition and processing

Confocal microscopy was performed at the core facility bioimaging of the Biomedical Center (BMC) with an inverted Leica SP8 microscope using the LASX software (Leica). Overview images were acquired with a 10x/0.30 objective, higher magnification pictures with a 20x/0.75, 40x/1.30 or 63x/1.40 objective, respectively. Image processing was performed using the NIH ImageJ software (version 2.1.0/1.53f). a minimum of three sections per animal was analyzed for five animals in total. In each section, an area of 300 µm was selected around the injury (150 µm on either side) and the number of positive cells in all individual z-planes of the optical stack was quantified using the Fiji plug-in tool 'Cell Counter'. Cell counts quantified within different sections were averaged per animal and the graph was generated using GraphPad Prism (v.9.4.1). Data are shown as mean ± standard error of the mean (SEM) with individual data points representing different animals.

References

Adusumilli, V. S., Walker, T. L., Overall, R. W., Klatt, G. M., Zeidan, S. A., Zocher, S., Kirova, D. G., Ntitsias, K., Fischer, T. J., Sykes, A. M., Reinhardt, S., Dahl, A., Mansfeld, J., Rünker, A. E., & Kempermann, G. (2021). ROS Dynamics Delineate Functional States of Hippocampal Neural Stem Cells and Link to Their Activity-Dependent Exit from Quiescence. *Cell Stem Cell*, *28*(2). https://doi.org/10.1016/j.stem.2020.10.019

Anderson, M. A., Burda, J. E., Ren, Y., Ao, Y., O'Shea, T. M., Kawaguchi, R., Coppola, G., Khakh, B. S., Deming, T. J., & Sofroniew, M. V. (2016). Astrocyte scar formation AIDS central nervous system axon regeneration. *Nature*. https://doi.org/10.1038/nature17623

Arredondo, S. B., Valenzuela-Bezanilla, D., Mardones, M. D., & Varela-Nallar, L. (2020). Role of Wnt Signaling in Adult Hippocampal Neurogenesis in Health and Disease. In *Frontiers in Cell and Developmental Biology* (Vol. 8). https://doi.org/10.3389/fcell.2020.00860

Bardehle, S., Kruger, M., Buggenthin, F., Schwausch, J., Ninkovic, J., Clevers, H., Snippert, H. J. J., Theis, F. J. J., Meyer-Luehmann, M., Bechmann, I., Dimou, L., Gotz, M., Krüger, M., Buggenthin, F., Schwausch, J., Ninkovic, J., Clevers, H., Snippert, H. J. J., Theis, F. J. J., … Götz, M. (2013). Live imaging of astrocyte responses to acute injury reveals selective juxtavascular proliferation. *Nat Neurosci*, *16*(5), 580–586. https://doi.org/10.1038/nn.3371

Baser, A., Skabkin, M., Kleber, S., Dang, Y., Gülcüler Balta, G. S., Kalamakis, G., Göpferich, M., Ibañez, D. C., Schefzik, R., Lopez, A. S., Bobadilla, E. L., Schultz, C., Fischer, B., & Martin-Villalba, A. (2019). Onset of differentiation is post-transcriptionally controlled in adult neural stem cells. *Nature*, *566*(7742), 100–104. https://doi.org/10.1038/s41586-019-0888-x

Baser, A., Skabkin, M., & Martin-Villalba, A. (2017). Neural Stem Cell Activation and the Role of Protein Synthesis. *Brain Plasticity*. https://doi.org/10.3233/bpl-160038

Batiuk, M. Y., Martirosyan, A., Wahis, J., de Vin, F., Marneffe, C., Kusserow, C., Koeppen, J., Viana, J. F., Oliveira, J. F., Voet, T., Ponting, C. P., Belgard, T. G., & Holt, M. G. (2020). Identification of region-specific astrocyte subtypes at single cell resolution. *Nature Communications*, *11*(1). https://doi.org/10.1038/s41467-019-14198-8

Baumgart, E. V. V, Barbosa, J. S. S., Bally-Cuif, L., Gotz, M., Ninkovic, J., Götz, M., & Ninkovic, J. (2012). Stab wound injury of the zebrafish telencephalon: a model for comparative analysis of reactive gliosis. *Glia*, *60*(3), 343–357. https://doi.org/10.1002/glia.22269

Beckervordersandforth, R., Ebert, B., Schaffner, I., Moss, J., Fiebig, C., Shin, J., Moore, D. L., Ghosh, L., Trinchero, M. F., Stockburger, C., Friedland, K., Steib, K., von Wittgenstein, J., Keiner, S., Redecker, C., Holter, S. M., Xiang, W., Wurst, W., Jagasia, R., … Lie, D. C. (2017). Role of Mitochondrial Metabolism in the Control of Early Lineage Progression and Aging Phenotypes in Adult Hippocampal Neurogenesis. *Neuron*, *93*(3), 560-573 e6. https://doi.org/10.1016/j.neuron.2016.12.017

Beckervordersandforth, R., Tripathi, P., Ninkovic, J., Bayam, E., Lepier, A., Stempfhuber, B., Kirchhoff, F., Hirrlinger, J., Haslinger, A., Lie, D. C. C., Beckers, J., Yoder, B., Irmler, M., & Götz, M. (2010). In vivo fate mapping and expression analysis reveals molecular hallmarks of prospectively isolated adult neural stem cells. *Cell Stem Cell*. https://doi.org/10.1016/j.stem.2010.11.017

Behrendt, G., Sirko, S., Tripathi, P., Costa, M., Bek, S., Heinrich, C., Tiedt, T., Colak, D., Dichgans, M., Fischer, I. R., Plesnila, N., Staufenbiel, M., Haass, C., Tsai, L., Fischer, A., Grobe, K., Dimou, L., & Götz, M. (2012). The stem cell response of reactive glia: differential regulation in diverse injury paradigms reveals the key role of sonic hedgehog. *Cell Stem Cell*, *In Revisio*.

Berninger, B., Guillemot, F., & Gotz, M. (2007). Directing neurotransmitter identity of neurones derived from expanded adult neural stem cells. *Eur J Neurosci*, *25*(9), 2581–2590. https://doi.org/10.1111/j.1460-9568.2007.05509.x

Bocchi, R., Masserdotti, G., & Götz, M. (2022). Direct neuronal reprogramming: Fast forward from new concepts toward therapeutic approaches. In *Neuron* (Vol. 110, Issue 3). https://doi.org/10.1016/j.neuron.2021.11.023

Bostick, M., Jong, K. K., Estève, P. O., Clark, A., Pradhan, S., & Jacobsen, S. E. (2007). UHRF1 plays a role in maintaining DNA methylation in mammalian cells. *Science*, *317*(5845). https://doi.org/10.1126/science.1147939

Bottes, S., Jaeger, B. N., Pilz, G. A., Jörg, D. J., Cole, J. D., Kruse, M., Harris, L., Korobeynyk, V. I., Mallona, I., Helmchen, F., Guillemot, F., Simons, B. D., & Jessberger, S. (2021). Long-term self-renewing stem cells in the adult mouse hippocampus identified by intravital imaging. *Nature Neuroscience*, *24*(2). https://doi.org/10.1038/s41593-020-00759-4

Bramlett, H. M., & Dietrich, W. D. (2015). Long-Term Consequences of Traumatic Brain Injury: Current Status of Potential Mechanisms of Injury and Neurological Outcomes. *Journal of Neurotrauma*, *32*(23), 1834–1848. https://doi.org/10.1089/neu.2014.3352

Buffo, A., Rite, I., Tripathi, P., Lepier, A., Colak, D., Horn, A. P., Mori, T., & Gotz, M. (2008). Origin and progeny of reactive gliosis: A source of multipotent cells in the injured brain. *Proc Natl Acad Sci U S A*, *105*(9), 3581–3586. https://doi.org/0709002105 [pii] 10.1073/pnas.0709002105

Buffo, A., Vosko, M. R., Erturk, D., Hamann, G. F., Jucker, M., Rowitch, D., & Gotz, M. (2005). Expression pattern of the transcription factor Olig2 in response to brain injuries: implications for neuronal repair. *Proc Natl Acad Sci U S A*, *102*(50), 18183–18188. https://doi.org/10.1073/pnas.0506535102

Bugiani, M., Plug, B. C., Man, J. H. K., Breur, M., & van der Knaap, M. S. (2022). Heterogeneity of white matter astrocytes in the human brain. In *Acta Neuropathologica* (Vol. 143, Issue 2). https://doi.org/10.1007/s00401-021-02391-3

Butler, A., Hoffman, P., Smibert, P., Papalexi, E., & Satija, R. (2018). Integrating single-cell transcriptomic data across different conditions, technologies, and species. *Nature Biotechnology*, *36*(5). https://doi.org/10.1038/nbt.4096

Cao, J., Spielmann, M., Qiu, X., Huang, X., Ibrahim, D. M., Hill, A. J., Zhang, F., Mundlos, S., Christiansen, L., Steemers, F. J., Trapnell, C., & Shendure, J. (2019). The single-cell transcriptional landscape of mammalian organogenesis. *Nature*, *566*(7745). https://doi.org/10.1038/s41586-019-0969-x

Chen, K., Zhang, J., Liang, F., Zhu, Q., Cai, S., Tong, X., He, Z., Liu, X., Chen, Y., & Mo, D. (2021). HMGB2 orchestrates mitotic clonal expansion by binding to the promoter of C/EBPβ to facilitate adipogenesis. *Cell Death and Disease*, *12*(7). https://doi.org/10.1038/s41419-021-03959-3

Clarke, L. E., Liddelow, S. A., Chakraborty, C., Münch, A. E., Heiman, M., & Barres, B. A. (2018). Normal aging induces A1-like astrocyte reactivity. *Proceedings of the National Academy of Sciences of the United States of America*, *115*(8). https://doi.org/10.1073/pnas.1800165115

Colak, D., Mori, T., Brill, M. S., Pfeifer, A., Falk, S., Deng, C., Monteiro, R., Mummery, C., Sommer, L., & Gotz, M. (2008). Adult neurogenesis requires Smad4-mediated bone morphogenic protein signaling in stem cells. *J Neurosci*, *28*(2), 434–446. http://www.ncbi.nlm.nih.gov/entrez/query.fcgi?cmd=Retrieve&db=PubMed&dopt=Citation&list_uids=18184786

D'Elia, K. P., Hameedy, H., Goldblatt, D., Frazel, P., Kriese, M., Zhu, Y., Hamling, K. R., Kawakami, K., Liddelow, S. A., Schoppik, D., & Dasen, J. S. (2023). Determinants of motor neuron functional subtypes important for locomotor speed. *Cell Reports*, *42*(9). https://doi.org/10.1016/j.celrep.2023.113049

Di Bella, D. J., Habibi, E., Stickels, R. R., Scalia, G., Brown, J., Yadollahpour, P., Yang, S. M., Abbate, C., Biancalani, T., Macosko, E. Z., Chen, F., Regev, A., & Arlotta, P. (2021). Molecular logic of cellular diversification in the mouse cerebral cortex. *Nature*, *595*(7868). https://doi.org/10.1038/s41586-021-03670-5

Dimou, L., & Gotz, M. (2014). Glial cells as progenitors and stem cells: new roles in the healthy and diseased brain. *Physiol Rev*, *94*(3), 709–737. https://doi.org/10.1152/physrev.00036.2013

Diotel, N., Lübke, L., Strähle, U., & Rastegar, S. (2020). Common and Distinct Features of Adult Neurogenesis and Regeneration in the Telencephalon of Zebrafish and Mammals. In *Frontiers in Neuroscience* (Vol. 14). Frontiers Media S.A. https://doi.org/10.3389/fnins.2020.568930

Dray, N., Mancini, L., Binshtok, U., Cheysson, F., Supatto, W., Mahou, P., Bedu, S., Ortica, S., Than-Trong, E., Krecsmarik, M., Herbert, S., Masson, J. B., Tinevez, J. Y., Lang, G., Beaurepaire, E., Sprinzak, D., & Bally-Cuif, L. (2021). Dynamic spatiotemporal coordination of neural stem cell fate decisions occurs through local feedback in the adult vertebrate brain. *Cell Stem Cell*, *28*(8). https://doi.org/10.1016/j.stem.2021.03.014

Escartin, C., Galea, E., Lakatos, A., O'Callaghan, J. P., Petzold, G. C., Serrano-Pozo, A., Steinhäuser, C., Volterra, A., Carmignoto, G., Agarwal, A., Allen, N. J., Araque, A., Barbeito, L., Barzilai, A., Bergles, D. E., Bonvento, G., Butt, A. M., Chen, W. T., Cohen-Salmon, M., …

Verkhratsky, A. (2021). Reactive astrocyte nomenclature, definitions, and future directions. In *Nature Neuroscience* (Vol. 24, Issue 3). https://doi.org/10.1038/s41593-020-00783-4

Fawcett, J. W., & Asher, R. A. (1999). The glial scar and central nervous system repair. *Brain Res Bull*, *49*(6), 377–391. http://www.ncbi.nlm.nih.gov/entrez/query.fcgi?cmd=Retrieve&db=PubMed&dopt=Citation&list_uids=10483914

Frik, J., Merl-Pham, J., Plesnila, N., Mattugini, N., Kjell, J., Kraska, J., Gomez, R. M., Hauck, S. M., Sirko, S., & Gotz, M. (2018). Cross-talk between monocyte invasion and astrocyte proliferation regulates scarring in brain injury. *EMBO Rep*, *19*(5). https://doi.org/10.15252/embr.201745294

Gascon, S., Masserdotti, G., Russo, G. L., & Gotz, M. (2017). Direct Neuronal Reprogramming: Achievements, Hurdles, and New Roads to Success. *Cell Stem Cell*, *21*(1), 18–34. https://doi.org/10.1016/j.stem.2017.06.011

Gascon, S., Murenu, E., Masserdotti, G., Ortega, E. O., Russo, G., Petrik, D., Deshpande, A., Heinrich, C., Karow, M., Robertson, S. R., Schroeder, T., Beckers, J., Irmler, M., Carsten, B., Friedmann Angeli, J. P., Conrad, M., Berninger, B., & Goetz, M. (2015). Identification and Successful Negotiation of a Metabolic Checkpoint in Direct Neuronal Reprogramming. *Cell Stem Cell*.

George, K. K., Heithoff, B. P., Shandra, O., & Robel, S. (2022). Mild Traumatic Brain Injury/Concussion Initiates an Atypical Astrocyte Response Caused by Blood-Brain Barrier Dysfunction. *Journal of Neurotrauma*, *39*(1–2). https://doi.org/10.1089/neu.2021.0204

Gotz, M., Sirko, S., Beckers, J., & Irmler, M. (2015). Reactive astrocytes as neural stem or progenitor cells: In vivo lineage, In vitro potential, and Genome-wide expression analysis. *Glia*, *63*(8), 1452–1468. https://doi.org/10.1002/glia.22850

Grade, S., & Götz, M. (2017). Neuronal replacement therapy: previous achievements and challenges ahead. *Regen Med*.

Griesbach, G. S., Masel, B. E., Helvie, R. E., & Ashley, M. J. (2018). The Impact of Traumatic Brain Injury on Later Life: Effects on Normal Aging and Neurodegenerative Diseases. *Journal of Neurotrauma*, *35*(1). https://doi.org/10.1089/neu.2017.5103

Hack, M. A., Saghatelyan, A., de Chevigny, A., Pfeifer, A., Ashery-Padan, R., Lledo, P. M., & Gotz, M. (2005). Neuronal fate determinants of adult olfactory bulb neurogenesis. *Nat Neurosci*, *8*(7), 865–872. http://www.ncbi.nlm.nih.gov/entrez/query.fcgi?cmd=Retrieve&db=PubMed&dopt=Citation&list_uids=15951811

Han, G., Wei, Z., Cui, H., Zhang, W., Wei, X., Lu, Z., & Bai, X. (2018). NUSAP1 gene silencing inhibits cell proliferation, migration and invasion through inhibiting DNMT1 gene expression in human colorectal cancer. *Experimental Cell Research*, *367*(2). https://doi.org/10.1016/j.yexcr.2018.03.039

Han, R. T., Kim, R. D., Molofsky, A. V., & Liddelow, S. A. (2021). Astrocyte-immune cell interactions in physiology and pathology. In *Immunity* (Vol. 54, Issue 2). https://doi.org/10.1016/j.immuni.2021.01.013

Heinrich, C., Bergami, M., Gascón, S., Lepier, A., Dimou, L., Sutor, B., Berninger, B., Götz, M., Gascon, S., Lepier, A., Vigano, F., Dimou, L., Sutor, B., Berninger, B., & Gotz, M. (2014). Sox2-mediated conversion of NG2 glia into induced neurons in the injured adult cerebral cortex. *Stem Cell Reports*, *in press*(6), 1000–1014. https://doi.org/10.1016/j.stemcr.2014.10.007

Heinrich, C., Blum, R., Gascon, S., Masserdotti, G., Tripathi, P., Sanchez, R., Tiedt, S., Schroeder, T., Gotz, M., & Berninger, B. (2010). Directing astroglia from the cerebral cortex into subtype specific functional neurons. *PLoS Biol*, *8*(5), e1000373. https://doi.org/10.1371/journal.pbio.1000373

Holt, M. G. (2023). Astrocyte heterogeneity and interactions with local neural circuits. In *Essays in Biochemistry* (Vol. 67, Issue 1). https://doi.org/10.1042/EBC20220136

Imayoshi, I., Sakamoto, M., Yamaguchi, M., Mori, K., & Kageyama, R. (2010). Essential roles of Notch signaling in maintenance of neural stem cells in developing and adult brains. *Journal of Neuroscience*, *30*(9). https://doi.org/10.1523/JNEUROSCI.4987-09.2010

Kageyama, R., Ohtsuka, T., Shimojo, H., & Imayoshi, I. (2009). Dynamic regulation of Notch signaling in neural progenitor cells. In *Current Opinion in Cell Biology* (Vol. 21, Issue 6). https://doi.org/10.1016/j.ceb.2009.08.009

Kamino, H., Moore, R., & Negishi, M. (2011). Role of a novel CAR-induced gene, TUBA8, in hepatocellular carcinoma cell lines. *Cancer Genetics*, *204*(7). https://doi.org/10.1016/j.cancergen.2011.05.007

Kimura, A., Matsuda, T., Sakai, A., Murao, N., & Nakashima, K. (2018). HMGB2 expression is associated with transition from a quiescent to an activated state of adult neural stem cells. *Developmental Dynamics*, *247*(1). https://doi.org/10.1002/dvdy.24559

Knobloch, M., Pilz, G. A., Ghesquière, B., Kovacs, W. J., Wegleiter, T., Moore, D. L., Hruzova, M., Zamboni, N., Carmeliet, P., & Jessberger, S. (2017). A Fatty Acid Oxidation-Dependent Metabolic Shift Regulates Adult Neural Stem Cell Activity. *Cell Reports*, *20*(9). https://doi.org/10.1016/j.celrep.2017.08.029

Korsunsky, I., Millard, N., Fan, J., Slowikowski, K., Zhang, F., Wei, K., Baglaenko, Y., Brenner, M., Loh, P. ru, & Raychaudhuri, S. (2019). Fast, sensitive and accurate integration of single-cell data with Harmony. *Nature Methods*, *16*(12). https://doi.org/10.1038/s41592-019-0619-0

Koupourtidou, C., Schwarz, V., Aliee, H., Frerich, S., Fischer-Sternjak, J., Bocchi, R., Simon-Ebert, T., Bai, X., Sirko, S., Kirchhoff, F., Dichgans, M., Götz, M., Theis, F. J., & Ninkovic, J. (2024). Shared inflammatory glial cell signature after stab wound injury, revealed by spatial, temporal, and cell-type-specific profiling of the murine cerebral cortex. *Nature Communications*, *15*(1), 2866. https://doi.org/10.1038/s41467-024-46625-w

Lange Canhos, L., Chen, M., Falk, S., Popper, B., Straub, T., Götz, M., & Sirko, S. (2021). Repetitive injury and absence of monocytes promote astrocyte self-renewal and neurological recovery. *GLIA*, *69*(1). https://doi.org/10.1002/glia.23893

Li, Y., He, X., Kawaguchi, R., Zhang, Y., Wang, Q., Monavarfeshani, A., Yang, Z., Chen, B., Shi, Z., Meng, H., Zhou, S., Zhu, J., Jacobi, A., Swarup, V., Popovich, P. G., Geschwind, D. H., & He, Z. (2020). Microglia-organized scar-free spinal cord repair in neonatal mice. *Nature*, *587*(7835), 613–618. https://doi.org/10.1038/s41586-020-2795-6

Liddelow, S. A., & Barres, B. A. (2017). Reactive Astrocytes: Production, Function, and Therapeutic Potential. In *Immunity* (Vol. 46, Issue 6). https://doi.org/10.1016/j.immuni.2017.06.006

Liddelow, S. A., Guttenplan, K. A., Clarke, L. E., Bennett, F. C., Bohlen, C. J., Schirmer, L., Bennett, M. L., Münch, A. E., Chung, W. S., Peterson, T. C., Wilton, D. K., Frouin, A., Napier, B. A., Panicker, N., Kumar, M., Buckwalter, M. S., Rowitch, D. H., Dawson, V. L., Dawson, T. M., … Barres, B. A. (2017). Neurotoxic reactive astrocytes are induced by activated microglia. *Nature*, *541*(7638). https://doi.org/10.1038/nature21029

Liu, F., Zhang, Y., Chen, F., Yuan, J., Li, S., Han, S., Lu, D., Geng, J., Rao, Z., Sun, L., Xu, J., Shi, Y., Wang, X., & Liu, Y. (2021). Neurog2 directly converts astrocytes into functional neurons in midbrain and spinal cord. *Cell Death and Disease*, *12*(3). https://doi.org/10.1038/s41419-021-03498-x

Madisen, L., Zwingman, T. A., Sunkin, S. M., Oh, S. W., Zariwala, H. A., Gu, H., Ng, L. L., Palmiter, R. D., Hawrylycz, M. J., Jones, A. R., Lein, E. S., & Zeng, H. (2010). A robust and high-throughput Cre reporting and characterization system for the whole mouse brain. *Nature Neuroscience*, *13*(1). https://doi.org/10.1038/nn.2467

Magnusson, J. P., Goritz, C., Tatarishvili, J., Dias, D. O., Smith, E. M., Lindvall, O., Kokaia, Z., & Frisen, J. (2014). A latent neurogenic program in astrocytes regulated by Notch signaling in the mouse. *Science*, *346*(6206), 237–241. https://doi.org/10.1126/science.346.6206.237

Malatesta, P., Hack, M. A., Hartfuss, E., Kettenmann, H., Klinkert, W., Kirchhoff, F., Götz, M., & Gotz, M. (2003). Neuronal or glial progeny: regional differences in radial glia fate. *Neuron*, *37*(5), 751–764. https://doi.org/S0896627303001168 [pii]

März, M., Chapouton, P., Diotel, N., Vaillant, C., Hesl, B., Takamiya, M., Lam, C. S., Kah, O., Bally-Cuif, L., Strähle, U., Marz, M., Chapouton, P., Diotel, N., Vaillant, C., Hesl, B., Takamiya, M., Lam, C. S., Kah, O., Bally-Cuif, L., & Strahle, U. (2010). Heterogeneity in progenitor cell subtypes in the ventricular zone of the zebrafish adult telencephalon. *Glia*, *58*(7), 870–888. https://doi.org/10.1002/glia.20971

Matias, I., Morgado, J., & Gomes, F. C. A. (2019). Astrocyte Heterogeneity: Impact to Brain Aging and Disease. In *Frontiers in Aging Neuroscience* (Vol. 11). https://doi.org/10.3389/fnagi.2019.00059

Mattugini, N., Bocchi, R., Scheuss, V., Russo, G. L., Torper, O., Lao, C. L., & Götz, M. (2019). Inducing Different Neuronal Subtypes from Astrocytes in the Injured Mouse Cerebral Cortex. *Neuron*, *103*(6). https://doi.org/10.1016/j.neuron.2019.08.009

Matusova, Z., Hol, E. M., Pekny, M., Kubista, M., & Valihrach, L. (2023). Reactive astrogliosis in the era of single-cell transcriptomics. In *Frontiers in Cellular Neuroscience* (Vol. 17). https://doi.org/10.3389/fncel.2023.1173200

Moore, D. L., Pilz, G. A., Araúzo-Bravo, M. J., Barral, Y., & Jessberger, S. (2015). A mechanism for the segregation of age in mammalian neural stem cells. *Science*, *349*(6254). https://doi.org/10.1126/science.aac9868

Mori, T., Buffo, A., & Gotz, M. (2005). The novel roles of glial cells revisited: the contribution of radial glia and astrocytes to neurogenesis. *Curr Top Dev Biol*, *69*, 67–99. https://doi.org/S0070-2153(05)69004-7 [pii] 10.1016/S0070-2153(05)69004-7

Nicolau-Neto, P., Palumbo, A., De Martino, M., Esposito, F., Simão, T. de A., Fusco, A., Nasciutti, L. E., Da Costa, N. M., & Pinto, L. F. R. (2018). UBE2C is a transcriptional target of the cell cycle regulator FOXM1. *Genes*, *9*(4). https://doi.org/10.3390/genes9040188

Ninkovic, J., & Götz, M. (2018). Understanding direct neuronal reprogramming — from pioneer factors to 3D chromatin. *Current Opinion in Genetics and Development*, *52*. https://doi.org/10.1016/j.gde.2018.05.011

Ninkovic, J., Steiner-Mezzadri, A., Jawerka, M., Akinci, U., Masserdotti, G., Petricca, S., Fischer, J., von Holst, A., Beckers, J., Lie, C. D. D., Petrik, D., Miller, E., Tang, J., Wu, J., Lefebvre, V., Demmers, J., Eisch, A., Metzger, D., Crabtree, G., … Gotz, M. (2013). The BAF Complex Interacts with Pax6 in Adult Neural Progenitors to Establish a Neurogenic Cross-Regulatory Transcriptional Network. *Cell Stem Cell*, *13*(4). https://doi.org/10.1016/j.stem.2013.07.002

Nishiyama, A., Shimizu, T., Sherafat, A., & Richardson, W. D. (2021). Life-long oligodendrocyte development and plasticity. *Seminars in Cell and Developmental Biology*, *116*. https://doi.org/10.1016/j.semcdb.2021.02.004

Ohlig, S., Clavreul, S., Thorwirth, M., Simon-Ebert, T., Bocchi, R., Ulbricht, S., Kannayian, N., Rossner, M., Sirko, S., Smialowski, P., Fischer-Sternjak, J., & Götz, M. (2021). Molecular diversity of diencephalic astrocytes reveals adult astrogenesis regulated by Smad4. *The EMBO Journal*, *40*(21). https://doi.org/10.15252/embj.2020107532

Ohtani, K., Iwanaga, R., Nakamura, M., Ikeda, M. A., Yabuta, N., Tsuruga, H., & Nojima, H. (1999). Cell growth-regulated expression of mammalian MCM5 and MCM6 genes mediated by the transcription factor E2F. *Oncogene*, *18*(14). https://doi.org/10.1038/sj.onc.1202544

Ortega, F., Gascon, S., Masserdotti, G., Deshpande, A., Simon, C., Fischer, J., Dimou, L., Chichung Lie, D., Schroeder, T., & Berninger, B. (2013). Oligodendrogliogenic and neurogenic adult subependymal zone neural stem cells constitute distinct lineages and exhibit differential responsiveness to Wnt signalling. *Nat Cell Biol*, *15*(6), 602–613. https://doi.org/10.1038/ncb2736

Patani, R., Hardingham, G. E., & Liddelow, S. A. (2023). Functional roles of reactive astrocytes in neuroinflammation and neurodegeneration. In *Nature Reviews Neurology* (Vol. 19, Issue 7). https://doi.org/10.1038/s41582-023-00822-1

Păun, O., Tan, Y. X., Patel, H., Strohbuecker, S., Ghanate, A., Cobolli-Gigli, C., Sopena, M. L., Gerontogianni, L., Goldstone, R., Ang, S. L., Guillemot, F., & Dias, C. (2023). Pioneer factor ASCL1 cooperates with the mSWI/SNF complex at distal regulatory elements to regulate human neural differentiation. *Genes and Development*, *37*(5–6). https://doi.org/10.1101/gad.350269.122

Pereira, M., Birtele, M., Shrigley, S., Benitez, J. A., Hedlund, E., Parmar, M., & Ottosson, D. R. (2017). Direct Reprogramming of Resident NG2 Glia into Neurons with Properties of Fast-Spiking Parvalbumin-Containing Interneurons. *Stem Cell Reports*, *9*(3), 742–751. https://doi.org/10.1016/j.stemcr.2017.07.023

Ramesh, V., Bayam, E., Cernilogar, F. M., Bonapace, I. M., Schulze, M., Riemenschneider, M. J., Schotta, G., & Gotz, M. (2016). Loss of Uhrf1 in neural stem cells leads to activation of retroviral elements and delayed neurodegeneration. *Genes Dev*, *30*(19), 2199–2212. https://doi.org/10.1101/gad.284992.116

Ramos, S. I., Makeyev, E. V., Salierno, M., Kodama, T., Kawakami, Y., & Sahara, S. (2020). Tuba8 Drives Differentiation of Cortical Radial Glia into Apical Intermediate Progenitors by Tuning

Modifications of Tubulin C Termini. *Developmental Cell*, *52*(4). https://doi.org/10.1016/j.devcel.2020.01.036

Sanchez-Gonzalez, R., Koupourtidou, C., Lepko, T., Zambusi, A., Novoselc, K. T., Durovic, T., Aschenbroich, S., Schwarz, V., Breunig, C. T., Straka, H., Huttner, H. B., Irmler, M., Beckers, J., Wurst, W., Zwergal, A., Schauer, T., Straub, T., Czopka, T., Trümbach, D., … Ninkovic, J. (2022). Innate Immune Pathways Promote Oligodendrocyte Progenitor Cell Recruitment to the Injury Site in Adult Zebrafish Brain. *Cells*, *11*(3). https://doi.org/10.3390/cells11030520

Santopolo, G., Magnusson, J. P., Lindvall, O., Kokaia, Z., & Frisén, J. (2020). Blocking Notch-Signaling Increases Neurogenesis in the Striatum after Stroke. *Cells*, *9*(7). https://doi.org/10.3390/cells9071732

Schmid, R. S., Simon, J. M., Vitucci, M., McNeill, R. S., Bash, R. E., Werneke, A. M., Huey, L., White, K. K., Ewend, M. G., Wu, J., & Miller, C. R. (2016). Core pathway mutations induce de-differentiation of murine astrocytes into glioblastoma stem cells that are sensitive to radiation but resistant to temozolomide. *Neuro-Oncology*, *18*(7). https://doi.org/10.1093/neuonc/nov321

Schober, A. L., Wicki-Stordeur, L. E., Murai, K. K., & Swayne, L. A. (2022). Foundations and implications of astrocyte heterogeneity during brain development and disease. In *Trends in Neurosciences* (Vol. 45, Issue 9). https://doi.org/10.1016/j.tins.2022.06.009

Shi, W., Feng, Z., Zhang, J., Gonzalez-Suarez, I., Vanderwaal, R. P., Wu, X., Powell, S. N., Roti Roti, J. L., Gonzalo, S., & Zhang, J. (2010). The role of RPA2 phosphorylation in homologous recombination in response to replication arrest. *Carcinogenesis*, *31*(6). https://doi.org/10.1093/carcin/bgq035

Shimada, I. S., LeComte, M. D., Granger, J. C., Quinlan, N. J., & Spees, J. L. (2012). Self-renewal and differentiation of reactive astrocyte-derived neural stem/progenitor cells isolated from the cortical peri-infarct area after stroke. *Journal of Neuroscience*, *32*(23). https://doi.org/10.1523/JNEUROSCI.4303-11.2012

Shimizu, Y., Ueda, Y., & Ohshima, T. (2018). Wnt signaling regulates proliferation and differentiation of radial glia in regenerative processes after stab injury in the optic tectum of adult zebrafish. *GLIA*, *66*(7). https://doi.org/10.1002/glia.23311

Simpson Ragdale, H., Clements, M., Tang, W., Deltcheva, E., Andreassi, C., Lai, A. G., Chang, W. H., Pandrea, M., Andrew, I., Game, L., Uddin, I., Ellis, M., Enver, T., Riccio, A., Marguerat, S., & Parrinello, S. (2023). Injury primes mutation-bearing astrocytes for dedifferentiation in later life. *Current Biology*, *33*(6). https://doi.org/10.1016/j.cub.2023.02.013

Sirko, S., Behrendt, G., Johansson, P. A., Tripathi, P., Costa, M., Bek, S., Heinrich, C., Tiedt, S., Colak, D., Dichgans, M., Fischer, I. R., Plesnila, N., Staufenbiel, M., Haass, C., Snapyan, M., Saghatelyan, A., Tsai, L. H., Fischer, A., Grobe, K., … Götz, M. (2013). Reactive glia in the injured brain acquire stem cell properties in response to sonic hedgehog. [corrected]. *Cell Stem Cell*, *12*(4), 426–439. https://doi.org/10.1016/j.stem.2013.01.019

Sirko, S., Irmler, M., Gascon, S., Bek, S., Schneider, S., Dimou, L., Obermann, J., De Souza Paiva, D., Poirier, F., Beckers, J., Hauck, S. M., Barde, Y. A., & Gotz, M. (2015). Astrocyte reactivity after brain injury-: The role of galectins 1 and 3. *Glia*, *63*(12), 2340–2361. https://doi.org/10.1002/glia.22898

Sirko, S., Schichor, C., Della Vecchia, P., Metzger, F., Sonsalla, G., Simon, T., Bürkle, M., Kalpazidou, S., Ninkovic, J., Masserdotti, G., Sauniere, J. F., Iacobelli, V., Iacobelli, S., Delbridge, C., Hauck, S. M., Tonn, J. C., & Götz, M. (2023). Injury-specific factors in the cerebrospinal fluid regulate astrocyte plasticity in the human brain. *Nature Medicine*, *29*(12). https://doi.org/10.1038/s41591-023-02644-6

Sofroniew, M. V. (2009). Molecular dissection of reactive astrogliosis and glial scar formation. *Trends in Neurosciences*, *32*(12), 638–647. https://doi.org/10.1016/j.tins.2009.08.002

Storer, M. A., Gallagher, D., Fatt, M. P., Simonetta, J. V., Kaplan, D. R., & Miller, F. D. (2018). Interleukin-6 Regulates Adult Neural Stem Cell Numbers during Normal and Abnormal Post-natal Development. *Stem Cell Reports*, *10*(5). https://doi.org/10.1016/j.stemcr.2018.03.008

Strzalka, W., & Ziemienowicz, A. (2011). Proliferating cell nuclear antigen (PCNA): A key factor in DNA replication and cell cycle regulation. In *Annals of Botany* (Vol. 107, Issue 7). https://doi.org/10.1093/aob/mcq243

Sun, D. (2014). The potential of endogenous neurogenesis for brain repair and regeneration following traumatic brain injury. *Neural Regeneration Research*, *9*(7). https://doi.org/10.4103/1673-5374.131567

Thorner, K., Zorn, A., & Chaturvedi, P. (2021). ELeFHAnt: A supervised machine learning approach for label harmonization and annotation of single cell RNA-seq data. *BioRxiv*.

Torper, O., & Götz, M. (2017). Brain repair from intrinsic cell sources: Turning reactive glia into neurons. In *Progress in Brain Research* (Vol. 230). https://doi.org/10.1016/bs.pbr.2016.12.010

Torper, O., Ottosson, D. R., Pereira, M., Lau, S., Cardoso, T., Grealish, S., & Parmar, M. (2015). In Vivo Reprogramming of Striatal NG2 Glia into Functional Neurons that Integrate into Local Host Circuitry. *Cell Rep*, *12*(3), 474–481. https://doi.org/10.1016/j.celrep.2015.06.040

Wang, T., Lu, J., Wang, R., Cao, W., & Xu, J. (2022). TOP2A promotes proliferation and metastasis of hepatocellular carcinoma regulated by miR-144-3p. *Journal of Cancer*, *13*(2). https://doi.org/10.7150/jca.64017

Wani, G. A., Sprenger, H. G., Ndoci, K., Chandragiri, S., Acton, R. J., Schatton, D., Kochan, S. M. V., Sakthivelu, V., Jevtic, M., Seeger, J. M., Müller, S., Giavalisco, P., Rugarli, E. I., Motori, E., Langer, T., & Bergami, M. (2022). Metabolic control of adult neural stem cell self-renewal by the mitochondrial protease YME1L. *Cell Reports*, *38*(7). https://doi.org/10.1016/j.celrep.2022.110370

Westphal, M., Panza, P., Kastenhuber, E., Wehrle, J., & Driever, W. (2022). Wnt/β-catenin signaling promotes neurogenesis in the diencephalospinal dopaminergic system of embryonic zebrafish. *Scientific Reports*, *12*(1). https://doi.org/10.1038/s41598-022-04833-8

Xu, M., Liu, Y., Wan, H. L., Wong, A. M., Ding, X., You, W., Lo, W. S., Ng, K. K. C., & Wong, N. (2022). Overexpression of nucleotide metabolic enzyme DUT in hepatocellular carcinoma potentiates a therapeutic opportunity through targeting its dUTPase activity. *Cancer Letters*, *548*. https://doi.org/10.1016/j.canlet.2022.215898

Yanardag, S., & Pugacheva, E. N. (2021). Primary cilium is involved in stem cell differentiation and renewal through the regulation of multiple signaling pathways. In *Cells* (Vol. 10, Issue 6). https://doi.org/10.3390/cells10061428

Yuan, J., Lan, H., Huang, D., Guo, X., Liu, C., Liu, S., Zhang, P., Cheng, Y., & Xiao, S. (2022). Multi-Omics Analysis of MCM2 as a Promising Biomarker in Pan-Cancer. *Frontiers in Cell and Developmental Biology*, *10*. https://doi.org/10.3389/fcell.2022.852135

Zamboni, M., Llorens-Bobadilla, E., Magnusson, J. P., & Frisén, J. (2020). A Widespread Neurogenic Potential of Neocortical Astrocytes Is Induced by Injury. *Cell Stem Cell*, *27*(4). https://doi.org/10.1016/j.stem.2020.07.006

Zambusi, A., & Ninkovic, J. (2020). Regeneration of the central nervous system-principles from brain regeneration in adult zebrafish. In *World Journal of Stem Cells* (Vol. 12, Issue 1, pp. 8–24). Baishideng Publishing Group Co. https://doi.org/10.4252/wjsc.v12.i1.8

Zambusi, A., Novoselc, K. T., Hutten, S., Kalpazidou, S., Koupourtidou, C., Schieweck, R., Aschenbroich, S., Silva, L., Yazgili, A. S., van Bebber, F., Schmid, B., Möller, G., Tritscher, C., Stigloher, C., Delbridge, C., Sirko, S., Günes, Z. I., Liebscher, S., Schlegel, J., … Ninkovic, J. (2022). TDP-43 condensates and lipid droplets regulate the reactivity of microglia and regeneration after traumatic brain injury. *Nature Neuroscience*, *25*(12), 1608–1625. https://doi.org/10.1038/s41593-022-01199-y

Zeng, T., Guan, Y., Li, Y. kun, Wu, Q., Tang, X. jun, Zeng, X., Ling, H., & Zou, J. (2021). The DNA replication regulator MCM6: An emerging cancer biomarker and target. In *Clinica Chimica Acta* (Vol. 517). https://doi.org/10.1016/j.cca.2021.02.005

Zhou, L., & Luo, H. (2013). Replication protein a links cell cycle progression and the onset of neurogenesis in Drosophila optic lobe development. *Journal of Neuroscience*, *33*(7). https://doi.org/10.1523/JNEUROSCI.3357-12.2013

Figures legends

Figure 1. Integration of mouse and zebrafish single cell transcriptomes.
(**A**) Schematic of datasets used for integration analysis from both species. (**B**) UMAP plots of unaligned (before integration) and aligned (after integration) datasets from a mouse (red) and zebrafish (blue). (**C**) UMAP plot depicting integrated dataset grouped into 25 transcriptionally distinct clusters, annotated by cell type-specific markers. (**D**) Bar plot depicts the contribution of cells from different conditions to identified cell cluster. (**E**) Alluvial plot visualizes contribution of the two species to identified clusters. (**F**,**G**) Heatmaps visualizing relative similarities among clusters between (F) unintegrated mouse and integrated mouse+zebrafish and (G) unintegrated zebrafish and integrated mouse+zebrafish datasets.

Figure 2. Integration of mouse and zebrafish species identifies SW injury-induced astrocytic population with radial glia properties.
(**A**) UMAP plot highlighting astrocytes/radial glia (Astro/RG) in the integrated dataset. (**B**) UMAP plots visualize cell distribution across species and conditions after sub-clustering of Astro/RG clusters. (**C**) UMAP plot depicting Astro/RG sub-clusters. (**D**) UMAP plots illustrating condition-specific distribution of cells within Astro/RG clusters mouse (above) and zebrafish (bellow). (**E**) Dot plot depicting top 5 enriched genes across Astro/RG sub-clusters. (**F**) Bar plot depicting cell distribution across injured and intact conditions in both species. Note that Astro/RG 3 and 6 clusters contain mouse cells only after injury. (**G**) Dot-plot showing the expression of top 5 enriched genes in Astro/RG 3 and 6 clusters, demonstrating elevated expression in injured mice (3 and 5 dpi) compared to intact mice. Note, only mouse cells from cluster 3 and 6 are considered for the analysis.

Figure 3. Visualizations of injury-induced Astro/RG clusters 3 and 6 cells after SW injury in mouse.
(**A**) UMAP highlighting Astro/RG 3 and 6 clusters. (**B**) Dot plot showing the expression of Astro/RG 3/6 enriched genes in all Astro/RG sub-clusters in mice. (**C**) Violin plots illustrating the expression of sub-clusters Astro/RG 3/6 across conditions in mouse. (**D**) Micrographs depicting the astrocyte reactivity in the intact and injured (3 dpi) cerebral cortex based on the GFAP staining. (**E**, **F**) Expression of RPA2 in reactive astrocyte. Micrographs in E and F are magnifications of boxed areas in D and E, retrospectively. (**G**-**K**) Micrographs showing the co-localization of GFAP, HMGB2 and *Uhrf1* RNA in the intact and injured (3 dpi) mouse cerebral cortex. H is magnification of boxed area in G. Micrographs in I, J and K are magnifications of boxed areas in H and depict triple positive cell (I), cell expressing only *Uhrf* (J) and cell expression only HMGB2 (K). All micrographs are maximum intensity projections of the confocal Z-stack and micrograph in F contains orthogonal projections. Scale bars in D, G are 100 mm;

50 mm in E, H; 10 mm in F, I, J, K. White dashed lines (D, E, G) and red dashed line in H show position of the injury.

Figure 4. Astro/RG 3 and 6 clusters contain proliferative astrocytes.

(**A**) PCA plots show injury-induced mouse clusters (green and blue) and cell cycle phases (G1, S, G2M). (**B**) Pie charts depict the distribution of Astro/RG 3 and 6 clusters amongst different cell cycle phases. (**C**) Heatmap showing GO terms enriched in injury-induced 3 and 6 Astro/RG clusters, colored by p-values. **(D)** UMAP plot displaying the enrichment score for genes associated with the Gene Ontology term "GO:0045787 positive regulation of cell cycle". (**E**) A schematic illustrating the experimental design to address proliferation of Astro/RG 3 and 6 astrocytes using incorporation of BrdU. (**F**-**J**) Micrographs depicting BrdU incorporation by Hmgb2+ reactive (GFAP+) astrocytes in the intact and injured (5 dpi) mouse cerebral cortex. G is magnification of boxed area in F. H-J are magnifications of boxed areas in G as indicated by color-code. Micrographs in F and G are maximum intensity projections of confocal Z-stack. Micrographs in H-J are single optical sections. Scale bar in F is 100 mm; in G 50 mm and in H, I, J 10 mm. Red line indicates SW injury. (**K**) Dot plot showing the proportion of HMGB2+ astrocytes (GFAP+) incorporating BrdU within 5 days labelling period after SW injury. Data are shown as mean±SEM. Every dot represents an independent animal.

Figure 5: Injury-induced 3 and 6 Astro/RG cluster cells upregulate neural progenitor genes and gain neurosphere-forming potential.

(**A**) UMAP depicting Monocle3 pseudotime trajectories (upper plot) across Astro/RG clusters (lower plot) in the mouse. (**B**, **C**) Plots depicting the dynamic changes in the expression of astrocytic marker genes (B) and injury induced Astro/RG clusters 3 and 6 specific genes (C) along pseudotime trajectories. Note that Astro/RG clusters 3 and 6 specific genes are typical neural progenitor genes. (**D**) A schematic illustrating a neurosphere assay using $Ascl1^{CreErt2}$ // tdTomato mouse line. (**E-G**) Micrographs depicting reporter positive (E, F) and reporter negative (G) differentiated neurosphare stained for the lineage specific markers after 7 days in vitro. F is maginifcation of boxed area in E. All images are maximum intensity projections of the confocal Z-stack. Scale bars are 50 mm in E and 10 mm in F and G. (**H**) Pie chart depicting the differentiation potential of reporter positive and negative neurospheres. 28 neursphares from 3 different animals have been analyzed.

Figure 6. Some injury-induced Astro/RG 3 and 6 cluster cells show similarities to Transit Amplifying Progenitors (TAPs).

(**A**) The schematic illustrating datasets used for the integration analysis. (**B**) The UMAP plot displays single cells grouped into 15 distinct cellular clusters annotated using known cell-type-specific markers. (**C**) The UMAP plot demonstrating subclustering of the neurogenic lineage

cells containing astrocyte/neural stem cells (Ast), TAPs and neuroblast (NBs) clusters. (**D**) Heatmap depicting expression of known cell type markers across Ast, TAPs, and NBs (Suppl. Table 6. (**E**) Bar plot illustrating frequency distribution of cells from cortex and SEZ conditions across Ast, TAPs, and NBs cell types. (**F**) Circos plot showing the distribution of cells from different conditions amongst specific Ast, TAPs, and NBs clusters. (**G)** UMAP plot showing the cells of injury-induced 3 and 6 Astro/RG clusters (from the zebrafish/mouse integration) identified in the integrated cortex and SEZ dataset. Inlets represent the enrichment score for homeostatic and reactive astrocytes calculated based on the gene expression published by Koupourtidou et al. (Koupourtidou et al., 2024) (**H**, **I**) Heatmaps representing similarities of the transcriptome of injury-induced cluster Astro/RG_3 (H) and Astro/RG_6 (I) with SEZ Ast, TAPs, and NBs.

Figure 7: TAP-like cells emerging after injury fail to upregulate neurogenic fate determinants.

(**A**) UMAP plot illustrating representative pseudotime trajectory in the SEZ (dotted black line) and injured cerebral cortex (solid blue line) (**B**, **C**) UMAP plots of pseudotime trajectory of SEZ only cells (B) and cerebral cortex only (C) based on pseudotime (upper panels) and across clusters (lower panels). (**D**) Heatmap depicting enriched GO terms in the set of DEGs between Ast_4 cluster from the injured cerebral cortex and SEZ, color-coded by p-values. (**E**) Heatmap illustrating enriched GO terms in the set of DEGs between Ast_4 and Ast_6 clusters isolated from the injured cerebral cortex, color-coded by p-values. (**F**) Heatmap of enriched GO terms in the DEG set between across TAPs_1 and TAPs_3 clusters of the integrated cortex and SEZ, colored by p-values. (**G**) Heatmap of GO terms enriched in DEGs between TAPs_1 of the injured cortex and TAPs_3 of SEZ, colored by p-values. (**H**) Violin plot displaying 7 significant DEGs between injured context and SEZ in TAPs_1 and TAPs_2 clusters, color-coded by TAPs clusters.

Supplementary Figures legends

Supplementary Figure S1. Comparison of Harmony- and Seurat-based integration of mouse and zebrafish datasets.

(**A**) UMAP plots depicting Seurat-based integration of cells from injured and intact mouse and zebrafish brain. (**B**) Alluvial plot showing the distribution of mouse and zebrafish cells amongst different clusters following harmony integration. **(C, E)** UMAPs depicting cellular clusters with their identity after Seurat (C) and harmony (E) based integration. (**D**) Relative similarity heatmap comparing integrated and annotated clusters by Seurat and harmony. Highlighted 3_Astrocytes/Radial cluster (yellow) in harmony analysis corresponds to 2_Astrocytes/Radial cluster (red) from Seurat integration. (**F**, **H**) UMAP plots highlighting clusters 2_Astrocytes/Radial cluster in the Seurat integration (F) and corresponding cluster 3_Astrocytes/Radial cluster in harmony-based integration (H). (**G**, **I**) Bar plots depicting the enrichment (log_2FC) of top 10 enriched genes in the corresponding 2_Astrocytes/Radial cluster in Seurat analysis (G) and 3_Astrocytes/Radial cluster in harmony analysis (I).

Supplementary Figure S2. Integration of brain datasets with the dataset of peripheral blood mononuclear cells (PBMCs).

(**A**) UMAP plot depicting integration of Mouse (intact+3dpi+5dpi), Zebrafish (intact+7dpi+7dpi) and PBMCs cells. (**B**-**F**) UMAP plots showing expression score for immune cells (B), astrocytes (C), neurons (D), microglia (E) and monocytes (F) in integrated dataset. Gene lists used for the expression score generation are provided in the Suppl. Table 1 and Suppl. Table 2.

Supplementary Figure S3. Expression of Astro/RG_6/3 enriched genes in reactive astrocyte population.

(**A**, **F**) Micrographs depicting GFAP expression in the injured (upper panel) and intact (lower panel) cerebral cortex at 3 dpi. (**B**-**E**) Micrographs showing the RNAscope® signal for Ascl1 in HMGB2 positive reactive, GFAP+ astrocytes 3 dpi. (**G**, **J**). Micrographs illustrating the RNAscope® signal for Ascl1 and Uhrf1 in reactive, GFAP+ astrocytes 3 dpi. Micrographs in C-E and H-J are magnifications of cells boxed in B and G according to the color code. Dashed lines indicate injury site. Micrographs A, B, F and G are maximum intensity projections of the confocal Z-stack. Micrographs C-E and H-J are single optical sections. Scale bars in A, F 100 mm; in B, G 50 mm; in C-E and H-J 10 mm.

Supplementary Figure S4. Cells from the Astro/RG 3 and 6 clusters are dispersed amongst different astrocytic clusters in unintegrated mouse dataset.

(**A**) UMAP plot depicting 7 distinct astrocytic clusters at resolution 0.3. (**B**) Dot plot highlighting the top 5 expressed genes in each astrocytic cluster shown in A, color-coded by expression

levels. (**C**-**H**) Bar plots highlighting distribution of Astro/RG clusters 3 (green) and 6 (blue) cells across astrocytes clusters in unintegrated dataset at resolutions of 0.3 (C), 0.4 (D), 0.5 (E), 0.6 (F), 0.7 (G), and 0.8 (H).

Supplementary Figure S5. Injury-induced mouse Astro/RG 3 and 6 cluster cells share molecular features with immature astrocytic progenitors.

(**A**) UMAP plots depict expression score for homeostatic and reactive astrocyte based on the classification in Koupourtidou et al. (Koupourtidou et al., 2024) in integrated astrocytic clusters. (**B**) Heatmaps depicting expression of genes identifying injury-induced (Astro/RG 6 and Astro/RG 3) clusters and homeostatic (Astro/RG 0) cluster in control (AC samples) and dedifferentiated (TRP samples) astrocytes. The astrocyte data are coming from the Schmid et al. dataset (REF). (**C**) UMAP plots illustrate the gene expression scores identifying cycling radial glia and astrocytes isolated from postnatal day 4 (P4) mouse cortex in integrated mouse and zebrafish Astro/RG clusters. The P4 dataset comes from Di Bella *et al.* 2021. (**D**, **E**) Volcano plots of depicting DEGs mouse and zebrafish in cells in Astro/RG 3 (D) and Astro/RG 6 (E) clusters. (**F**, **G**) Heatmaps depicting enriched GO terms in the set of DEGs between mouse and zebrafish cells in Astro/RG 3 cluster (F) and Astro/RG 3 cluster (G), color-coded by p-values.

Supplementary Figure S6. Identification of SEZ cell types and their differentiation trajectories.

(**A**) UMAP plot depicting SEZ cells grouped into 20 distinct transcriptional clusters, annotated by cell type-specific markers (Suppl. Table 1 and 6). (**B**-**D**) UMAP plots depict the expression of known marker genes used for annotation of NSCs (qNSCs/Astro and aNSCs) (B), TAPs (C), and Neuroblasts (D). (**E**) UMAP plot of pseudotime trajectory starting with qNSC, transiting via aNSC and TAPs, and ending in Neuroblasts clusters of SEZ. (**F**) UMAP plots locating the cells of the SEZ lineage within the integrated SEZ+cortex dataset. Cells from the specific SEZ cluster are marked in red.

Supplementary Figure S7. Diffusion map-based definition of the lineage trajectory and gene expression changes along the trajectory.

(**A**, **B**) Diffusion component plot of SEZ (A), and cortex (B) from integrated SEZ+cortex dataset displaying the position of Ast, TAPs and Neuroblast states. (**C**) Dot plot showing expression of genes downstream of notch receptor in TAPs clusters from injured cortex. (**D**-**E**) Heatmap plots depicting enrichment expression score of genes downstream of notch signaling (shown in C) in TAPs clusters from integrated injured cortex (D), and NSCs and TAPs clusters from SEZ only dataset (E). (**F**-**G**) Expression dynamics of selected genes along pseudotime trajectory in SEZ (F), and cortex (G) within the integrated SEZ+cortex dataset.

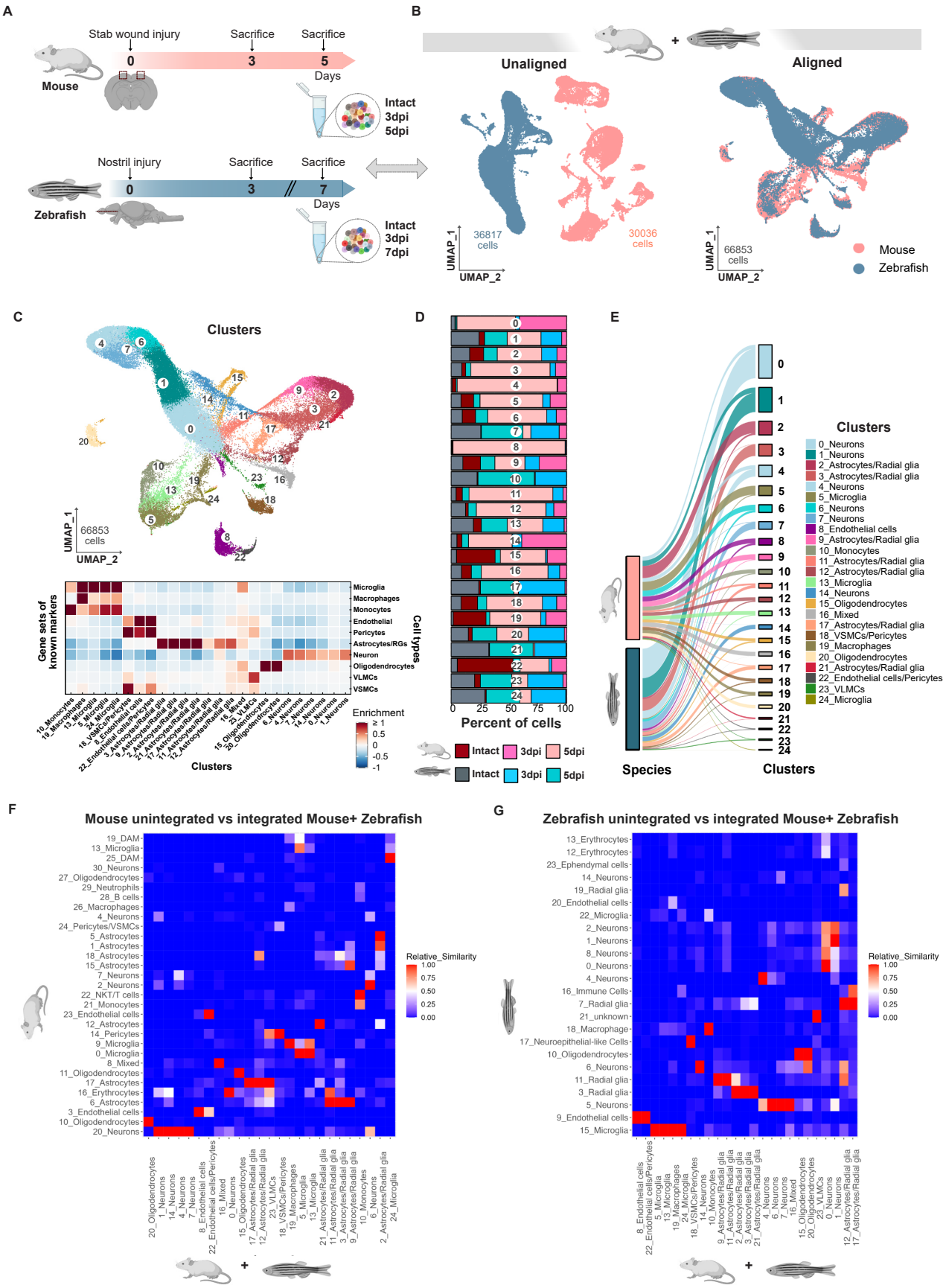

Figure 1, Maddhesiya *et al.*

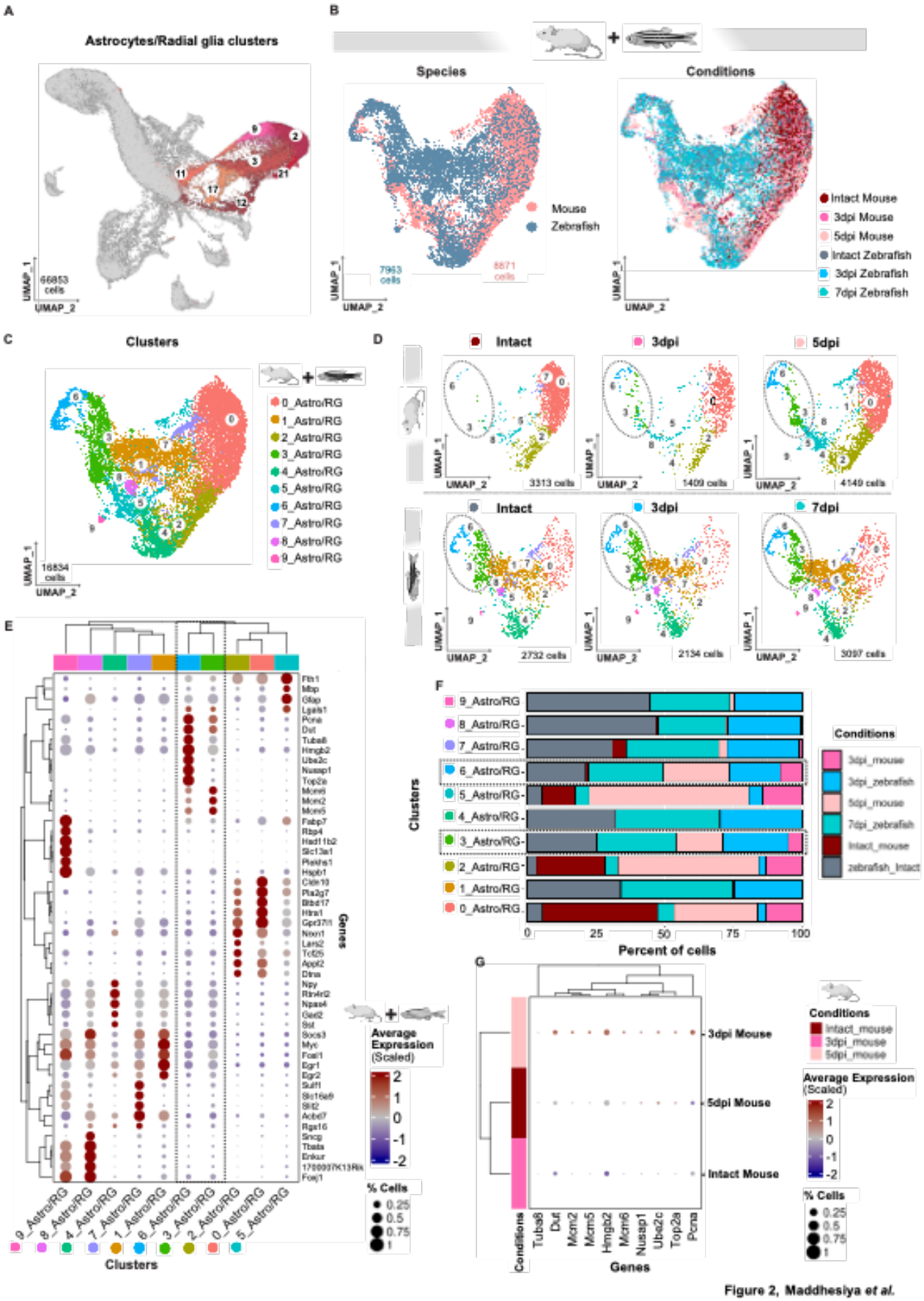

Figure 2, Maddhesiya *et al.*

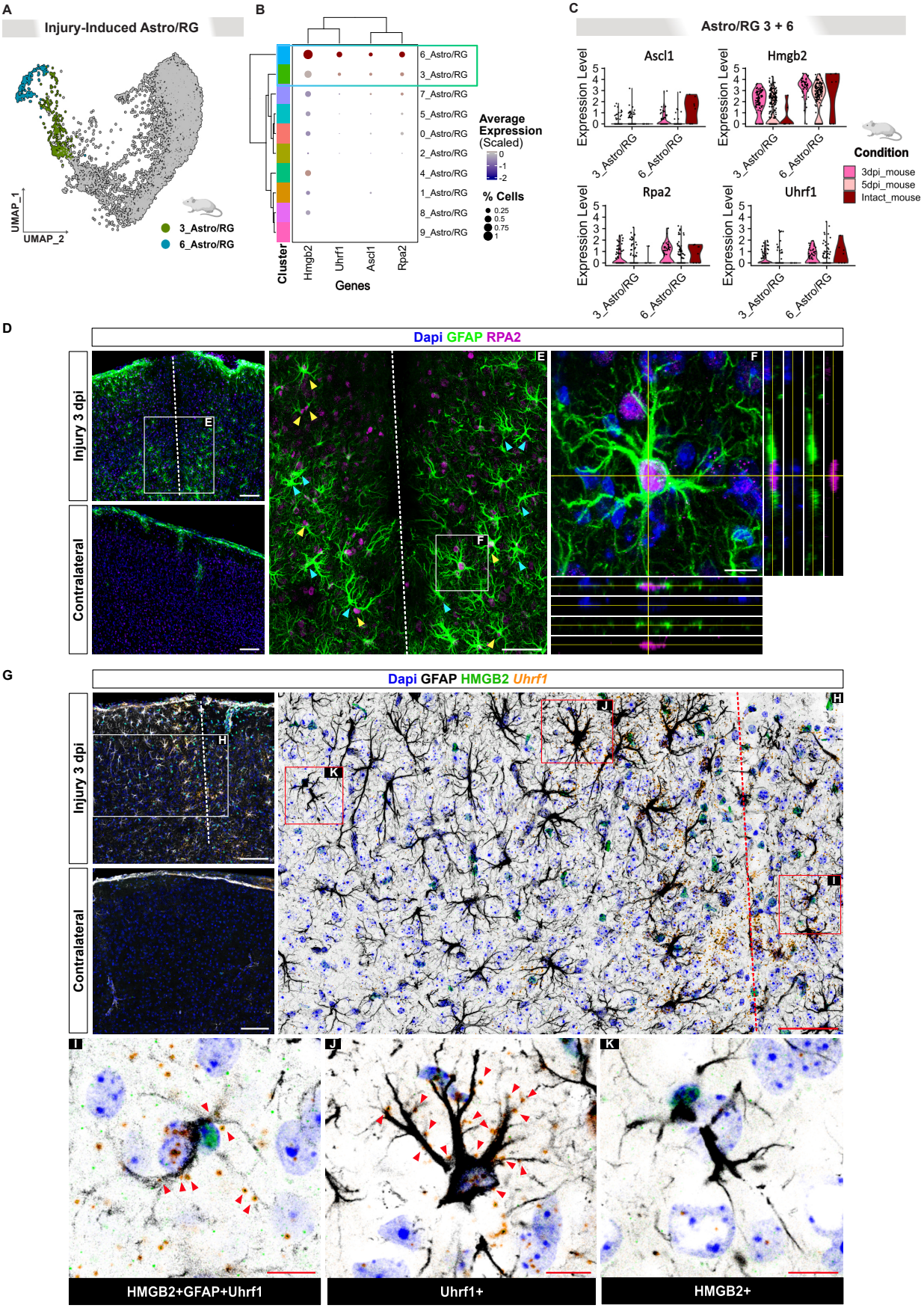

Figure 3, Maddhesiya *et al.*

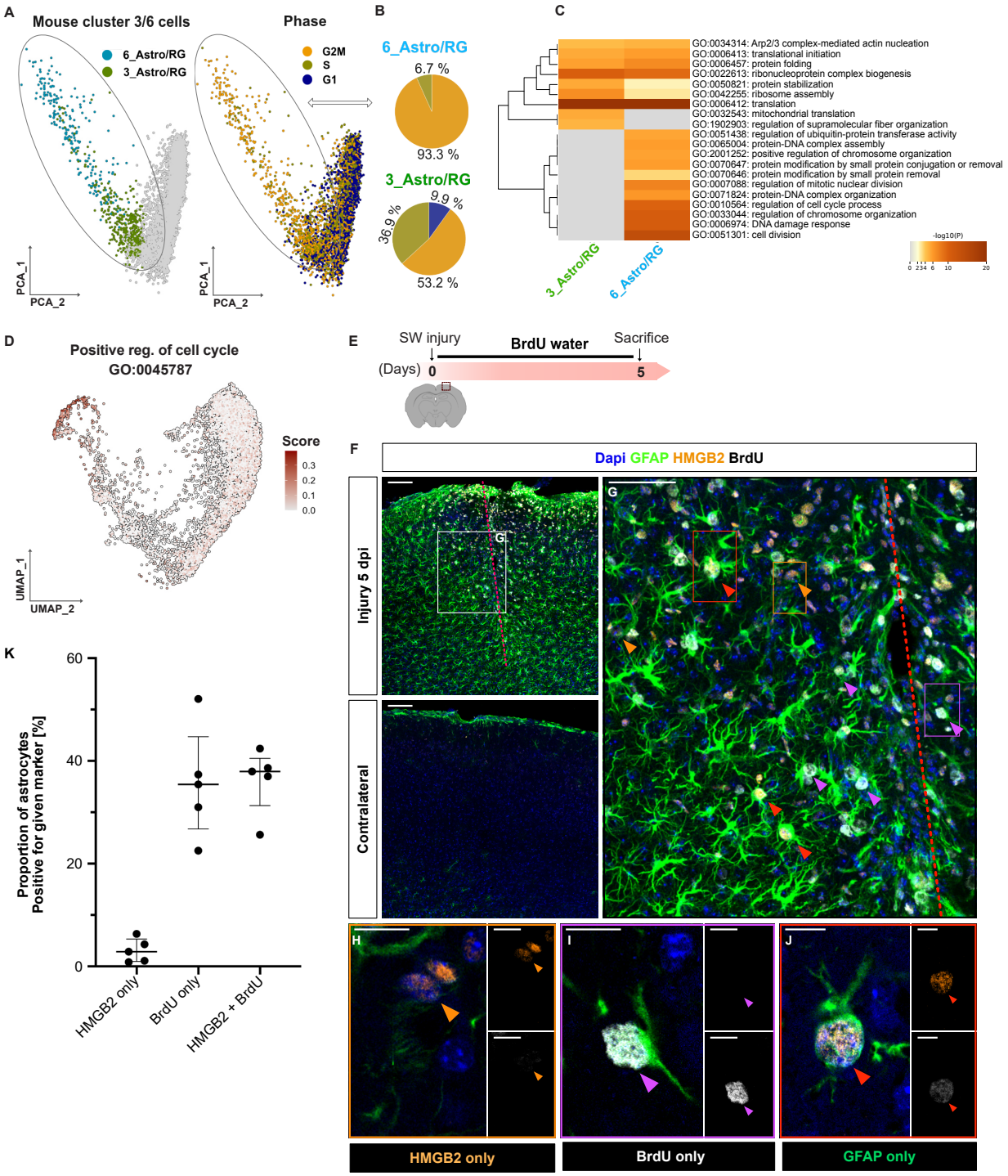

Figure 4, Maddhesiya *et al.*

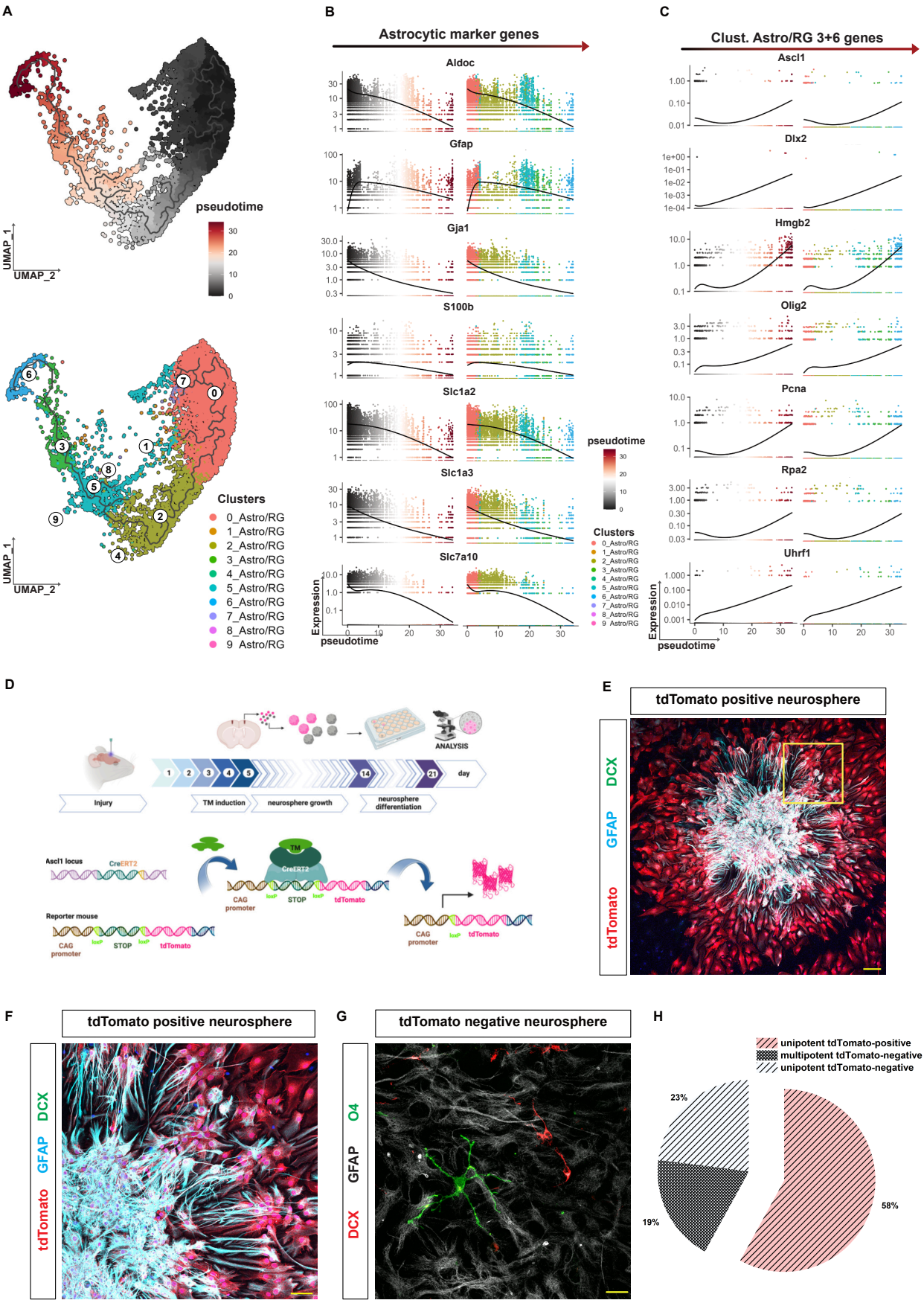

Figure 5, Maddhesiya *et al.*

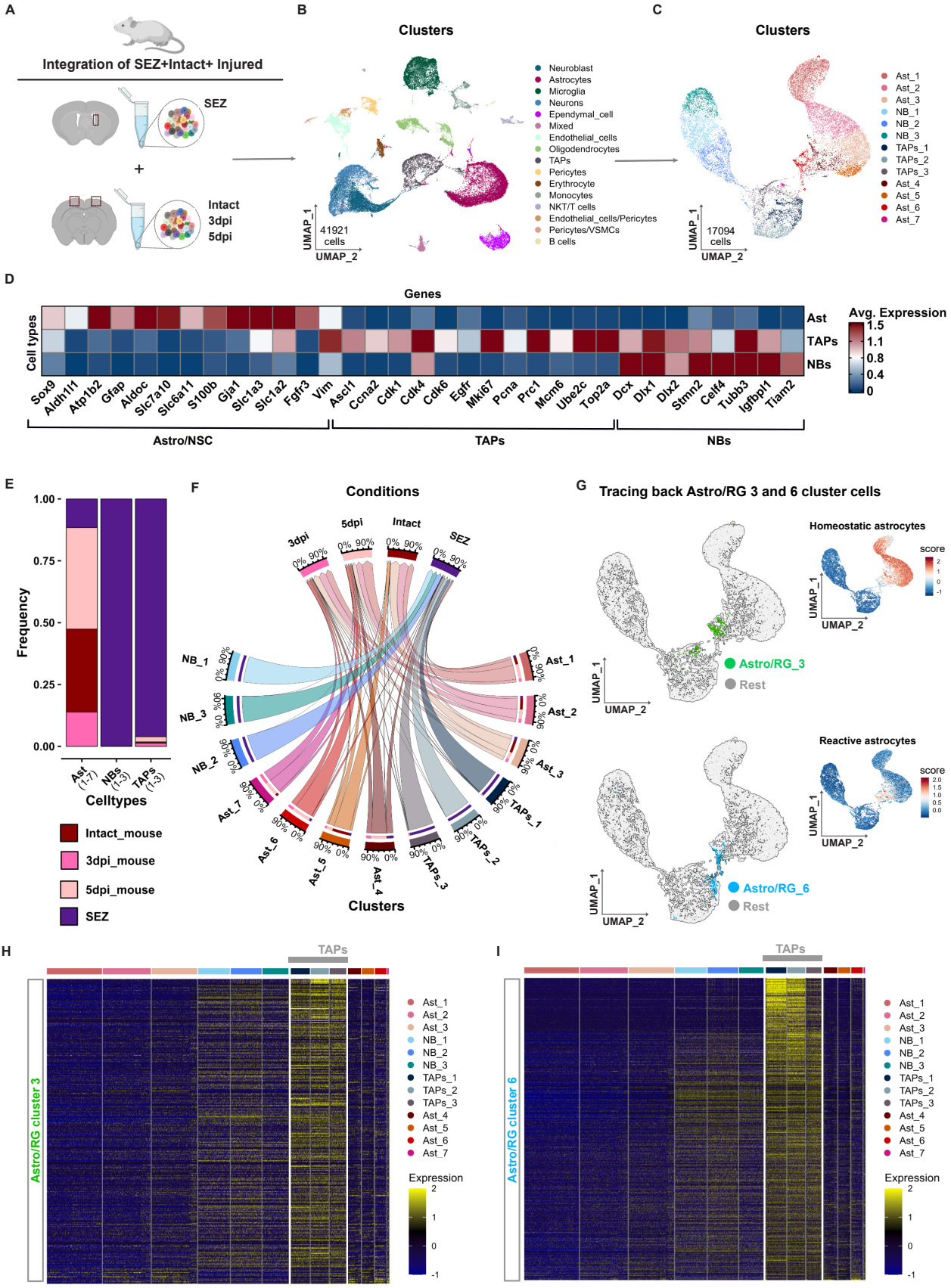

Figure 6, Maddhesiya *et al.*

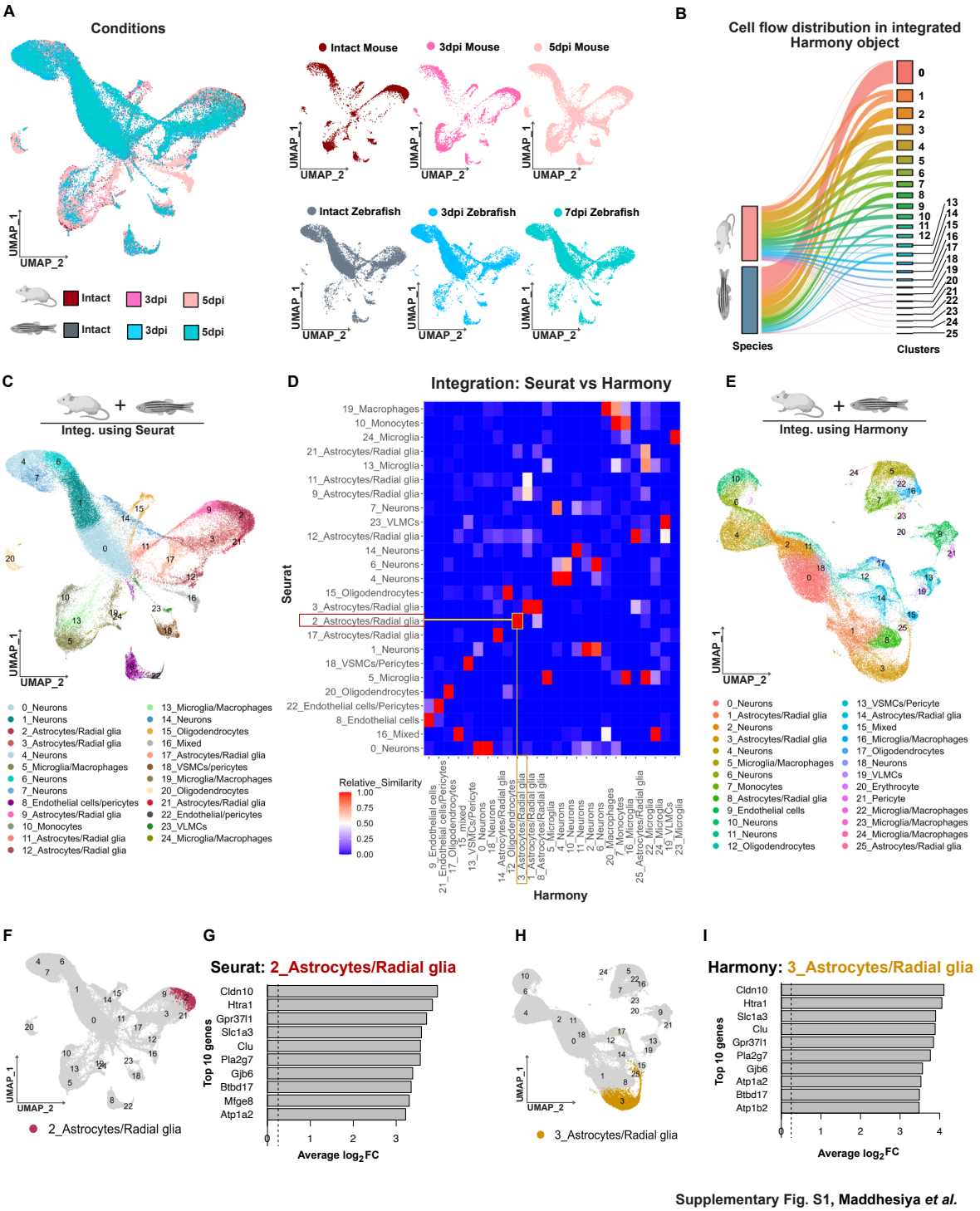

Supplementary Fig. S1, Maddhesiya *et al.*

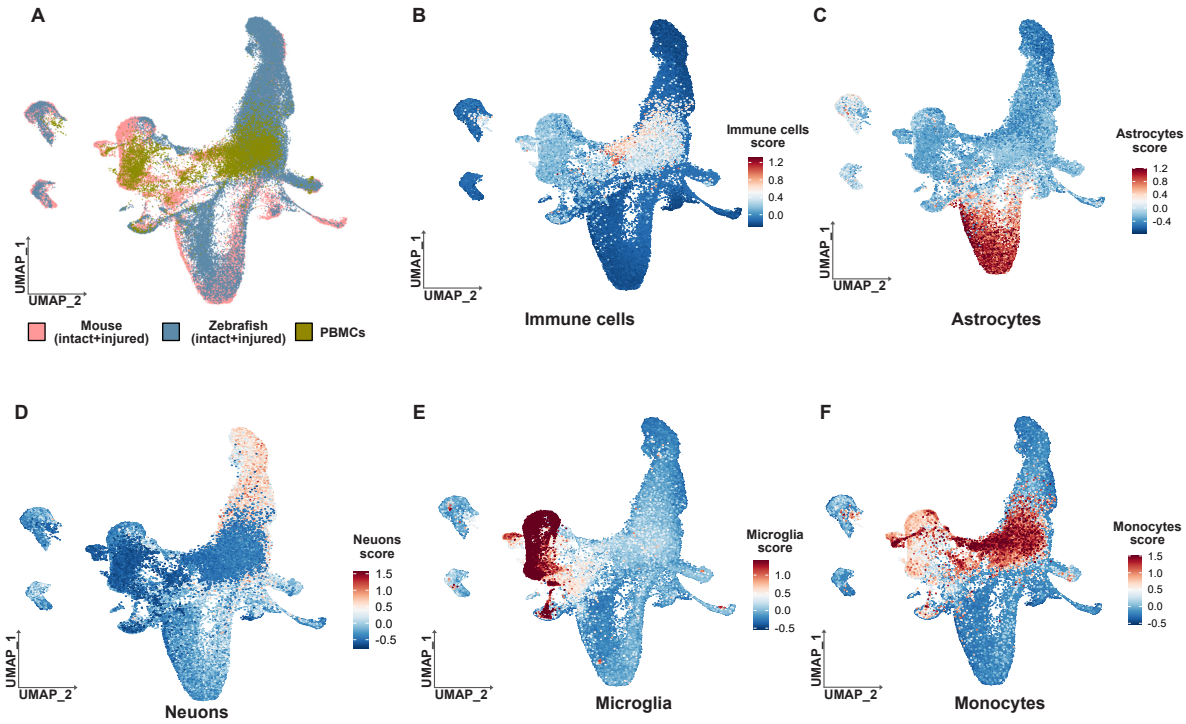

Supplementary Fig. S2, Maddhesiya *et. al.*

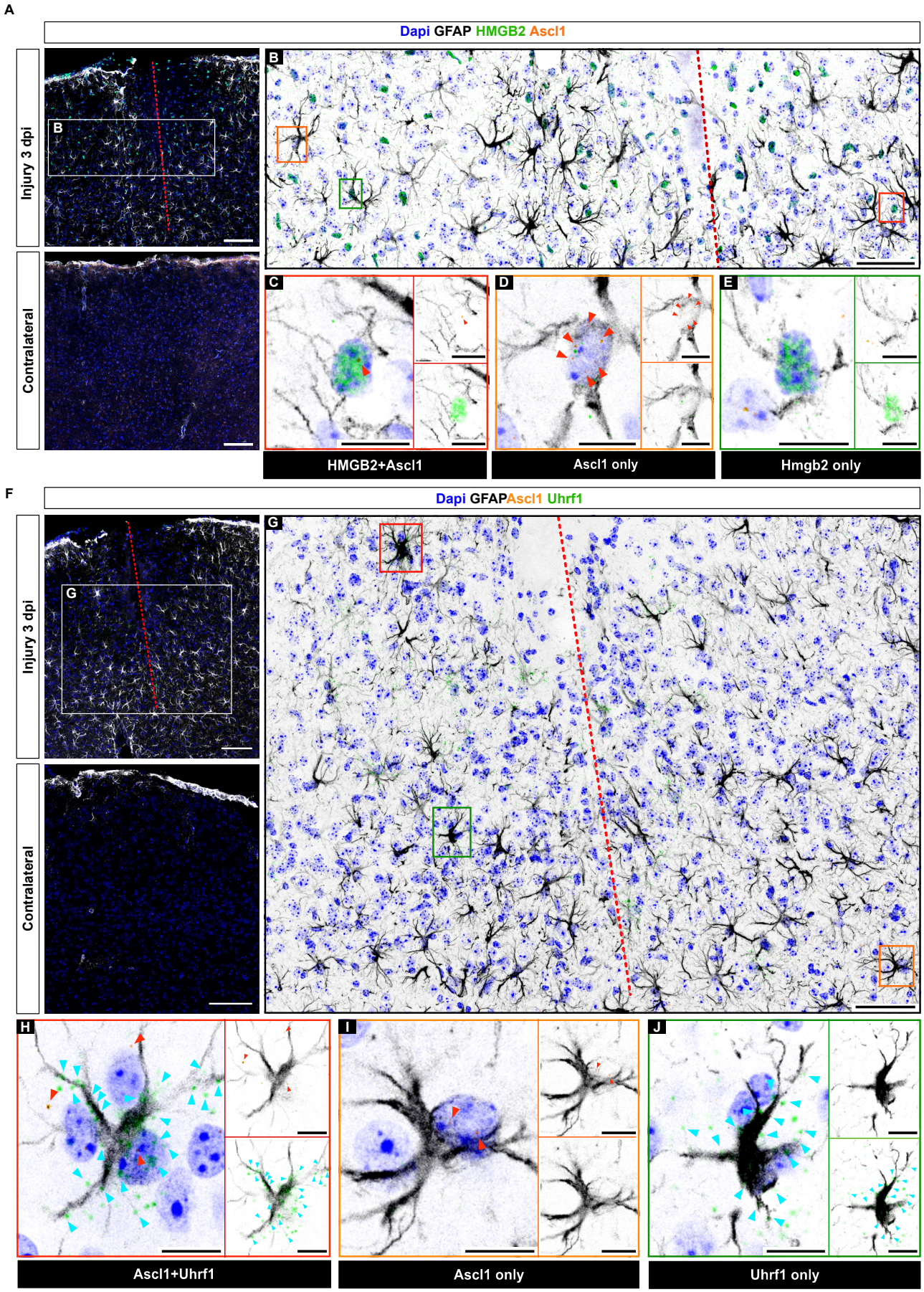

Supplementary Fig. S3, Maddhesiya *et al.*

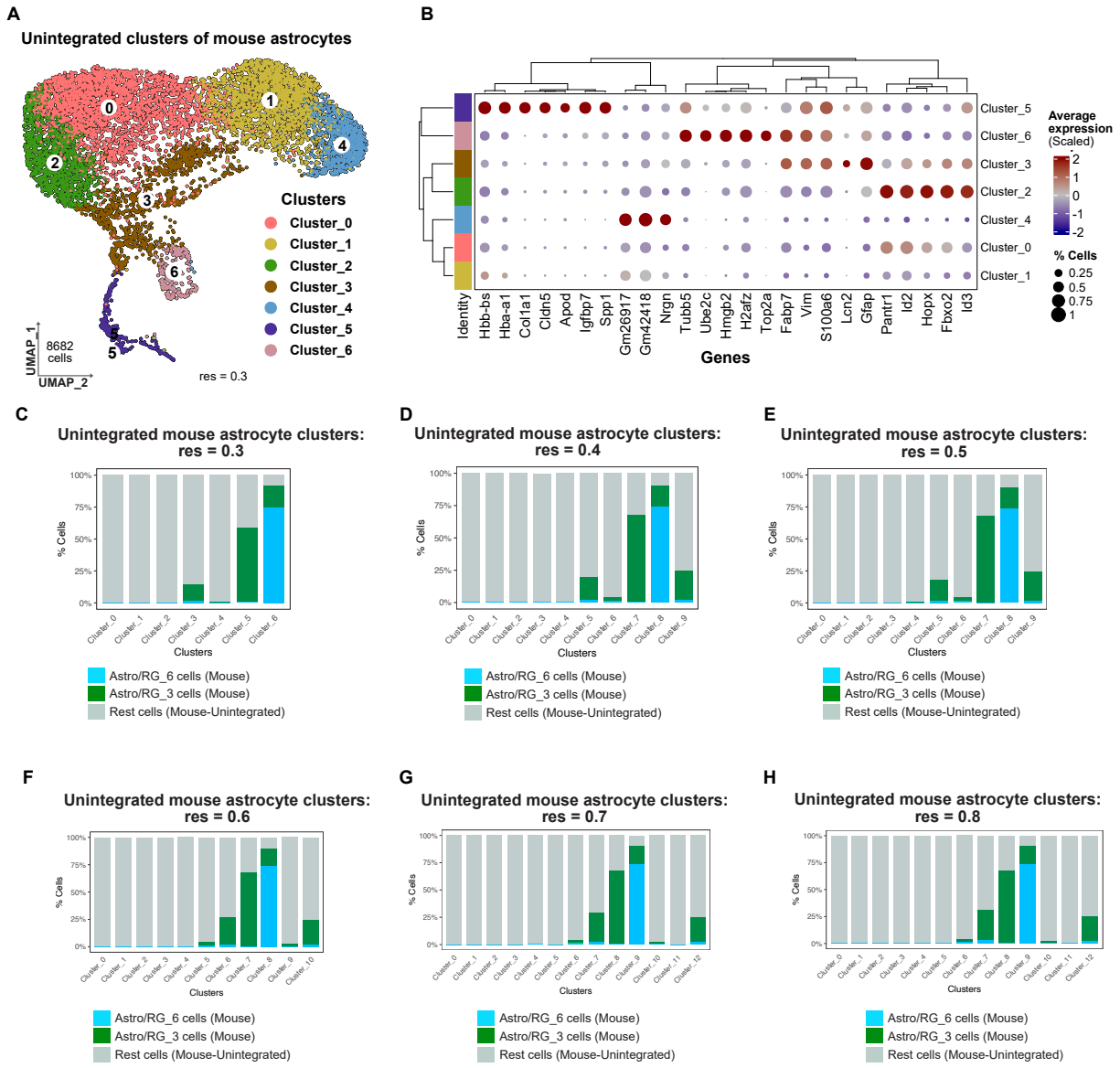

Supplementary Fig. S4, Maddhesiya *et al.*

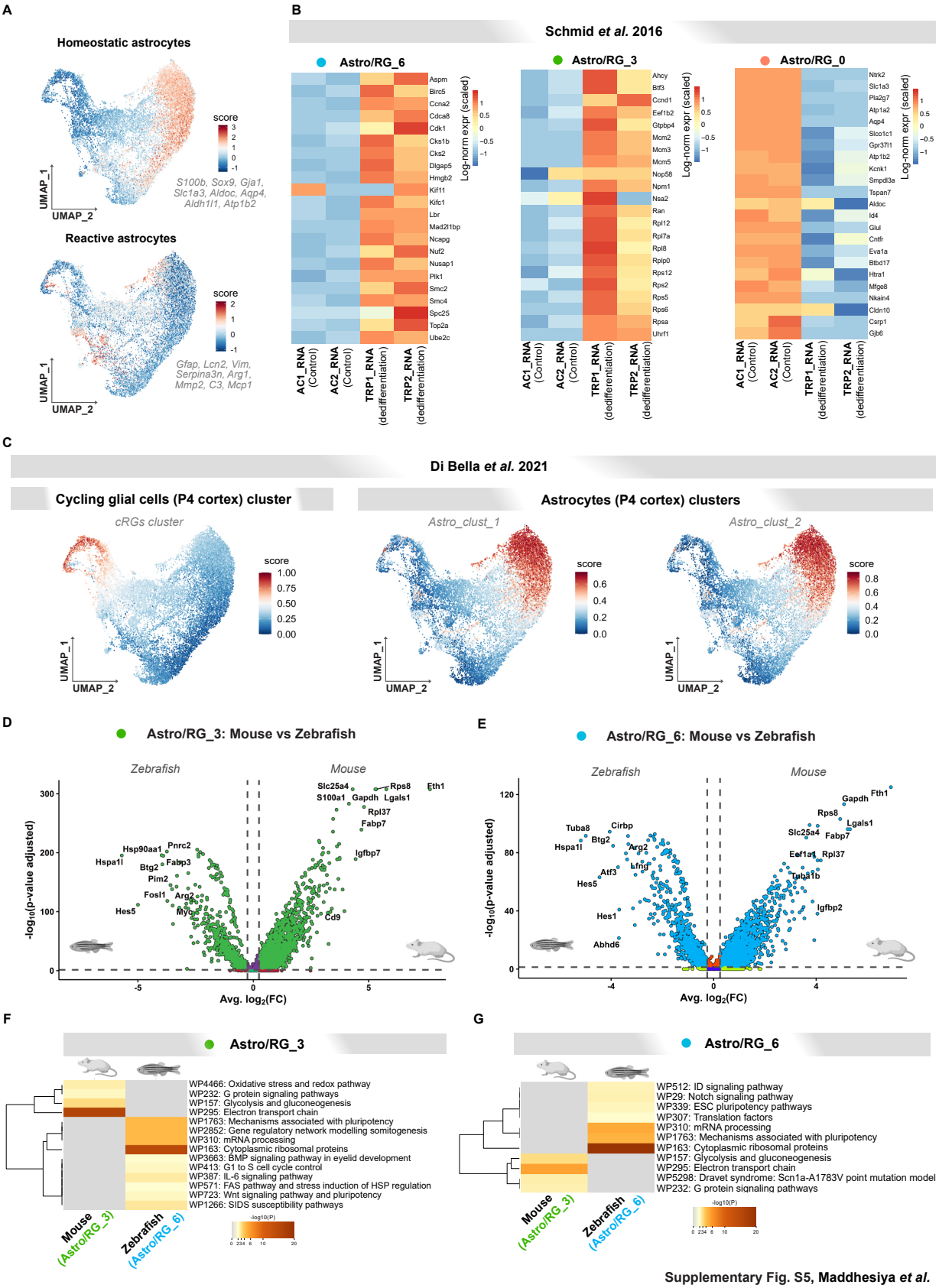

Supplementary Fig. S5, Maddhesiya *et al.*

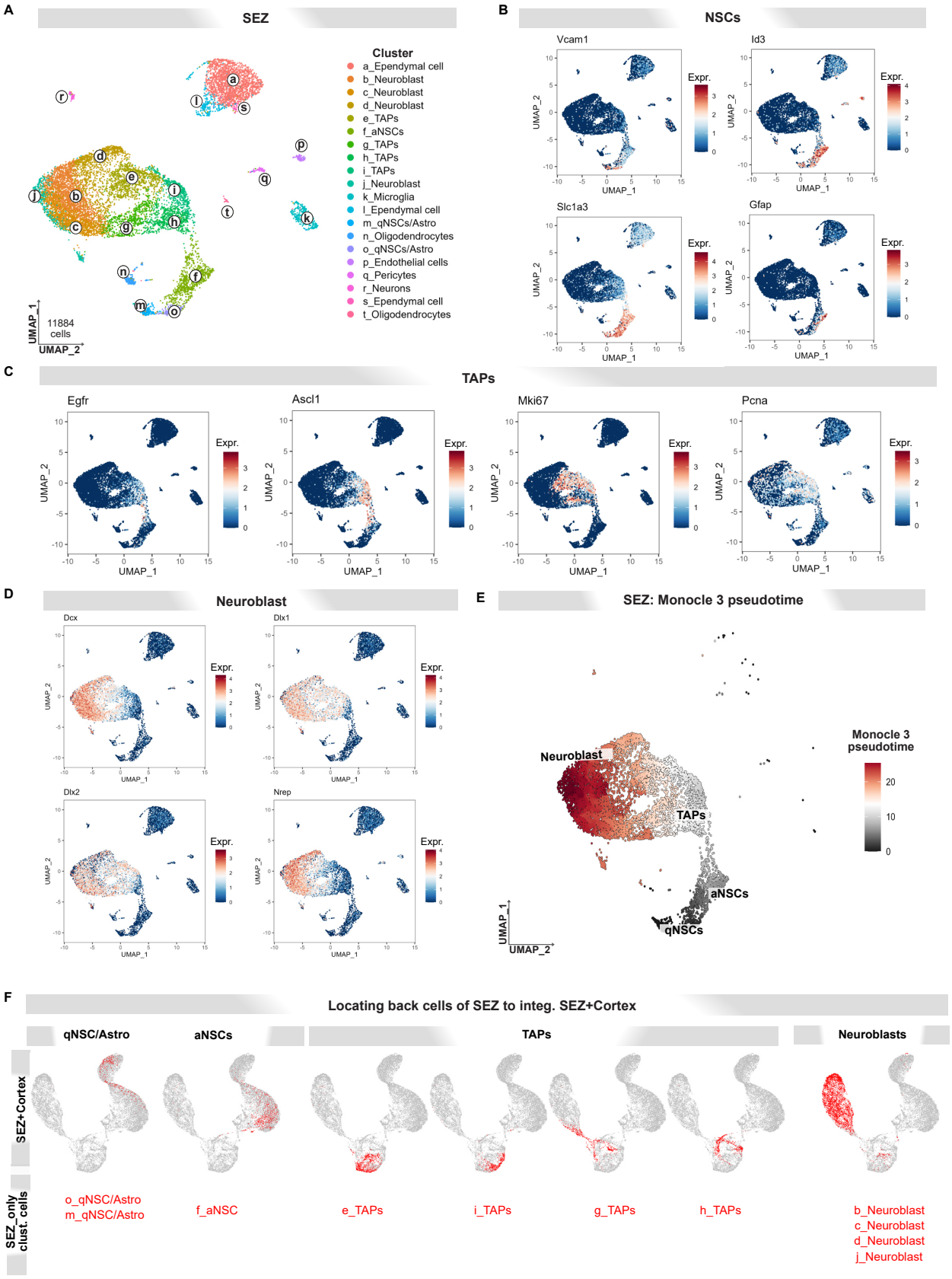

Supplementary Fig. S6, Maddhesiya *et al.*

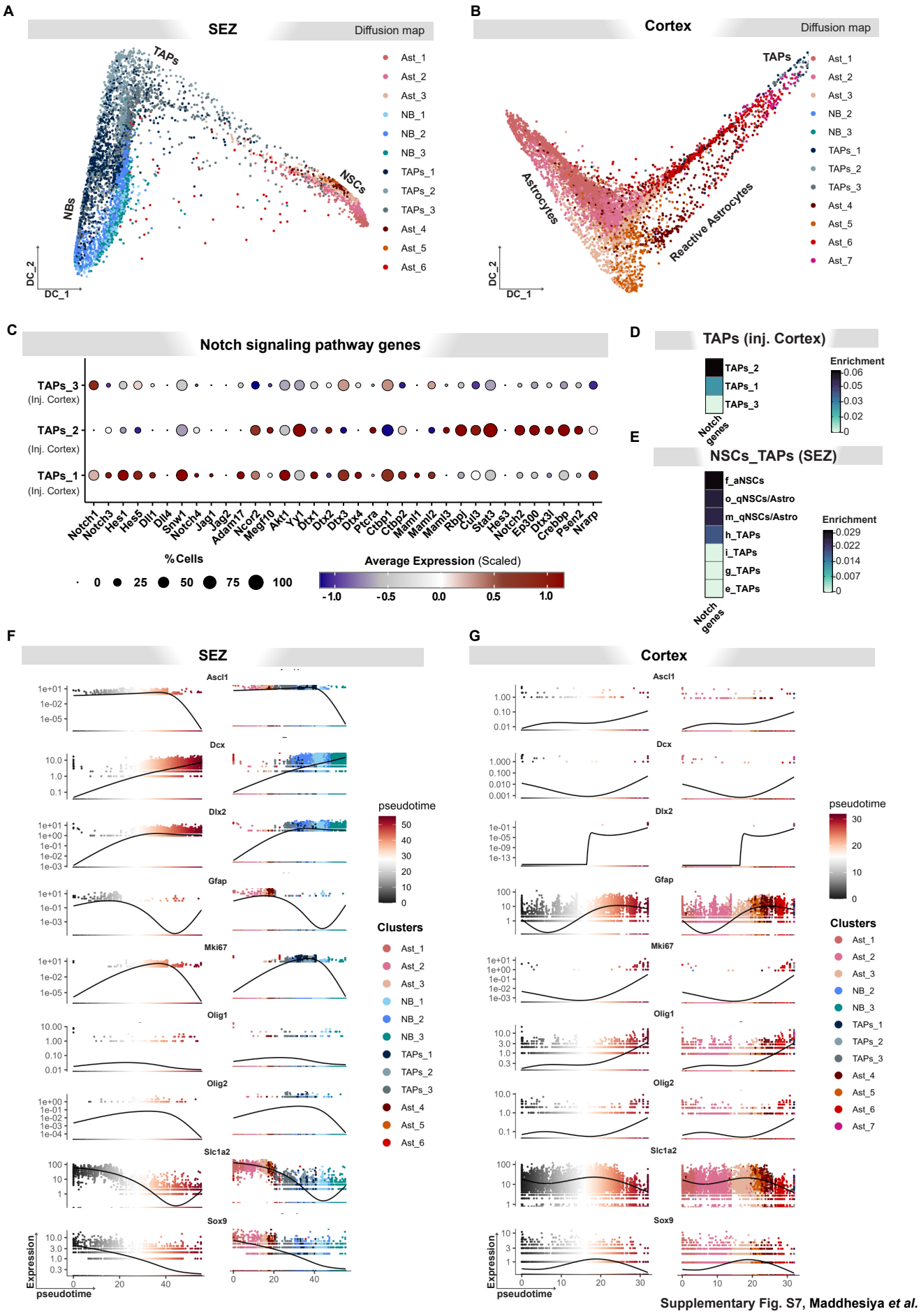

Supplementary Fig. S7, Maddhesiya *et al.*

Supplementary Tables

Supplementary Tables 1: Cell type-specific marker genes used for annotation of integrated mouse and zebrafish clusters.

Supplementary Table 2: Known immune cell markers used for annotation of peripheral blood mononuclear cells (PBMCs).

Supplementary Table 3: Gene list used to generate score for positive regulation of cell cycle (GO:0045787).

Supplementary Table 4: Gene list used to generate score for cycling glial progenitors and astrocytes clusters of P4 cortex (Di Bella et al., 2021).

Supplementary Table 5: Differentially expressed genes between Astro/RG cluster 3 and 6 cells originating from mouse and zebrafish.

Supplementary Table 6: Marker genes used to identify NSC/Astro, TAPs and NBs.

Supplementary Table 7: Differentially expressed genes between TAPs_1 cortical cluster and TAPs_3 SEZ cluster.

Supplementary Table 8: List of notch signaling genes.

Authors contribution

P.M, J.N., and F.B. conceived the project and designed bioinformatic experiments. C.K., A.Z., J.F.S. generated single cell sequencing data. P.M. performed the bioinformatic analyses. F.B. performed Immunohistochemical analyses. J.N, K.T.N, S.J, and T.S. performed neurosphere assay. P. M. and J.N. wrote the manuscript with input from all authors.

2.2 Aim of study II

The aim of this study is to investigate how the direct conversion of astrocytes to neurons is affected by the growth factor environment and the chromatin structural protein HMGB2. It demonstrates that Hmgb2 improves the reprogramming efficiency by opening the chromatin and expression of neuronal genes in cooperation with the neurogenic factor Neurog2.

Hmgb2 improves astrocyte to neuron conversion by increasing the chromatin accessibility of genes associated with neuronal maturation in a proneuronal factor-dependent manner

Priya Maddhesiya*, Tjasa Lepko Modic*, Andrea Steiner-Mezzardi, Veronika Schwarz, Juliane Merl-Pham, Finja Berger, Stefanie M. Hauck, Lorenza Ronfani, Marco Bianchi, Giacomo Masserdotti, Magdalena Götz, Jovica Ninkovic

* These authors contributed equally to the manuscript

My contribution to this manuscript in detail:

For the manuscript, I performed bioinformatic analyses of RNA-seq and ATAC-seq data to investigate the specific changes in gene expression and chromatin accessibility associated with efficient astrocyte-to-neuron conversion by Hmgb2 and Neurog2. I evaluated the effects of Hmgb2, Neurog2, and their combination under EGF+FGF2 and FGF2 culture conditions. I used different tools to visualize and perform downstream analysis. Furthermore, I contributed to the writing and editing of the manuscript.

The current manuscript is under revision to Genome Biology and the pre-print is available in bioRxiv (2023). doi: https://doi.org/10.1101/2023.08.31.555708

bioRxiv preprint doi: https://doi.org/10.1101/2023.08.31.555708; this version posted September 3, 2023. The copyright holder for this preprint (which was not certified by peer review) is the author/funder. All rights reserved. No reuse allowed without permission.

Hmgb2 improves astrocyte to neuron conversion by increasing the chromatin accessibility of genes associated with neuronal maturation in a proneuronal factor-dependent manner

Priya Maddhesiya[1, 2, 3, §], Tjasa Lepko[1, 2, 3, §], Andrea Steiner-Mezzardi[3], Veronika Schwarz[1, 2, 3], Juliane Merl-Pham[4], Finja Berger[1, 2, 3], Stefanie M. Hauck[4], Lorenza Ronfani[5], Marco Bianchi[5], Giacomo Masserdotti[3, 7], Magdalena Götz[3, 7, 8] and Jovica Ninkovic[1, 2, 3, 8, *]

[1] Biomedical Center Munich (BMC), Department of Cell Biology and Anatomy, Medical Faculty, LMU, Munich, Germany

[2] Graduate School of Systemic Neurosciences, LMU, Munich, Germany

[3] Institute of Stem Cell Research, Helmholtz Zentrum Munich, Munich, Germany

[4] Research Unit Protein Science and Metabolomics and Proteomics Core, Helmholtz Centre Munich, German Research Center for Environmental Health, Neuherberg, Germany

[5] School of Medicine, Vita-Salute San Raffaele University, Milan, Italy

[6] Division of Genetics and Cell Biology, IRCCS San Raffaele Hospital, Milan, Italy

[7] Biomedical Center Munich (BMC), Institute of Physiological Genomics, LMU, Munich, Germany

[8] Munich Cluster for Systems Neurology SYNERGY, LMU, Munich, Germany

[§] These authors contributed equally to this work

* Correspondence to jovica.ninkovic@helmholtz-munich.de

bioRxiv preprint doi: https://doi.org/10.1101/2023.08.31.555708; this version posted September 3, 2023. The copyright holder for this preprint (which was not certified by peer review) is the author/funder. All rights reserved. No reuse allowed without permission.

Abstract

Background:

Direct conversion of reactive glial cells to neurons is a promising avenue for neuronal replacement therapies after brain injury or neurodegeneration. The overexpression of neurogenic fate determinants in glial cells results in conversion to neurons. For repair purposes, the conversion should ideally be induced in the pathology-induced neuroinflammatory environment. However, very little is known regarding the influence of the injury-induced neuroinflammatory environment and released growth factors on the direct conversion process.

Results:

We established a new *in vitro* culture system of postnatal astrocytes without epidermal growth factor that reflects the direct conversion rate in the injured, neuroinflammatory environment *in vivo*. We demonstrated that the growth factor combination corresponding to the injured environment defines the ability of glia to be directly converted to neurons. Using this culture system, we showed that chromatin structural protein high mobility group box 2 (HMGB2) regulates the direct conversion rate downstream of the growth factor combination. We further demonstrated that Hmgb2 cooperates with neurogenic fate determinants, such as Neurog2, in opening chromatin at the loci of genes regulating neuronal maturation and synapse formation. Consequently, early chromatin rearrangements occur during direct fate conversion and are necessary for full fate conversion.

Conclusions:

Our data demonstrate novel growth factor-controlled regulation of gene expression during direct fate conversion. This regulation is crucial for proper maturation of induced neurons and could be targeted to improve the repair process.

bioRxiv preprint doi: https://doi.org/10.1101/2023.08.31.555708; this version posted September 3, 2023. The copyright holder for this preprint (which was not certified by peer review) is the author/funder. All rights reserved. No reuse allowed without permission.

Background

Innovative approaches to stimulate tissue regeneration and functional restoration of the central nervous system are required, because the adult mammalian brain has limited ability to replace lost neurons [1–4]. Direct conversion of glial cells to neurons (induced neurons, iN) is a promising avenue for successful repair [2,5,6]. The overexpression of several neurogenic factors, alone or in combination, induces the conversion of several cell types, including astrocytes, pericytes, oligodendrocyte progenitors and fibroblasts, into post-mitotic neurons with different well-defined neurotransmitter identities [7–24]. These strong inducers of the neurogenic fate are transcription factors (TFs) that specify neuronal fate during development [7]. Many of these TFs have recently been shown to have pioneering factor activity and to bind closed chromatin configurations [5,25,26]. Indeed, recent insights regarding the fundamentals of neuronal fate specification have revealed that changes in chromatin structure might be a key factor in the stable acquisition of neuronal fate [27,28], in line with the pioneering activity of fate determinants inducing fate conversion. Despite their remarkable strength, defined single pioneering TFs (e.g., Neurog2) cannot successfully reprogram some starting cell types or cell states induced by culturing conditions [14]. The inability of Neurog2 to activate gene expression has been associated with epigenetic silencing of target loci [14,29]. Interestingly, forskolin (an agonist of adenylyl cyclase) and dorsomorphin (an inhibitor of BMP signaling) enhance the chromatin accessibility mediated by Neurog2, thus suggesting that additional pathways contribute to Neurog2's trailblazing properties [30,31]. In fact, treating Neurog2-expressing cells with these small molecules results in chromatin opening at a substantial number of sites, including CRE half-sites or HMG box motifs [30]. Thus, small molecules or a combination of other TFs may be necessary to induce successful or efficient reprogramming, depending on the starting populations, although Neurog2 is a pioneer factor that can overcome the lineage barrier. In addition to several factors associated with chromatin, microRNAs and

bioRxiv preprint doi: https://doi.org/10.1101/2023.08.31.555708; this version posted September 3, 2023. The copyright holder for this preprint (which was not certified by peer review) is the author/funder. All rights reserved. No reuse allowed without permission.

small molecules have been found to improve the conversion efficiency and maturation status of reprogrammed neurons despite being unable to induce conversion on their own [12,15,32,33]. These findings support a model in which multi-level lineage barriers maintain cell identity and must be overcome for cells to acquire neuronal fate adequate for repair purposes. Comprehensive understanding of these barriers is at the core of successful iN generation and the functional restoration of the damaged CNS.

Importantly, most of these barriers have been identified through the use of defined and stable *in vitro* systems. However, for repair purposes, iNs must be generated in the injured environment. The intricacy of the injured milieu is an obstacle to understanding the molecular mechanisms of direct neuronal conversion *in vivo*. Injury triggers the release of several signaling factors with precise temporal resolution that can either resolve or strengthen the lineage barriers [34]. For example, epidermal growth factor (EGF) levels spike within 24 hours after brain injury and remain elevated for 3 days before returning to baseline. In contrast, basic fibroblast growth factor (bFGF) levels begin to rise 4 hours after damage and remain elevated for 14 days [34]. Infusion of bFGF into the brain after traumatic brain injury, for example, greatly enhances cognitive performance in animals by increasing neurogenesis [35]. Additionally, EGF infusion enhances neurogenesis via enlargement of the neurogenic precursor pool in the neurogenic niche after ischemia injury [36]. Moreover, forced Neurog2 expression in glial cells, along with the bFGF2 and EGF growth factors, enhances neuronal reprogramming *in vivo* [37]. Importantly, EGF receptor (EGFR) signaling has been proposed to regulate both global chromatin state and the accessibility of specific loci [38]. Furthermore, interaction of EGFR signaling and chromatin remodelers from the SWI/SNF family is critical for the expansion of beta cells after pancreas injury [39]. Similarly, FGF signaling orchestrates chromatin organization during neuronal differentiation [40]. Together, environmental signals

bioRxiv preprint doi: https://doi.org/10.1101/2023.08.31.555708; this version posted September 3, 2023. The copyright holder for this preprint (which was not certified by peer review) is the author/funder. All rights reserved. No reuse allowed without permission.

93 are likely to be integrated into the lineage barriers defining the propensity of starting glial cells
94 to be converted to postmitotic neurons.

95 To investigate the embedding of growth factors in lineage barriers relevant to *in vivo* direct
96 neuronal reprogramming after brain injury, we developed an *in vitro* model with altered growth
97 factor composition. We showed that, in this model, neurogenic fate determinants induced
98 astrocyte to neuron conversion with a diminished efficiency comparable to the conversion rate
99 observed *in vivo.* This system allowed us to identify Hmgb2 as a novel regulator in the context
100 of direct astrocyte to neuron conversion. We showed that high levels of Hmgb2 alleviate the
101 lineage barrier and promote efficient establishment of neuronal fate. Our data suggest that
102 Hmgb2-dependent chromatin opening of regulatory elements controls the expression of
103 neuronal maturation genes and enables the establishment of the full neurogenic program,
104 thereby resulting in efficient astrocyte to neuron conversion.

105

bioRxiv preprint doi: https://doi.org/10.1101/2023.08.31.555708; this version posted September 3, 2023. The copyright holder for this preprint (which was not certified by peer review) is the author/funder. All rights reserved. No reuse allowed without permission.

Results

Growth factors shape the lineage barriers to glia to neuron conversion

To investigate the contributions of injury-induced growth factors to lineage barriers to maintaining glial fate in the injured mammalian brain, we established a new *in vitro* model with the growth factor composition adjusted to better reflect the local environment after injury. After brain injury, levels of EGF peak within the first 24 h and return to baseline levels 3 days post injury (dpi). In contrast, FGF levels increase by 4 h after injury and persist until 14 dpi [41]. To mimic the dynamics in the *in vivo* environment, we cultured astrocytes, obtained from postnatal murine cerebral cortex (P5–P7) for 10 days in the presence of only bFGF, then compared the direct conversion rates to neurons in this culture with the conversion efficiency in the widely used culture conditions containing both EGF and bFGF [42,43]. To convert astrocytes into neurons, we transduced cells with an MLV-based retrovirus for expression of the neurogenic TFs reported to reprogram astrocytes (Neurog2, Pou3f2 or Sox11; Fig. 1a) *in vitro* and a fluorescent reporter protein. The expression of the fluorescent reporter protein was used to identify the transduced cells. The identity of the transduced cells was probed 7 days after viral transduction (days *in vitro* (div); Fig. 1a). Only cells expressing doublecortin (DCX) and having at least one process longer than three cell somata diameters were identified as neuronal cells, according to Gascon et al. [44] (Fig. 1b, c). The transduction of astrocytes with control viruses for expression of either GFP or dsRed did not induce glia to neuron conversion in any culturing conditions (Suppl. Fig. 1a-d). In contrast, the transduction of astrocytes isolated from EGF+bFGF culture with several neurogenic fate determinants did induce their conversion, and neurons at different maturation stages (on the basis of the complexity of their processes) were observed after 7 div (Fig. 1b, d). Interestingly, neither Neurog2 nor Pou3f2 induced the direct conversion of astrocytes grown in the presence of only bFGF, whereas the culturing conditions did not significantly alter the conversion by overexpression of Sox 11 (Fig.

bioRxiv preprint doi: https://doi.org/10.1101/2023.08.31.555708; this version posted September 3, 2023. The copyright holder for this preprint (which was not certified by peer review) is the author/funder. All rights reserved. No reuse allowed without permission.

1d). Because the culture condition with bFGF contained only half the usual growth factors, we assessed the conversion rate of cultures containing only EGF. Importantly, Neurog2 induced the conversion of astrocytes grown with only EGF at the same rate as astrocytes grown in EGF+bFGF culture medium (Suppl. Fig. 1d-f), in line with the specific role of bFGF in decreasing the conversion rate.

This difference in direct conversion could be explained by the selection of particular cell types during astrocyte expansion with growth factors. Therefore, we assessed the identity of the transduced cells 24 h after transduction by using immunocytochemistry (Suppl. Fig. 2a). Most cells expressed the astrocyte marker S100β in both culture conditions, without any significant differences (Suppl. Fig. 2b, c, f). Similarly, we did not observe any differences in the proportion of GFAP+ cells (Suppl. Fig. 2d-f). In line with reports that astrocytes *in vitro* express the TF Olig2 [45], most cells in both culture conditions expressed Olig2 (Suppl. Fig. 2g-i). Moreover, we observed only a small proportion of DCX+ neuronal progenitors or αSMA+ pericytes in both cultures (Suppl. Fig. 2d-i), thus indicating comparable cellular compositions between cultures, according to the analyzed marker expression. Interestingly, we observed lower proliferation rates of astrocytes grown in bFGF than EGF+bFGF conditions, on the basis of the expression of Ki67 or pH3 (Suppl. Fig. 2j-n). This finding suggested that bFGF-grown astrocytes might further differentiate, epigenetically silence neuronal loci and become less prone to direct conversion, as previously shown for long-term astrocyte cultures [46]. To examine this possibility, we cultured astrocytes for 7 days in bFGF culture conditions, added EGF and grew astrocytes for an additional 7 days with EGF+bFGF (Suppl. Fig 3a). The conversion rate of these astrocytes was compared with that of astrocytes cultured in either EGF+bFGF or bFGF for 14 days (Suppl. Fig. 3b, f). As expected, longer culturing of cells in either bFGF or EGF+bFGF decreased the direct reprogramming rate (Suppl. Fig. f), as previously described [46]. However, the post-culturing of initially bFGF-grown astrocytes in

bioRxiv preprint doi: https://doi.org/10.1101/2023.08.31.555708; this version posted September 3, 2023. The copyright holder for this preprint (which was not certified by peer review) is the author/funder. All rights reserved. No reuse allowed without permission.

156 EGF+bFGF for 7 days improved their reprogrammability, and we observed no differences in
157 the proportions of generated neurons compared with astrocytes continuously cultured in
158 EGF+bFGF (Suppl. Fig. 3b, c, f). Moreover, the conversion rate of EGF+bFGF-grown
159 astrocytes decreased after culturing in bFGF for 7 days, and no differences were observed
160 between this culture and continuously bFGF cultured astrocytes (Suppl. Fig. 3d-f). Together,
161 the cell identity marker analysis and the alterations in the culture composition experiments
162 suggested that growth factor conditions define the astrocytic lineage barriers and consequently
163 the rate of direct conversion to neurons, on the basis of neurogenic factor overexpression.

164

165 **High mobility group box 2 (Hmgb2) levels are decreased in bFGF astrocyte culture**

166 To identify factors responsible for maintaining the astrocytic lineage barrier, we
167 performed label-free LC-MS/MS-based proteome analysis of astrocytes cultured with either
168 bFGF or EGF+bFGF for 10 days. In total, we detected approximately 1700 proteins, of which
169 157 showed differences in levels between culture conditions (1.5-fold change, $p<0.05$): 68
170 significantly enriched in the EGF+bFGF culture and 89 significantly enriched in the bFGF
171 culture (Fig. 1e, Suppl. Table 1). Gene Ontology (GO) analysis revealed an enrichment of
172 cytoskeleton-associated processes in the protein set enriched in the bFGF-grown culture (Fig.
173 1f; Suppl. Table 1), whereas transport across the mitochondrial membrane, metabolic processes
174 and chromatin-associated processes were enriched in the EFG+bFGF induced proteome (2-
175 fold enrichment, $p<0.05$; Fig. 1g). These data are in line with recent evidence indicating that
176 changes in the mitochondrial proteome during astroglia to neuron conversion determine the
177 extent of the direct conversion [47]. Moreover, because chromatin state has been reported to
178 regulate lineage barriers in reprogramming [44,48–52], we searched for chromatin-associated
179 factors differentially enriched between culture systems. The chromatin architectural protein

bioRxiv preprint doi: https://doi.org/10.1101/2023.08.31.555708; this version posted September 3, 2023. The copyright holder for this preprint (which was not certified by peer review) is the author/funder. All rights reserved. No reuse allowed without permission.

Hmgb2 was 1,88-fold enriched in EGF+bFGF compared with bFGF cultures (Fig. 1e). This enrichment was confirmed by western blotting (Fig. 1h, j). Interestingly, we also observed that the HMGB2 protein family member HMGB1 was enriched in the EGF+bFGF culture condition, although at a lower level (Fig. 1e). In the adult mouse brain, Hmgb2 is specifically expressed in cells committed to the neurogenic lineage (transit amplifying progenitors, neuroblasts) in both neurogenic niches [53] in addition, traumatic brain injury induces Hmgb2 expression in a subset of reactive astrocytes (Suppl. Fig. 4). These findings suggest that HMGB2 might be an important factor improving direct conversion in the EGF+bFGF culture.

Hmgb2 levels define the rate of direct astrocyte to neuron conversion

To test whether Hmgb2 might have functional relevance in fate conversion, we transduced astrocytes, grown for 10 days in medium containing either EGF+bFGF or bFGF, with Hmgb2-encoding retrovirus (Fig. 2a), and assessed the identity of the transduced cells 7 days later, on the basis of DCX expression and cell morphology (see above; Fig. 1b-d). Overexpression of Hmgb2 did not alter cell identity in either culture condition (Fig. 2b-e). Most cells retained their astrocyte identity and expressed GFAP (Fig. 2e). However, when we co-transduced the bFGF-grown astrocytes with retroviruses for expression of Neurog2-dsRED and Hmgb2-GFP, we observed a 2.5-fold greater conversion rate in the co-transduced cells than cells transduced with Neurog2 only (Fig. 2c, d). Interestingly, the co-overexpression of Neurog2+Hmgb2 did not further improve the conversion of EGF+bFGF-grown astrocytes, because the conversion rate of Neurog2+Hmgb2 co-transduced astrocytes was comparable to that of Neurog2-transduced astrocytes in this culture condition (Fig. 2b, d).

Improvement in the Neurog2-mediated conversion rate of bFGF-grown astrocytes prompted us to investigate whether this improvement might be factor-specific. Therefore, we

bioRxiv preprint doi: https://doi.org/10.1101/2023.08.31.555708; this version posted September 3, 2023. The copyright holder for this preprint (which was not certified by peer review) is the author/funder. All rights reserved. No reuse allowed without permission.

assessed the effect of Hmgb2 overexpression on Pou3f2-mediated fate conversion, given that the neurogenic capability of Pou3f2 was also diminished in bFGF-grown astrocytes (Fig. 1d). Similarly to the Neurog2-mediated conversion, the simultaneous overexpression of Hmgb2 and Pou3f2 in EGF+bFGF-grown astrocytes did not result in higher conversion rates, whereas the factor combination significantly increased the conversion rate in bFGF-grown astrocytes (Suppl. Fig. 1g). Together, these data suggested that Hmgb2 does not induce direct conversion on its own but increases the ability of neurogenic factors to overcome the lineage barriers.

To test whether Hmgb2 might be necessary for direct astrocyte to neuron conversion, we isolated astroglia from Hmgb2-deficient mice ($Hmgb2^{MUT/MUT}$) and their siblings ($Hmgb2^{WT/MUT}$ and $Hmgb2^{WT/WT}$), cultured them in the direct conversion permissive conditions (EGF+bFGF) and induced conversion by Neurog2 overexpression (Fig. 3a). Neurog2 overexpression induced direct conversion of $Hmgb2^{WT/WT}$ and $Hmgb2^{WT/MUT}$ astrocytes (Fig. 3b-d), in agreement with our previous findings demonstrating high responsiveness of EGF+bFGF-grown astrocytes (Fig. 1d). However, the conversion rate of Hmgb2-deficient ($Hmgb2^{MUT/MUT}$) astroglia significantly decreased compared to WT siblings (Fig. 3c, d). These findings supported our hypothesis that Hmgb2 levels define the astrocytic lineage barrier.

Prospero homeobox protein 1 (Prox1) overexpression improves direct glia to neuron conversion in FGF only culture

To understand the Hmgb2-dependent lineage barrier in direct glia to neuron conversion, we compared the transcriptional changes induced by Neurog2 overexpression in the bFGF and EGF+bFGF cultured cells 48 h after transduction. Cells transduced with different viruses were purified by FACS, and genes regulated by Neurog2 overexpression were compared (Suppl.

bioRxiv preprint doi: https://doi.org/10.1101/2023.08.31.555708; this version posted September 3, 2023. The copyright holder for this preprint (which was not certified by peer review) is the author/funder. All rights reserved. No reuse allowed without permission.

228 Fig. 5). We identified differences in the expression of 443 genes (321 up-regulated and 122
229 down-regulated genes, fold change > 2, padj < 0.05) induced by Neurog2, as compared with
230 that in control CAG-GFP virally transduced cells in the EGF+bFGF culture condition (Suppl.
231 Fig. 6 a, Suppl. Table 2). In the bFGF culture, Neurog2, as compared with the respective CAG-
232 GFP transduced control, induced 171 genes (137 up-regulated and 34 down-regulated genes,
233 fold change > 2, padj < 0.05) (Suppl. Fig. 6 b, Suppl. Table 2). GO analysis (biological
234 processes, fold enrichment > 2 and $p < 0.05$) of genes (321) upregulated in EGF+bFGF culture
235 revealed enrichment in the terms nervous system development, neuronal differentiation, and
236 migration (Fig. 4a), in line with the ability of Neurog2 to successfully convert astroglia to
237 neurons. Unexpectedly, the significantly enriched biological processes in the set of the 137 up-
238 regulated genes in the bFGF culture were also associated with regulation of neurogenesis,
239 nervous system development and synaptic signaling (Fig. 4b), thereby indicating that Neurog2
240 overexpression at least partially induced the neuronal fate in astrocytes grown in the bFGF
241 condition. Indeed, we observed that 96 genes were induced by Neurog2 in both bFGF and
242 EGF+bFGF cultures (Fig. 4c), and were enriched in GO biological processes associated with
243 regulation of neurogenesis, nervous system development, neuronal differentiation and
244 migration (Suppl. Fig. 6c). In addition, in the bFGF culture, the 41 genes uniquely induced by
245 Neurog2 (Fig. 4c) were associated with GO biological processes of cardiac muscle tissue
246 development, leukocyte differentiation, response to lithium-ion and neurotransmitter receptor
247 to the plasma membrane (Suppl. Fig. 6d). These findings suggested that, in contrast to the
248 EGF+bFGF culture, in the bFGF culture, Neurog2 induced other fates along with neuronal
249 processes possibly interfering with the establishment of the neuronal identity [54]. Furthermore,
250 we identified 225 uniquely Neurog2-induced genes in the EGF+bFGF culture (Fig. 4c)
251 associated with the GO biological processes regulation of membrane potential and ephrin
252 receptor pathway (Suppl. Fig. 6d), which regulate neuronal maturation and axonogenesis

bioRxiv preprint doi: https://doi.org/10.1101/2023.08.31.555708; this version posted September 3, 2023. The copyright holder for this preprint (which was not certified by peer review) is the author/funder. All rights reserved. No reuse allowed without permission.

[55,56]. Moreover, previously reported Neurog2-induced genes necessary for successful conversion, such as *Neurod4*, *Insm1*, *Hes6*, *Slit1*, *Sox11* and *Gang4* [46] were up-regulated in both cultures (Fig. 4d). Nevertheless, genes such as *Dscaml1*, *Prox1*, *Lrp8* and *Shf* were induced in only the EGF+bFGF culture. Importantly, the co-expression of Neurog2 and Hmgb2 in bFGF-grown astrocytes induced the expression of these genes to levels similar to those detected in the Neurog2-transduced EGF+bFGF culture (Fig. 4d). Therefore, the bFGF culture established the lineage barrier by interfering with the induction of a small, specific set of genes relevant for the conversion. To test this hypothesis, we selected one candidate, Prox1, and evaluated whether it might help overcome the bFGF only medium restrictive conditions. We overexpressed Prox1 in the bFGF-cultured cells and observed only a small increase in the conversion rate (Fig. 4e). However, after the co-expression of Neurog2 and Prox1 in bFGF-cultured astrocytes, we observed a significant increase in the proportion of generated neurons similar to the conversion rate induced by Neurog2 in the EGF+bFGF culture and the bFGF-cultured astrocytes co-transduced with Neurog2 and Hmgb2 (Fig. 4e). Moreover, microRNA-mediated knockdown of Prox1 decreased the Neurog2-mediated conversion of EGF+bFGF cultured astrocytes, in line with previous reports [46]. This conversion rate was also comparable to the rate of Neurog2-mediated conversion of bFGF-cultured astrocytes (Fig. 4e).

Hmgb2-dependent expression of a specific set of neuronal maturation genes is necessary for efficient direct glia to neuron conversion

Our data suggested that low Hmgb2 expression levels in the bFGF culture could decrease astrocyte to neuron conversion via several non-mutually exclusive mechanisms: a) failure to activate the full neurogenic program induced in EGF+bFGF culture, b) prevention of the silencing of the conflicting alternative lineages and c) induction of a different neurogenic program from that in the EGF+bFGF culture. To directly test these possibilities, we analyzed

bioRxiv preprint doi: https://doi.org/10.1101/2023.08.31.555708; this version posted September 3, 2023. The copyright holder for this preprint (which was not certified by peer review) is the author/funder. All rights reserved. No reuse allowed without permission.

277 the transcriptomic changes induced by the overexpression of Hmgb2 alone or in combination
278 with Neurog2 in both bFGF and EGF+bFGF cultures.

279 Interestingly, Hmgb2 overexpression induced only several differentially expressed genes
280 (DEGs) in either EGF+bFGF or bFGF cultures with respect to CAG-GFP control viral
281 transduction ((Suppl. Fig. 6e, f; FC >2, padj < 0.05): two DEGs in the bFGF condition and four
282 DEGs in the EGF+bFGF culture condition, Suppl. Table 2). This transcriptomic analysis,
283 together with the lack of change in the conversion rate after Hmgb2 overexpression in both
284 bFGF and EGF+bFGF astrocytes (Fig. 2d), suggested that Hmgb2 did not implement any
285 specific neurogenic program on its own. Notably, the overexpression of Hmgb2 together with
286 Neurog2 in the bFGF culture, as compared with control viral transduction, induced 255 genes
287 (Fig. 3 g). This gene set was significantly enriched in GO biological processes associated with
288 neural development, neuronal migration, axon guidance and synaptic signaling (Fig. 4f),
289 similarly to the GO biological processes induced by Neurog2 alone in the EGF+bFGF
290 condition (Fig. 4a). In addition, we observed downregulation of 164 genes (Suppl. Table 3)
291 enriched in regulation of cell adhesion, actin filament organization, stress fiber assembly, and
292 regulation of protein phosphorylation (Suppl. Fig. 6g), thus suggesting that simultaneous
293 overexpression of Neurog2 and Hmgb2 suppresses gene expression that may block successful
294 conversion of astroglia to neurons, possibly through post-translational modifications [57].
295 However, the down-regulated genes were not associated with specific glial or alternative fates
296 induced by Neurog2 in the bFGF culture (Suppl. Fig. 6g).

297 To determine whether the dual overexpression of Neurog2+Hmgb2 might trigger similar
298 transcriptional programs in the bFGF culture and the Neurog2-transduced the EGF+bFGF
299 culture, we compared induced genes among three conditions: reprogramming prone culture
300 (EGF+bFGF transduced with Neurog2 vs control virus), reprogramming resistant culture
301 (bFGF transduced with Neurog2 vs control virus) and revived reprogramming culture (bFGF

bioRxiv preprint doi: https://doi.org/10.1101/2023.08.31.555708; this version posted September 3, 2023. The copyright holder for this preprint (which was not certified by peer review) is the author/funder. All rights reserved. No reuse allowed without permission.

transduced with Neurog2+Hmgb2 vs control virus). We identified 88 genes that were shared across all three conditions (Fig. 4g) and were enriched in GO biological processes associated with neurogenesis, neuronal differentiation and migration, and trans-synaptic signaling (Suppl. Fig. 6h), in line with our findings that all conditions at least partially induced the neurogenic program. Furthermore, 46 genes (for example, *Prox1*, *Lrp8*, *Shf* and *Dscaml1*) were shared exclusively between the reprogramming prone conditions (bFGF Neurog2+Hmgb2 and EGF+bFGF Neurog2). This gene set was enriched in GO biological processes associated with axonogenesis, positive regulation of neurogenesis, neuron projection guidance, and nervous system development, thus implying that the upregulation of genes induced by the simultaneous overexpression of Neurog2 and Neurog2+Hmgb2 in the bFGF culture are associated with the acquisition of a more mature neuronal phenotype.

Together, our data suggested that the Hmgb2 protein aids in implementing the Neurog2-dependent, neurogenic program in astrocytes by facilitating the induction of a specific set of neurogenic, neuronal maturation-associated genes.

Hmgb2 increases the chromatin accessibility of regions associated with the neurogenic program

We hypothesized that the establishment of the full neurogenic program by high levels of Hmgb2 is associated with Hmgb2-dependent chromatin changes. Therefore, we performed assay for transposase-accessible chromatin with high-throughput sequencing (ATAC-seq) on the cells from the same sorting samples used to generate transcriptomic libraries (Suppl. Fig. 5). We first examined the genome-wide chromatin accessibility profile at transcription start sites (TSSs ± 3.0 Kb) in both bFGF and EGF+bFGF cultures after the overexpression of Hmgb2, Neurog2, Neurog2+Hmgb2 and CAG-GFP control. The accessibility profile of

bioRxiv preprint doi: https://doi.org/10.1101/2023.08.31.555708; this version posted September 3, 2023. The copyright holder for this preprint (which was not certified by peer review) is the author/funder. All rights reserved. No reuse allowed without permission.

Hmgb2 overexpressing astrocytes was comparable to that of the control regardless of the culture condition (Fig. 5a), in line with the lack of changes in the transcriptome and conversion rate analysis (Fig. 2e; Suppl. Fig. 6e, f). We did not observe any discernible increase in chromatin accessibility with simultaneous overexpression of Neurog2+Hmgb2 compared with Neurog2 in EGF+bFGF culture. However, we observed a substantial increase in chromatin accessibility after simultaneous overexpression of Neurog2+Hmgb2 compared with Neurog2 in the bFGF culture (Fig. 5b). This increase in TSS (±3 kb) accessibility might have been due to at least two mutually non-exclusive mechanisms: a) widespread TSS opening after Hmgb2 overexpression, or b) lineage specific changes. Therefore, we analyzed the TSS accessibility of neuronal cell-type-specific genes [58] (Fig. 5c). Whereas we observed the accessibility of these sites increased after both Neurog2 and Neurog2+Hmgb2 overexpression in the EGF+bFGF culture condition, in the bFGF culture condition, the increase in these sites was detectable only after simultaneous overexpression of Neurog2+Hmgb2 but not Neurog2 alone (Fig. 5c). Interestingly, the TSS opening was comparable between bFGF and EGF+bFGF astrocytes after Neurog2+Hmgb2 overexpression (Fig. 5c), in line with an increased conversion rate. Next, we wondered whether the Hmgb2-dependent increase in accessibility might be confined to neuronal genes or whether it might also occur in genes specific for other cell lineages. Therefore, we analyzed the dependence of the promoter accessibility of genes identifying ES cells [59,60], endothelial cells [61–63], and microglial cells [64,65] on Hmgb2 levels in bFGF culture (Fig. 5d). We found no significant differences in accessibility between the Hmgb2, Neurog2 or Neurog2+Hmgb2 treated astrocytes and the controls, thus indicating that the accessibility change after Neurog2+Hmgb2 overexpression was specific for neuronal fate.

To identify direct conversion relevant changes in chromatin accessibility dependent on Hmgb2 levels, we determined the significant differentially accessible sites (DASs) after

bioRxiv preprint doi: https://doi.org/10.1101/2023.08.31.555708; this version posted September 3, 2023. The copyright holder for this preprint (which was not certified by peer review) is the author/funder. All rights reserved. No reuse allowed without permission.

overexpression of Neurog2 and Neurog2+Hmgb2, compared with CAG-GFP-transduced cells, in the bFGF and EGF+bFGF culture conditions. In the bFGF culture, Neurog2 overexpression resulted in 612 DASs (445 more accessible sites (MASs) and 167 less accessible sites (LASs); Fig. 5e, Suppl. Table 4). Combined overexpression of Neurog2+Hmgb2 in the bFGF culture resulted in 1213 DASs (1062 MASs and 151 LASs; Fig. 5e, Suppl. Fig. 7a). However, this increase in accessibility did not change the accessibility profile induced by Neurog2 and Neurog2+Hmgb2 in the bFGF culture, because we observed a similar distribution of MAS in the gene bodies, promoters and intergenic regions (Suppl. Fig. 7b, c). Importantly, the Hmgb2-associated increase in MASs was not observed in EGF+bFGF astrocyte culture (Fig 5e), in agreement with our transcriptome analysis. To reveal the processes influenced by MASs, we analyzed genes associated with these sites (defined as genes within 3 kb upstream and downstream of the MAS) in GO analysis. MASs induced by the simultaneous overexpression of Neurog2+Hmgb2 in the bFGF culture were associated with nervous system development, synaptic membrane adhesion, axon guidance, synapse assembly and chemical synaptic transmission (Fig. 5f, Suppl. Table 5). This finding suggests that Hmgb2 (together with Neurog2) increases the accessibility of genes involved in neuronal maturation. Indeed, the promoters of synapse-associated genes such as *Kif1a* [66,67], *Artn* [68] and *Rasd2* [69] were closed in the bFGF culture after either control viral transduction or Hmgb2 overexpression (Fig. 5h), in line with the astrocytic fate of these cells. Moreover, Neurog2+Hmgb2 overexpression opened the synapse-associated promoters to a significantly greater extent than Neurog2 alone (Fig. 5g, h). We then asked whether the chromatin opening state of all or only a subset of Neurog2-induced maturation genes depended on the expression of Hmgb2. Therefore, we compared the MASs induced by Neurog2 in the two conversion prone conditions (overexpression of Neurog2 in EGF+bFGF and overexpression of Neurog2+Hmgb2 in bFGF culture) with MASs induced by Neurog2 in the conversion resistant condition (overexpression

bioRxiv preprint doi: https://doi.org/10.1101/2023.08.31.555708; this version posted September 3, 2023. The copyright holder for this preprint (which was not certified by peer review) is the author/funder. All rights reserved. No reuse allowed without permission.

of Neurog2 in bFGF culture). We identified 395 MASs commonly induced in both conversion prone conditions (Fig. 6a). These MASs were enriched in processes associated with synapse formation (GO biological processes such as nervous system development, synaptic organization, trans-synaptic signals, potassium transport, and synaptic membrane adhesion; Fig. 6b, Suppl. Table 6). Importantly, the increase in the accessibility of these synapse-associated loci correlated with the increased expression of these genes after Neurog2+Hmgb2 overexpression in bFGF culture (Suppl. Fig. 8 a, b). However, we also observed 268 MASs induced by Neurog2 in all three conditions (Fig. 6a) that were enriched in synaptic processes (Fig. 6c, Suppl. Table 6). Therefore, these data suggested that the chromatin containing only a subset of genes associated with neuronal maturation was dependent on Hmgb2. However, the accessibility of these genes appeared to be instrumental for direct conversion.

Together, our data supported a model in which Hmgb2 fosters the establishment of the full neurogenic program by increasing the accessibility and consequently the expression of neuronal maturation genes, thus leading to improved neuronal maturation.

Hmgb2-dependent chromatin sites contain both E-boxes and Pou factor binding sites important for neuronal maturation

HMG proteins play a major role in controlling gene expression by increasing chromatin accessibility [70–72]. Therefore, we sought to identify the potential TF binding motifs enriched in the Hmgb2-dependent set of MASs (395 sites in Fig. 6a). To do so, we performed *de novo* motif enrichment analysis using BaMMmotif software. Motifs containing the consensus binding sequence of the Tal-associated TF family (Neurod1, Neurog2, Neurod2, Atoh1 and Msgn1) were enriched in Hmgb2-dependent set of MASs (Fig. 6d, Suppl. Table 7). In addition, we identified the motif that best matched the consensus sequence of the TF family of POU

bioRxiv preprint doi: https://doi.org/10.1101/2023.08.31.555708; this version posted September 3, 2023. The copyright holder for this preprint (which was not certified by peer review) is the author/funder. All rights reserved. No reuse allowed without permission.

400 domain factors, such as Pou2f2 (Fig. 6e, Suppl. Table 7). Pou2f2 is a direct Neurog2 target [73]
401 and has been reported to be involved in the implementation of proper neuronal identity [74,75].
402 This finding suggested that in the bFGF culture, some of the E-box motif sites bound by
403 Neurog2 (Tal related factors) were inaccessible, but with the addition of Hmgb2, these sites
404 became accessible, thereby increasing Neurog2-binding and enhancing reprogramming
405 efficiency. Additionally, we investigated MASs with consensus binding sequences for both
406 Tal-associated factors (Neurog2) and POU domain factors. We identified that 56 of 395 MASs
407 contained binding motifs for both TF families, and were associated with neuronal maturation
408 (GO processes: regulating actin filaments assembly, chemotaxis, and potassium ion transport;
409 Suppl. Fig. 8d and Suppl. Table 7), including the Robo-Slit pathway. Robo-Slit pathway has
410 been reported to regulate not only axonal pathfinding but also neuronal maturation [76].
411 Moreover, we observed enrichment in genes associated with the negative regulation of
412 proliferation, thus possibly improving the terminal differentiation of converted cells.
413 Interestingly, *de novo* motif analysis of the common 268 Neurog2-induced MASs identified
414 the binding motif of the TF family of Tal-associated factors, but not of the POU domain factors
415 (Fig. 6d). These data suggested that Hmgb2 levels set the lineage barrier by controlling the
416 accessibility of both the direct Neurog2 targets and targets of TFs downstream of Neurog2,
417 such as Pou3f2 or Neurod.

418 To directly test the importance of Hmgb2 in neuronal maturation, we analyzed the
419 neurite complexity of the converted neurons in the conversion prone cultures (overexpression
420 of Neurog2 in EGF+bFGF and overexpression of Neurog2+Hmgb2 in bFGF culture) and the
421 conversion resistant culture (overexpression of Neurog2 in bFGF culture) in induced neurons
422 with Sholl analysis 7 days after viral transduction (Fig. 7a). Indeed, Neurog2-induced neurons
423 in the bFGF culture showed fewer intersections than the Neurog2-induced neurons in the
424 EGF+bFGF culture (Fig. 7b, c). Lower neurite complexity is indicative of less mature neurons.

bioRxiv preprint doi: https://doi.org/10.1101/2023.08.31.555708; this version posted September 3, 2023. The copyright holder for this preprint (which was not certified by peer review) is the author/funder. All rights reserved. No reuse allowed without permission.

425 The complexity of neurites in neurons generated from bFGF astrocytes by the combined
426 overexpression of Neurog2 and Hmgb2 increased compared to overexpression of Neurog2
427 only. These converted neurons were indistinguishable from those generated by overexpression
428 of Neurog2 in the EGF+bFGF-cultured astrocytes (Fig. 7b, c).

429

bioRxiv preprint doi: https://doi.org/10.1101/2023.08.31.555708; this version posted September 3, 2023. The copyright holder for this preprint (which was not certified by peer review) is the author/funder. All rights reserved. No reuse allowed without permission.

Discussion

The establishment of neuronal identity during direct astrocyte to neuron conversion is achieved in very different environmental context from that of the bona fide neurogenesis occurring during embryonic development or in adult brain neurogenic niches [49,51]. This includes not only the different starting populations [49] but also the unique signaling milieus [77–79]. The growth factors released after injury regulate the conversion process, including neuronal maturation and neural circuit repair. Here, we presented a novel *in vitro* system to study the influence of growth factors on fate conversion. Using this system, we showed that EGF, potentially provided by the injured environment, is necessary for efficient neuronal conversion and proper maturation via the regulation of the chromatin binding protein Hmgb2. In combination with several different neurogenic fate determinants, Hmgb2 is capable of inducing the full neurogenic program, as indicated by Hmgb2 gain and loss of function experiments. Our model predicted that prolonged injury-induced elevation in bFGF levels decreased the reprogrammability of astrocytes to neurons. However, the FGF signal per se did not prevent the induction of a set of processes associated with neurogenesis and neuronal fate in astrocytes during Neurog2-mediated conversion. This finding is in line with reports that the FGF promotes neurogenesis [80–82], although the neuronal subtypes generated in such context differ [82]. Importantly, the chromatin states in direct conversion and during embryonic neurogenesis may differ: the chromatin states during neurogenesis require fewer re-arrangements in embryonic development, because large numbers of neurogenic gene loci in radial glial cells, the neuronal stem cells of the developing CNS, are already in an open configuration [83,84]. Interestingly, genes involved in synapse formation and neuronal maturation are already in an active chromatin state without detectable gene expression in both radial glia and committed neuronal progenitors [83,85], thus implying the existence of an active inhibitory mechanism keeping the progenitor state primed toward neurogenesis and preventing

bioRxiv preprint doi: https://doi.org/10.1101/2023.08.31.555708; this version posted September 3, 2023. The copyright holder for this preprint (which was not certified by peer review) is the author/funder. All rights reserved. No reuse allowed without permission.

455 their premature differentiation. Importantly, Hmgb2 opens the loci of these classes of genes
456 during astrocyte to neuron conversion, thus supporting the concept that overexpression of
457 Neurog2+Hmgb2 endows postnatal astrocytes with some stem cell features. This concept is
458 also in line with the expression of Hmgb2 during activation of quiescent neural stem cells in
459 the adult brain [53] and its role in adult neurogenesis [86]. However, we did observe immediate
460 expression of synaptic genes in postnatal astrocytes without the maintenance of these primed
461 neuronal states, thus suggesting that the mechanisms preventing premature differentiation
462 operating in the neuronal stem cells are not established during astrocyte to neuron conversion.
463 This possibility reinforces the concept that direct neuronal conversion does not fully
464 recapitulate the developmental trajectory underlying neuronal differentiation [44,48]. Instead,
465 the overexpression of reprogramming factors induces early re-arrangements of chromatin along
466 with changes in gene expression. However, during late morphological and functional
467 maturation stages of the induced neurons, changes in chromatin are negligible [87]. Moreover,
468 in our *in vitro* system, we did not observe any changes in astrocyte proliferation due to the
469 overexpression of Hmgb2 alone or in combination with different neurogenic TFs, thus further
470 limiting the spectrum of neural stem cell features induced in the postnatal astrocytes.
471 Interestingly, Hmgb2 induces similar chromatin changes in postnatal astrocytes to the HMG
472 group protein A2, a different HMG-box-containing family member in gliogenic radial glial
473 cells. These chromatin changes are sufficient to prolong the neurogenic phase during cortical
474 development and lead to the generation of new postnatal neurons [88]. During this period,
475 progenitors normally generate glial cells, thus potentially implicating similar mechanisms in
476 the Hmga2-mediated extension of neurogenic period and the Hmgb2-mediated direct astrocyte
477 to neuron conversion. Because Hmga2 is associated with Polycomb signaling [89], testing
478 whether the same system would be operational during the Hmgb2-dependent conversion
479 should prove interesting, because Ezh2 maintains the lineage barriers during fibroblast to

bioRxiv preprint doi: https://doi.org/10.1101/2023.08.31.555708; this version posted September 3, 2023. The copyright holder for this preprint (which was not certified by peer review) is the author/funder. All rights reserved. No reuse allowed without permission.

480 neuron conversion [90]. Both Hmgb2 and Hmga2 bind AT-rich DNA segments with little to
481 no sequence specificity [91][71]. Nevertheless, we observed highly specific Hmgb2-dependent
482 opening of chromatin containing late neuronal maturation genes, thus prompting questions
483 regarding HMG protein binding specificity. This specificity could be provided by an interacting
484 protein, e.g., neurogenic TF Neurog2, because we observed an enrichment of the typical E-box
485 binding sequence in the promoters when Hmgb2 was overexpressed in astrocytes. However,
486 our findings did not reveal a direct interaction of Hmgb2 with Neurog2 via WB or mass
487 spectrometry, thus making this scenario unlikely. An alternative explanation may be that
488 Hmgb2 stabilizes the regulatory loops (transactivation domains, TADs) involved in the
489 expression of synaptic genes. The regulatory roles of such domains have been demonstrated
490 for neurogenesis downstream of Neurog2 during embryonal cerebral cortex development [92].
491 Moreover, both Hmgb2 and Hmga2 have been implicated in TAD establishment [93,94]. The
492 stabilization of regulatory loops induced by Neurog2 may indeed provide a mechanistic
493 explanation for the Hmgb2-dependent opening of chromatin regions containing the Neurog2
494 binding E-boxes. These data further challenge the common belief that Neurog2 is a pioneer
495 TF. In contrast to the on-target pioneering function of Ascl1 during reprogramming [87,95], in
496 fibroblast to neuron conversion, Neurog2 requires additional factors, such as forskolin and
497 dorsomorphin or Sox4, that are necessary for not only late neuronal maturation but also the
498 induction of early reprogramming changes [73,96]. We demonstrated that, at least in the case
499 of astrocyte to neuron conversion, Neurog2 function is dependent on Hmgb2. Because Hmgb2
500 increases the accessibility of various sites, including the binding motif of the Neurog2 target
501 Pou2f2 [92], our data suggested that Neurog2 must open the chromatin of maturation genes
502 that are transcriptionally regulated by direct Neurog2 targets. Our study provides mechanistic
503 insights into previously described improvements in neuronal reprogramming with the infusion
504 of EGF and FGF [37]. Interestingly, EGF and FGF exhibit different temporal dynamics post-

bioRxiv preprint doi: https://doi.org/10.1101/2023.08.31.555708; this version posted September 3, 2023. The copyright holder for this preprint (which was not certified by peer review) is the author/funder. All rights reserved. No reuse allowed without permission.

505 injury, with a very narrow expression window and a presumably diminished activity window
506 of EGF [41]. This window correlates with the expression of Hmgb2, thus suggesting that
507 prolonged expression the either EGF or Hmgb2 after TBI might be important in the success of
508 neuronal replacement therapies. Furthermore, our model may also explain the lower direct
509 conversion rates induced by Neurog2 in some starting cellular populations, such as
510 oligodendrocyte precursor cells [97], in which the promoters might not yet be open. Similarly,
511 such multilevel control is compatible with the ability of Neurog2 to induce different neuronal
512 subtypes or maturation stages in different, permissive starting cells [46,96,98,99], given that
513 maturation loci defining the neuronal subtype could be differentially accessible for Neurog2
514 direct targets.

515 Interestingly, the overexpression of Neurog2 in bFGF-grown astrocytes induced not only a
516 partial neurogenic program but also additional transcriptional programs associated with
517 alternative fates, such as cartilage formation and immune cell differentiation. The induction of
518 alternative fates or a failure to repress the original fate can lead to abortive conversion and
519 concomitant death of reprogrammed cells [100], thereby possibly mechanistically explaining
520 the lower Neurog2-mediated conversion efficiency in the bFGF culture. Because Hmgb2
521 overexpression does not specifically repress the astrocytic fate, yet significantly improves the
522 conversion efficiency, the abortive direct conversion is unlikely to explain the lower efficiency
523 in direct conversion. Interestingly, we did not observe Hmgb2-dependent opening of regions
524 associated with alternative fate genes, thus supporting the idea that alternative fate induction is
525 independent of the Hmgb2-induced changes in chromatin states. Hmgb2-dependent changes in
526 the transcription rate [101], RNA stability or RNA splicing could account for the enrichment
527 of alternative fates observed in mRNA analysis, because Hmgb2 has been proposed to have an
528 RNA-binding domain [91]. Importantly, we observed changes in chromatin opening for only
529 genes associated with the neurogenic lineage.

bioRxiv preprint doi: https://doi.org/10.1101/2023.08.31.555708; this version posted September 3, 2023. The copyright holder for this preprint (which was not certified by peer review) is the author/funder. All rights reserved. No reuse allowed without permission.

Conclusions

Together, our results provide a mechanistic framework for translating environmental signals into a specific program involved in neuronal maturation downstream of the neurogenic fate determinants via chromatin modification. Interestingly, this aspect of neuronal reprogramming is the least understood and stands to be further improved, particularly *in vivo*.

bioRxiv preprint doi: https://doi.org/10.1101/2023.08.31.555708; this version posted September 3, 2023. The copyright holder for this preprint (which was not certified by peer review) is the author/funder. All rights reserved. No reuse allowed without permission.

Figure Legends:

Figure 1. Astrocyte growth conditions define the rate of direct astrocyte to neuron conversion

(**a**) Schemes depicting viral vector design and the experimental paradigm used for astrocyte to neuron conversion. (**b-c´´**) Micrographs illustrating the identity of Neurog-Neurog2 transduced cells 7 days after transduction in the EGF+bFGF (b) and bFGF (c) culture conditions. b´, b´´, c´ and c´ are magnifications of boxed areas in b and c, respectively. Yellow arrows indicate successfully converted cells, whereas white arrowheads indicate cells failing to convert. Scale bars: 100 µm in b and c; 50 µm in b´, b´´, c´ and c´´. (**d**) Dot plot depicting the proportion of transduced cells converting to neurons in EGF+bFGF and bFGF cultures 7 days after transduction with different neurogenic fate determinants. Data are shown as median±IQR; each single dot represents an independent biological replicate. Significance was tested with two-tailed Mann-Whitney test. p-values: black font corresponds to the comparison to the control and colored to the comparison between EGF+bFGF and bFGF. (**e**) Volcano plot depicting proteins enriched in astrocytes cultured in bFGF (magenta circles) and EGF+bFGF (green diamonds) culture conditions (fold change >1,5; p value <0,05). (**f, g**) Plots depicting the top five enriched GO terms in protein sets enriched in bFGF (f) and EGF+bFGF (g) cultures. (**h**) Western blot depicting levels of Hmgb2 protein in EGF+bFGF and bFGF astrocyte cultures. (**j**) Dot plot showing the relative levels of Hmgb2 (normalized to actin) in EGF+bFGF and bFGF cultures. Data are shown as median±IQR; single dots represent independent biological replicates. Paired-t-test was used for the significance test. Abbreviation: GO, Gene Ontology.

bioRxiv preprint doi: https://doi.org/10.1101/2023.08.31.555708; this version posted September 3, 2023. The copyright holder for this preprint (which was not certified by peer review) is the author/funder. All rights reserved. No reuse allowed without permission.

559 **Figure 2. Hmgb2 is sufficient for successful Neurog2-mediated direct astrocyte to neuron**
560 **conversion.**

561 (**a**) Scheme depicting the experimental paradigm used for astrocyte to neuron conversion. (**b-**
562 **c´´´**) Micrographs showing the identity of Neurog2- and Hmgb2-expressing virally transduced
563 cells 7 days after transduction in EGF+bFGF (a) and bFGF cultures (b). b´, b´´, b´´´, c´, c´´ and
564 c´´´ are magnifications of the boxed areas in a and b, respectively. Yellow arrows indicate co-
565 transduced cells expressing Neurog2 and Hmgb2, yellow arrowheads indicate cells transduced
566 only with Hmgb2-encoding virus, and blue arrowheads indicate cells transduced with only
567 Neurog2-encoding virus. Scale bars: 100 µm in b and c; 50 µm in b´. b´´, b´´´, c´, c´´ and cb´´´.
568 (**d**) Dot plot depicting the proportion of transduced cells converting to neurons in EGF+bFGF
569 and bFGF cultures 7 days after transduction. Data are shown as median±IQR; single dots
570 represent independent biological replicates. Significance was tested with two-tailed Mann-
571 Whitney test. (**e**) Histogram depicting the identities of cells transduced with the indicated
572 factors 7 days after transduction. Abbreviation: FP, fluorescent protein.

573

574 **Figure 3. Hmgb2 is necessary for successful Neurog2-mediated direct astrocyte to neuron**
575 **conversion.**

576 (**a**) Scheme depicting the experimental paradigm used for astrocyte to neuron conversion. (**b,**
577 **c**) Micrographs showing the identities of Neurog2-expressing virally transduced cells 7 days
578 after transduction in EGF+bFGF culture of astrocytes derived from Hmgb2-deficient animals
579 (c) and their siblings (b). Scale bars: 100 µm. (**d**) Dot plot depicting the proportion of Hmgb2-
580 deficient or control cells converting to neurons 7 days after transduction with Neurog2. Data
581 are shown as median±IQR; single dots represent independent biological replicates.

bioRxiv preprint doi: https://doi.org/10.1101/2023.08.31.555708; this version posted September 3, 2023. The copyright holder for this preprint (which was not certified by peer review) is the author/funder. All rights reserved. No reuse allowed without permission.

582 Significance was tested with two-tailed Mann-Whitney test. Abbreviation: FP, fluorescent
583 protein.

584

585 **Figure 4. Neurog2 induces incomplete neuronal fate in bFGF culture.**

586 (**a, b**) Plots depicting enriched GO biological process terms in gene sets induced by Neurog2
587 in EGF+bFGF culture (a) and bFGF culture (b) 48 hours after viral transduction. Orange text
588 represents the GO terms not associated with neuronal fate. Green and magenta text represent
589 GO terms specifically enriched in EGF+bFGF culture and bFGF culture, respectively. (**c**) Venn
590 diagram illustrating the overlap of Neurog2-induced transcripts in EGF+bFGF and bFGF
591 culture 48 h after viral transduction. (**d**) Heat map showing Neurog2- or Neurog2+HMGB2-
592 mediated induction of core neurogenic factors (according to Masserdotti et al., 2013) in
593 EGF+bFGF and bFGF cultures. (**e**) Dot plot depicting the proportion of transduced cells
594 converting to neurons in EGF+bFGF and bFGF cultures 7 days after transduction in Prox1
595 deficient or Prox-1 overexpressing cells. Data are shown as median±IQR; single dots represent
596 independent biological replicates. Significance was tested with two-tailed Mann-Whitney test.
597 (**f**) Plot showing GO terms enriched in the gene set upregulated in bFGF culture by Neurog2
598 and Hmgb2 expression 48 h after viral transduction. GO terms in green text are also induced
599 by Neurog2 alone in EGF+bFGF culture (panel a). (**g**) Venn diagram illustrating the overlap
600 of Neurog2-induced transcripts in EGF+bFGF and bFGF culture with Neurog2 and Hmgb2-
601 induced transcripts after overexpression in bFGF culture 48 h after viral transduction. (**h**) Plot
602 depicting enriched GO biological process terms in gene sets induced in the reprogramming
603 prone condition (46 genes set; Fig. 4g). GO terms in green text are also induced by Neurog2
604 alone in EGF+bFGF culture. Abbreviations: FP, fluorescent protein; GO, Gene Ontology.

605

bioRxiv preprint doi: https://doi.org/10.1101/2023.08.31.555708; this version posted September 3, 2023. The copyright holder for this preprint (which was not certified by peer review) is the author/funder. All rights reserved. No reuse allowed without permission.

606 **Figure 5. Hmgb2 improves the capability of Neurog2 to open promoters of neuronal**
607 **maturation-associated genes.**

608 (**a,b**) Heat maps depicting opening of promoters by Neurog2 and Hmgb2 or their combination
609 in EGF+bFGF (green, a) and bFGF (magenta, b) culture. Scale: 1 kb (**c**) Heat maps depicting
610 ATAC signals in the promoters of the core neurogenic genes (Fig. 4d) 48 h after Neurog2,
611 Hmgb2 or Neurog2+Hmgb2 overexpression in EGF+bFGF and bFGF cultures. (**d**) IGV tracks
612 showing the ATAC signal in the promoters of genes identifying non-neuronal lineages 48 h
613 after Neurog2, Hmgb2 or Neurog2+Hmgb2 overexpression in bFGF culture. (**e**) Histogram
614 depicting the number of more (MAS) or less (LAS) accessible sites identified by ATAC 48 h
615 after Neurog2, Hmgb2 or Neurog2+Hmgb2 overexpression in EGF+bFGF (green) and bFGF
616 (magenta) cultures. (**f**) Plot depicting enriched GO biological process terms in the promoter set
617 opened by Neurog2+Hmgb2 in bFGF culture 48 hours after viral transduction. (**g**) Heat map
618 showing ATAC signal in the promoters of neuronal maturation related genes (red in panel e)
619 48 h after Neurog2, Hmgb2 or Neurog2+Hmgb2 overexpression in bFGF culture. (g) IGV
620 tracks showing the ATAC signal in the promoters of representative genes involved in neuronal
621 maturation 48 h after Neurog2, Hmgb2 or Neurog2+Hmgb2 overexpression in FGF culture.
622 Green boxes indicate differentially accessible sites.

623

624 **Figure 6. Hmgb2-dependent promoters contain an E-box and Pou2f2 factor binding**
625 **motif.**

626 (**a**) Venn diagram illustrating the overlap in ATAC signals for MASs after Neurog2
627 overexpression in EGF+bFGF and bFGF cultures, with MASs induced by Neurog2 and Hmgb2
628 overexpression in bFGF culture 48 h after viral transduction. (**b**, **c**) Plots depicting enriched
629 GO biological process terms in 395 peak set MASs in panel a (b) and 268 peak set MASs in

bioRxiv preprint doi: https://doi.org/10.1101/2023.08.31.555708; this version posted September 3, 2023. The copyright holder for this preprint (which was not certified by peer review) is the author/funder. All rights reserved. No reuse allowed without permission.

630 panel a (b). (**d, e**) Transcription factor consensus sequences identified in 268 peak set MASs in
631 panel a (d) and 395 peak set MASs in panel a (e), identified with *de novo* motif analysis. The
632 motif image from the BaMM web server shows the likelihood of each nucleotide at each motif
633 position. The color intensity reflects the probability, with darker colors indicating higher
634 probabilities. Tables show transcription factors binding these motifs. Abbreviations: MAS,
635 more accessible site; TF, transcription factor.

636

637 **Figure 7. Hmgb2 and Neurog2 overexpression increases complexity of iN.**

638 (**a**) Scheme depicting the experimental paradigm used for Shool analysis. (**b**) Representative
639 thresholded images of neuronal cells used for Sholl analysis. (**c**) Sholl analysis of induced
640 neurons by concurrent overexpression of Neurog2 and Neurog2+Hmgb2 in EGF and
641 EGF+bFGF culture 7 days after viral transduction. Abbreviations: MAS, more accessible site;
642 TF, transcription factor.

643

644

bioRxiv preprint doi: https://doi.org/10.1101/2023.08.31.555708; this version posted September 3, 2023. The copyright holder for this preprint (which was not certified by peer review) is the author/funder. All rights reserved. No reuse allowed without permission.

Suppl. Figure Legends:

Suppl. Figure 1. Growth conditions define the direct conversion rate.

(**a**) Scheme depicting the experimental paradigm used for astrocyte to neuron conversion. (**b-e**) Micrographs depicting the fate of transduced cells after control viral transduction in EGF+bFGF (b), bFGF (c), EGF (d) culture and Neurog2 overexpression in EGF culture (e) 7 days after viral transduction. Scale bars: 50 µm. (**f**, **g**) Dot plots showing direct conversion efficacy of Neurog2 overexpression in EGF culture (f) as well as Pou2f2, and Pou3f2+Hmgb2 overexpression in EGF+bFGF and bFGF culture (g). Data are shown as median±IQR; single dots represent independent biological replicates. Significance was tested with two-tailed Mann-Whitney test. Abbreviations: FP, fluorescent protein.

Suppl. Figure 2: Characterization of the starting population in EGF+bFGF and bFGF culture.

(**a**) Scheme depicting the experimental paradigm used to characterize initially transduced cells. (**b**, **c**, **d**, **e**, **g**, **h**, **j**, **k**, **l**, **m**) Micrographs illustrating identity assessment of control virally transduced cells 24 h after transduction. Yellow arrows indicate identity marker positive transduced, GFP-positive cells. Scale bars: 50 µm. (**f, i, n**) Dot plots showing the proportion of transduced cells with the indicated identity. Data are shown as median±IQR; single dots represent independent biological replicates. Significance was tested with two-tailed Mann-Whitney test.

Suppl. Figure 3: The growth factor induced barrier is reversible.

bioRxiv preprint doi: https://doi.org/10.1101/2023.08.31.555708; this version posted September 3, 2023. The copyright holder for this preprint (which was not certified by peer review) is the author/funder. All rights reserved. No reuse allowed without permission.

668 (**a**) Scheme depicting the experimental paradigm used to address the stability of the growth
669 factor induced lineage barrier. (**b-e**) Micrographs illustrating the identity of control virus (b, d)
670 and Neurog2-encoding virus (c, e) transduced cells cultured first in bFGF and then in
671 EGF+bFGF (b, c), and of cells cultured first in EGF+bFGF and then bFGF (d, e). Identity
672 assessment was performed 7 days after viral transduction. Scale bar in b-e: 50 μm. (**f**) Dot plots
673 showing the proportions of transduced cells acquiring neuronal identity 7 days after viral
674 transduction. Data are shown as median±IQR; single dots represent independent biological
675 replicates. Significance was tested with two-tailed Mann-Whitney test.

676

677 **Suppl. Figure 4: Traumatic brain injury induces Hmgb2 expression in gray matter**
678 **reactive astrocytes.**

679 (**a**) Scheme depicting the experimental paradigm. (**b-c´**) Micrographs showing the expression
680 of Hmgb2 in the intact (b) and injured hemisphere (c) 5 days after injury. (c´) Orthogonal
681 projections of the optical Z-stack depicting the expression of Hmgb2 in astrocytes of the injured
682 hemisphere. Scale bars in b and c 100 μm and in c´ 10 μm.

683

684 **Suppl. Figure 5: Isolation of transduced cells for RNAseq and ATACseq.**

685 (**a**) Scheme depicting the workflow used to isolate transduced cells 48 h after transduction for
686 omic analysis. (**b**) Plots demonstrating the FACS sorting gates and settings used to sort cells
687 transduced with control, Neurog2 and Hmgb2 expressing viruses.

688

689 **Suppl. Figure 6. Neurog2+Hmgb2 overexpression in bFGF culture induces a**
690 **transcriptional subset necessary for successful direct conversion.**

bioRxiv preprint doi: https://doi.org/10.1101/2023.08.31.555708; this version posted September 3, 2023. The copyright holder for this preprint (which was not certified by peer review) is the author/funder. All rights reserved. No reuse allowed without permission.

691 (**a-b**) Volcano plots of differentially expressed genes (DEGs) induced by Neurog2 in
692 EGF+bFGF culture (a) and bFGF culture (b) 48 hours after viral transduction. (**c**) Plot depicting
693 enriched GO biological processes of 96 shared genes (Fig. 4c) induced by Neurog2 in both
694 EGF+bFGF and bFGF culture 48 hours after viral transduction. (**d**) Plot depicting enriched GO
695 biological processes of uniquely induced genes by Neurog2 in EGF+bFGF culture (225 gene
696 set; in Fig. 4c, green text) and bFGF culture (41 gene set in Fig. 4c, magenta text) 48 hours
697 after viral transduction. (**e**, **f**) Volcano plot of DEGs induced by Hmgb2 in EGF+bFGF culture
698 (f) and bFGF culture (g) 48 hours after viral transduction. (**g**) Plot depicting enriched GO
699 biological processes of genes downregulated by Neurog2+Hmgb2 overexpression in bFGF
700 culture 48 hours after viral transduction. Red text highlights processes associated with
701 cytoskeletal remodeling, and blue depicts processes involved in adhesion. (**h**) Plot depicting
702 enriched GO biological processes of the gene set commonly induced by Neurog2 in
703 EGF+bFGF, bFGF culture and by Neurog2+Hmgb2 in bFGF culture (88 genes in Fig. 4g).
704 Black text highlights processes associated with neurogenesis.

705

706 **Suppl. Figure 7. Hmgb2 increases the ability of Neurog2 to open chromatin in bFGF**
707 **culture.**

708 (**a**) Heat map depicting accessibility of MASs induced by Hmgb2 (9 MASs), Neurog2 (445
709 MASs) and the combination of Neurog2+Hmgb2 (1062 MASs) in bFGF culture 48 h after viral
710 transduction. Scale: 1 kb. (**b-c**) Pie charts of genomic distribution of MASs induced by
711 Neurog2 (b) and the combination of Neurog2+Hmgb2 (c) in bFGF culture 48 h after viral
712 transduction.

713

bioRxiv preprint doi: https://doi.org/10.1101/2023.08.31.555708; this version posted September 3, 2023. The copyright holder for this preprint (which was not certified by peer review) is the author/funder. All rights reserved. No reuse allowed without permission.

Suppl. Figure 8. Additional sites opened by Hmgb2 and Neurog2 overexpression are associated with the establishment of synaptic contacts and/or maturation of neurons.

(**a**) IGV tracks showing the ATAC signals of genes associated with synapse formation/function 48 h after viral transduction in bFGF culture. Boxes indicate signals significantly broadened by co-expression of Neurog2 and Hmgb2. (**b**) Box plots depicting expression of synapse-associated genes (from panel a) after control, Neurog2, Hmgb2 and Neurog2+Hmgb2 overexpression in bFGF culture 48 hours after viral transduction. (**c**) Venn diagram illustrating the overlap of MASs with the Tal-associated factor binding motif (motif 1, E-box) and POU domain factor binding motif (motif 2, POU) induced by Neurog2 in EGF+bFGF culture and induced by Neurog2+Hmgb2 in bFGF culture. (**d**) Plot depicting GO biological processes enriched in genes with promoters containing binding motifs for both Tal-associated factors and POU domain factors (56 promoters in c).

bioRxiv preprint doi: https://doi.org/10.1101/2023.08.31.555708; this version posted September 3, 2023. The copyright holder for this preprint (which was not certified by peer review) is the author/funder. All rights reserved. No reuse allowed without permission.

Suppl. Table Legends:

Suppl. Table 1. GO analysis of processes enriched in the EGF+bFGF and bFGF only proteomes.

Suppl. Table 2. Full list of differentially regulated genes between different conditions.

Suppl. Table 3. GO analysis associated with RNA-seq analysis.

Suppl. Table 4. Full list of MAS and DAS with their genomic location.

Suppl. Table 5. GO analysis associated with ATAC analysis.

Suppl. Table 6. GO analysis associated ATAC peaks enriched in different reprogramming conditions.

Suppl. Table 7. Full list of MAS and DAS with Neurog2 and Pou TF binding motifs.

bioRxiv preprint doi: https://doi.org/10.1101/2023.08.31.555708; this version posted September 3, 2023. The copyright holder for this preprint (which was not certified by peer review) is the author/funder. All rights reserved. No reuse allowed without permission.

Material and Methods

Experimental animals

Experiments were conducted on both, female and male animals, which were either wild types (C57BL/6J mice) or transgenic Hmgb2-/- animals on a C57BL/6 background [102]. The Hmgb2-/- mice do not show gross phenotypical abnormalities and do not differ to wild-type siblings (Ronfani et al., 2001). For all *in vitro* experiments, animals at postnatal stage P5-P6 were used. Injuries were done in adult 8-10 weeks old animals. Animals were kept under standard conditions with access to water and food ad libitum. All animal experimental procedures were performed in accordance with the German and European Union guidelines and were approved by the Institutional Animal Care and Use Committee (IACUC) and the Government of Upper Bavaria under license number: AZ 55.2-1-54-2532-171-2011 and AZ 55.2-1-54-2532-150-11. All efforts were made to minimize animal suffering and to reduce the number of animals used.

Stab wound injury

Prior to every surgery, mice were deeply anesthetised by intra-peritoneal injection of sleep solution (Medetomidin (0,5mg/kg) / Midazolam (5mg/kg) / Fentanyl (0,05mg/kg)) complemented by local lidocaine application (20 mg/g). After the injection of the anaesthesia, mice were checked for pain reactions by pinching their tail and toes. Stab wound injury was performed in the somatosensory cortex, as previously described [97,103]. The following coordinates relative to Bregma were used: medio-lateral: 1,0 µm; rostro-caudal: -1,2 µm to -2,2 µm; dorso-ventral: -0,6 µm. Anaesthesia was antagonized with an subcutan injection of awake solution (Atipamezol (2,5mg/kg) / Flumazenil (0,5mg/kg) / Buprenorphin (0,1mg/kg))

bioRxiv preprint doi: https://doi.org/10.1101/2023.08.31.555708; this version posted September 3, 2023. The copyright holder for this preprint (which was not certified by peer review) is the author/funder. All rights reserved. No reuse allowed without permission.

760 and the mice were kept on a pre-warmed pad until they were awake and recovered from the
761 surgery.

762

763 **Perfusion and tissue section preparation**

764 Prior to perfusion, animals were deeply anesthetized with overdoses of cocktail of ketamine
765 (100 mg/kg) / xylazine (10 mg/kg). Subsequently, they were transcardially perfused first with
766 cold PBS, followed by fresh ice-cold 4% PFA in PBS for 20 minutes. The brain was then
767 removed from the skull, post-fixed in the same fixative overnight at 4 °°C, cryoprotected in 30%
768 sucrose and cut at the cryostat at 40 µm tick sections.

769

770 **Preparation of PDL-coated glass coverslips**

771 Glass coverslips were washed first with acetone and boiled for 30 min in ethanol containing
772 0,7% (v/v) HCl. After two washing steps with 100% ethanol, coverslips were dried at RT and
773 autoclaved for 2 h at 180 °C. Coverslips were washed with D-PBS and coated with poly-D-
774 lysine (PDL, 0.02 mg/ml) solution for at least 2 h at 37 °C. Following coating, coverslips were
775 washed three times with autoclaved ultrapure water, dried in the laminar flow and stored at
776 4 °C until needed.

777

778 **Primary culture of postnatal cortical astroglial cells**

779 Postnatal cortical astroglia were isolated and cultured as described previously [104]. Following
780 decapitation of postnatal (P5-P6) wild-type C57BL/6J mice, the skin and the skull were
781 removed, and the brain was extracted avoiding any tissue damage and placed into the 10 mM
782 HEPES solution for dissection. After separating the two hemispheres, the meninges was

bioRxiv preprint doi: https://doi.org/10.1101/2023.08.31.555708; this version posted September 3, 2023. The copyright holder for this preprint (which was not certified by peer review) is the author/funder. All rights reserved. No reuse allowed without permission.

783 removed and white matter of cerebral cortex was dissected using fine forceps and collected in
784 a tube with astrocyte medium (Fetal calf serum-FCS (10% (v/v)); Horse serum-HS (5% (v/v));
785 glucose (3,5 mM); B27 supplement; Penicillin/Streptomycin (100 I.U/ml Pen and 100 µg/ml
786 Strep) in DMEM/F12+GlutaMAX). The tissue was mechanical dissociated with a 5 ml pipette
787 and placed into uncoated plastic flasks for cell expansion in astrocyte medium supplemented
788 with the two growth factors EGF (10 ng/ml) + bFGF (10 ng/ml each) or with bFGF (10 ng/ml)
789 only as specified for each experiment. After 4-5 days, the medium was exchanged and supplied
790 with the fresh growth factors. After 10 days of culturing, cultured cells were rinsed with DPBS
791 and contaminating oligodendrocyte precursor cells were removed by brusquely shaking the
792 culture flasks several times. Astroglial cells were then detached from the flask by trypsinization
793 and seeded onto poly-D-lysine (PDL)-coated glass coverslips at a density of $8x10^4$ cells per
794 well in a 24-well plate with astrocyte medium for immunohistochemical analysis. For the
795 ATAC-seq and RNA-seq experiments, cells were plated in T75 flasks with a seeding density
796 of $3x10^6$ cells per flask. 2-4 h after seeding, the cells were transduced with different retroviral
797 vectors in a ratio of 1 µl virus per 1 ml medium to prevent virus toxicity. Astrocyte medium
798 was changed 12-18 h after viral transduction to differentiation medium (glucose (3,5 mM); B27
799 supplement; Penicillin/Streptomycin (100 I.U/ml Pen and 100 µg/ml Strep) in
800 DMEM/F12+GlutaMAX) containing neither EGF nor bFGF up to the immunocytochemical
801 analysis timepoint. The cells were cultured as indicated in each experiment. Cells were fixed
802 in cold 4% PFA for 20 min and rinsed with cold D-PBS before immunocytochemical analysis.

803 For the ATAC-seq and RNA-seq experiments, the cells were kept in the astrocyte medium and
804 collected 48 h after viral transduction. Astrocytes were detached from the flask by
805 trypsinization, prepared for the FACS and sorted for the following ATAC-seq and RNA-seq
806 experiments according to the fluorophore expression.

bioRxiv preprint doi: https://doi.org/10.1101/2023.08.31.555708; this version posted September 3, 2023. The copyright holder for this preprint (which was not certified by peer review) is the author/funder. All rights reserved. No reuse allowed without permission.

807 The astroglial cultures from the Hmgb2-/- transgenic animals were prepared as described above,
808 however, the cortical tissue from each animal was kept separately and placed into the small
809 T25 flask. In addition, the tips of the tails were used for genotyping as described in [102]. The
810 cultures from Hmgb2-/- transgenic mice were grown only in the double growth factor condition
811 containing EGF+bFGF.

812

813 **Immunocytochemistry and immunohistochemistry**

814 Immunostaining was performed on cell culture samples or free-floating brain sections.
815 Specimens were treated with blocking buffer (0,5% Triton-X-100; 10% normal goat serum
816 (NGS) in D-PBS) to reduce non-specific binding. The same buffer was used to dilute the
817 primary antibodies. The specimens were incubated with the primary antibody mixture
818 overnight at 4°C (brain tissue) °C or for 2 hours at RT (cell culture samples), followed by 3x
819 10 min washing steps with PBS. In order to visualize primary antibody binding, samples were
820 exposed to appropriate species and/or subclass specific secondary antibodies conjugated to
821 Alexa Fluor 488, 546 or 647 (Invitrogen) for about 90 min at RT protected from light.
822 Secondary antibodies were diluted 1:1000 in blocking buffer. Nuclei were visualized with
823 DAPI (4',6-diamidino-2-phenylindole) that was added to the mix of secondary antibodies.
824 Following extensive washing steps with PBS, coverslips or sections were mounted with Aqua
825 Poly/Mount (Polysciences) and imaged.

826 Following primary antibodies were used: Chick-anti-GFP (Aves Lab, GFP-120; 1:1000);
827 Rabbit-anti-RFP (Rockland, 600-401-379; 1:500); Mouse IgG1-anti-GFAP (Sigma-Aldrich,
828 G3893; 1:500); Rabbit-anti-GFAP (DakoCytomation, Z0334; 1:1000); Mouse IgG1κ-anti-
829 S100β (Sigma-Aldrich, S2644; 1:500); Rabbit-anti-OLIG2 (Thermo Fischer, AB9610; 1:500);
830 Mouse IgG2a-anti-αSMA (Sigma-Aldrich, A2547; 1:400); Rabbit-anti-Ki67 (Abcam, 15580;

bioRxiv preprint doi: https://doi.org/10.1101/2023.08.31.555708; this version posted September 3, 2023. The copyright holder for this preprint (which was not certified by peer review) is the author/funder. All rights reserved. No reuse allowed without permission.

1:200); Rat-anti-Ki67 (DakoCytomation, M7249; 1:200); Rabbit-anti-PH3 (Ser10) (Thermo Fischer, 06-570; 1:200); Guinea pig-anti-DCX (Thermo Fischer, AB-2253; 1:1000); Mouse IgG2b-anti-β-III-TUBULIN (Sigma-Aldrich, T8660; 1:500); Mouse IgG1-anti-NEUN (Chemicon, MAB 377; 1:250); Rabbit-anti-HMGB2 (Abcam, ab67282; 1:1000); Mouse IgG2aκ-anti-HMGB2 (Sigma-Aldrich, 07173-3E5; 1:500); Mouse IgG2aκ-anti-HMGB2 antibody requires termal (15 min at 95°C) antigen retrieval using the citrate buffer (10 mM; pH 6). Primary antibody binding was revealed using class-specific secondary antibody coupled to Alexa fluorophore (Invitrogen, Germany). All secondary antibodies were used at dilution 1:1000.

Image acquisition and quantifications

Immunostainings were analysed with a fluorescent Microscope Axio Imager M2m (Zeiss) using the ZEN software (Zeiss) with a 20x or 40x objective. Fluorescent-labelled sections were photographed with FV1000 confocal laser-scanning microscope (Olympus), using the FW10-ASW 4.0 software (Olympus). The quantifications of *in vitro* cultured cells were performed using the ZEN software (Zeiss) analysing at least 25 randomly taken pictures per coverslip depending on the number of transduced cells. In total, 100-200 retroviral vector-transduced cells were quantified from randomly chosen fields on a single coverslip. 3 coverslips in each experiment (biological replicate) were analysed. The number of experiments is indicated in corresponding Figure. The number of induced neurons was expressed as a percentage out of all transduced cells.

To analyse the number of apoptotic cells, between 350-550 DAPI labelled cells were counted from 5 randomly selected fields on one coverslip.

bioRxiv preprint doi: https://doi.org/10.1101/2023.08.31.555708; this version posted September 3, 2023. The copyright holder for this preprint (which was not certified by peer review) is the author/funder. All rights reserved. No reuse allowed without permission.

In the reprogramming experiments of the astrocytes isolated from Hmgb2+/+, Hmgb2+/- and Hmgb2-/- animals, each of the single animals was considered as a biological replicate and at least 3 coverslips were counted per animal. We analysed in total 6 litters containing wild-type, heterozygous or homozygous littermates.

Western blots using the Fiji software as previously described [105] . All lanes of interest were outlined using the rectangular selection tool and the signal intensity of each band was calculated by determining the area under the peak. The measurements of the corresponding α-ACTIN bands were used to normalize the amount of proteins loaded on the gel.

Sholl Analysis

We analysed only DCX positive cells 7 days after viral transduction. Single cells were isolated and subjected to Sholl analysis using the ImageJ plug-in 'Sholl Analysis'. We used the following parameters: starting radius 5µm; ending radius 500 µm; radius step size 5 µm. The number of crossings per cell were visualized and analysed using Origin.

FACS analysis and sorting

Astrocytes were collected by trypsinization 48 h after retroviral transduction, washed, resuspended in DPBS and analysed using a FACS Aria II instrument (BD Biosciences) in the FACSFlowTM medium. Debris and aggregated cells were gated out by forward-scatter area (FSC-A) and side-scatter area (SSC-A). Forward scatter area (FSC-A) vs. forward scatter width (FSC-W) was used to discriminate doublets from single cells. To set the gates for the sorting, untransduced astrocytes were recorded. Sorted cells were collected in DPBS, counted and

bioRxiv preprint doi: https://doi.org/10.1101/2023.08.31.555708; this version posted September 3, 2023. The copyright holder for this preprint (which was not certified by peer review) is the author/funder. All rights reserved. No reuse allowed without permission.

876 divided into two batches: 50000 cells were immediately processed for ATAC-seq and the
877 remaining cells were collected for RNA-seq library preparation.

878

879 **ATAC-sequencing**

880 Assay for Transposase Accessible Chromatin with high-throughput sequencing (ATAC-seq),
881 a method to detect genome-wide chromatin accessibility, was performed following the
882 published protocol [106,107]. Briefly, right after the FACS sorting, 50000 cells were lysed, the
883 nuclei were extracted and resuspended with the transposase reaction mix (25 µl 2x TD buffer
884 (Illumina); 2,5 µl Transposase (Illumina); 22,5 µl nuclease free water), following by
885 transposition reaction for 30 minutes at 37°C °C. To stop the transposition reaction, samples
886 were purified using a Qiagen MinElute PCR (Qiagen) purification kit according to the
887 manufacturer instructions. Open chromatin fragments were first amplified for 5 cycles and then
888 for additional 7-8 cycles, as determined by RT-qPCR, using the combination of primer
889 Ad1_noMX (5'
890 AATGATACGGCGACCACCGAGATCTACACTCGTCGGCAGCGTCAGATGTG 3') and
891 the Nextera Index Kit (Illumina) primer N701-N706. Libraries were purified using a Qiagen
892 MinElute PCR purification kit (Qiagen) and their quality was assessed using the Bioanalyzer
893 High-Sensitivity DNA kit (Agilent) according to the manufacturer's instructions. The
894 concentration of each library was measured by Qubit using the provided protocol. Libraries
895 were pooled for sequencing and the pool contained 20 ng of each library. Prior to sequencing,
896 pooled libraries were additionally purified with AMPure beads (ratio 1:1) to remove
897 contaminating primer dimers and quantified using Qubit and the Bioanalyzer High-Sensitivity
898 DNA kit (Agilent). 50-bp paired-end deep sequencing was carried out on HiSeq 4000
899 (Illumina).

bioRxiv preprint doi: https://doi.org/10.1101/2023.08.31.555708; this version posted September 3, 2023. The copyright holder for this preprint (which was not certified by peer review) is the author/funder. All rights reserved. No reuse allowed without permission.

ATAC-sequencing analysis:

For the analysis of bulk ATAC-seq data, we followed the Harvard FAS Informatics ATAC-seq guidelines. The quality of raw FASTQ reads were checked using FastQC (Version 0.11.9). The low quality read (< 20bp) and adapter sequences were trimmed by Cutadapt (Version 4.0). The trimmed reads were mapped to the mouse reference genome (mm10) by using Bowtie2 (parameter: --very-sensitive -X 1000 --dovetail). Samtools were then used to convert and sort the sam files into bam files. Peak calling step was performed with Genrich for each sample separately to identify accessible regions. Genrich peak caller has a mode (-j) assigned to ATAC-Seq analysis mode and allows running all of the post-alignment steps via peak-calling with one command. Mitochondrial reads and PCR duplicates were removed by -e chrM and -r argument respectively. To generate count table matrix for differential analysis bam2counts (intePareto R-based package) was used to count reads fall into specific genomic positions by importing all the bam files and merging all the bed files into one (importing GenomicRanges and GenomicAlignments libraries). DESeq2 (version 1.26.0) was used for differential accessibility analysis of the count data. The relatively more open and closed sites are called MAS and LAS respectively (fold change (FC) > 2 and adjusted P-value < 0.05) and the annotation of these sites were performed using R-based packages Chip-seeker (TSS ± 3.0 Kb) (version 1.28.3). For visualization, the bamcovage deeptools (version 3.5.1) were used to normalize the data by importing the scaling factor from DESeq2 (version 1.36.0). The normalized bigwig files used to visualize the coverage using deeptools and samtools. These bigwig files were loaded into the IGV tool to visualize the peak at the gene level. The Venn diagrams were made using the BioVenn web application tool. The Gorilla tool was used to generate the GO Biological processes, with a cut-off of enrichment > 2 and p-value of < 0.01.

bioRxiv preprint doi: https://doi.org/10.1101/2023.08.31.555708; this version posted September 3, 2023. The copyright holder for this preprint (which was not certified by peer review) is the author/funder. All rights reserved. No reuse allowed without permission.

924 **Motif analysis**

925 BaMMmotif (https://bammmotif.soedinglab.org/home/) was used to perform *de novo* motif
926 enrichment analysis by providing MASs fasta sequence [108] as input and all detected
927 accessible sites fasta sequences as background using default parameters. We selected the motifs
928 with an AvRec score above 0.5 as candidates for further analysis. The mouse database
929 HOCOMOCO v11 was used for motif annotation, and the most significant transcription factors
930 matching the motif with e-values below 0.001 were considered as potential binders.

931

932 **Preparation of libraries for RNA-sequencing**

933 Sorted cells were resuspended in 100 µl extraction buffer of the PicoPureTM RNA isolation
934 kit (Thermo Fischer Scientific) and the RNA was extracted according to the manufacturer's
935 instructions. The Agilent 2100 Bioanalyzer was used to assess RNA quality and concentration.
936 For the RNA-seq library preparation, only high-quality RNA with RIN values >8 were used.
937 cDNA was synthesized from 10 ng of total RNA using SMART-Seq v4 Ultra Low Input RNA
938 Kit (Takara Bio), according to the manufacturer's instructions. The total number of
939 amplification cycles was determined by RT-qPCR side reaction according to manufacturer's
940 instruction. PCR-amplified cDNA was purified by immobilization on AMPure XP beads. Prior
941 to generating the final library for sequencing, the Covaris AFA system was used to perform
942 cDNA shearing in Covaris microtubes (microTUBE AFA Fiber Pre-Slit Snap-Cap 6x16mm),
943 resulting in 200-500 bp long cDNA fragments that were subsequently purified by ethanol
944 precipitation. Prior to library preparation using the MicroPlex Library Preparation kit v2
945 (Diagenode) according to the user manual, the quality and concentration of the sheared cDNA
946 were assessed using an Agilent 2100 Bioanalyzer. Final libraries were evaluated using an
947 Agilent 2100 Bioanalyzer and the concentration was measured with Qubit Fluorometer

bioRxiv preprint doi: https://doi.org/10.1101/2023.08.31.555708; this version posted September 3, 2023. The copyright holder for this preprint (which was not certified by peer review) is the author/funder. All rights reserved. No reuse allowed without permission.

(Thermo Fischer Scientific). The uniquely barcoded libraries were multiplexed onto one lane and 100-bp paired-end deep sequencing was carried out at the HiSeq 4000 (Illumina) generating ~20 million reads per sample.

Transcriptome data analysis (Bulk RNA Seq):

The raw paired-end FASTQ files were mapped to the mouse reference genome (mm10) using STAR RNA-seq aligner (version 2.7.2b). Aligned reads in the BAM files were then quantified by HTSeq-count (Version 0.9.1) based on annotation file GENCODE Release M25 (GRCm38.p6). The gene-level count matrix was imported into the R/Bioconductor package DESeq2 (version 1.26.0) for normalization and differential expression with FC > 2, adjusted P-value < 0.05. Venn diagrams were created using the web application BioVenn tool and heatmaps were generated using gplots and RColorBrewer R-based/Bioconductor tools. For GO enrichment analysis of the assigned set of genes we used the GOrilla tool by providing background genes. The enriched GO term (biological processes) possessing enrichment > 2, containing at least 1% of the input genes and p-value specified in the figure legend were visualized using Origin.

Protein isolation and Western blot

Postnatal cortical astroglia were isolated and cultured as described above. After 10 days of culturing with growth factors EGF+bFGF or bFGF, cells were detached from the flask by trypsinization, washed and counted. $0{,}5x10^6$ cells were lysed in RIPA buffer containing cOmplete Protease Inhibitor cocktail (Roche). Protein extraction and Western blotting is performed as previously described [109]. The following antibodies were used: Rabbit-anti-HMGB2 (Abcam, ab67282; 1:5000); Mouse-anti-ACTIN (Millipore, MAB1501; 1:10000);

bioRxiv preprint doi: https://doi.org/10.1101/2023.08.31.555708; this version posted September 3, 2023. The copyright holder for this preprint (which was not certified by peer review) is the author/funder. All rights reserved. No reuse allowed without permission.

HRP-coupled anti-mouse IgG1 (GE Healthcare, NA931; 1:20000) and HRP-coupled anti-rabbit IgG (Jackson ImmunoResearch,111-036-045; 1:20000).

Quantitative mass spectrometry

Treated adherent astrocytes were lysed and subjected to tryptic protein digest using a modified FASP protocol [110]. Proteomic measurements were performed on a LTQ Orbitrap XL mass spectrometer (Thermo Scientific) online coupled to an Ultimate 3000 nano-HPLC (Dionex). Peptides were enriched on a nano trap column (100 µm i.d. × 2 cm, packed with Acclaim PepMap100 C18, 5 µm, 100 Å, Dionex) prior to separation on an analytical C18 PepMap column (75 µm i.d. × 25 cm, Acclaim PepMap100 C18, 3 µm, 100Å, Dionex) in a 135 min linear acetonitrile gradient from 3% to 34% ACN. From the high resolution orbitrap MS pre-scan (scan range 300 – 1500 m/z), the ten most intense peptide ions of charge ≥ +2 were selected for fragment analysis in the linear ion trap if they exceeded an intensity of at least 200 counts. The normalized collision energy for CID was set to a value of 35. Every ion selected for fragmentation was excluded for 30 s by dynamic exclusion. The individual raw-files were loaded to the Progenesis software (version 4.1, Waters) for label free quantification and analyzed as described [111,112]. MS/MS spectra were exported as Mascot generic file and used for peptide identification with Mascot (version 2.4, Matrix Science Inc., Boston, MA, USA) in the Ensembl Mouse protein database (release 75, 51765 sequences). Search parameters used were as follows: 10 ppm peptide mass tolerance and 0.6 Da fragment mass tolerance, one missed cleavage allowed, carbamidomethylation was set as fixed modification, methionine oxidation and asparagine or glutamine deamidation were allowed as variable modifications. A Mascot-integrated decoy database search was included. Peptide assignments were filtered for an ion score cut-off of 30 and a significance threshold of $p < 0.01$ and were

bioRxiv preprint doi: https://doi.org/10.1101/2023.08.31.555708; this version posted September 3, 2023. The copyright holder for this preprint (which was not certified by peer review) is the author/funder. All rights reserved. No reuse allowed without permission.

reimported into the Progenesis software. After summing up the abundances of all peptides allocated to each protein, resulting normalized protein abundances were used for calculation of fold-changes and corresponding p-values.

Expression plasmids

In order to overexpress different neurogenic transcription factors in the astroglial cells, we used Moloney murine leukemia virus (MMLV)-derived retroviral vectors, expressing neurogenic fate determinants under the regulatory control of a strong and silencing-resistant pCAG promoter. All our construct encode a neurogenic factor followed by an internal ribosomal entry site (IRES) and either GFP or dsRED as reporter proteins, allowing simultaneous reporter expression. For control experiments, we used a retrovirus encoding for the fluorescent proteins (GFP or dsRED) behind the IRES driven by the same CAG promoter. We used the following expression vectors: pCAG-IRES-GFP [43]; pCAG-IRES-dsRED [43]; pCAG-Neurog2-IRES-dsRED [43]; pCAG-Pou3f2 -IRES-dsRED [113]; pCAG-Sox11-IRES-GFP [46]; pCAG-Hmgb2-IRES-GFP(this work).

Cloning pCAG-Hmgb2-IRES-GFP construct

cDNA for Hmgb2 were synthetized at Genscript, containing BamHI and HindIII in order to clone them into the pENTR1A entry vector. The cDNAs were then transferred to the retroviral destination vector pCAG-IRES-dsRED/GFP using the Gateway cloning method (Invitrogen) according to the manufacturer's instructions. The correct sequence was confirmed using Sanger sequencing before viral vector production.

bioRxiv preprint doi: https://doi.org/10.1101/2023.08.31.555708; this version posted September 3, 2023. The copyright holder for this preprint (which was not certified by peer review) is the author/funder. All rights reserved. No reuse allowed without permission.

1019 **Retroviral vector production**

1020 The VSV-G-pseudotyped retroviruses were prepared using the HEK293-derived retroviral
1021 packaging cell line (293GPG) (Ory et al., 1996) that stably express the gag-pol genes of murine
1022 leukemia virus and vsv-g under the control of a tet/VP16 transactivator as previously described
1023 (Heinrich et al., 2011). The viral particles were stored in TNE (Tris-HCl pH=7,8 (50mM);
1024 NaCl (130mM); EDTA (1mM)) buffer at -80 0C until use.

1025 **Statistical analysis**

1026 Numbers of biological replicates can be seen on the dot plots or in the figure legend in case of
1027 the bar charts. All results are presented as median ± interquartile range (IQR). IQR was
1028 calculated in RStudio [114], using the default method based on type 7 continuous sample
1029 quantile. For the reprogramming experiments, statistical analysis was performed in Origin
1030 using non-parametric Mann-Whitney U test unless differently specified for particular
1031 experiments.

bioRxiv preprint doi: https://doi.org/10.1101/2023.08.31.555708; this version posted September 3, 2023. The copyright holder for this preprint (which was not certified by peer review) is the author/funder. All rights reserved. No reuse allowed without permission.

Declarations

Availability of data and materials

Proteome data set is available at PRIDE database (https://www.ebi.ac.uk/pride/). The dataset identifier is PXD044288. During the review process the data could be accessed using the following username: reviewer_pxd044288@ebi.ac.uk and password: C9naS7jL.

The RNAseq and ATACseq datasets are available at Gene Expression Omnibus (GEO). The accession number is pending. The reviewer token will be provided upon request.

Competing interests

All authors declare no competing interest.

Funding

This work was supported by the German research foundation (DFG) through SFB 870 (J.N. and M.G.); TRR274/1 (ID 408885537) (J.N.); SPP 1738 "Emerging roles of non-coding RNAs in nervous system development, plasticity & disease" (J.N.); SPP1757 "Glial heterogeneity" (J.N.); the Fritz Thyssen Foundation (J.N.); SPP2191 "Molecular mechanisms of functional phase separation" (ID 402723784, project number 419139133) (J.N.); SPP1935 "Deciphering the mRNP code: RNA-bound determinants of post-transcriptional gene regulation" (J.N.); ERC Chrono Neurorepair (M.G.) and the Graduate School for Systemic Neurosciences GSN-LMU (V.S., F.B., P.M. and T.L.).

Authors' contributions

bioRxiv preprint doi: https://doi.org/10.1101/2023.08.31.555708; this version posted September 3, 2023. The copyright holder for this preprint (which was not certified by peer review) is the author/funder. All rights reserved. No reuse allowed without permission.

1054 P.M., T.L. and J. N. conceived the project and designed experiments. A.S.-M., V.S., F.B., and
1055 J.N. performed experiments. J. M.-P. and S.M.H. analyzed proteome. L.R. and M. B. provided
1056 Hmgb2 KO animals. P. M. and J.N. wrote the manuscript with input from all authors.

1057

1058 **Acknowledgments**

1059 We thank all members of the Neurogenesis and Regeneration group for experimental input,
1060 discussions and critical reading of the manuscript. We acknowledge the support of the
1061 following core facilities: the Bioimaging Core Facility at the BioMedical Center of LMU
1062 Munich and the Sequencing Facility at the Helmholtz Zentrum München.

1063

1064

bioRxiv preprint doi: https://doi.org/10.1101/2023.08.31.555708; this version posted September 3, 2023. The copyright holder for this preprint (which was not certified by peer review) is the author/funder. All rights reserved. No reuse allowed without permission.

References:

1. Barker RA, Götz M, Parmar M. New approaches for brain repair—from rescue to reprogramming. Nature 2018 557:7705 [Internet]. 2018 [cited 2022 Aug 16];557:329–34. Available from: https://www.nature.com/articles/s41586-018-0087-1

2. Götz M, Bocchi R. Neuronal replacement: Concepts, achievements, and call for caution. Curr Opin Neurobiol [Internet]. 2021 [cited 2022 Aug 18];69:185–92. Available from: https://pubmed.ncbi.nlm.nih.gov/33984604/

3. Torper O, Götz M. Brain repair from intrinsic cell sources: Turning reactive glia into neurons. Prog Brain Res. 2017.

4. Griesbach GS, Masel BE, Helvie RE, Ashley MJ. The Impact of Traumatic Brain Injury on Later Life: Effects on Normal Aging and Neurodegenerative Diseases. J Neurotrauma. 2018;35.

5. Bocchi R, Masserdotti G, Götz M. Direct neuronal reprogramming: Fast forward from new concepts toward therapeutic approaches. Neuron [Internet]. 2022 [cited 2022 Aug 18];110:366–93. Available from: https://pubmed.ncbi.nlm.nih.gov/34921778/

6. Zhou Y, Shao A, Yao Y, Tu S, Deng Y, Zhang J. Dual roles of astrocytes in plasticity and reconstruction after traumatic brain injury. Cell Communication and Signaling. BioMed Central Ltd.; 2020.

7. Amamoto R, Arlotta P. Development-inspired reprogramming of the mammalian central nervous system. Science (1979) [Internet]. 2014;343:1239882. Available from: http://www.ncbi.nlm.nih.gov/pubmed/24482482

8. Berninger B, Costa MR, Koch U, Schroeder T, Sutor B, Grothe B, et al. Functional properties of neurons derived from in vitro reprogrammed postnatal astroglia. J Neurosci [Internet]. 2007;27:8654–64. Available from: http://www.ncbi.nlm.nih.gov/entrez/query.fcgi?cmd=Retrieve&db=PubMed&dopt=Citation&list_uids=17687043

9. Buffo A, Vosko MR, Erturk D, Hamann GF, Jucker M, Rowitch D, et al. Expression pattern of the transcription factor Olig2 in response to brain injuries: implications for neuronal repair. Proc Natl Acad Sci U S A [Internet]. 2005/12/07. 2005;102:18183–8. Available from: http://www.ncbi.nlm.nih.gov/entrez/query.fcgi?cmd=Retrieve&db=PubMed&dopt=Citation&list_uids=16330768

bioRxiv preprint doi: https://doi.org/10.1101/2023.08.31.555708; this version posted September 3, 2023. The copyright holder for this preprint (which was not certified by peer review) is the author/funder. All rights reserved. No reuse allowed without permission.

1097 10. Grande A, Sumiyoshi K, López-Juárez A, Howard J, Sakthivel B, Aronow B, et al.
1098 Environmental impact on direct neuronal reprogramming in vivo in the adult brain. Nat
1099 Commun [Internet]. 2013;4. Available from: http://dx.doi.org/10.1038/ncomms3373

1100 11. Heinrich C, Blum R, Gascón S, Masserdotti G, Tripathi P, Sánchez R, et al. Directing
1101 Astroglia from the Cerebral Cortex into Subtype Specific Functional Neurons. McKay
1102 RDG, editor. PLoS Biol [Internet]. 2010/05/27. 2010;8:e1000373. Available from:
1103 http://www.ncbi.nlm.nih.gov/entrez/query.fcgi?cmd=Retrieve&db=PubMed&dopt=Cita
1104 tion&list_uids=20502524

1105 12. Herrero-Navarro Á, Puche-Aroca L, Moreno-Juan V, Sempere-Ferràndez A,
1106 Espinosa A, Susín R, et al. Astrocytes and neurons share region-specific transcriptional
1107 signatures that confer regional identity to neuronal reprogramming. Sci Adv. 2021;7.

1108 13. Liu F, Zhang Y, Chen F, Yuan J, Li S, Han S, et al. Neurog2 directly converts
1109 astrocytes into functional neurons in midbrain and spinal cord. Cell Death Dis. 2021;12.

1110 14. Masserdotti G, Gillotin S, Sutor B, Drechsel D, Irmler M, Jørgensen HF, et al.
1111 Transcriptional Mechanisms of Proneural Factors and REST in Regulating Neuronal
1112 Reprogramming of Astrocytes. Cell Stem Cell [Internet]. 2015;17:74–88. Available from:
1113 https://linkinghub.elsevier.com/retrieve/pii/S1934590915002234

1114 15. Mattugini N, Bocchi R, Scheuss V, Russo GL, Torper O, Lao CL, et al. Inducing
1115 Different Neuronal Subtypes from Astrocytes in the Injured Mouse Cerebral Cortex.
1116 Neuron [Internet]. 2019;103:1086-1095.e5. Available from:
1117 https://linkinghub.elsevier.com/retrieve/pii/S0896627319306932

1118 16. Ninkovic J, Steiner-Mezzadri A, Jawerka M, Akinci U, Masserdotti G, Petricca S, et al.
1119 The BAF complex interacts with Pax6 in adult neural progenitors to establish a
1120 neurogenic cross-regulatory transcriptional network. Cell Stem Cell. 2013;13.

1121 17. Niu W, Zang T, Zou Y, Fang S, Smith DK, Bachoo R, et al. In vivo reprogramming of
1122 astrocytes to neuroblasts in the adult brain. Nat Cell Biol [Internet]. 2013;15:1164–75.
1123 Available from: http://www.ncbi.nlm.nih.gov/pubmed/24056302

1124 18. Pereira M, Birtele M, Shrigley S, Benitez JA, Hedlund E, Parmar M, et al. Direct
1125 Reprogramming of Resident NG2 Glia into Neurons with Properties of Fast-Spiking
1126 Parvalbumin-Containing Interneurons. Stem Cell Reports [Internet]. 2017;9:742–51.
1127 Available from: https://www.ncbi.nlm.nih.gov/pubmed/28844658

1128 19. Zhang L, Lei Z, Guo Z, Pei Z, Chen Y, Zhang F, et al. Development of
1129 Neuroregenerative Gene Therapy to Reverse Glial Scar Tissue Back to Neuron-Enriched
1130 Tissue. Front Cell Neurosci. 2020;14.

bioRxiv preprint doi: https://doi.org/10.1101/2023.08.31.555708; this version posted September 3, 2023. The copyright holder for this preprint (which was not certified by peer review) is the author/funder. All rights reserved. No reuse allowed without permission.

1131 20. Vierbuchen T, Wernig M. Direct lineage conversions: unnatural but useful? Nat
1132 Biotechnol [Internet]. 2011/10/15. 2011;29:892–907. Available from:
1133 http://www.ncbi.nlm.nih.gov/entrez/query.fcgi?cmd=Retrieve&db=PubMed&dopt=Cita
1134 tion&list_uids=21997635

1135 21. Lujan E, Chanda S, Ahlenius H, Sudhof TC, Wernig M. Direct conversion of mouse
1136 fibroblasts to self-renewing, tripotent neural precursor cells. Proc Natl Acad Sci U S A
1137 [Internet]. 2012/02/07. 2012;109:2527–32. Available from:
1138 http://www.ncbi.nlm.nih.gov/entrez/query.fcgi?cmd=Retrieve&db=PubMed&dopt=Cita
1139 tion&list_uids=22308465

1140 22. Marro S, Pang ZP, Yang N, Tsai MC, Qu K, Chang HY, et al. Direct lineage
1141 conversion of terminally differentiated hepatocytes to functional neurons. Cell Stem Cell
1142 [Internet]. 2011/10/04. 2011;9:374–82. Available from:
1143 http://www.ncbi.nlm.nih.gov/entrez/query.fcgi?cmd=Retrieve&db=PubMed&dopt=Cita
1144 tion&list_uids=21962918

1145 23. Treutlein B, Lee QY, Camp JG, Mall M, Koh W, Shariati SA, et al. Dissecting direct
1146 reprogramming from fibroblast to neuron using single-cell RNA-seq. Nature [Internet].
1147 2016;534:391–5. Available from: https://www.ncbi.nlm.nih.gov/pubmed/27281220

1148 24. Pfisterer U, Kirkeby A, Torper O, Wood J, Nelander J, Dufour A, et al. Direct
1149 conversion of human fibroblasts to dopaminergic neurons. Proceedings of the National
1150 Academy of Sciences [Internet]. 2011;108:10343–8. Available from:
1151 http://www.ncbi.nlm.nih.gov/pubmed/21646515

1152 25. Wapinski OL, Vierbuchen T, Qu K, Lee QY, Chanda S, Fuentes DR, et al. Hierarchical
1153 mechanisms for direct reprogramming of fibroblasts to neurons. Cell [Internet].
1154 2013;155:621–35. Available from: http://www.ncbi.nlm.nih.gov/pubmed/24243019

1155 26. Wapinski OL, Lee QY, Chen AC, Li R, Corces MR, Ang CE, et al. Rapid Chromatin
1156 Switch in the Direct Reprogramming of Fibroblasts to Neurons. Cell Rep [Internet].
1157 2017;20:3236–47. Available from: https://www.ncbi.nlm.nih.gov/pubmed/28954238

1158 27. Noack F, Vangelisti S, Raffl G, Carido M, Diwakar J, Chong F, et al. Multimodal
1159 profiling of the transcriptional regulatory landscape of the developing mouse cortex
1160 identifies Neurog2 as a key epigenome remodeler. Nat Neurosci. 2022;25.

1161 28. Pataskar A, Jung J, Smialowski P, Noack F, Calegari F, Straub T, et al. NeuroD1
1162 reprograms chromatin and transcription factor landscapes to induce the neuronal
1163 program. Embo J [Internet]. 2016;35:24–45. Available from:
1164 https://www.ncbi.nlm.nih.gov/pubmed/26516211

bioRxiv preprint doi: https://doi.org/10.1101/2023.08.31.555708; this version posted September 3, 2023. The copyright holder for this preprint (which was not certified by peer review) is the author/funder. All rights reserved. No reuse allowed without permission.

1165 29. Heinrich C, Bergami M, Gascón S, Lepier A, Dimou L, Sutor B, et al. Sox2-mediated
1166 conversion of NG2 glia into induced neurons in the injured adult cerebral cortex. Stem
1167 Cell Reports [Internet]. 2014;in press:1000–14. Available from:
1168 http://www.ncbi.nlm.nih.gov/pubmed/25458895

1169 30. Liu M-L, Zang T, Zou Y, Chang JC, Gibson JR, Huber KM, et al. Small molecules
1170 enable neurogenin 2 to efficiently convert human fibroblasts into cholinergic neurons.
1171 Nat Commun [Internet]. 2013;4. Available from: http://dx.doi.org/10.1038/ncomms3183

1172 31. Russo GL, Sonsalla G, Natarajan P, Breunig CT, Bulli G, Merl-Pham J, et al. CRISPR-
1173 Mediated Induction of Neuron-Enriched Mitochondrial Proteins Boosts Direct Glia-to-
1174 Neuron Conversion. Cell Stem Cell. 2021;28.

1175 32. Gascón S, Murenu E, Masserdotti G, Ortega F, Russo GL, Petrik D, et al. Identification
1176 and Successful Negotiation of a Metabolic Checkpoint in Direct Neuronal
1177 Reprogramming. Cell Stem Cell [Internet]. 2016;18:396–409. Available from:
1178 https://linkinghub.elsevier.com/retrieve/pii/S1934590915005482

1179 33. Hu X, Qin S, Huang X, Yuan Y, Tan Z, Gu Y, et al. Region-Restrict Astrocytes Exhibit
1180 Heterogeneous Susceptibility to Neuronal Reprogramming. Stem Cell Reports. 2019;12.

1181 34. Addington CP, Roussas A, Dutta D, Stabenfeldt SE. Endogenous Repair Signaling
1182 after Brain Injury and Complementary Bioengineering Approaches to Enhance Neural
1183 Regeneration: Supplementary Issue: Stem Cell Biology. Biomark Insights. 2015.

1184 35. Sun D, Bullock MR, McGinn MJ, Zhou Z, Altememi N, Hagood S, et al. Basic
1185 fibroblast growth factor-enhanced neurogenesis contributes to cognitive recovery in
1186 rats following traumatic brain injury. Exp Neurol. 2009;216.

1187 36. Ninomiya M, Yamashita T, Araki N, Okano H, Sawamoto K. Enhanced neurogenesis
1188 in the ischemic striatum following EGF-induced expansion of transit-amplifying cells in
1189 the subventricular zone. Neurosci Lett. 2006;403.

1190 37. Grande A, Sumiyoshi K, López-Juárez A, Howard J, Sakthivel B, Aronow B, et al.
1191 Environmental impact on direct neuronal reprogramming in vivo in the adult brain. Nat
1192 Commun [Internet]. 2013;4. Available from: http://dx.doi.org/10.1038/ncomms3373

1193 38. Hung LY, Tseng JT, Lee YC, Xia W, Wang YN, Wu ML, et al. Nuclear epidermal
1194 growth factor receptor (EGFR) interacts with signal transducer and activator of
1195 transcription 5 (STAT5) in activating Aurora-A gene expression. Nucleic Acids Res.
1196 2008;36.

1197 39. Choi HS, Choi BY, Cho YY, Mizuno H, Kang BS, Bode AM, et al. Phosphorylation of
1198 histone H3 at serine 10 is indispensable for neoplastic cell transformation. Cancer Res.
1199 2005;65.

bioRxiv preprint doi: https://doi.org/10.1101/2023.08.31.555708; this version posted September 3, 2023. The copyright holder for this preprint (which was not certified by peer review) is the author/funder. All rights reserved. No reuse allowed without permission.

1200 40. Patel NS, Rhinn M, Semprich CI, Halley PA, Dollé P, Bickmore WA, et al. FGF
1201 Signalling Regulates Chromatin Organisation during Neural Differentiation via
1202 Mechanisms that Can Be Uncoupled from Transcription. PLoS Genet. 2013;9.

1203 41. Addington CP, Roussas A, Dutta D, Stabenfeldt SE. Endogenous Repair Signaling
1204 after Brain Injury and Complementary Bioengineering Approaches to Enhance Neural
1205 Regeneration: Supplementary Issue: Stem Cell Biology. Biomark Insights. 2015.

1206 42. Heinrich C, Blum R, Gascon S, Masserdotti G, Tripathi P, Sanchez R, et al. Directing
1207 astroglia from the cerebral cortex into subtype specific functional neurons. PLoS Biol
1208 [Internet]. 2010/05/27. 2010;8:e1000373. Available from:
1209 http://www.ncbi.nlm.nih.gov/entrez/query.fcgi?cmd=Retrieve&db=PubMed&dopt=Cita
1210 tion&list_uids=20502524

1211 43. Heinrich C, Gotz M, Berninger B. Reprogramming of postnatal astroglia of the
1212 mouse neocortex into functional, synapse-forming neurons. Methods Mol Biol
1213 [Internet]. 2012;814:485–98. Available from:
1214 http://www.ncbi.nlm.nih.gov/pubmed/22144327

1215 44. Gascon S, Masserdotti G, Russo GL, Gotz M. Direct Neuronal Reprogramming:
1216 Achievements, Hurdles, and New Roads to Success. Cell Stem Cell [Internet].
1217 2017;21:18–34. Available from: http://www.ncbi.nlm.nih.gov/pubmed/28686866

1218 45. Hack MA, Sugimori M, Lundberg C, Nakafuku M, Götz M, Gotz M. Regionalization
1219 and fate specification in neurospheres: the role of Olig2 and Pax6. Mol Cell Neurosci
1220 [Internet]. 2004/04/15. 2004;25:664–78. Available from:
1221 http://www.ncbi.nlm.nih.gov/pubmed/15080895

1222 46. Masserdotti G, Gillotin S, Sutor B, Drechsel D, Irmler M, Jørgensen HF, et al.
1223 Transcriptional Mechanisms of Proneural Factors and REST in Regulating Neuronal
1224 Reprogramming of Astrocytes. Cell Stem Cell. 2015;

1225 47. Russo GL, Sonsalla G, Natarajan P, Breunig CT, Bulli G, Merl-Pham J, et al. CRISPR-
1226 Mediated Induction of Neuron-Enriched Mitochondrial Proteins Boosts Direct Glia-to-
1227 Neuron Conversion. Cell Stem Cell. 2021;28.

1228 48. Masserdotti G, Götz M. A decade of questions about the fluidity of cell identity.
1229 Nature. 2020;578.

1230 49. Bocchi R, Masserdotti G, Götz M. Direct neuronal reprogramming: Fast forward
1231 from new concepts toward therapeutic approaches. Neuron. 2022.

1232 50. Gascón S, Masserdotti G, Russo GL, Götz M. Direct Neuronal Reprogramming:
1233 Achievements, Hurdles, and New Roads to Success. Cell Stem Cell. 2017.

bioRxiv preprint doi: https://doi.org/10.1101/2023.08.31.555708; this version posted September 3, 2023. The copyright holder for this preprint (which was not certified by peer review) is the author/funder. All rights reserved. No reuse allowed without permission.

1234 51. Ninkovic J, Götz M. Fate specification in the adult brain - lessons for eliciting
1235 neurogenesis from glial cells. BioEssays. 2013;35.

1236 52. Ninkovic J, Götz M. Understanding direct neuronal reprogramming — from pioneer
1237 factors to 3D chromatin. Curr Opin Genet Dev. 2018;52.

1238 53. Kimura A, Matsuda T, Sakai A, Murao N, Nakashima K. HMGB2 expression is
1239 associated with transition from a quiescent to an activated state of adult neural stem
1240 cells. Developmental Dynamics. 2018;247.

1241 54. Mall M, Kareta MS, Chanda S, Ahlenius H, Perotti N, Zhou B, et al. Myt1l safeguards
1242 neuronal identity by actively repressing many non-neuronal fates. Nature [Internet].
1243 2017;544:245–9. Available from: https://www.ncbi.nlm.nih.gov/pubmed/28379941

1244 55. Hsieh CY, Nakamura PA, Luk SO, Miko IJ, Henkemeyer M, Cramer KS. Ephrin-B
1245 reverse signaling is required for formation of strictly contralateral auditory brainstem
1246 pathways. Journal of Neuroscience. 2010;30.

1247 56. Kania A, Klein R. Mechanisms of ephrin-Eph signalling in development, physiology
1248 and disease. Nat Rev Mol Cell Biol. 2016.

1249 57. Hindley C, Ali F, McDowell G, Cheng K, Jones A, Guillemot F, et al. Post-translational
1250 modification of Ngn2 differentially affects transcription of distinct targets to regulate
1251 the balance between progenitor maintenance and differentiation. Development.
1252 2012;139.

1253 58. Zhang ZH, Jhaveri DJ, Marshall VM, Bauer DC, Edson J, Narayanan RK, et al. A
1254 comparative study of techniques for differential expression analysis on RNA-seq data.
1255 PLoS One. 2014;9.

1256 59. Pan G, Thomson JA. Nanog and transcriptional networks in embryonic stem cell
1257 pluripotency. Cell Res. 2007.

1258 60. Tokuzawa Y, Kaiho E, Maruyama M, Takahashi K, Mitsui K, Maeda M, et al. Fbx15 Is
1259 a Novel Target of Oct3/4 but Is Dispensable for Embryonic Stem Cell Self-Renewal and
1260 Mouse Development. Mol Cell Biol. 2003;23.

1261 61. Petrovic N, Schacke W, Gahagan JR, O'Conor CA, Winnicka B, Conway RE, et al.
1262 CD13/APN regulates endothelial invasion and filopodia formation. Blood. 2007;110.

1263 62. Mina-Osorio P, Winnicka B, O'Conor C, Grant CL, Vogel LK, Rodriguez-Pinto D, et
1264 al. CD13 is a novel mediator of monocytic/endothelial cell adhesion. J Leukoc Biol.
1265 2008;84.

bioRxiv preprint doi: https://doi.org/10.1101/2023.08.31.555708; this version posted September 3, 2023. The copyright holder for this preprint (which was not certified by peer review) is the author/funder. All rights reserved. No reuse allowed without permission.

1266 63. Lin G, Finger E, Gutierrez-Ramos JC. Expression of CD34 in endothelial cells,
1267 hematopoietic progenitors and nervous cells in fetal and adult mouse tissues. Eur J
1268 Immunol. 1995;25.

1269 64. Jung S, Aliberti J, Graemmel P, Sunshine MJ, Kreutzberg GW, Sher A, et al. Analysis
1270 of Fractalkine Receptor CX 3 CR1 Function by Targeted Deletion and Green Fluorescent
1271 Protein Reporter Gene Insertion . Mol Cell Biol. 2000;20.

1272 65. Schwab JM, Frei E, Klusman I, Schnell L, Schwab ME, Schluesener HJ. AIF-1
1273 expression defines a proliferating and alert microglial/macrophage phenotype
1274 following spinal cord injury in rats. J Neuroimmunol. 2001;119.

1275 66. Okada Y, Yamazaki H, Sekine-Aizawa Y, Hirokawa N. The neuron-specific kinesin
1276 superfamily protein KIF1A is a uniqye monomeric motor for anterograde axonal
1277 transport of synaptic vesicle precursors. Cell. 1995;81.

1278 67. Niwa S, Tanaka Y, Hirokawa N. KIF1Bβ- and KIF1A-mediated axonal transport of
1279 presynaptic regulator Rab3 occurs in a GTP-dependent manner through DENN/MADD.
1280 Nat Cell Biol. 2008;10.

1281 68. Wang R, Rossomando A, Sah DWY, Ossipov MH, King T, Porreca F. Artemin induced
1282 functional recovery and reinnervation after partial nerve injury. Pain. 2014;155.

1283 69. Errico F, Santini E, Migliarini S, Borgkvist A, Centonze D, Nasti V, et al. The GTP-
1284 binding protein Rhes modulates dopamine signalling in striatal medium spiny neurons.
1285 Molecular and Cellular Neuroscience. 2008;37.

1286 70. Bianchi ME, Agresti A. HMG proteins: Dynamic players in gene regulation and
1287 differentiation. Curr Opin Genet Dev. 2005.

1288 71. Štros M. HMGB proteins: Interactions with DNA and chromatin. Biochim Biophys
1289 Acta Gene Regul Mech. 2010.

1290 72. Thomas JO, Travers AA. HMG1 and 2, and related “architectural” DNA-binding
1291 proteins. Trends Biochem Sci. 2001.

1292 73. Smith DK, Yang J, Liu ML, Zhang CL. Small Molecules Modulate Chromatin
1293 Accessibility to Promote NEUROG2-Mediated Fibroblast-to-Neuron Reprogramming.
1294 Stem Cell Reports. 2016;7.

1295 74. Javed A, Mattar P, Lu S, Kruczek K, Kloc M, Gonzalez-Cordero A, et al. Pou2f1 and
1296 Pou2f2 cooperate to control the timing of cone photoreceptor production in the
1297 developing mouse retina. Development (Cambridge). 2020;147.

bioRxiv preprint doi: https://doi.org/10.1101/2023.08.31.555708; this version posted September 3, 2023. The copyright holder for this preprint (which was not certified by peer review) is the author/funder. All rights reserved. No reuse allowed without permission.

1298 75. Harris A, Masgutova G, Collin A, Toch M, Hidalgo-Figueroa M, Jacob B, et al.
1299 Onecut factors and Pou2f2 regulate the distribution of V2 interneurons in the mouse
1300 developing spinal cord. Front Cell Neurosci. 2019;13.

1301 76. Gonda Y, Namba T, Hanashima C. Beyond Axon Guidance: Roles of Slit-Robo
1302 Signaling in Neocortical Formation. Front Cell Dev Biol. 2020.

1303 77. Hevner RF. From Radial Glia to Pyramidal-Projection Neuron: Transcription Factor
1304 Cascades in Cerebral Cortex Development. Mol Neurobiol [Internet]. 2006 [cited 2019
1305 Nov 3];33:033–50. Available from: http://www.ncbi.nlm.nih.gov/pubmed/16388109

1306 78. Sofroniew M V. Astrocyte Reactivity: Subtypes, States, and Functions in CNS Innate
1307 Immunity. Trends Immunol. 2020.

1308 79. Burda JE, Sofroniew M V. Reactive gliosis and the multicellular response to CNS
1309 damage and disease. Neuron [Internet]. 2014;81:229–48. Available from:
1310 http://www.ncbi.nlm.nih.gov/pubmed/24462092

1311 80. Kang W, Hébert JM. FGF signaling is necessary for neurogenesis in young mice and
1312 sufficient to reverse its decline in old mice. Journal of Neuroscience. 2015;35.

1313 81. Goldshmit Y, Tang JKKY, Siegel AL, Nguyen PD, Kaslin J, Currie PD, et al. Different
1314 Fgfs have distinct roles in regulating neurogenesis after spinal cord injury in zebrafish.
1315 Neural Dev. 2018;13.

1316 82. Smith KM, Fagel DM, Stevens HE, Rabenstein RL, Maragnoli ME, Ohkubo Y, et al.
1317 Deficiency in Inhibitory Cortical Interneurons Associates with Hyperactivity in Fibroblast
1318 Growth Factor Receptor 1 Mutant Mice. Biol Psychiatry. 2008;63.

1319 83. Pataskar A, Jung J, Smialowski P, Noack F, Calegari F, Straub T, et al. NeuroD1
1320 reprograms chromatin and transcription factor landscapes to induce the neuronal
1321 program. Embo J [Internet]. 2016;35:24–45. Available from:
1322 https://www.ncbi.nlm.nih.gov/pubmed/26516211

1323 84. Noack F, Pataskar A, Schneider M, Buchholz F, Tiwari VK, Calegari F. Assessment and
1324 site-specific manipulation of DNA (hydroxy-)methylation during mouse corticogenesis.
1325 Life Sci Alliance. 2019;2.

1326 85. Aprea J, Prenninger S, Dori M, Ghosh T, Monasor LS, Wessendorf E, et al.
1327 Transcriptome sequencing during mouse brain development identifies long non-
1328 coding RNAs functionally involved in neurogenic commitment. EMBO Journal. 2013;32.

1329 86. Abraham AB, Bronstein R, Reddy AS, Maletic-Savatic M, Aguirre A, Tsirka SE.
1330 Aberrant Neural Stem Cell Proliferation and Increased Adult Neurogenesis in Mice
1331 Lacking Chromatin Protein HMGB2. PLoS One. 2013;8:e84838.

bioRxiv preprint doi: https://doi.org/10.1101/2023.08.31.555708; this version posted September 3, 2023. The copyright holder for this preprint (which was not certified by peer review) is the author/funder. All rights reserved. No reuse allowed without permission.

1332 87. Wapinski OL, Lee QY, Chen AC, Li R, Corces MR, Ang CE, et al. Rapid Chromatin
1333 Switch in the Direct Reprogramming of Fibroblasts to Neurons. Cell Rep [Internet].
1334 2017;20:3236–47. Available from: https://www.ncbi.nlm.nih.gov/pubmed/28954238

1335 88. Kishi Y, Fujii Y, Hirabayashi Y, Gotoh Y. HMGA regulates the global chromatin state
1336 and neurogenic potential in neocortical precursor cells. Nat Neurosci [Internet].
1337 2012;15:1127–33. Available from: http://www.ncbi.nlm.nih.gov/pubmed/22797695

1338 89. Zhou X, Zhong S, Peng H, Liu J, Ding W, Sun L, et al. Cellular and molecular
1339 properties of neural progenitors in the developing mammalian hypothalamus. Nat
1340 Commun. 2020;11.

1341 90. Lee SW, Oh YM, Lu YL, Kim WK, Yoo AS. MicroRNAs Overcome Cell Fate Barrier by
1342 Reducing EZH2-Controlled REST Stability during Neuronal Conversion of Human Adult
1343 Fibroblasts. Dev Cell. 2018;46.

1344 91. Starkova T, Polyanichko A, Tomilin AN, Chikhirzhina E. Structure and Functions of
1345 HMGB2 Protein. Int J Mol Sci. 2023;24:8334.

1346 92. Noack F, Vangelisti S, Raffl G, Carido M, Diwakar J, Chong F, et al. Multimodal
1347 profiling of the transcriptional regulatory landscape of the developing mouse cortex
1348 identifies Neurog2 as a key epigenome remodeler. Nat Neurosci. 2022;25.

1349 93. Zirkel A, Nikolic M, Sofiadis K, Mallm JP, Brackley CA, Gothe H, et al. HMGB2 Loss
1350 upon Senescence Entry Disrupts Genomic Organization and Induces CTCF Clustering
1351 across Cell Types. Mol Cell. 2018;70.

1352 94. Divisato G, Chiariello AM, Esposito A, Zoppoli P, Zambelli F, Elia MA, et al. Hmga2
1353 protein loss alters nuclear envelope and 3D chromatin structure. BMC Biol. 2022;20.

1354 95. Wapinski OL, Vierbuchen T, Qu K, Lee QY, Chanda S, Fuentes DR, et al. Hierarchical
1355 mechanisms for direct reprogramming of fibroblasts to neurons. Cell [Internet].
1356 2013;155:621–35. Available from: http://www.ncbi.nlm.nih.gov/pubmed/24243019

1357 96. Liu M-L, Zang T, Zou Y, Chang JC, Gibson JR, Huber KM, et al. Small molecules
1358 enable neurogenin 2 to efficiently convert human fibroblasts into cholinergic neurons.
1359 Nat Commun [Internet]. 2013;4. Available from: http://dx.doi.org/10.1038/ncomms3183

1360 97. Heinrich C, Bergami M, Gascón S, Lepier A, Dimou L, Sutor B, et al. Sox2-mediated
1361 conversion of NG2 glia into induced neurons in the injured adult cerebral cortex. Stem
1362 Cell Reports [Internet]. 2014;in press:1000–14. Available from:
1363 http://www.ncbi.nlm.nih.gov/pubmed/25458895

1364 98. Liu ML, Zang T, Zhang CL. Direct Lineage Reprogramming Reveals Disease-Specific
1365 Phenotypes of Motor Neurons from Human ALS Patients. Cell Rep. 2016;14.

bioRxiv preprint doi: https://doi.org/10.1101/2023.08.31.555708; this version posted September 3, 2023. The copyright holder for this preprint (which was not certified by peer review) is the author/funder. All rights reserved. No reuse allowed without permission.

1366 99. Kempf J, Knelles K, Hersbach BA, Petrik D, Riedemann T, Bednarova V, et al.
1367 Heterogeneity of neurons reprogrammed from spinal cord astrocytes by the proneural
1368 factors Ascl1 and Neurogenin2. Cell Rep. 2021;36.

1369 100. Treutlein B, Lee QY, Camp JG, Mall M, Koh W, Shariati SA, et al. Dissecting direct
1370 reprogramming from fibroblast to neuron using single-cell RNA-seq. Nature [Internet].
1371 2016;534:391–5. Available from: https://www.ncbi.nlm.nih.gov/pubmed/27281220

1372 101. Chen K, Zhang J, Liang F, Zhu Q, Cai S, Tong X, et al. HMGB2 orchestrates mitotic
1373 clonal expansion by binding to the promoter of C/EBPβ to facilitate adipogenesis. Cell
1374 Death Dis. 2021;12.

1375 102. Ronfani L, Ferraguti M, Croci L, Ovitt CE, Schöler HR, Consalez GG, et al. Reduced
1376 fertility and spermatogenesis defects in mice lacking chromosomal protein Hmgb2.
1377 Development. 2001;128:1265–73.

1378 103. Buffo A, Rite I, Tripathi P, Lepier A, Colak D, Horn AP, et al. Origin and progeny of
1379 reactive gliosis: A source of multipotent cells in the injured brain. Proc Natl Acad Sci U S
1380 A [Internet]. 2008/02/27. 2008;105:3581–6. Available from:
1381 http://www.ncbi.nlm.nih.gov/entrez/query.fcgi?cmd=Retrieve&db=PubMed&dopt=Cita
1382 tion&list_uids=18299565

1383 104. Blum R, Heinrich C, Sanchez R, Lepier A, Gundelfinger ED, Berninger B, et al.
1384 Neuronal network formation from reprogrammed early postnatal rat cortical glial cells.
1385 Cereb Cortex [Internet]. 2010/06/22. 2011;21:413–24. Available from:
1386 http://www.ncbi.nlm.nih.gov/pubmed/20562320

1387 105. Schindelin J, Arganda-Carreras I, Frise E, Kaynig V, Longair M, Pietzsch T, et al. Fiji:
1388 An open-source platform for biological-image analysis. Nat Methods. 2012.

1389 106. Buenrostro JD, Wu B, Chang HY, Greenleaf WJ. ATAC-seq: A method for assaying
1390 chromatin accessibility genome-wide. Curr Protoc Mol Biol. 2015;2015.

1391 107. Buenrostro JD, Giresi PG, Zaba LC, Chang HY, Greenleaf WJ. Transposition of
1392 native chromatin for fast and sensitive epigenomic profiling of open chromatin, DNA-
1393 binding proteins and nucleosome position. Nat Methods. 2013;10.

1394 108. Quinlan AR, Hall IM. BEDTools: A flexible suite of utilities for comparing genomic
1395 features. Bioinformatics. 2010;26.

1396 109. Ninkovic J, Pinto L, Petricca S, Lepier A, Sun J, Rieger MAA, et al. The transcription
1397 factor Pax6 regulates survival of dopaminergic olfactory bulb neurons via crystallin
1398 alphaA. Neuron [Internet]. 2010/11/26. 2010;68:682–94. Available from:
1399 http://www.ncbi.nlm.nih.gov/entrez/query.fcgi?cmd=Retrieve&db=PubMed&dopt=Cita
1400 tion&list_uids=21092858

bioRxiv preprint doi: https://doi.org/10.1101/2023.08.31.555708; this version posted September 3, 2023. The copyright holder for this preprint (which was not certified by peer review) is the author/funder. All rights reserved. No reuse allowed without permission.

1401 110. Wiśniewski JR, Zougman A, Nagaraj N, Mann M. Universal sample preparation
1402 method for proteome analysis. Nat Methods. 2009;6:359–62.

1403 111. Hauck SM, Dietter J, Kramer RL, Hofmaier F, Zipplies JK, Amann B, et al.
1404 Deciphering Membrane-Associated Molecular Processes in Target Tissue of
1405 Autoimmune Uveitis by Label-Free Quantitative Mass Spectrometry. Molecular &
1406 Cellular Proteomics. 2010;9:2292–305.

1407 112. Merl J, Ueffing M, Hauck SM, von Toerne C. Direct comparison of MS-based label-
1408 free and SILAC quantitative proteome profiling strategies in primary retinal Müller cells.
1409 Proteomics. 2012;12:1902–11.

1410 113. Ninkovic J, Steiner-Mezzadri A, Jawerka M, Akinci U, Masserdotti G, Petricca S, et
1411 al. The BAF Complex Interacts with Pax6 in Adult Neural Progenitors to Establish a
1412 Neurogenic Cross-Regulatory Transcriptional Network. Cell Stem Cell [Internet].
1413 2013;13. Available from: http://www.ncbi.nlm.nih.gov/pubmed/23933087

1414 114. RStudio Team. RStudio: Integrated Development for R. RStudio, Inc., Boston, MA.
1415 URL http://www.rstudio.com/. RStudio, Inc. 2015;

1416

bioRxiv preprint doi: https://doi.org/10.1101/2023.08.31.555708; this version posted September 3, 2023. The copyright holder for this preprint (which was not certified by peer review) is the author/funder. All rights reserved. No reuse allowed without permission.

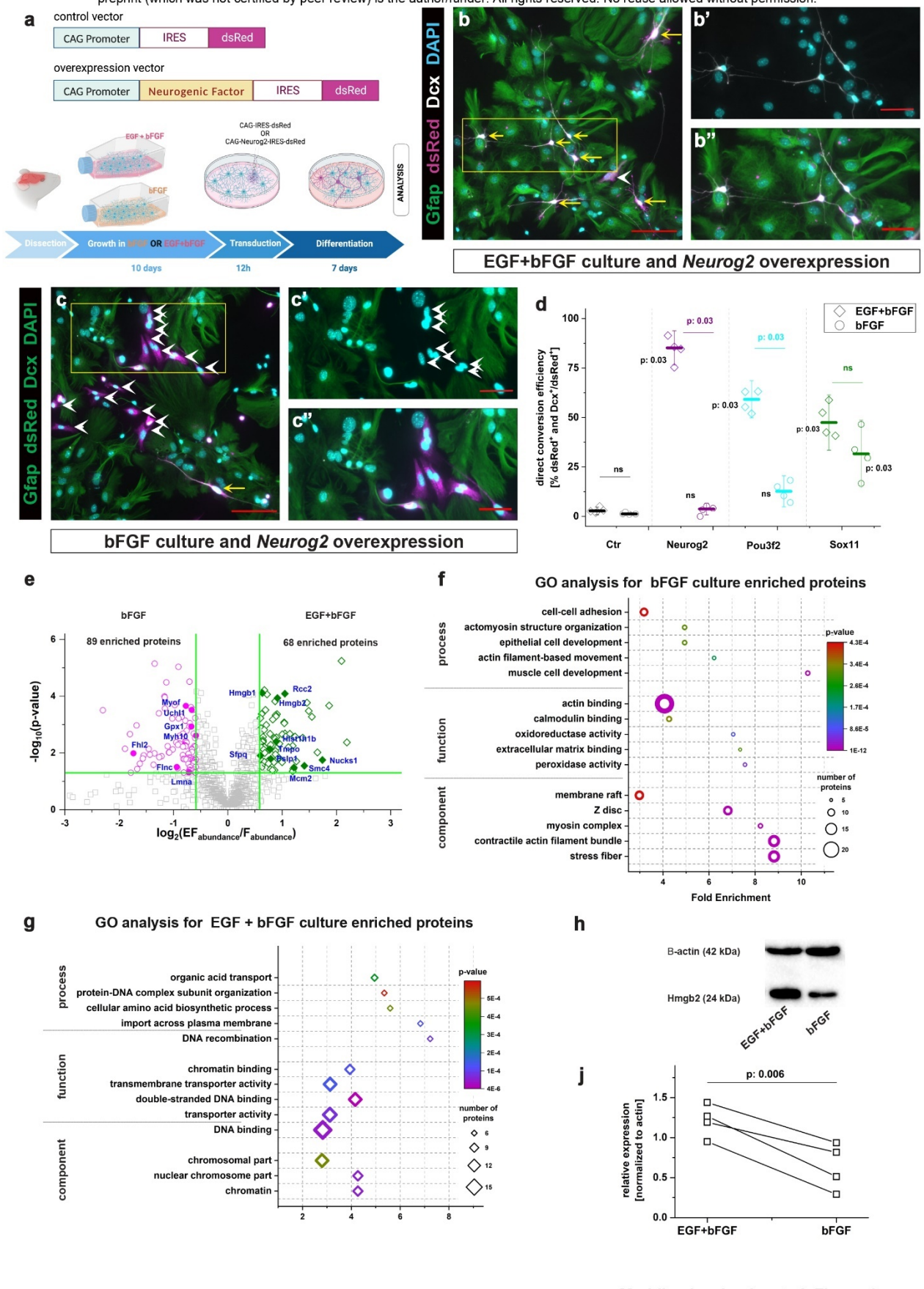

Maddhesiya, Lepko et al, Figure 1

bioRxiv preprint doi: https://doi.org/10.1101/2023.08.31.555708; this version posted September 3, 2023. The copyright holder for this preprint (which was not certified by peer review) is the author/funder. All rights reserved. No reuse allowed without permission.

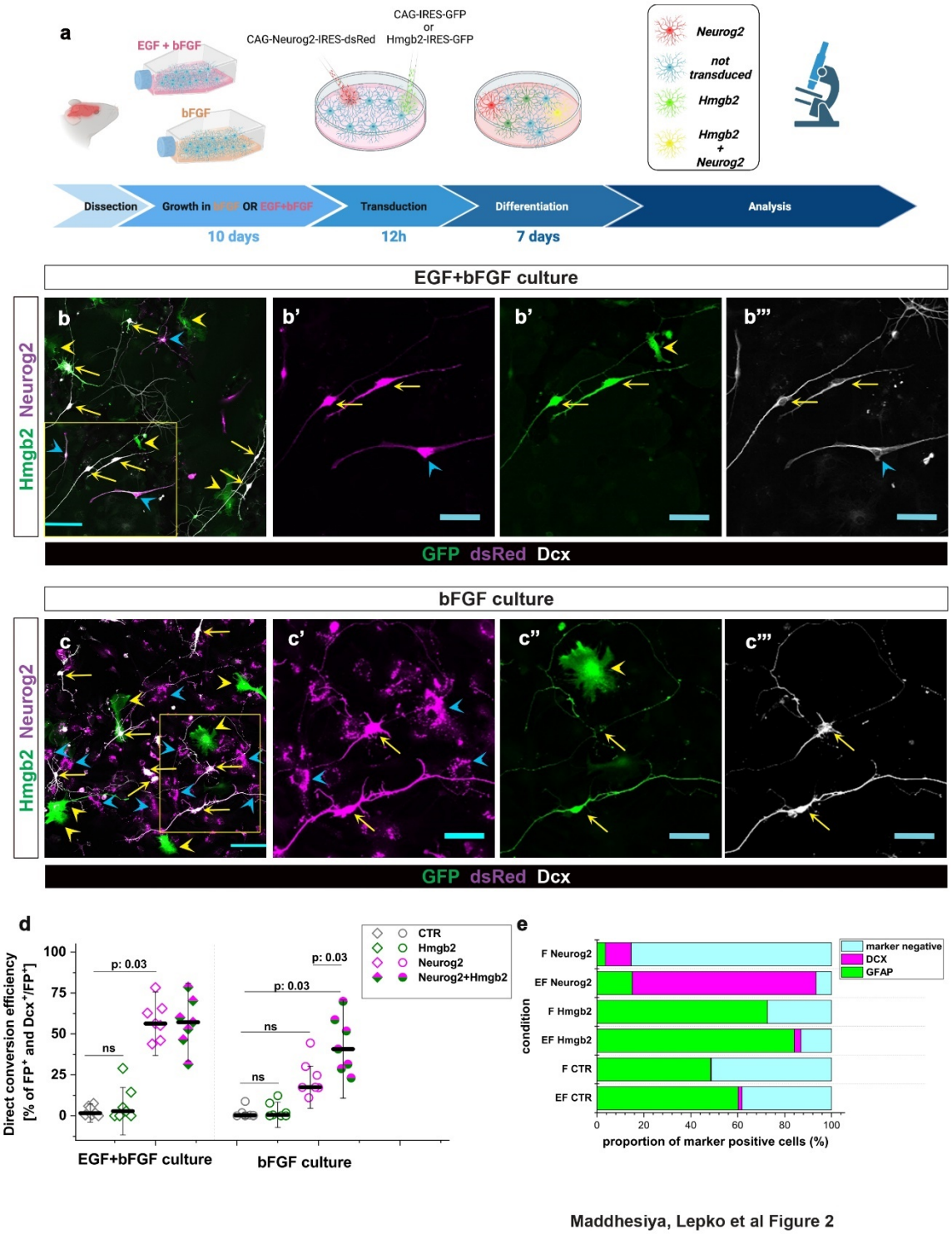

Maddhesiya, Lepko et al Figure 2

bioRxiv preprint doi: https://doi.org/10.1101/2023.08.31.555708; this version posted September 3, 2023. The copyright holder for this preprint (which was not certified by peer review) is the author/funder. All rights reserved. No reuse allowed without permission.

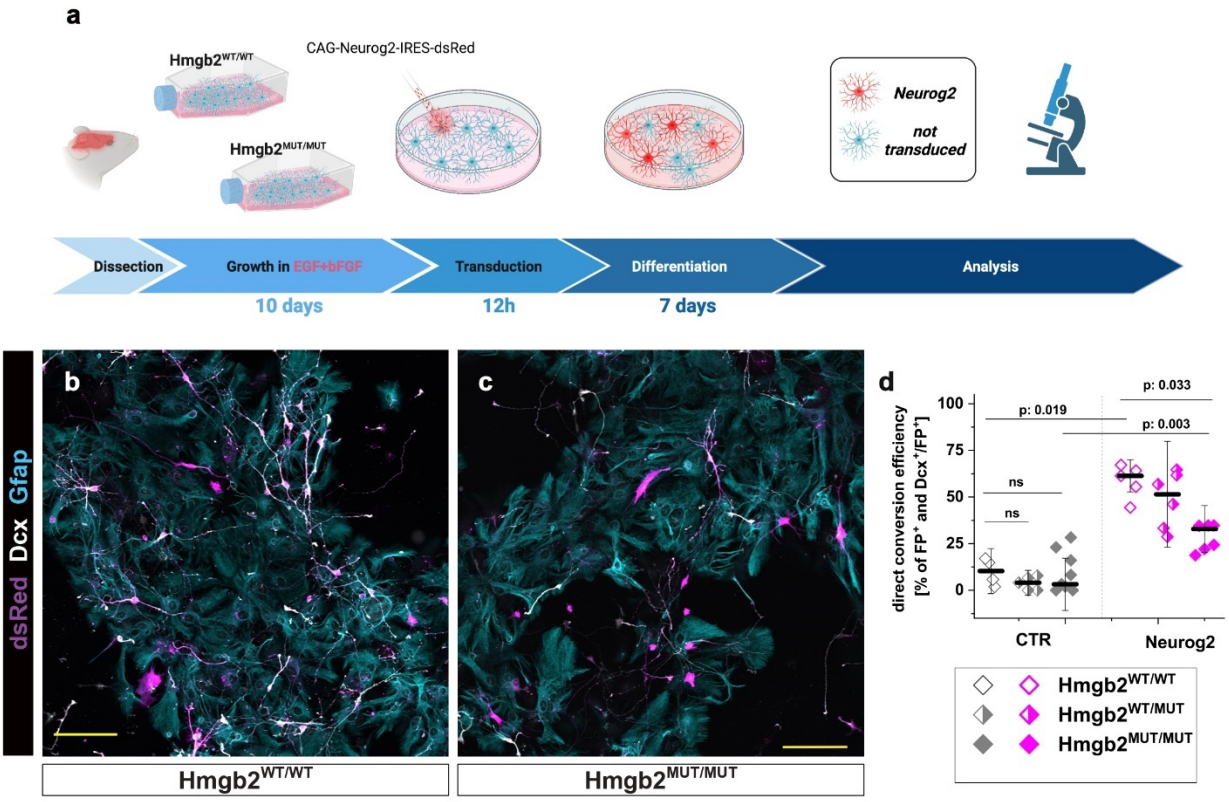

Maddhesiya, Lepko et al Figure 3

bioRxiv preprint doi: https://doi.org/10.1101/2023.08.31.555708; this version posted September 3, 2023. The copyright holder for this preprint (which was not certified by peer review) is the author/funder. All rights reserved. No reuse allowed without permission.

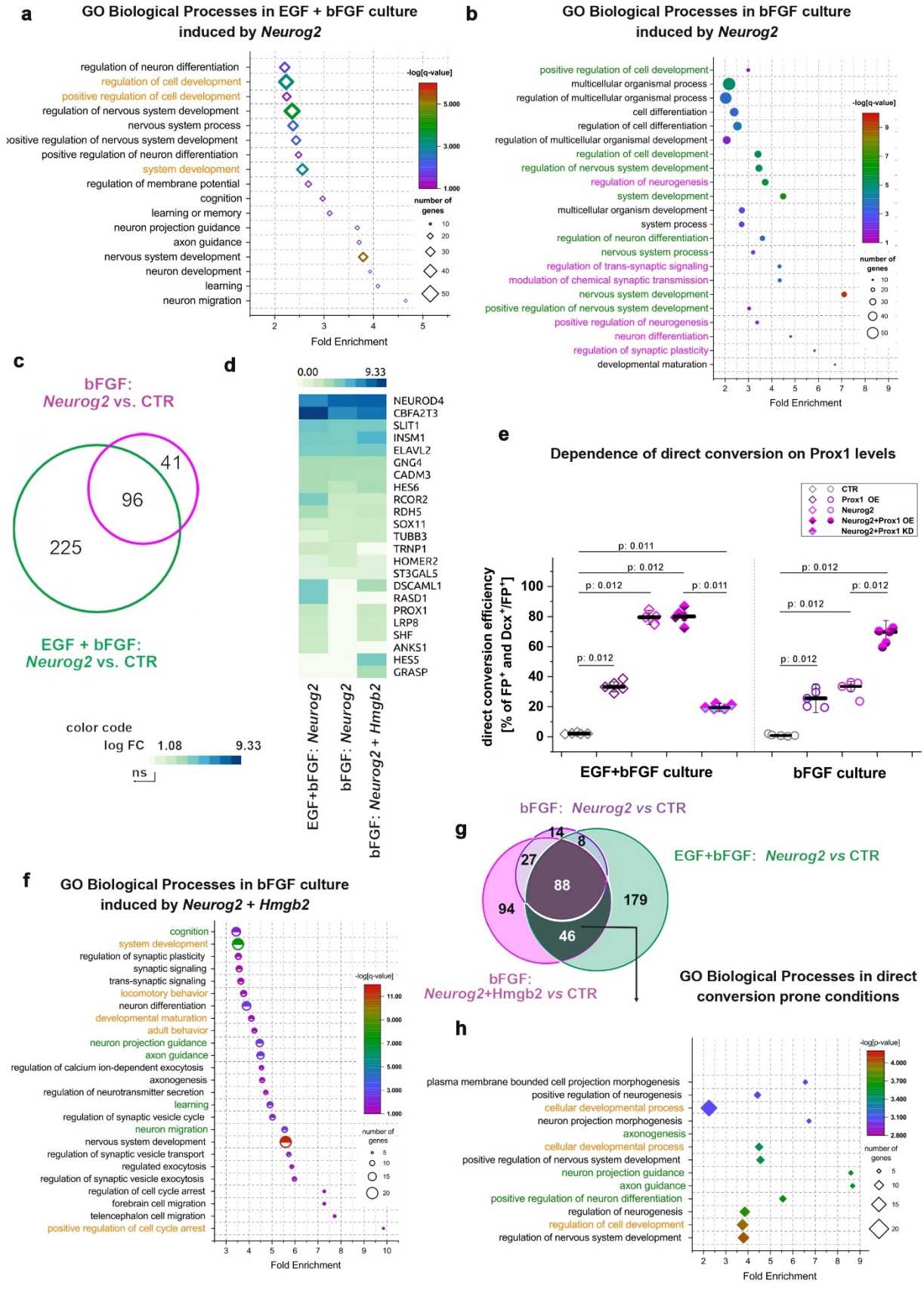

Maddhesiya, Lepko et al, Figure 4

bioRxiv preprint doi: https://doi.org/10.1101/2023.08.31.555708; this version posted September 3, 2023. The copyright holder for this preprint (which was not certified by peer review) is the author/funder. All rights reserved. No reuse allowed without permission.

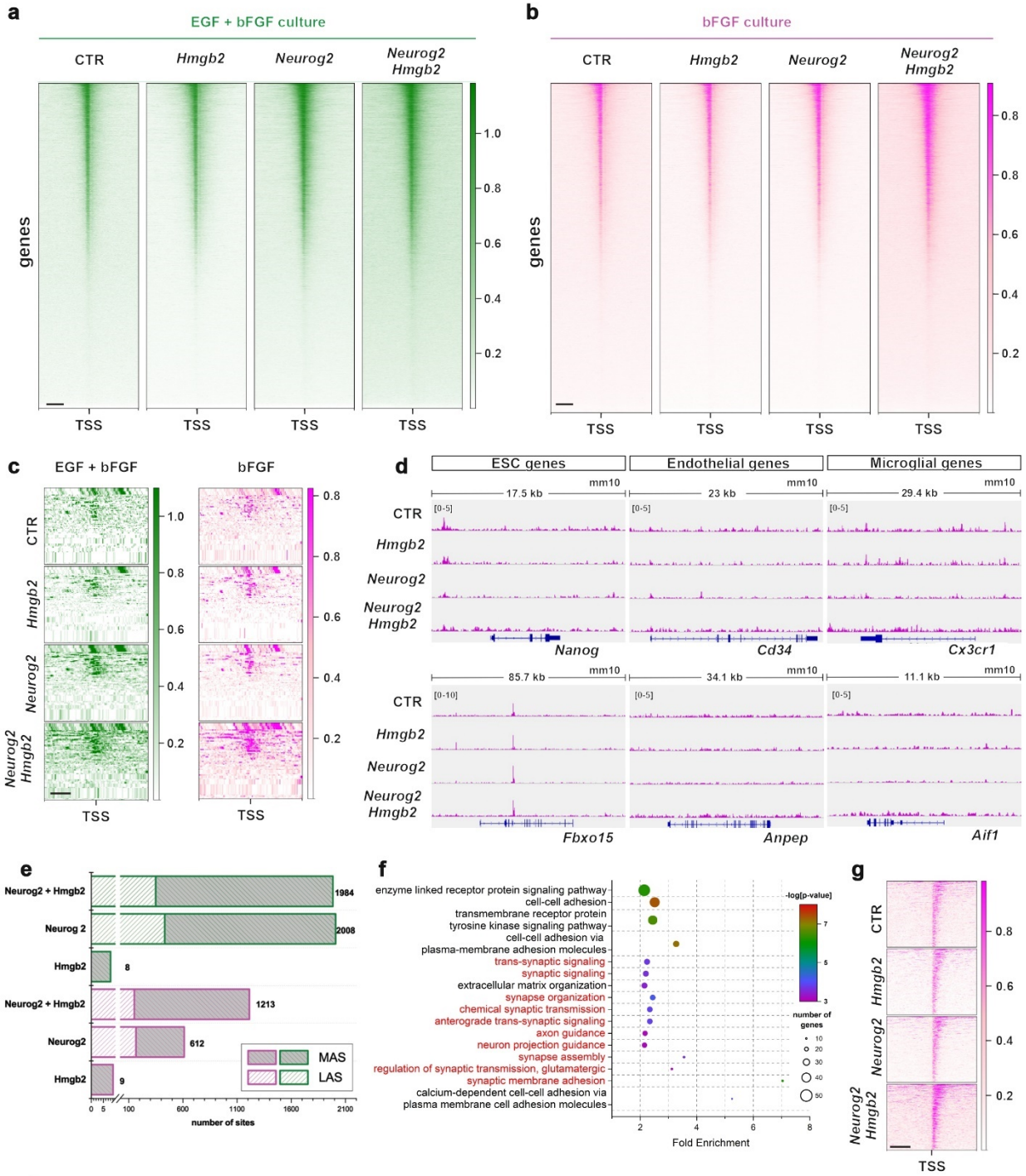

Maddhesiya, Lepko et al, Figure 5

bioRxiv preprint doi: https://doi.org/10.1101/2023.08.31.555708; this version posted September 3, 2023. The copyright holder for this preprint (which was not certified by peer review) is the author/funder. All rights reserved. No reuse allowed without permission.

a

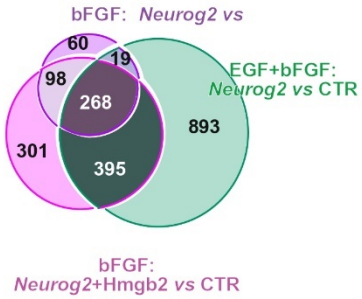

b

GO Biological Processes enriched in direct conversion relevant peaks induced by *Neurog2+Hmgb2* (395 MASs)

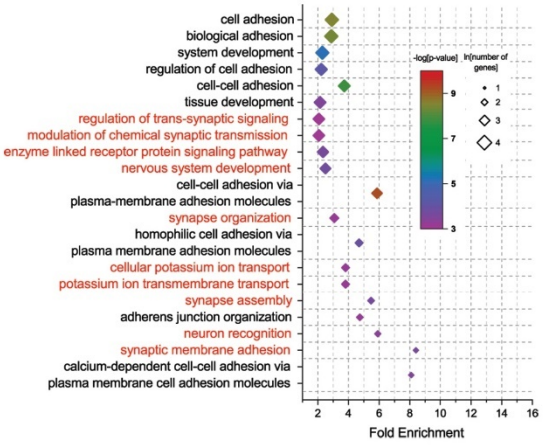

c

GO Biological Processes enriched in shared peaks induced by *Neurog2* (268 MASs)

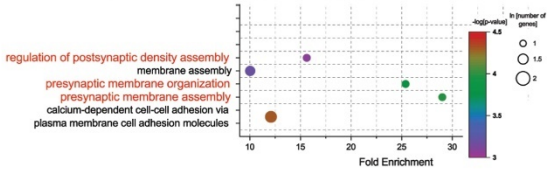

d

TF binding site consensus sequence in shared peaks induced by *Neurog2* (268 MASs)

Motif 1

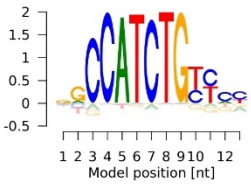

Binding motif for Tal-related TFs

TF	E-value
Neurog2	2.9E-06
Neurod1	3.1E-06
Neurod2	5.4E-06
Atoh1	8.4E-06
Msgn1	3.2E-05

identified in 202 MASs

e

TF binding site consensus sequence in direct conversion relevant peaks induced by *Neurog2+Hmgb2* (395 MASs)

Motif 1

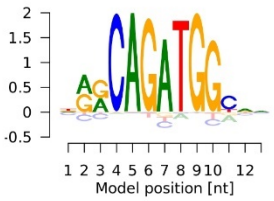

Binding motif for Tal-related TFs

TF	E-value
Neurog2	1.9E-08
Neurod1	4.1E-08
Neurod2	4.2E-08
Atoh1	5.4E-08
Msgn1	1.8E-06

identified in 261 MASs

Motif 2

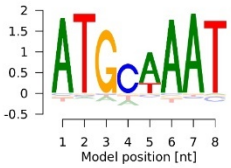

Binding motif for POU TFs

TF	E-value
Pou2f2	7.6E-03

identified in 90 MASs

Maddhesiya, Lepko et al, Figure 6

bioRxiv preprint doi: https://doi.org/10.1101/2023.08.31.555708; this version posted September 3, 2023. The copyright holder for this preprint (which was not certified by peer review) is the author/funder. All rights reserved. No reuse allowed without permission.

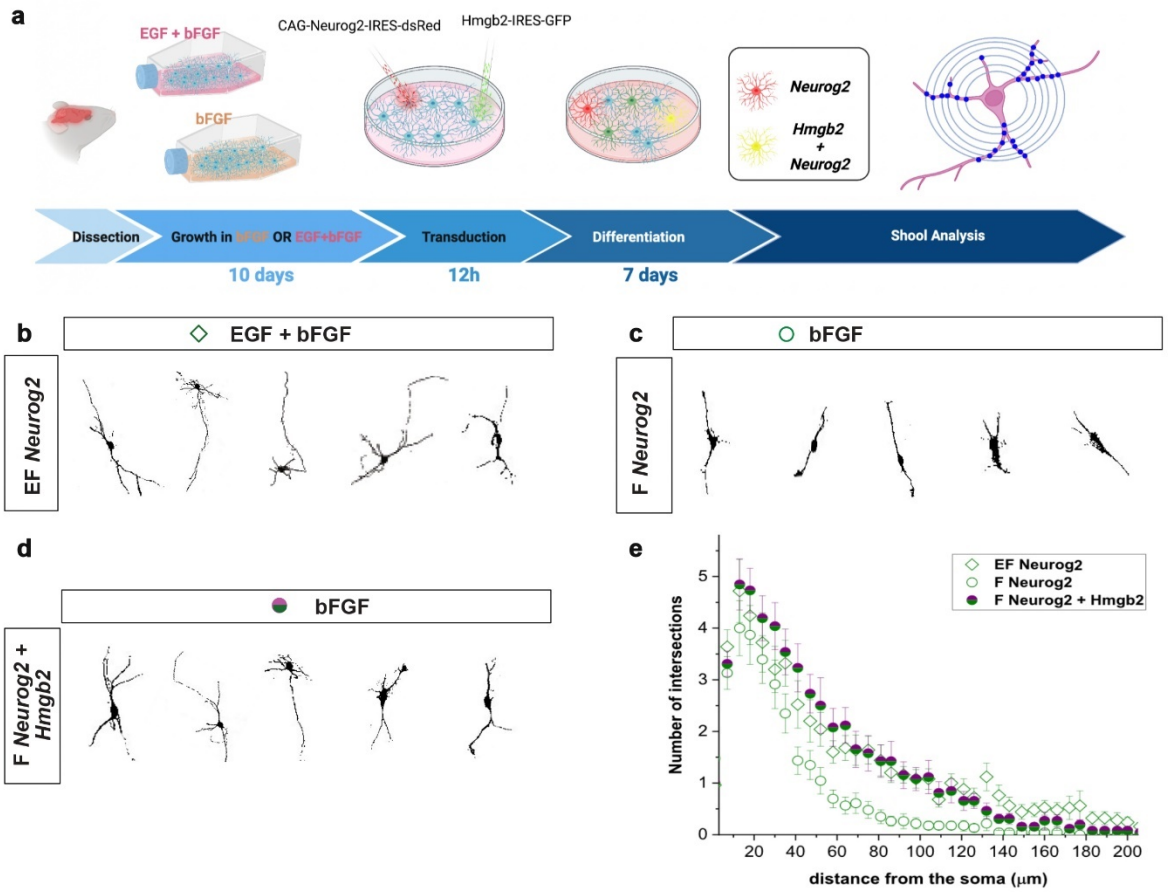

Maddhesiya, Lepko et al, Figure 7

3. Discussion

3.1 Cross-Species Insights into identifying injury-induced proliferative astrocytic subset

The limited neurogenic capacity of the adult mammalian brain poses a significant obstacle to repairing and rejuvenating damaged or diseased brains (Jessberger, 2016; Sun, 2014). Nonetheless, there has been a notable paradigm shift suggests that reactive astrocytes in the cerebral cortex can exhibit remarkable plasticity and dedifferentiate into a stem cell-like state following injury (Buffo et al., 2008). These astrocytic subsets share characteristics with NSCs, including the ability to proliferate and form multipotent neurospheres *in vitro* (M. Götz et al., 2015; Robel et al., 2011; Sirko et al., 2013). This revelation opens new avenues for regenerative medicine, potentially leveraging these plastic astrocytes for direct neuronal reprogramming, a promising approach for neuronal replacement (Guo et al., 2014; Heinrich et al., 2012). Yet, a significant challenge remains in the prospective identification and isolation of these plastic subsets due to their low frequency (approximately 5% in stab wound injuries (Buffo et al., 2008)). Moreover, despite the advancements in single-cell transcriptomics that have revealed the extensive heterogeneity of astrocytes (Batiuk et al., 2020; Bayraktar et al., 2020; Llorens-Bobadilla et al., 2015; Ohlig et al., 2021; Zamboni et al., 2020), the lack of specific markers continues to hinder their effective identification.

To overcome these challenges, we hypothesized that leveraging the regenerative abilities of zebrafish RGCs, known for their stem cell-like properties, could be instrumental in identifying plastic astrocytic subsets (possessing proliferative and neurosphere-forming capacities) in mice post-injury. Given the RGCs' capacity to initiate neurogenesis in response to injury, as evidenced by their proliferation and neuroblast production (Kizil, Kyritsis, et al., 2012; Kroehne et al., 2011), we posited that pinpointing these rare plastic astrocytic subsets in mice post-injury would be beneficial. Therefore, we integrated single-cell transcriptomics data of mouse astrocytes with that of zebrafish RGCs following injury. The analysis revealed distinct clusters, with clusters 3 and 6 being particularly noteworthy. These clusters were predominantly composed of zebrafish cells, with a minor fraction (around 6%) from mice species. What makes these clusters interesting is that they lack cells from the intact mouse brain, primarily originating from the injured cortex. Cells within these injury-induced clusters expressed genes associated with proliferation, including top 10 genes such as Pcna, Top2a, Ube2c, Nusap1, Mcm2, Mcm5, Mcm6, Hmgb2, Dut, and

Tuba8—a significant feature of plastic astrocytes. Importantly, the integrated analysis was crucial for identifying these rare injury-induced proliferative astrocytic subsets as clusters. Without integration, we have demonstrated that these cells have remained scattered and potentially overlooked in unintegrated mouse datasets. These findings highlight the value of our cross-species transcriptomic approach, which provides a resolution to identify and study marker genes of these subsets.

3.2 Molecular profile of identified injury-induced proliferative astrocytic subset

In search for marker genes representing these cluster 3/6, we found that post-injury, these clusters exhibited expression of genes such as achaete-scute family bHLH transcription factor 1 (Ascl1), high mobility group box 2 (Hmgb2), ubiquitin-like with PHD and ring finger domains 1 (Uhrf1), and replication protein A2 (Rpa2) after injury. Notably, these genes are involved in various aspects of neurogenesis, such as transcriptional regulation, chromatin remodelling, epigenetic modification, DNA metabolism, replication, and cell cycle (Bayin et al., 2021; Bostick et al., 2007; Castro et al., 2011; Kimura et al., 2018; Păun et al., 2023; Ramesh et al., 2016; Shi et al., 2010; L. Zhou & Luo, 2013). For example, Ascl1 acts as a pioneer transcription factor capable of reprogramming astrocytes into functional neurons (iN cells) both *in vitro* and *in vivo* (Y. Liu et al., 2015; Rao et al., 2021), while Uhrf1 is essential for the renewal of NSCs and the proliferation of progenitors, with its absence severely impairing neurogenesis (Blanchart et al., 2018). The presence of these genes in the injury-induced clusters suggests the activation of a latent neurogenic program within the mouse astrocytes, potentially induced by the injury.

Further analysis of the metabolic pathways activated by mouse cells within these clusters 3/6 highlighted a significant shift. There was an upregulation of pathways related to oxidative stress, redox reactions, the electron transport chain, and G protein signalling within these clusters. This observation is particularly intriguing given the traditional glycolytic metabolism of astrocytes, which is geared towards supporting neuronal activity through lactate production (Bélanger et al., 2011; Bonvento & Bolaños, 2021; Gascón et al., 2017). The shift towards oxidative phosphorylation—a metabolic pathway more characteristic of neurons—that supports higher energy demands suggests that these astrocytic subsets might be undergoing a metabolic transition towards a more neurogenic state (Bélanger et al., 2011; Gascón et al., 2016; Zheng et al., 2016). The switching quite evidently seems to be in direct reprogramming of astrocytes to neurons upon forced

overexpression of neurogenic factors. However, to fully understand the implications of these neurogenic and metabolic shifts in injured astrocytes, further studies are imperative.

Overall, these findings suggest the identified injury-induced proliferative clusters exhibit a significant degree of plasticity, potentially transitioning towards a neurogenic phase or by initiating induction of lineage-specific genes (e.g. proneural gene Ascl1). Further studies are needed on dynamic changes in these genes and employing functional assays to corroborate these findings.

3.3 Unipotent nature of identified injury-induced proliferative astrocytic subset

Building upon the intriguing gene expression profile observed in the injury-induced astrocyte clusters (3/6), led us to investigate their potential for neurosphere formation (a characteristic often associated with the latent stem cell capacity of reactive astrocytes (Sirko et al., 2013)). To achieve this, we employed the Ascl1:CreERT2 mouse line, which allows fate mapping of Ascl1-expressing cells. Our findings revealed that Ascl1-positive astrocytes (one of marker of cluster 3/6) were indeed capable of forming neurospheres *in vitro*.

Initially, the neurogenic gene expression within clusters 3/6 hinted at a possible shift towards a neurogenic phenotype. However, the resultant neurospheres displayed a unipotent, predominantly gliogenic phenotype, challenges this notion, underscoring a more restricted differentiation capacity than anticipated. This unexpected gliogenic dominance may underscore the adult brain's inherent bias towards glial differentiation (Ninkovic & Götz, 2013), further evidenced by the inability of neurospheres derived from reactive astrocytes to generate neurons in neurogenic regions like the SVZ (M. Götz et al., 2015).

Prompted by this discrepancy, we delved into the gene expression dynamics of clusters 3 and 6 through pseudotime trajectory analysis to understand the underlying cellular states and potential lineage decisions. This analysis uncovered a complex gene expression landscape, exemplified by the upregulation of Olig2 (Oligodendrocyte Transcription Factor 2), a bHLH transcription factor. Studies have shown that Olig2 represses neurogenesis following brain injury by inhibiting the generation of immature neurons and suppressing neurogenic factors such as Pax6 (Buffo, 2007; Buffo et al., 2005). When the function of Olig2 is blocked, there is an increase in the production of new neurons, highlighting its

role as a repressor of the neurogenic process in cells that are reacting to brain injury. Within the same clusters, we also noted the expression of Dlx2 (Distal-Less Homeobox 2) in a subset of cells. Dlx2 is known to promote the proliferation of neuronal progenitor cells and contribute to neurogenesis (Suh et al., 2009). Studies have also shown Dlx2's ability to efficiently convert striatal astrocytes into neurons (M.-H. Liu et al., 2022).

This intricate expression pattern indicates a state of lineage ambiguity within these clusters, with cells not fully committed to neurogenic fate and still having glial fate. These observations open questions like how does this observed plasticity within the injury-induced clusters compare to the well-established neurogenic lineage of niches like the SVZ? And what implications does this have for understanding the mechanisms of CNS repair and regeneration?

3.4 Transcriptional parallels between injury-induced plastic astrocytes and transient amplifying progenitors

The transcriptional landscape of the injury-induced proliferative astrocytic subset (clusters 3/6) presents a compelling narrative of cellular plasticity and lineage ambiguity. These clusters, exhibiting a blend of glial and neurogenic gene expressions, suggest an intermediate, perhaps transitional, phase in the lineage specification of reactive astrocytes following injury. This leads us to ponder whether the shift of reactive astrocytes towards neuronal identities might be incomplete, characterized by an inability to fully repress glial-specific genes. To explore this possibility, we conducted an integrative analysis of single-cell transcriptomic data from the adult mouse SVZ and cortex, encompassing both injured and intact conditions. Our goal was to discern any parallels between the cellular dynamics within clusters 3/6 and the established neurogenic trajectories within the SVZ. This comparative approach aimed to elucidate the extent to which injury influences astrocytic subsets to adopt or diverge from the neurogenic lineages of SVZ.

SVZ, a region renowned for its role in harbouring NSCs and facilitating adult neurogenesis (Fischer et al., 2011; D. K. Ma et al., 2009). The integration and subsequent analysis successfully delineated known cell types within the SEZ's neurogenic lineage. This included quiescent NSCs (qNSCs), activated NSCs (aNSCs), transient amplifying progenitors (TAPs), neuroblasts (NBs), and astrocytes (Doetsch et al., 1999; Kazanis, 2009; Taupin & Gage, 2002). This comparative analysis revealed that the clusters 3/6

share more similarities with TAPs than with NSCs, suggesting that the injury-induced astrocytic subsets may exhibit TAP-like properties. This observation was further substantiated by tracing the origins of cluster 3/6 cells within the integrated cortex and SVZ data, where their congruence with TAP populations was evident, reinforcing the notion that these clusters might embody a TAP-like state. TAPs, as intermediate progenitors originating from NSCs, undergo several rounds of cell division before committing to a specific lineage (Beckervordersandforth et al., 2010; M. Götz et al., 2016; Kazanis, 2009). TAPs are heterogeneous progenitors and express varying levels of neurogenic or gliogenic transcription factors, hints at the pivotal decision-making phase for lineage commitment (Azim et al., 2015; Marshall et al., 2003). The expression of Pax6 in TAPs, for instance, is linked to neuronal differentiation, whereas Olig2 expression heralds a glial fate (Hack et al., 2004). Intriguingly, our injury-induced clusters, akin to TAPs, predominantly express Olig1/2, indicating a bias towards gliogenesis, a tendency corroborated by the gliogenic nature of their derived neurospheres. This raises intriguing questions about the lineage trajectories of these injury-induced, TAP-like cells compared to bonafide TAPs. Specifically, it prompts us to explore whether the injury context redirects these cells along a divergent path from their conventional trajectory, favouring gliogenesis over neurogenesis.

By employing pseudotime trajectory analysis, we aimed to dissect the distinctions and similarities in the lineage specification processes between these injury-induced TAP-like cells in relation to endogenous TAPs. Our findings revealed divergent progression trajectories for bonafide TAPs and injury-induced TAP-like cells. In the SEZ, notable heterogeneity within the TAP populations was noted, with TAPs_3 transitioning to NBs and bifurcating into TAPs_2 and TAPs_1, indicating diverse subpopulations. In contrast, the pseudotime trajectory of the cortex revealed a progression from homeostatic astrocytes to reactive astrocytes and further to the TAPs_1 cluster. However, unlike in the SEZ, TAPs-like cells (TAPs_1) within the cortex did not advance towards TAPs_3 or NBs. This suggests a potential interruption or incomplete activation of the neurogenic program in these injury-induced TAP-like cells. While these cells exhibit characteristics suggestive of plasticity, their limited progression towards a fully neurogenic fate necessitates further investigation.

In our study, the gene expression analysis of these TAP-like cells along pseudotime trajectories in the cortex revealed a discernible decrease in the expression of astrocytic markers such as Sox9 and Slc1a2, suggesting a transition of these cells towards a

progenitor state. This observation is consistent with the findings of Zamboni *et al.,* where clusters of neurogenic astrocytes demonstrated a decrease in genes linked to astrocyte-specific functions, while simultaneously adopting a transcriptional landscape akin to that of NSCs in a latent, primed state (Zamboni et al., 2020). Additionally, the activation of progenitor-related genes in TAPs-like cells such as Nestin, Gfap, Ascl1, Olig1/2, Mki67, and notably Dlx2, further supports this transition (Azim et al., 2015; Bayin et al., 2021; Bernal & Arranz, 2018; Castro et al., 2011; Dimou et al., 2008; Garcia et al., 2004; Suh et al., 2009; Q. Zhou & Anderson, 2002). To further explore why these TAP-like cells in the cortex do not adopt the NB trajectory observed in the SVZ, we conducted a differential analysis between bona fide TAPs (going to NBs) and injury-induced TAP-like cells (which are more gliogenic, favour a glial fate, and do not switch to a neurogenic trajectory). The comparisons showed upregulation of genes, for example, Hopx, which has been shown to be predominantly expressed in NSC subsets within the postnatal SVZ that are biased to acquire an astroglial fate (Zweifel et al., 2018). Galectin 1 (encoded by Lgals1), following brain injury, influences the proliferation and NSC-like potential of specific reactive astrocytes (M. Götz et al., 2015) and has also been shown to strongly inhibit astrocyte proliferation, contributing to the regulation of astrocyte populations (Sasaki et al., 2004). Apart from this, TAP-like cells were still enriched for glial fate-related genes compared to bona fide TAPs. The bona fide TAPs upregulated genes that regulate the establishment of neuronal fates, such as Sox4 and Sox11 (Bergsland et al., 2006), Nfib (Ninkovic et al., 2013), Dlx1/2 and Meis2 (Agoston et al., 2014), Ascl1 (Aydin et al., 2019), Pou3f2 or Brn2 (Hagino-Yamagishi et al., 1997; Y. M. J. Lin et al., 2018). The trend in expression of these genes was also seen in TAP-like cells but not at a significant level. This finding indicates that the TAP-like cells indeed express neurogenic-related genes but not at a level like the bonafide TAPs and still express glial fate-related genes, suggesting that the transition of injury-induced TAP-like cells to neurogenic fates is not complete and that they stall at the TAP level.

Furthermore, we investigated the molecular pathways that might be involved in the neurogenic potential of TAPs (SVZ) and TAP-like cells (cortex). Notch signalling, an evolutionary conserved pathway first identified in fruit flies, is crucial in fate acquisition, spatiotemporal patterning, and regulation of neuronal and glial cell fates (Androutsellis-Theotokis et al., 2006; Basak et al., 2012; Basak & Taylor, 2007; Gozlan & Sprinzak, 2023; Morrison et al., 2000; Santopolo et al., 2020; Zamboni et al., 2020). Studies have shown that ablating Notch signalling following a stab wound injury in the cortex induces the emergence of neurogenic astrocyte clusters expressing neurogenic genes such as

Neurog1 and Ascl1 (Zamboni et al., 2020). Notably, Neurog1 expression was absent in injury-induced TAP-like cells identified in our model, but Ascl1 was expressed. By analysing the expression of Notch pathway genes, higher levels of Notch signalling components were observed in injury-induced TAP-like cells compared to bona fide TAPs. This indicates that elevated Notch signalling may underlie why TAP-like cells fail to adopt a neurogenic trajectory similar to bonafide TAPs, as Notch signalling is known to promote the maintenance of stem-cell-like properties over differentiation into neuroblasts.

3.5 High efficiency of direct conversion of astrocytes to neurons using a marker of identified injury-induced plastic astrocytes

As we identified injury-induced proliferative plastic astrocytic subsets (cluster 3/6) exhibiting TAP-like characteristics, albeit with an incomplete neurogenic lineage, these cells still expressed few progenitor-related genes. We hypothesized that these plastic astrocytic subsets would be suitable for direct astrocyte-to-neuron conversion. Given their down regulation of astrocytic markers and upregulation of neurogenic-related genes, these subsets could be conducive to efficient neuronal fate conversion. To test this hypothesis, we overexpressed chromatin architectural protein Hmgb2, a marker of these plastic subsets, along with the pioneer factor Neurog2, in astrocytes and assessed their neuronal conversion efficiency. We also mimicked the *in vivo* injury microenvironment by using different combinations of mitogen EGF and FGF2 (EGF+FGF2 or FGF2 only) in the culture conditions. While EGF+FGF2 are often used for *in vitro* reprogramming due to their synergistic effects, FGF2 is the dominant mitogen in the *in vivo* injury microenvironment (Addington et al., 2015). Our study compares the reprogramming outcomes of Hmgb2 alone, Neurog2 alone, and their combination (Neurog2+Hmgb2) under proposed mitogen conditions. We observed that both the growth factor and transcription factor expression levels significantly influenced the reprogramming efficiency of astrocytes to neuron conversion. Neurog2 alone exhibited greater reprogramming efficiencies in the presence of EGF+FGF2 compared to FGF2 alone. This suggests that Neurog2 alone may not sufficiently alter the chromatin structure of astrocytes to facilitate neuronal gene activation in cultures with FGF alone, making such conditions restrictive for reprogramming. However, co-expression of Hmgb2 with Neurog2 overcame this barrier, enhancing reprogramming efficiency in FGF2 cultures. This cooperative action suggests that Hmgb2 facilitates the opening of genes crucial for reprogramming and drives the specification of neuronal identity, a task unattainable by proneural transcription factors Neurog2 alone in

FGF2 condition. Interestingly, Hmgb2 by itself was insufficient to induce neuronal reprogramming, regardless of the growth factor environment. Furthermore, under EGF+FGF2 conditions, there was no difference in efficiency between Neurog2 alone and Neurog2+Hmgb2, suggesting that chromatin remodelling and activation of reprogramming-related genes can be fully enhanced without Hmgb2 in this condition.

These observations raise questions such as: How does the combination of Hmgb2 and Neurog2 enhance the reprogramming efficiency of astrocytes to neurons under FGF2 culture? How does this combination overcome the lineage barriers and induce neuronal fate and function in astrocytes? What are the key genes and processes involved in this process?

3.6 Hmgb2 in corporation with Neurog2 enhances direct astrocyte-to-neuron conversion by modulating chromatin accessibility and gene expression

To examine how Hmgb2, a chromatin-associated protein, enhances the reprogramming efficiency of astrocytes to neurons, I performed a comprehensive analysis of the transcriptome (RNA-Seq) and chromatin accessibility (ATAC-Seq) of astrocytes under three distinct culture conditions: reprogramming-prone (EGF+FGF2 induced by Neurog2), reprogramming-restricted (FGF2 induced by Neurog2), and reprogramming-permissive (FGF2 induced by Neurog2+Hmgb2). By comparing the gene expression and chromatin accessibility profiles among these conditions, I aimed to identify the differentially expressed and accessible genes, particularly in reprogramming-permissive conditions, to elucidate how Hmgb2 collaborates with Neurog2 to overcome the lineage barriers and induce neuronal fate and function in astrocytes.

Our differential expression analysis revealed that the reprogramming-prone and reprogramming-restricted conditions shared the expression of essential Neurog2-induced genes, such as Neurod4, Insm1, Hes6, Slit1, Sox11, and Gang4, which have been previously reported to be involved in astrocyte-to-neuron conversion (Masserdotti et al., 2015). However, these genes were not sufficient to ensure efficient reprogramming, as the reprogramming-restricted condition exhibited low conversion rates. We hypothesized that additional genes may be required to facilitate efficient reprogramming process. Indeed, we found that genes, such as Dscaml1, Prox1, Lrp8, and Shf (Masserdotti et al., 2015), were exclusively induced in the reprogramming-prone and reprogramming-permissive

conditions, but not in the reprogramming-restricted condition. Gene ontology analysis linked these genes to critical neuronal maturation processes, including axonogenesis, neurogenesis, axon guidance, and nervous system development, suggesting their relevance to reprogramming. To corroborate these findings, we overexpressed Prox1 alongside Neurog2 in the reprogramming-restricted condition, which resulted in enhanced reprogramming efficiency of astrocytes to neurons. This finding supports the hypothesis that Hmgb2 is instrumental in reprogramming, as it activates genes that lead to more efficient neuronal conversion upon overexpression in reprogramming-restricted conditions. The concept that additional factors or molecules are required to boost reprogramming efficiency is well-established in the field (Vasan et al., 2021). Consistent with this, previous studies like Smith *et al.* have demonstrated Neurog2's limited reprogramming capacity in human fibroblasts, akin to our observations in FGF culture. However, the addition of small molecules such as forskolin and dorsomorphin enabled chromatin remodelling and the activation of neuronal transcription factors, culminating in successful neuronal conversion (Smith et al., 2016).

Next, we examined how Hmgb2 improved the efficiency of astrocyte-to-neuron conversion and transitioned the condition from reprogramming-restrictive to reprogramming-prone at the chromatin level. Employing ATAC-Seq, we assessed chromatin accessibility across different culture conditions: reprogramming-prone, permissive, and restrictive. Our analysis revealed an increase in chromatin accessibility of reprogramming-relevant genes in the Hmgb2-induced permissive condition compared to the reprogramming-restrictive condition. This enhanced accessibility aligns more closely with the reprogramming-prone condition. Further analysis revealed that the Hmgb2-induced permissive condition facilitated the opening of chromatin regions associated with neuronal maturation and synaptic functions, which were not accessible in the reprogramming-restrictive condition. These regions included the promoters of neuronal maturation genes, such as Kif1a12, Artn34, and Rasd25 (Errico et al., 2008; Niwa et al., 2008; Okada et al., 1995; R. Wang et al., 2014; Wong et al., 2015), and synaptic genes, such as Mical3, Enc1, Foxo6, and Dscaml1 (Hernandez et al., 1997; Q. Liu et al., 2016; Ogata et al., 2021; Salih et al., 2012). Moreover, neurons that underwent conversion from astrocytes in the Hmgb2-induced permissive condition displayed features indicative of enhanced maturity. This was evidenced by their extended and more complex branching processes and increased dendritic complexity, as determined by Sholl analysis, compared to those derived under reprogramming restrictive conditions. Thus, Hmgb2 not only boosts the rate of astrocytes to neuronal conversion but also improves the quality of the resulting neurons.

These insights are significant for the field of neuronal replacement therapies, suggesting that Hmgb2 could potentially improve the functionality and integration of neurons directly converted from astrocytes within injured brain tissue. Nonetheless, additional research is required to fully understand the collaborative mechanisms of Hmgb2 and Neurog2 in the *in vivo* reprogramming process.

3.7 Summary and conclusions

In a nutshell, the findings of my PhD projects addressed the persisting challenge of reliably identifying and isolating rare, injury-induced plastic astrocytic subpopulations in mice following stab wound injuries. To overcome this challenge, I employed an innovative trans-species approach, integrating single-cell transcriptomic data from regenerative zebrafish ependymoglia stem cells with mouse astrocytes. This approach led to the identification of key marker combinations, including Hmgb2, Ascl1, Rpa2, and Uhrf1, which are expressed in actively proliferating plastic reactive astrocyte subpopulations. These subsets, notably those that are Ascl1-positive, were found to acquire neurosphere-forming capacities and give rise to unipotent gliogenic neurospheres. Interestingly, these plastic astrocytes express a unique combination of progenitor-related and gliogenic genes. Transcriptionally, these subsets exhibit TAP-like features, resembling bona fide TAPs of the SEZ. However, unlike bonafide TAPs, they exhibit partial trajectories toward neurogenic lineages, indicating injury-induced plasticity in these astrocytes. Furthermore, we explored the potential of utilizing these identified markers, particularly Hmgb2, to enhance astrocyte-to-neuron conversion. Overexpression of chromatin binding protein Hmgb2 alongside the pioneer transcription factor Neurog2 significantly improved the efficiency of neuronal conversion *in vitro*, particularly under conditions mimicking the *in vivo* injury microenvironment. Additionally, we have shown that co-expression of Hmgb2 and Neurog2 promoted the maturation of iNs. This enhancement was attributed to the chromatin remodelling effects of Hmgb2, which facilitated accessibility and expression of neurogenic genes, as confirmed by chromatin and transcriptome analysis.

In conclusion, the findings from my PhD research lay the groundwork for a deeper exploration of astrocyte plasticity following injury. Through the identification of key marker genes, this study provides crucial insights for pinpointing these specific astrocytic populations. Further investigation into the identified markers reveals their potential roles in augmenting the efficiency of astrocyte-to-neuron conversion. This underscores the

potential of plastic astrocytic subsets as a valuable source for direct neuronal reprogramming, presenting promising prospects for regenerative approaches in CNS repair.

3.8 Outlook

This work opens new avenues for exploring astrocyte plasticity and its prospective role in CNS repair. However, further research is essential to understand the mechanisms and complex interactions between astrocytic subsets, other cell types, and factors within the CNS. Additionally, a few questions and challenges remain to be addressed in future research that could enhance the quality and impact.

While this study focused on plastic astrocyte transcriptome profiles, a comprehensive understanding of molecular, cellular, and injury-induced epigenetic changes warrants a multi-omics approach. Integrating transcriptomics with proteomics, metabolomics, and epigenomics could provide a more holistic view. Additionally, characterizing plastic astrocyte marker genes across various injury and disease conditions, like stroke, epilepsy, and spinal cord injury, is crucial to assess reliability and variability of the identified markers.

Moreover, the study has yet to address the morphological changes in plastic astrocytes and their distinctions from reactive astrocytes throughout injury or disease. Advanced imaging techniques could offer a window into these changes, potentially revealing how they influence interactions with other cell types in the CNS. Given that the shape, size, and branching patterns of astrocytes potentially signify their functional states, influence interactions within the CNS.

Furthermore, while Hmgb2 serves as one marker for plastic astrocytes and is also expressed by a subset of reactive astrocytes, achieving specificity and precision in targeting plastic astrocytic subsets for efficient neuronal reprogramming necessitates requires the use of a combination of other identified markers. Additionally, in the study, the collaborative overexpression of Hmgb2 with Neurog2 has shown promise in inducing a more mature neuronal phenotype, upregulating synaptic and neuronal maturation-related genes. However, assessing the electrical properties of the converted neurons and conducting Chromatin immunoprecipitation (ChIP) assays to identify direct binding sites of Hmgb2 and neurogenic factors on target gene promoters remain crucial steps. Although this study has focused on *in vitro* reprogramming as a model for what happens *in vivo*,

validating these findings is essential for understanding their contributions to the reprogramming process.

Addressing these research areas will enhance our understanding of the regenerative process and and pave the way for future therapeutic strategies, marking significant strides toward harnessing astrocyte plasticity for CNS repair.

4. Bibliography

Abbott, N. J., Rönnbäck, L., & Hansson, E. (2006). Astrocyte-endothelial interactions at the blood-brain barrier. *Nature Reviews. Neuroscience*, *7*(1), 41–53. https://doi.org/10.1038/NRN1824

Abraham, A. B., Bronstein, R., Chen, E. I., Koller, A., Ronfani, L., Maletic-Savatic, M., & Tsirka, S. E. (2013). Members of the high mobility group B protein family are dynamically expressed in embryonic neural stem cells. *Proteome Science*, *11*(1), 1–11. https://doi.org/10.1186/1477-5956-11-18/FIGURES/4

Abraham, A. B., Bronstein, R., Reddy, A. S., Maletic-Savatic, M., Aguirre, A., & Tsirka, S. E. (2013). Aberrant Neural Stem Cell Proliferation and Increased Adult Neurogenesis in Mice Lacking Chromatin Protein HMGB2. *PLoS ONE*, *8*(12). https://doi.org/10.1371/JOURNAL.PONE.0084838

Adams, K. L., & Gallo, V. (2018). The diversity and disparity of the glial scar. In *Nature Neuroscience* (Vol. 21, Issue 1, pp. 9–15). Nature Publishing Group. https://doi.org/10.1038/s41593-017-0033-9

Adams, K. V., & Morshead, C. M. (2018). Neural stem cell heterogeneity in the mammalian forebrain. *Progress in Neurobiology*, *170*, 2–36. https://doi.org/10.1016/J.PNEUROBIO.2018.06.005

Addington, C. P., Roussas, A., Dutta, D., & Stabenfeldt, S. E. (2015). Endogenous Repair Signaling after Brain Injury and Complementary Bioengineering Approaches to Enhance Neural Regeneration. *Biomarker Insights*, *10*(Suppl 1), 43. https://doi.org/10.4137/BMI.S20062

Adolf, B., Chapouton, P., Lam, C. S., Topp, S., Tannhauser, B., Strahle, U., Gotz, M., & Bally-Cuif, L. (2006). Conserved and acquired features of adult neurogenesis in the zebrafish telencephalon. *Dev Biol*, *295*(1), 278–293. https://doi.org/10.1016/j.ydbio.2006.03.023

Agarwala, R., Barrett, T., Beck, J., Benson, D. A., Bollin, C., Bolton, E., Bourexis, D., Brister, J. R., Bryant, S. H., Canese, K., Charowhas, C., Clark, K., Dicuccio, M., Dondoshansky, I., Federhen, S., Feolo, M., Funk, K., Geer, L. Y., Gorelenkov, V., … Zbicz, K. (2016). Database resources of the National Center for Biotechnology Information. *Nucleic Acids Research*, *44*(D1), D7–D19. https://doi.org/10.1093/NAR/GKV1290

Agoston, Z., Heine, P., Brill, M. S., Grebbin, B. M., Hau, A. C., Kallenborn-Gerhardt, W., Schramm, J., Götz, M., & Schulte, D. (2014). Meis2 is a Pax6 co-factor in neurogenesis and dopaminergic periglomerular fate specification in the adult olfactory bulb. *Development*, *141*(1), 28–38. https://doi.org/10.1242/DEV.097295

Allen, N. J., & Lyons, D. A. (2018). Glia as architects of central nervous system formation and function. *Science*, *362*(6411), 181–185. https://doi.org/10.1126/science.aat0473

Alunni, A., & Bally-Cuif, L. (2016). A comparative view of regenerative neurogenesis in vertebrates. *Development*, *143*(5), 741–753. https://doi.org/10.1242/DEV.122796

Amamoto, R., & Arlotta, P. (2014). Development-inspired reprogramming of the mammalian central nervous system. *Science (New York, N.Y.)*, *343*(6170). https://doi.org/10.1126/SCIENCE.1239882

Anderson, M. A., Burda, J. E., Ren, Y., Ao, Y., O'Shea, T. M., Kawaguchi, R., Coppola, G., Khakh, B. S., Deming, T. J., & Sofroniew, M. V. (2016). Astrocyte scar formation aids central nervous system axon regeneration. *Nature*, *532*(7598), 195–200. https://doi.org/10.1038/NATURE17623

Androutsellis-Theotokis, A., Leker, R. R., Soldner, F., Hoeppner, D. J., Ravin, R., Poser, S. W., Rueger, M. A., Bae, S.-K., Kittappa, R., & McKay, R. D. G. (2006). Notch signalling regulates stem cell numbers in vitro and in vivo. *Nature*, *442*(7104), 823–826. http://dx.doi.org/10.1038/nature04940

Augusto-Oliveira, M., Arrifano, G. P., Lopes-Araújo, A., Santos-Sacramento, L., Takeda, P. Y., Anthony, D. C., Malva, J. O., & Crespo-Lopez, M. E. (2019). What Do Microglia Really Do in Healthy Adult Brain? *Cells*, *8*(10). https://doi.org/10.3390/CELLS8101293

Aydin, B., Kakumanu, A., Rossillo, M., Moreno-Estellés, M., Garipler, G., Ringstad, N., Flames, N., Mahony, S., & Mazzoni, E. O. (2019). Proneural factors Ascl1 and Neurog2 contribute to neuronal subtype identities by establishing distinct chromatin landscapes. *Nature Neuroscience 2019 22:6*, *22*(6), 897–908. https://doi.org/10.1038/s41593-019-0399-y

Azim, K., Hurtado-Chong, A., Fischer, B., Kumar, N., Zweifel, S., Taylor, V., & Raineteau, O. (2015). Transcriptional Hallmarks of Heterogeneous Neural Stem Cell Niches of the Subventricular Zone. *Stem Cells*, *33*(7), 2232–2242. https://doi.org/10.1002/STEM.2017

Barbosa, J. S. S., & Ninkovic, J. (2016). Adult neural stem cell behavior underlying constitutive and restorative neurogenesis in zebrafish. *Neurogenesis (Austin)*, *3*(1), e1148101. https://doi.org/10.1080/23262133.2016.1148101

Bardehle, S., Krüger, M., Buggenthin, F., Schwausch, J., Ninkovic, J., Clevers, H., Snippert, H. J., Theis, F. J., Meyer-Luehmann, M., Bechmann, I., Dimou, L., & Götz, M. (2013). Live imaging of astrocyte responses to acute injury reveals selective juxtavascular proliferation. *Nature Neuroscience*, *16*(5), 580–586. https://doi.org/10.1038/NN.3371

Barkas, N., Petukhov, V., Nikolaeva, D., Lozinsky, Y., Demharter, S., Khodosevich, K., & Kharchenko, P. V. (2019). Joint analysis of heterogeneous single-cell RNA-seq dataset collections. *Nature Methods*, *16*(8), 695. https://doi.org/10.1038/S41592-019-0466-Z

Basak, O., Giachino, C., Fiorini, E., Macdonald, H. R., & Taylor, V. (2012). Neurogenic subventricular zone stem/progenitor cells are Notch1-dependent in their active but not quiescent state. *J Neurosci*, *32*(16), 5654–5666. https://doi.org/10.1523/JNEUROSCI.0455-12.2012

Basak, O., & Taylor, V. (2007). Identification of self-replicating multipotent progenitors in the embryonic nervous system by high Notch activity and Hes5 expression. *Eur J Neurosci*, *25*(4), 1006–1022. https://doi.org/10.1111/j.1460-9568.2007.05370.x

Batiuk, M. Y., Martirosyan, A., Wahis, J., de Vin, F., Marneffe, C., Kusserow, C., Koeppen, J., Viana, J. F., Oliveira, J. F., Voet, T., Ponting, C. P., Belgard, T. G., & Holt, M. G. (2020). Identification of region-specific astrocyte subtypes at single cell resolution. *Nature Communications 2020 11:1*, *11*(1), 1–15. https://doi.org/10.1038/s41467-019-14198-8

Bayin, N. S., Mizrak, D., Stephen, D. N., Lao, Z., Sims, P. A., & Joyner, A. L. (2021). Injury-induced ASCL1 expression orchestrates a transitory cell state required for repair of the neonatal cerebellum. *Science Advances*, *7*(50). https://doi.org/10.1126/SCIADV.ABJ1598/SUPPL_FILE/SCIADV.ABJ1598_SUPPLEMENTARY_TABLES.ZIP

Bayraktar, O. A., Bartels, T., Holmqvist, S., Kleshchevnikov, V., Martirosyan, A., Polioudakis, D., Haim, L. Ben, Young, A. M. H., Batiuk, M. Y., Prakash, K., Brown, A., Roberts, K., Paredes, M. F., Kawaguchi, R., Stockley, J. H., Sabeur, K., Chang, S. M., Huang, E., Hutchinson, P., … Rowitch, D. H. (2020). Astrocyte layers in the mammalian cerebral cortex revealed by a single-cell in situ transcriptomic map. *Nature Neuroscience*, *23*(4), 500–509. https://doi.org/10.1038/s41593-020-0602-1

Beckervordersandforth, R., Tripathi, P., Ninkovic, J., Bayam, E., Lepier, A., Stempfhuber, B., Kirchhoff, F., Hirrlinger, J., Haslinger, A., Lie, D. C., Beckers, J., Yoder, B., Irmler, M., & Götz, M. (2010). In vivo fate mapping and expression analysis reveals molecular hallmarks of prospectively isolated adult neural stem cells. *Cell Stem Cell*, *7*(6), 744–758. https://doi.org/10.1016/J.STEM.2010.11.017

Bélanger, M., Allaman, I., & Magistretti, P. J. (2011). Brain Energy Metabolism: Focus on Astrocyte-Neuron Metabolic Cooperation. *Cell Metabolism*, *14*(6), 724–738. https://doi.org/10.1016/j.cmet.2011.08.016

Bergsland, M., Werme, M., Malewicz, M., Perlmann, T., & Muhr, J. (2006). The establishment of neuronal properties is controlled by Sox4 and Sox11. *Genes & Development*, *20*(24), 3475. https://doi.org/10.1101/GAD.403406

Bernal, A., & Arranz, L. (2018). Nestin-expressing progenitor cells: function, identity and therapeutic implications. *Cellular and Molecular Life Sciences 2018 75:12*, *75*(12), 2177–2195. https://doi.org/10.1007/S00018-018-2794-Z

Berninger, B., Costa, M. R., Koch, U., Schroeder, T., Sutor, B., Grothe, B., & Götz, M. (2007). Functional properties of neurons derived from in vitro reprogrammed postnatal astroglia. *Journal of Neuroscience*, *27*(32), 8654–8664. https://doi.org/10.1523/JNEUROSCI.1615-07.2007

Berwick, D., Bowman, K., & Matney, C. (2022). Traumatic Brain Injury: A Roadmap for Accelerating Progress (2022). *Traumatic Brain Injury*, 1–228. https://doi.org/10.17226/25394

Bioconductor - orthogene. (n.d.). Retrieved March 8, 2024, from https://bioconductor.org/packages/release/bioc/html/orthogene.html

Blanchart, A., Navis, A. C., Assaife-Lopes, N., Usoskin, D., Aranda, S., Sontheimer, J., & Ernfors, P. (2018). UHRF1 Licensed Self-Renewal of Active Adult Neural Stem Cells. *Stem Cells (Dayton, Ohio)*, *36*(11), 1736–1751. https://doi.org/10.1002/STEM.2889

Blum, R., Heinrich, C., Sanchez, R., Lepier, A., Gundelfinger, E. D., Berninger, B., & Gotz, M. (2011). Neuronal network formation from reprogrammed early postnatal rat cortical glial cells. *Cereb Cortex*, *21*(2), 413–424. https://doi.org/bhq107 [pii] 10.1093/cercor/bhq107

Bocchi, R., Masserdotti, G., & Götz, M. (2022). Direct neuronal reprogramming: Fast forward from new concepts toward therapeutic approaches. *Neuron*, *110*(3), 366–393. https://doi.org/10.1016/J.NEURON.2021.11.023

Bonvento, G., & Bolaños, J. P. (2021). Astrocyte-neuron metabolic cooperation shapes brain activity. *Cell Metabolism*, *33*(8), 1546–1564. https://doi.org/10.1016/j.cmet.2021.07.006

Bostick, M., Jong, K. K., Estève, P. O., Clark, A., Pradhan, S., & Jacobsen, S. E. (2007). UHRF1 plays a role in maintaining DNA methylation in mammalian cells. *Science (New York, N.Y.)*, *317*(5845), 1760–1764. https://doi.org/10.1126/SCIENCE.1147939

Bovolenta, P., Wandosell, F., & Nieto-Sampedro, M. (1993). Characterization of a neurite outgrowth inhibitor expressed after CNS injury. *The European Journal of Neuroscience*, *5*(5), 454–465. https://doi.org/10.1111/J.1460-9568.1993.TB00512.X

Bradl, M., & Lassmann, H. (2010). Oligodendrocytes: biology and pathology. *Acta Neuropathologica*, *119*(1), 37. https://doi.org/10.1007/S00401-009-0601-5

Brain research - European Commission. (n.d.). Retrieved December 31, 2023, from https://research-and-innovation.ec.europa.eu/research-area/health/brain-research_en

Brandao, M., Simon, T., Critchley, G., & Giamas, G. (2019). Astrocytes, the rising stars of the glioblastoma microenvironment. In *GLIA* (Vol. 67, Issue 5, pp. 779–790). John Wiley and Sons Inc. https://doi.org/10.1002/glia.23520

Bronstein, R., Kyle, J., Abraham, A. B., & Tsirka, S. E. (2017). Neurogenic to gliogenic fate transition perturbed by loss of HMGB2. *Frontiers in Molecular Neuroscience*, *10*. https://doi.org/10.3389/FNMOL.2017.00153/FULL

Brulet, R., Matsuda, T., Zhang, L., Miranda, C., Giacca, M., Kaspar, B. K., Nakashima, K., & Hsieh, J. (2017). NEUROD1 Instructs Neuronal Conversion in Non-Reactive Astrocytes. *Stem Cell Reports*, *8*(6), 1506–1515. https://doi.org/10.1016/J.STEMCR.2017.04.013

Buffo, A. (2007). Fate Determinant Expression in the Lesioned Brain: Olig2 Induction and Its Implications for Neuronal Repair. *Neurodegenerative Diseases*, *4*(4), 328–332. https://doi.org/10.1159/000101890

Buffo, A., Rite, I., Tripathi, P., Lepier, A., Colak, D., Horn, A.-P., Mori, T., & Götz, M. (2008). Origin and progeny of reactive gliosis: A source of multipotent cells in the injured brain. *Proceedings of the National Academy of Sciences*, *105*(9), 3581–3586. https://doi.org/10.1073/pnas.0709002105

Buffo, A., Rolando, C., & Ceruti, S. (2010). Astrocytes in the damaged brain: Molecular and cellular insights into their reactive response and healing potential. *Biochemical Pharmacology*, *79*(2), 77–89. http://www.sciencedirect.com/science/article/B6T4P-4X7R7Y3-2/2/1be5e717ebfa19b3b66994ba40e7ee93

Buffo, A., Vosko, M. R., Erturk, D., Hamann, G. F., Jucker, M., Rowitch, D., & Gotz, M. (2005). Expression pattern of the transcription factor Olig2 in response to brain injuries: implications for neuronal repair. *Proc Natl Acad Sci U S A*, *102*(50), 18183–18188. https://doi.org/10.1073/pnas.0506535102

Bulcha, J. T., Wang, Y., Ma, H., Tai, P. W. L., & Gao, G. (2021). Viral vector platforms within the gene therapy landscape. *Signal Transduction and Targeted Therapy 2021 6:1*, *6*(1), 1–24. https://doi.org/10.1038/s41392-021-00487-6

Burda, J. E., Bernstein, A. M., & Sofroniew, M. V. (2016). Astrocyte roles in traumatic brain injury. In *Experimental Neurology* (Vol. 275, Issue 0 3, pp. 305–315). Academic Press Inc. https://doi.org/10.1016/j.expneurol.2015.03.020

Burda, J. E., & Sofroniew, M. V. (2014). Reactive Gliosis and the Multicellular Response to CNS Damage and Disease. *Neuron*, *81*(2), 229–248. https://doi.org/10.1016/j.neuron.2013.12.034

Busch, S. A., & Silver, J. (2007). The role of extracellular matrix in CNS regeneration. *Curr Opin Neurobiol*, *17*(1), 120–127. https://doi.org/S0959-4388(07)00002-5 [pii] 10.1016/j.conb.2006.09.004

Bush, T. G., Puvanachandra, N., Horner, C. H., Polito, A., Ostenfeld, T., Svendsen, C. N., Mucke, L., Johnson, M. H., & Sofroniew, M. V. (1999). Leukocyte infiltration, neuronal degeneration, and neurite outgrowth after ablation of scar-forming, reactive astrocytes in adult transgenic mice. *Neuron*, *23*(2), 297–308. https://doi.org/10.1016/S0896-6273(00)80781-3

Butler, A., Hoffman, P., Smibert, P., Papalexi, E., & Satija, R. (2018). Integrating single-cell transcriptomic data across different conditions, technologies, and species. *Nature Biotechnology*, *36*(5). https://doi.org/10.1038/nbt.4096

Cacialli, P., & Lucini, C. (2019). Adult neurogenesis and regeneration in zebrafish brain: are the neurotrophins involved in? *Neural Regeneration Research*, *14*(12), 2067–2068. https://doi.org/10.4103/1673-5374.262574

Castro, D. S., Martynoga, B., Parras, C., Ramesh, V., Pacary, E., Johnston, C., Drechsel, D., Lebel-Potter, M., Garcia, L. G., Hunt, C., Dolle, D., Bithell, A., Ettwiller, L., Buckley, N., & Guillemot, F. (2011). A novel function of the proneural factor Ascl1 in progenitor proliferation identified by genome-wide characterization of its targets. *Genes & Development*, *25*(9), 930. https://doi.org/10.1101/GAD.627811

Cates, K., McCoy, M. J., Kwon, J. S., Liu, Y., Abernathy, D. G., Zhang, B., Liu, S., Gontarz, P., Kim, W. K., Chen, S., Kong, W., Ho, J. N., Burbach, K. F., Gabel, H. W., Morris, S. A., & Yoo, A. S. (2021). Deconstructing Stepwise Fate Conversion of Human Fibroblasts to Neurons by MicroRNAs. *Cell Stem Cell*, *28*(1), 127-140.e9. https://doi.org/10.1016/J.STEM.2020.08.015

Chaboub, L. S., & Deneen, B. (2013). Developmental Origins of Astrocyte Heterogeneity: The Final Frontier of CNS Development. *Developmental Neuroscience*, *34*(5), 379–388. https://doi.org/10.1159/000343723

Chanda, S., Ang, C. E., Davila, J., Pak, C., Mall, M., Lee, Q. Y., Ahlenius, H., Jung, S. W., Südhof, T. C., & Wernig, M. (2014). Generation of induced neuronal cells by the single

reprogramming factor ASCL1. *Stem Cell Reports*, *3*(2), 282–296. https://doi.org/10.1016/J.STEMCR.2014.05.020

Chen, J., Poskanzer, K. E., Freeman, M. R., & Monk, K. R. (2020). Live-imaging of astrocyte morphogenesis and function in zebrafish neural circuits. *Nature Neuroscience*, *23*(10), 1297. https://doi.org/10.1038/S41593-020-0703-X

Chen, X., Sokirniy, I., Wang, X., Jiang, M., Mseis-Jackson, N., Williams, C., Mayes, K., Jiang, N., Puls, B., Du, Q., Shi, Y., & Li, H. (2023). MicroRNA-375 Is Induced during Astrocyte-to-Neuron Reprogramming and Promotes Survival of Reprogrammed Neurons when Overexpressed. *Cells*, *12*(17), 2202. https://doi.org/10.3390/CELLS12172202/S1

Chouchane, M., Melo de Farias, A. R., Moura, D. M. de S., Hilscher, M. M., Schroeder, T., Leão, R. N., & Costa, M. R. (2017). Lineage Reprogramming of Astroglial Cells from Different Origins into Distinct Neuronal Subtypes. *Stem Cell Reports*, *9*(1), 162–176. https://doi.org/10.1016/J.STEMCR.2017.05.009

Clarke, L. E., Liddelow, S. A., Chakraborty, C., Münch, A. E., Heiman, M., & Barres, B. A. (2018). Normal aging induces A1-like astrocyte reactivity. *Proceedings of the National Academy of Sciences of the United States of America*, *115*(8). https://doi.org/10.1073/pnas.1800165115

Codega, P., Silva-Vargas, V., Paul, A., Maldonado-Soto, A. R., Deleo, A. M., Pastrana, E., & Doetsch, F. (2014). Prospective identification and purification of quiescent adult neural stem cells from their in vivo niche. *Neuron*, *82*(3), 545–559. https://doi.org/10.1016/j.neuron.2014.02.039

Cosacak, M. I., Bhattarai, P., De Jager, P. L., Menon, V., Tosto, G., & Kizil, C. (2022). Single Cell/Nucleus Transcriptomics Comparison in Zebrafish and Humans Reveals Common and Distinct Molecular Responses to Alzheimer's Disease. *Cells*, *11*(11). https://doi.org/10.3390/CELLS11111807/S1

Cosentino, S., & Iwasaki, W. (2019). SonicParanoid: fast, accurate and easy orthology inference. *Bioinformatics (Oxford, England)*, *35*(1), 149–151. https://doi.org/10.1093/BIOINFORMATICS/BTY631

Couillard-Despres, S., Winner, B., Schaubeck, S., Aigner, R., Vroemen, M., Weidner, N., Bogdahn, U., Winkler, J., Kuhn, H. G., & Aigner, L. (2005). Doublecortin expression levels in adult brain reflect neurogenesis. *European Journal of Neuroscience*, *21*(1), 1–14. https://doi.org/10.1111/j.1460-9568.2004.03813.x

De Donno, C., Hediyeh-Zadeh, S., Moinfar, A. A., Wagenstetter, M., Zappia, L., Lotfollahi, M., & Theis, F. J. (2023). Population-level integration of single-cell datasets enables multi-scale analysis across samples. *Nature Methods 2023 20:11*, *20*(11), 1683–1692. https://doi.org/10.1038/s41592-023-02035-2

DEL RIO-HORTEGA, P. (1921). Estudios sobre la neurogia. La glia de escasas rediaciones (oligodendroglia). *Bol Real Soc Esp Hist Nat*, *21*, 63–92.

Dellarole, A., & Grilli, M. (2008). Adult dorsal root ganglia sensory neurons express the early neuronal fate marker doublecortin. *The Journal of Comparative Neurology*, *511*(3), 318–328. https://doi.org/10.1002/CNE.21845

Demlie, T. A., Alemu, M. T., Messelu, M. A., Wagnew, F., & Mekonen, E. G. (2023). Incidence and predictors of mortality among traumatic brain injury patients admitted to Amhara region Comprehensive Specialized Hospitals, northwest Ethiopia, 2022. *BMC Emergency Medicine*, *23*(1). https://doi.org/10.1186/S12873-023-00823-9

Dewan, M. C., Rattani, A., Gupta, S., Baticulon, R. E., Hung, Y. C., Punchak, M., Agrawal, A., Adeleye, A. O., Shrime, M. G., Rubiano, A. M., Rosenfeld, J. V., & Park, K. B. (2019). Estimating the global incidence of traumatic brain injury. *Journal of Neurosurgery*, *130*(4), 1080–1097. https://doi.org/10.3171/2017.10.JNS17352

Dimou, L., Simon, C., Kirchhoff, F., Takebayashi, H., & Gotz, M. (2008). Progeny of Olig2-expressing progenitors in the gray and white matter of the adult mouse cerebral cortex. *J Neurosci*, *28*(41), 10434–10442. https://doi.org/28/41/10434 [pii] 10.1523/JNEUROSCI.2831-08.2008

Ding, Z., Dai, C., Shan, W., Liu, R., Lu, W., Gao, W., Zhang, H., Huang, W., Guan, J., & Yin, Z. (2021). TNF-α up-regulates Nanog by activating NF-κB pathway to induce primary rat spinal cord astrocytes dedifferentiation. *Life Sciences*, *287*, 120126. https://doi.org/10.1016/J.LFS.2021.120126

Diotel, N., Lübke, L., Strähle, U., & Rastegar, S. (2020). Common and Distinct Features of Adult Neurogenesis and Regeneration in the Telencephalon of Zebrafish and Mammals. *Frontiers in Neuroscience*, *14*. https://doi.org/10.3389/FNINS.2020.568930

Doetsch, F., Caille, I., Lim, D. A., Garcia-Verdugo, J. M., & Alvarez-Buylla, A. (1999). Subventricular zone astrocytes are neural stem cells in the adult mammalian brain. *Cell*, *97*(6), 703–716. https://doi.org/10.1016/S0092-8674(00)80783-7

Doetsch, F., Petreanu, L., Caille, I., Garcia-Verdugo, J.-M., & Alvarez-Buylla, A. (2002). EGF Converts Transit-Amplifying Neurogenic Precursors in the Adult Brain into Multipotent Stem Cells. *Neuron*, *36*(6), 1021–1034. https://doi.org/10.1016/S0896-6273(02)01133-9

Duan, Q., Li, S., Wen, X., Sunnassee, G., Chen, J., Tan, S., & Guo, Y. (2019). Valproic Acid Enhances Reprogramming Efficiency and Neuronal Differentiation on Small Molecules Staged-Induction Neural Stem Cells: Suggested Role of mTOR Signaling. *Frontiers in Neuroscience*, *13*. https://doi.org/10.3389/FNINS.2019.00867

Dulken, B. W., Leeman, D. S., Boutet, S. C., Hebestreit, K., & Brunet, A. (2017). Single-Cell Transcriptomic Analysis Defines Heterogeneity and Transcriptional Dynamics in the Adult Neural Stem Cell Lineage. *Cell Rep*, *18*(3), 777–790. https://doi.org/10.1016/j.celrep.2016.12.060

Emms, D. M., & Kelly, S. (2019). OrthoFinder: phylogenetic orthology inference for comparative genomics. *Genome Biology*, *20*(1). https://doi.org/10.1186/S13059-019-1832-Y

Endo, F., Kasai, A., Soto, J. S., Yu, X., Qu, Z., Hashimoto, H., Gradinaru, V., Kawaguchi, R., & Khakh, B. S. (2022). Molecular basis of astrocyte diversity and morphology across the CNS in health and disease. *Science*, *378*(6619). https://doi.org/10.1126/science.adc9020

Errico, F., Santini, E., Migliarini, S., Borgkvist, A., Centonze, D., Nasti, V., Carta, M., Chiara, V. De, Prosperetti, C., Spano, D., Herve, D., Pasqualetti, M., Lauro, R. Di, Fisone, G., & Usiello, A. (2008). The GTP-binding protein Rhes modulates dopamine signalling in striatal medium spiny neurons. *Molecular and Cellular Neuroscience*, *37*(2). https://doi.org/10.1016/j.mcn.2007.10.007

Escartin, C., Galea, E., Lakatos, A., O'Callaghan, J. P., Petzold, G. C., Serrano-Pozo, A., Steinhäuser, C., Volterra, A., Carmignoto, G., Agarwal, A., Allen, N. J., Araque, A., Barbeito, L., Barzilai, A., Bergles, D. E., Bonvento, G., Butt, A. M., Chen, W. T., Cohen-Salmon, M., … Verkhratsky, A. (2021). Reactive astrocyte nomenclature, definitions, and future directions. *Nature Neuroscience 2021 24:3*, *24*(3), 312–325. https://doi.org/10.1038/s41593-020-00783-4

Fan, H., Yang, J., Zhang, K., Xing, J., Guo, B., Mao, H., Wang, W., Hu, Y., Lin, W., Huang, Y., Ding, J., Yu, C., Fu, F., Sun, L., Wu, J., Zhao, Y., Deng, W., Zhou, C., Qiu, M., … Wang, Y. (2022). IRES-mediated Wnt2 translation in apoptotic neurons triggers astrocyte dedifferentiation. *Npj Regenerative Medicine 2022 7:1*, *7*(1), 1–17. https://doi.org/10.1038/s41536-022-00248-1

Faulkner, J. R., Herrmann, J. E., Woo, M. J., Tansey, K. E., Doan, N. B., & Sofroniew, M. V. (2004). Reactive astrocytes protect tissue and preserve function after spinal cord injury. *Journal of Neuroscience*, *24*(9), 2143–2155. https://doi.org/10.1523/JNEUROSCI.3547-03.2004

Fawcett, J. W., & Asher, R. A. (1999). The glial scar and central nervous system repair. *Brain Res Bull*, *49*(6), 377–391. http://www.ncbi.nlm.nih.gov/entrez/query.fcgi?cmd=Retrieve&db=PubMed&dopt=Citation&list_uids=10483914

Fischer, J., Beckervordersandforth, R., Tripathi, P., Steiner-Mezzadri, A., Ninkovic, J., Gotz, M., & Götz, M. (2011). Prospective isolation of adult neural stem cells from the mouse subependymal zone. *Nat Protoc*, *6*(12), 1981–1989. https://doi.org/nprot.2011.412 [pii] 10.1038/nprot.2011.412

Fitch, M. T., & Silver, J. (2008). CNS Injury, Glial Scars, and Inflammation: Inhibitory extracellular matrices and regeneration failure. *Experimental Neurology*, *209*(2), 294. https://doi.org/10.1016/J.EXPNEUROL.2007.05.014

Frik, J., Merl-Pham, J., Plesnila, N., Mattugini, N., Kjell, J., Kraska, J., Gómez, R. M., Hauck, S. M., Sirko, S., & Götz, M. (2018). Cross-talk between monocyte invasion and astrocyte proliferation regulates scarring in brain injury. *EMBO Reports*, *19*(5). https://doi.org/10.15252/EMBR.201745294

Gabel, S., Koncina, E., Dorban, G., Heurtaux, T., Birck, C., Glaab, E., Michelucci, A., Heuschling, P., & Grandbarbe, L. (2016). Inflammation Promotes a Conversion of Astrocytes into Neural Progenitor Cells via NF-κB Activation. *Molecular Neurobiology*, *53*(8), 5041–5055. https://doi.org/10.1007/S12035-015-9428-3/FIGURES/8

Gantner, C. W., de Luzy, I. R., Kauhausen, J. A., Moriarty, N., Niclis, J. C., Bye, C. R., Penna, V., Hunt, C. P. J., Ermine, C. M., Pouton, C. W., Kirik, D., Thompson, L. H., & Parish, C. L. (2020). Viral Delivery of GDNF Promotes Functional Integration of Human Stem Cell Grafts in Parkinson's Disease. *Cell Stem Cell*, *26*(4). https://doi.org/10.1016/j.stem.2020.01.010

Ganz, J., & Brand, M. (2016). Adult Neurogenesis in Fish. *Cold Spring Harbor Perspectives in Biology*, *8*(7). https://doi.org/10.1101/CSHPERSPECT.A019018

Garcia, A. D., Doan, N. B., Imura, T., Bush, T. G., & Sofroniew, M. V. (2004). GFAP-expressing progenitors are the principal source of constitutive neurogenesis in adult mouse forebrain. *Nat Neurosci*, *7*(11), 1233–1241. https://doi.org/nn1340 [pii] 10.1038/nn1340

Gascón, S., Masserdotti, G., Russo, G. L., & Götz, M. (2017). Direct Neuronal Reprogramming: Achievements, Hurdles, and New Roads to Success. *Cell Stem Cell*, *21*(1), 18–34. https://doi.org/10.1016/j.stem.2017.06.011

Gascón, S., Murenu, E., Masserdotti, G., Ortega, F., Russo, G. L., Petrik, D., Deshpande, A., Heinrich, C., Karow, M., Robertson, S. P., Schroeder, T., Beckers, J., Irmler, M., Berndt, C., Angeli, J. P. F., Conrad, M., Berninger, B., & Götz, M. (2016). Identification and Successful Negotiation of a Metabolic Checkpoint in Direct Neuronal Reprogramming. *Cell Stem Cell*, *18*(3), 396–409. https://doi.org/10.1016/j.stem.2015.12.003

Götz, M., & Bocchi, R. (2021). Neuronal replacement: Concepts, achievements, and call for caution. *Current Opinion in Neurobiology*, *69*, 185–192. https://doi.org/10.1016/j.conb.2021.03.014

Götz, M., Nakafuku, M., & Petrik, D. (2016). Neurogenesis in the Developing and Adult Brain—Similarities and Key Differences. *Cold Spring Harbor Perspectives in Biology*, *8*(7). https://doi.org/10.1101/CSHPERSPECT.A018853

Götz, M., Sirko, S., Beckers, J., & Irmler, M. (2015). Reactive astrocytes as neural stem or progenitor cells: In vivo lineage, In vitro potential, and Genome-wide expression analysis. *Glia*, *63*(8), 1452–1468. https://doi.org/10.1002/GLIA.22850

Götz, S., Bribian, A., López-Mascaraque, L., Götz, M., Grothe, B., & Kunz, L. (2021). Heterogeneity of astrocytes: Electrophysiological properties of juxtavascular astrocytes before and after brain injury. *Glia*, *69*(2), 346–361. https://doi.org/10.1002/glia.23900

Gozlan, O., & Sprinzak, D. (2023). Notch signaling in development and homeostasis. *Development*, *150 4*(4). https://doi.org/10.1242/DEV.201138

Grade, S., & Götz, M. (2017). Neuronal replacement therapy: previous achievements and challenges ahead. *Npj Regenerative Medicine 2017 2:1*, *2*(1), 1–11. https://doi.org/10.1038/s41536-017-0033-0

Grande, A., Sumiyoshi, K., López-Juárez, A., Howard, J., Sakthivel, B., Aronow, B., Campbell, K., & Nakafuku, M. (2013). Environmental impact on direct neuronal reprogramming in vivo in the adult brain. *Nature Communications*, *4*. https://doi.org/10.1038/NCOMMS3373

Guo, Z., Zhang, L., Wu, Z., Chen, Y., Wang, F., & Chen, G. (2014). In vivo direct reprogramming of reactive glial cells into functional neurons after brain injury and in an Alzheimer's disease model. *Cell Stem Cell*, *14*(2). https://doi.org/10.1016/j.stem.2013.12.001

Hack, M. A., Sugimori, M., Lundberg, C., Nakafuku, M., Götz, M., & Gotz, M. (2004). Regionalization and fate specification in neurospheres: the role of Olig2 and Pax6. *Mol Cell Neurosci*, *25*(4), 664–678. https://doi.org/10.1016/j.mcn.2003.12.012

Hagino-Yamagishi, K., Saijoh, Y., Ikeda, M., Ichikawa, M., Minamikawa-Tachino, R., & Hamada, H. (1997). Predominant expression of Brn-2 in the postmitotic neurons of the developing mouse neocortex. *Brain Research*, *752*(1–2), 261–268. https://doi.org/10.1016/S0006-8993(96)01472-2

Haim, L. Ben, Carrillo-de Sauvage, M. A., Ceyzériat, K., & Escartin, C. (2015). Elusive roles for reactive astrocytes in neurodegenerative diseases. *Frontiers in Cellular Neuroscience*, *9*(AUGUST), 278. https://doi.org/10.3389/FNCEL.2015.00278

Han, R. T., Kim, R. D., Molofsky, A. V, & Liddelow, S. A. (2021). Astrocyte-immune cell interactions in physiology and pathology. *Immunity*, *54*(2), 211–224. https://doi.org/10.1016/j.immuni.2021.01.013

Hasel, P., Rose, I. V. L., Sadick, J. S., Kim, R. D., & Liddelow, S. A. (2021). Neuroinflammatory astrocyte subtypes in the mouse brain. *Nature Neuroscience*, *24*(10), 1475–1487. https://doi.org/10.1038/s41593-021-00905-6

Heinrich, C., Bergami, M., Gascón, S., Lepier, A., Dimou, L., Sutor, B., Berninger, B., Götz, M., Gascon, S., Lepier, A., Vigano, F., Dimou, L., Sutor, B., Berninger, B., & Gotz, M. (2014). Sox2-mediated conversion of NG2 glia into induced neurons in the injured adult cerebral cortex. *Stem Cell Reports*, *in press*(6), 1000–1014. https://doi.org/10.1016/j.stemcr.2014.10.007

Heinrich, C., Blum, R., Gascón, S., Masserdotti, G., Tripathi, P., Sánchez, R., Tiedt, S., Schroeder, T., Götz, M., & Berninger, B. (2010). Directing Astroglia from the Cerebral Cortex into Subtype Specific Functional Neurons. *PLoS Biology*, *8*(5), e1000373. https://doi.org/10.1371/journal.pbio.1000373

Heinrich, C., Gotz, M., & Berninger, B. (2012). Reprogramming of postnatal astroglia of the mouse neocortex into functional, synapse-forming neurons. *Methods Mol Biol*, *814*, 485–498. https://doi.org/10.1007/978-1-61779-452-0_32

Hernandez, M. C., Andres-Barquin, P. J., Martinez, S., Bulfone, A., Rubenstein, J. L. R., & Israel, M. A. (1997). ENC-1: A Novel MammalianKelch-Related Gene Specifically Expressed in the Nervous System Encodes an Actin-Binding Protein. *Journal of Neuroscience*, *17*(9), 3038–3051. https://doi.org/10.1523/JNEUROSCI.17-09-03038.1997

Hernández-Plaza, A., Szklarczyk, D., Botas, J., Cantalapiedra, C. P., Giner-Lamia, J., Mende, D. R., Kirsch, R., Rattei, T., Letunic, I., Jensen, L. J., Bork, P., von Mering, C., & Huerta-Cepas, J. (2023). eggNOG 6.0: enabling comparative genomics across 12 535 organisms. *Nucleic Acids Research*, *51*(D1), D389. https://doi.org/10.1093/NAR/GKAC1022

Herrero, J., Muffato, M., Beal, K., Fitzgerald, S., Gordon, L., Pignatelli, M., Vilella, A. J., Searle, S. M. J., Amode, R., Brent, S., Spooner, W., Kulesha, E., Yates, A., & Flicek, P. (2016). Ensembl comparative genomics resources. *Database*. https://doi.org/10.1093/database/baw053

Herrmann, J. E., Imura, T., Song, B., Qi, J., Ao, Y., Nguyen, T. K., Korsak, R. A., Takeda, K., Akira, S., & Sofroniew, M. V. (2008). STAT3 is a critical regulator of astrogliosis and scar formation after spinal cord injury. *The Journal of Neuroscience : The Official*

Journal of the Society for Neuroscience, *28*(28), 7231–7243. https://doi.org/10.1523/JNEUROSCI.1709-08.2008

Hoang, T., Wang, J., Boyd, P., Wang, F., Santiago, C., Jiang, L., Yoo, S., Lahne, M., Todd, L. J., Jia, M., Saez, C., Keuthan, C., Palazzo, I., Squires, N., Campbell, W. A., Rajaii, F., Parayil, T., Trinh, V., Kim, D. W., … Blackshaw, S. (2020). Gene regulatory networks controlling vertebrate retinal regeneration. *Science*, *370*(6519). https://doi.org/10.1126/SCIENCE.ABB8598/SUPPL_FILE/ABB8598_TABLES9.XLSX

Hol, E. M., & Pekny, M. (2015). Glial fibrillary acidic protein (GFAP) and the astrocyte intermediate filament system in diseases of the central nervous system. *Curr Opin Cell Biol*, *32*, 121–130. https://doi.org/10.1016/j.ceb.2015.02.004

Hsieh, J., Nakashima, K., Kuwabara, T., Mejia, E., & Gage, F. H. (2004). Histone deacetylase inhibition-mediated neuronal differentiation of multipotent adult neural progenitor cells. *Proceedings of the National Academy of Sciences of the United States of America*, *101*(47), 16659–16664. https://doi.org/10.1073/PNAS.0407643101

Hyder, A. A., Wunderlich, C. A., Puvanachandra, P., Gururaj, G., & Kobusingye, O. C. (2007). The impact of traumatic brain injuries: A global perspective. *NeuroRehabilitation*, *22*(5), 341–353. https://doi.org/10.3233/NRE-2007-22502

Iwafuchi-Doi, M., & Zaret, K. S. (2014). Pioneer transcription factors in cell reprogramming. *Genes Dev*, *28*(24), 2679–2692. https://doi.org/10.1101/gad.253443.114

Jäkel, S., & Dimou, L. (2017). Glial cells and their function in the adult brain: A journey through the history of their ablation. *Frontiers in Cellular Neuroscience*, *11*, 235525. https://doi.org/10.3389/FNCEL.2017.00024/BIBTEX

Jessberger, S. (2016). Neural repair in the adult brain. *F1000Research*, *5*, 1000. https://doi.org/10.12688/F1000RESEARCH.7459.1

Jørgensen, H. F., Terry, A., Beretta, C., Pereira, C. F., Leleu, M., Chen, Z. F., Kelly, C., Merkenschlager, M., & Fisher, A. G. (2009). REST selectively represses a subset of RE1-containing neuronal genes in mouse embryonic stem cells. *Development (Cambridge, England)*, *136*(5), 715–721. https://doi.org/10.1242/DEV.028548

Jurisch-Yaksi, N., Yaksi, E., & Kizil, C. (2020). Radial glia in the zebrafish brain: Functional, structural, and physiological comparison with the mammalian glia. In *GLIA* (Vol. 68, Issue 12, pp. 2451–2470). John Wiley and Sons Inc. https://doi.org/10.1002/glia.23849

Kazanis, I. (2009). The subependymal zone neurogenic niche: a beating heart in the centre of the brain: How plastic is adult neurogenesis? Opportunities for therapy and questions to be addressed. *Brain*, *132*(11), 2909. https://doi.org/10.1093/BRAIN/AWP237

Kettenmann, H., & Verkhratsky, A. (2022). Glial Cells: Neuroglia. In *Neuroscience in the 21st Century* (pp. 825–860). Springer International Publishing. https://doi.org/10.1007/978-3-030-88832-9_19

Khakh, B. S., & Deneen, B. (2019). The Emerging Nature of Astrocyte Diversity. *Https://Doi.Org/10.1146/Annurev-Neuro-070918-050443*, *42*, 187–207. https://doi.org/10.1146/ANNUREV-NEURO-070918-050443

Kim, Y., Comte, I., Szabo, G., Hockberger, P., & Szele, F. G. (2009). Adult Mouse Subventricular Zone Stem and Progenitor Cells Are Sessile and Epidermal Growth Factor Receptor Negatively Regulates Neuroblast Migration. *PLOS ONE*, *4*(12), e8122. https://doi.org/10.1371/JOURNAL.PONE.0008122

Kim, Y., Park, J., & Choi, Y. K. (2019). The Role of Astrocytes in the Central Nervous System Focused on BK Channel and Heme Oxygenase Metabolites: A Review. *Antioxidants*, *8*(5). https://doi.org/10.3390/ANTIOX8050121

Kimura, A., Matsuda, T., Sakai, A., Murao, N., & Nakashima, K. (2018). HMGB2 expression is associated with transition from a quiescent to an activated state of adult

neural stem cells. *Developmental Dynamics*, *247*(1), 229–238. https://doi.org/10.1002/DVDY.24559

Kishimoto, N., Alfaro-Cervello, C., Shimizu, K., Asakawa, K., Urasaki, A., Nonaka, S., Kawakami, K., Garcia-Verdugo, J. M., & Sawamoto, K. (2011). Migration of neuronal precursors from the telencephalic ventricular zone into the olfactory bulb in adult zebrafish. *J Comp Neurol*, *519*(17), 3549–3565. https://doi.org/10.1002/cne.22722

Kizil, C., Kaslin, J., Kroehne, V., & Brand, M. (2012). Adult neurogenesis and brain regeneration in zebrafish. *Developmental Neurobiology*, *72*(3), 429–461. https://doi.org/10.1002/DNEU.20918

Kizil, C., Kyritsis, N., Dudczig, S., Kroehne, V., Freudenreich, D., Kaslin, J., & Brand, M. (2012). Regenerative Neurogenesis from Neural Progenitor Cells Requires Injury-Induced Expression of Gata3. *Developmental Cell*, *23*(6), 1230–1237. https://doi.org/10.1016/j.devcel.2012.10.014

Korsunsky, I., Millard, N., Fan, J., Slowikowski, K., Zhang, F., Wei, K., Baglaenko, Y., Brenner, M., Loh, P. ru, & Raychaudhuri, S. (2019). Fast, sensitive, and accurate integration of single cell data with Harmony. *Nature Methods*, *16*(12), 1289. https://doi.org/10.1038/S41592-019-0619-0

Kozol, R. A., Abrams, A. J., James, D. M., Buglo, E., Yan, Q., & Dallman, J. E. (2016). Function over form: Modeling groups of inherited neurological conditions in zebrafish. *Frontiers in Molecular Neuroscience*, *9*(JUL), 203484. https://doi.org/10.3389/FNMOL.2016.00055/ABSTRACT

Kreutzberg, G. W. (1996). Microglia: a sensor for pathological events in the CNS. *Trends Neurosci*, *19*(8), 312–318. https://doi.org/0166223696100497 [pii]

Kroehne, V., Freudenreich, D., Hans, S., Kaslin, J., & Brand, M. (2011). Regeneration of the adult zebrafish brain from neurogenic radial glia-type progenitors. *Development*, *138*(22), 4831–4841. https://doi.org/10.1242/dev.072587

Kuznetsov, D., Tegenfeldt, F., Manni, M., Seppey, M., Berkeley, M., Kriventseva, E. V., & Zdobnov, E. M. (2023). OrthoDB v11: annotation of orthologs in the widest sampling of organismal diversity. *Nucleic Acids Research*, *51*(D1), D445. https://doi.org/10.1093/NAR/GKAC998

Lang, B., Liu, H. L., Liu, R., Feng, G. D., Jiao, X. Y., & Ju, G. (2004). Astrocytes in injured adult rat spinal cord may acquire the potential of neural stem cells. *Neuroscience*, *128*(4), 775–783. https://doi.org/10.1016/j.neuroscience.2004.06.033

Lanjakornsiripan, D., Pior, B.-J., Kawaguchi, D., Furutachi, S., Tahara, T., Katsuyama, Y., Suzuki, Y., Fukazawa, Y., & Gotoh, Y. (2018). Layer-specific morphological and molecular differences in neocortical astrocytes and their dependence on neuronal layers. *Nature Communications*, *9*(1), 1623. https://doi.org/10.1038/s41467-018-03940-3

Lawrence, J. M., Schardien, K., Wigdahl, B., & Nonnemacher, M. R. (2023). Roles of neuropathology-associated reactive astrocytes: a systematic review. *Acta Neuropathologica Communications*, *11*(1). https://doi.org/10.1186/S40478-023-01526-9

Lee Chong, T., Ahearn, E. L., & Cimmino, L. (2019). Reprogramming the Epigenome With Vitamin C. *Frontiers in Cell and Developmental Biology*, *7*. https://doi.org/10.3389/FCELL.2019.00128

Liao, L. Y., Lau, B. W. M., Sánchez-Vidaña, D. I., & Gao, Q. (2019). Exogenous neural stem cell transplantation for cerebral ischemia. *Neural Regeneration Research*, *14*(7), 1129. https://doi.org/10.4103/1673-5374.251188

Liddelow, S. A., & Barres, B. A. (2017). Reactive Astrocytes: Production, Function, and Therapeutic Potential. *Immunity*, *46*(6), 957–967. https://doi.org/10.1016/J.IMMUNI.2017.06.006

Lim, D. A., & Alvarez-Buylla, A. (2016). The Adult Ventricular-Subventricular Zone (V-SVZ) and Olfactory Bulb (OB) Neurogenesis. *Cold Spring Harbor Perspectives in Biology*, *8*(5). https://doi.org/10.1101/CSHPERSPECT.A018820

Lin, Y., Ghazanfar, S., Wang, K. Y. X., Gagnon-Bartsch, J. A., Lo, K. K., Su, X., Han, Z. G., Ormerod, J. T., Speed, T. P., Yang, P., & Yang, J. Y. H. (2019). ScMerge leverages factor analysis, stable expression, and pseudoreplication to merge multiple single-cell RNA-seq datasets. *Proceedings of the National Academy of Sciences of the United States of America*, *116*(20), 9775–9784. https://doi.org/10.1073/PNAS.1820006116/SUPPL_FILE/PNAS.1820006116.SD02.XLSX

Lin, Y. M. J., Hsin, I. L., Sun, H. S., Lin, S., Lai, Y. L., Chen, H. Y., Chen, T. Y., Chen, Y. P., Shen, Y. T., & Wu, H. M. (2018). NTF3 Is a Novel Target Gene of the Transcription Factor POU3F2 and Is Required for Neuronal Differentiation. *Molecular Neurobiology*, *55*(11), 8403–8413. https://doi.org/10.1007/S12035-018-0995-Y/FIGURES/8

Liu, F., Zhang, Y., Chen, F., Yuan, J., Li, S., Han, S., Lu, D., Geng, J., Rao, Z., Sun, L., Xu, J., Shi, Y., Wang, X., & Liu, Y. (2021). Neurog2 directly converts astrocytes into functional neurons in midbrain and spinal cord. *Cell Death and Disease*, *12*(3). https://doi.org/10.1038/s41419-021-03498-x

Liu, J., Gao, C., Sodicoff, J., Kozareva, V., Macosko, E. Z., & Welch, J. D. (2020). Jointly defining cell types from multiple single-cell datasets using LIGER. *Nature Protocols*, *15*(11), 3632–3662. https://doi.org/10.1038/S41596-020-0391-8

Liu, M. L., Zang, T., Zou, Y., Chang, J. C., Gibson, J. R., Huber, K. M., & Zhang, C. L. (2013). Small molecules enable neurogenin 2 to efficiently convert human fibroblasts into cholinergic neurons. *Nature Communications*, *4*. https://doi.org/10.1038/NCOMMS3183

Liu, M.-H., Xu, Y.-G., Bai, X.-N., Lin, J.-H., Xiang, Z.-Q., Wang, T., Xu, L., Li, W., & Chen, G. (2022). Efficient Dlx2-mediated astrocyte-to-neuron conversion and inhibition of neuroinflammation by NeuroD1. *BioRxiv*, 2022.07.11.499522. https://doi.org/10.1101/2022.07.11.499522

Liu, Q., Liu, F., Yu, K. Lou, Tas, R., Grigoriev, I., Remmelzwaal, S., Serra-Marques, A., Kapitein, L. C., Heck, A. J. R., & Akhmanova, A. (2016). MICAL3 Flavoprotein Monooxygenase Forms a Complex with Centralspindlin and Regulates Cytokinesis. *The Journal of Biological Chemistry*, *291*(39), 20617–20629. https://doi.org/10.1074/JBC.M116.748186

Liu, Y., Miao, Q., Yuan, J., Han, S., Zhang, P., Li, S., Rao, Z., Zhao, W., Ye, Q., Geng, J., Zhang, X., & Cheng, L. (2015). Ascl1 Converts Dorsal Midbrain Astrocytes into Functional Neurons In Vivo. *Journal of Neuroscience*, *35*(25), 9336–9355. https://doi.org/10.1523/JNEUROSCI.3975-14.2015

Llorens-Bobadilla, E., Zhao, S., Baser, A., Saiz-Castro, G., Zwadlo, K., & Martin-Villalba, A. (2015). Single-Cell Transcriptomics Reveals a Population of Dormant Neural Stem Cells that Become Activated upon Brain Injury. *Cell Stem Cell*, *17*(3), 329–340. https://doi.org/10.1016/j.stem.2015.07.002

Lotfollahi, M., Wolf, F. A., & Theis, F. J. (2019). scGen predicts single-cell perturbation responses. *Nature Methods 2019 16:8*, *16*(8), 715–721. https://doi.org/10.1038/s41592-019-0494-8

Lu, Y. L., & Yoo, A. S. (2018). Mechanistic Insights Into MicroRNA-Induced Neuronal Reprogramming of Human Adult Fibroblasts. *Frontiers in Neuroscience*, *12*(AUG). https://doi.org/10.3389/FNINS.2018.00522

Lust, K., & Tanaka, E. M. (2019). A Comparative Perspective on Brain Regeneration in Amphibians and Teleost Fish. *Developmental Neurobiology*, *79*(5), 424. https://doi.org/10.1002/DNEU.22665

Ma, D. K., Bonaguidi, M. A., Ming, G. L., & Song, H. (2009). Adult neural stem cells in the mammalian central nervous system. *Cell Research 2009 19:6*, *19*(6), 672–682. https://doi.org/10.1038/cr.2009.56

Ma, N. X., Yin, J. C., & Chen, G. (2019). Transcriptome analysis of small molecule–mediated astrocyte-to-neuron reprogramming. *Frontiers in Cell and Developmental Biology*, *7*(May). https://doi.org/10.3389/FCELL.2019.00082/FULL

Maas, A. I. R., Menon, D. K., Manley, G. T., Abrams, M., Åkerlund, C., Andelic, N., Aries, M., Bashford, T., Bell, M. J., Bodien, Y. G., Brett, B. L., Büki, A., Chesnut, R. M., Citerio, G., Clark, D., Clasby, B., Cooper, D. J., Czeiter, E., Czosnyka, M., … Zumbo, F. (2022). Traumatic brain injury: progress and challenges in prevention, clinical care, and research. *The Lancet. Neurology*, *21*(11), 1004–1060. https://doi.org/10.1016/S1474-4422(22)00309-X

Maas, A. I. R., Stocchetti, N., & Bullock, R. (2008). Moderate and severe traumatic brain injury in adults. *The Lancet Neurology*, *7*(8), 728–741. https://doi.org/10.1016/S1474-4422(08)70164-9

Magnusson, J. P., Göritz, C., Tatarishvili, J., Dias, D. O., Smith, E. M. K., Lindvall, O., Kokaia, Z., & Frisén, J. (2014). A latent neurogenic program in astrocytes regulated by Notch signaling in the mouse. *Science (New York, N.Y.)*, *346*(6206), 237–241. https://doi.org/10.1126/SCIENCE.346.6206.237

Makarava, N., Mychko, O., Molesworth, K., Chang, J. C. Y., Henry, R. J., Tsymbalyuk, N., Gerzanich, V., Simard, J. M., Loane, D. J., & Baskakov, I. V. (2023). Region-Specific Homeostatic Identity of Astrocytes Is Essential for Defining Their Response to Pathological Insults. *Cells*, *12*(17), 2172. https://doi.org/10.3390/CELLS12172172/S1

Maldonado, K. A., & Alsayouri, K. (2023). Physiology, Brain. *StatPearls*. https://www.ncbi.nlm.nih.gov/books/NBK551718/

Mall, M., Kareta, M. S., Chanda, S., Ahlenius, H., Perotti, N., Zhou, B., Grieder, S. D., Ge, X., Drake, S., Ang, C. E., Walker, B. M., Vierbuchen, T., Fuentes, D. R., Brennecke, P., Nitta, K. R., Jolma, A., Steinmetz, L. M., Taipale, J., Sudhof, T. C., & Wernig, M. (2017). Myt1l safeguards neuronal identity by actively repressing many non-neuronal fates. *Nature*, *544*(7649), 245–249. https://doi.org/10.1038/nature21722

Marshall, C. A. G., Suzuki, S. O., & Goldman, J. E. (2003). Gliogenic and neurogenic progenitors of the subventricular zone: who are they, where did they come from, and where are they going? *Glia*, *43*(1), 52–61. https://doi.org/10.1002/GLIA.10213

Masserdotti, G., Gillotin, S., Sutor, B., Drechsel, D., Irmler, M., Jørgensen, H. F., Sass, S., Theis, F. J., Beckers, J., Berninger, B., Guillemot, F., & Götz, M. (2015). Transcriptional Mechanisms of Proneural Factors and REST in Regulating Neuronal Reprogramming of Astrocytes. *Cell Stem Cell*, *17*(1), 74–88. https://doi.org/10.1016/j.stem.2015.05.014

Mattugini, N., Bocchi, R., Scheuss, V., Russo, G. L., Torper, O., Lao, C. L., & Götz, M. (2019). Inducing Different Neuronal Subtypes from Astrocytes in the Injured Mouse Cerebral Cortex. *Neuron*, *103*(6), 1086-1095.e5. https://doi.org/10.1016/j.neuron.2019.08.009

Matusova, Z., Hol, E. M., Pekny, M., Kubista, M., & Valihrach, L. (2023). Reactive astrogliosis in the era of single-cell transcriptomics. *Frontiers in Cellular Neuroscience*, *17*. https://doi.org/10.3389/FNCEL.2023.1173200

McKeon, R. J., Jurynec, M. J., & Buck, C. R. (1999). The Chondroitin Sulfate Proteoglycans Neurocan and Phosphacan Are Expressed by Reactive Astrocytes in the Chronic CNS Glial Scar. *Journal of Neuroscience*, *19*(24), 10778–10788. https://doi.org/10.1523/JNEUROSCI.19-24-10778.1999

Michinaga, S., & Koyama, Y. (2019). Dual Roles of Astrocyte-Derived Factors in Regulation of Blood-Brain Barrier Function after Brain Damage. *International Journal of Molecular Sciences 2019, Vol. 20, Page 571*, *20*(3), 571. https://doi.org/10.3390/IJMS20030571

Miller, R. H., & Raff, M. C. (1984). Fibrous and protoplasmic astrocytes are biochemically and developmentally distinct. *The Journal of Neuroscience : The Official Journal of*

the Society for Neuroscience, *4*(2), 585–592. https://doi.org/10.1523/JNEUROSCI.04-02-00585.1984

Ming, G. li, & Song, H. (2011). Adult Neurogenesis in the Mammalian Brain: Significant Answers and Significant Questions. *Neuron*, *70*(4), 687. https://doi.org/10.1016/J.NEURON.2011.05.001

Morris, S. A. (2016). Direct lineage reprogramming via pioneer factors; a detour through developmental gene regulatory networks. *Development*, *143*(15), 2696–2705. https://doi.org/10.1242/dev.138263

Morrison, S. J., Perez, S. E., Qiao, Z., Verdi, J. M., Hicks, C., Weinmaster, G., & Anderson, D. J. (2000). Transient Notch activation initiates an irreversible switch from neurogenesis to gliogenesis by neural crest stem cells. *Cell*, *101*(5), 499–510.

Myer, D. J., Gurkoff, G. G., Lee, S. M., Hovda, D. A., & Sofroniew, M. V. (2006). Essential protective roles of reactive astrocytes in traumatic brain injury. *Brain*, *129*(10), 2761–2772. https://doi.org/10.1093/brain/awl165

Nedergaard, M., Ransom, B., & Goldman, S. A. (2003). New roles for astrocytes: redefining the functional architecture of the brain. *Trends in Neurosciences*, *26*(10), 523–530. https://doi.org/10.1016/J.TINS.2003.08.008

Ninkovic, J., & Götz, M. (2013). Fate specification in the adult brain--lessons for eliciting neurogenesis from glial cells. *BioEssays : News and Reviews in Molecular, Cellular and Developmental Biology*, *35*(3), 242–252. https://doi.org/10.1002/BIES.201200108

Ninkovic, J., Steiner-Mezzadri, A., Jawerka, M., Akinci, U., Masserdotti, G., Petricca, S., Fischer, J., von Holst, A., Beckers, J., Lie, C. D. D., Petrik, D., Miller, E., Tang, J., Wu, J., Lefebvre, V., Demmers, J., Eisch, A., Metzger, D., Crabtree, G., … Gotz, M. (2013). The BAF Complex Interacts with Pax6 in Adult Neural Progenitors to Establish a Neurogenic Cross-Regulatory Transcriptional Network. *Cell Stem Cell*, *13*(4). https://doi.org/10.1016/j.stem.2013.07.002

Ninomiya, M., Yamashita, T., Araki, N., Okano, H., & Sawamoto, K. (2006). Enhanced neurogenesis in the ischemic striatum following EGF-induced expansion of transit-amplifying cells in the subventricular zone. *Neuroscience Letters*, *403*(1–2). https://doi.org/10.1016/j.neulet.2006.04.039

Niu, W., Zang, T., Zou, Y., Fang, S., Smith, D., … R. B.-N. cell, & 2013, undefined. (n.d.). In vivo reprogramming of astrocytes to neuroblasts in the adult brain. *Nature.ComW Niu, T Zang, Y Zou, S Fang, DK Smith, R Bachoo, CL ZhangNature Cell Biology, 2013•nature.Com*. Retrieved January 3, 2024, from https://www.nature.com/articles/ncb2843

Niwa, S., Tanaka, Y., & Hirokawa, N. (2008). KIF1Bβ- and KIF1A-mediated axonal transport of presynaptic regulator Rab3 occurs in a GTP-dependent manner through DENN/MADD. *Nature Cell Biology*, *10*(11). https://doi.org/10.1038/ncb1785

Oberheim, N. A., Goldman, S. A., & Nedergaard, M. (2012). Heterogeneity of Astrocytic Form and Function. *Methods in Molecular Biology (Clifton, N.J.)*, *814*, 23. https://doi.org/10.1007/978-1-61779-452-0_3

Ogata, S., Hashizume, K., Hayase, Y., Kanno, Y., Hori, K., Balan, S., Yoshikawa, T., Takahashi, H., Taya, S., & Hoshino, M. (2021). Potential involvement of DSCAML1 mutations in neurodevelopmental disorders. *Genes to Cells : Devoted to Molecular & Cellular Mechanisms*, *26*(3), 136–151. https://doi.org/10.1111/GTC.12831

Ohlig, S., Clavreul, S., Thorwirth, M., Simon-Ebert, T., Bocchi, R., Ulbricht, S., Kannayian, N., Rossner, M., Sirko, S., Smialowski, P., Fischer-Sternjak, J., & Götz, M. (2021). Molecular diversity of diencephalic astrocytes reveals adult astrogenesis regulated by Smad4. *The EMBO Journal*, *40*(21). https://doi.org/10.15252/embj.2020107532

Okada, Y., Yamazaki, H., Sekine-Aizawa, Y., & Hirokawa, N. (1995). The neuron-specific kinesin superfamily protein KIF1A is a uniqye monomeric motor for anterograde axonal transport of synaptic vesicle precursors. *Cell*, *81*(5). https://doi.org/10.1016/0092-8674(95)90538-3

O'Shea, T. M., Ao, Y., Wang, S., Ren, Y., Cheng, A., Kawaguchi, R., Swarup, V., & Sofroniew, M. V. (2023). Border-forming wound repair astrocytes. *BioRxiv*, 2023.08.25.554857. https://doi.org/10.1101/2023.08.25.554857

Pandey, S., Moyer, A. J., & Thyme, S. B. (2023). A single-cell transcriptome atlas of the maturing zebrafish telencephalon. *Genome Research*, *33*(4), 658–671. https://doi.org/10.1101/GR.277278.122/-/DC1

Pascale, E., Caiazza, C., Paladino, M., Parisi, S., Passaro, F., & Caiazzo, M. (2022). MicroRNA Roles in Cell Reprogramming Mechanisms. *Cells*, *11*(6). https://doi.org/10.3390/CELLS11060940

Patabendige, A., Singh, A., Jenkins, S., Sen, J., & Chen, R. (2021). Astrocyte Activation in Neurovascular Damage and Repair Following Ischaemic Stroke. *International Journal of Molecular Sciences 2021, Vol. 22, Page 4280*, *22*(8), 4280. https://doi.org/10.3390/IJMS22084280

Păun, O., Tan, Y. X., Patel, H., Strohbuecker, S., Ghanate, A., Cobolli-Gigli, C., Sopena, M. L., Gerontogianni, L., Goldstone, R., Ang, S. L., Guillemot, F., & Dias, C. (2023). Pioneer factor ASCL1 cooperates with the mSWI/SNF complex at distal regulatory elements to regulate human neural differentiation. *Genes and Development*, *37*(5–6), 218–242. https://doi.org/10.1101/gad.350269.122

Pekny, M., & Nilsson, M. (2005). Astrocyte activation and reactive gliosis. *Glia*, *50*(4), 427–434. https://doi.org/10.1002/glia.20207

Pekny, M., & Pekna, M. (2004). Astrocyte intermediate filaments in CNS pathologies and regeneration. *The Journal of Pathology*, *204*(4), 428–437. https://doi.org/10.1002/path.1645

Pekny, M., Wilhelmsson, U., & Pekna, M. (2014). The dual role of astrocyte activation and reactive gliosis. *Neuroscience Letters*, *565*, 30–38. https://doi.org/10.1016/J.NEULET.2013.12.071

Pencea, V., Bingaman, K. D., Freedman, L. J., & Luskin, M. B. (2001). Neurogenesis in the subventricular zone and rostral migratory stream of the neonatal and adult primate forebrain. *Experimental Neurology*, *172*(1), 1–16. https://doi.org/10.1006/EXNR.2001.7768

Poss, K. D., Keating, M. T., & Nechiporuk, A. (2003). Tales of regeneration in zebrafish. *Dev Dyn*, *226*(2), 202–210. https://doi.org/10.1002/dvdy.10220

Qian, Z., Qin, J., Lai, Y., Zhang, C., & Zhang, X. (2023). Large-Scale Integration of Single-Cell RNA-Seq Data Reveals Astrocyte Diversity and Transcriptomic Modules across Six Central Nervous System Disorders. *Biomolecules*, *13*(4). https://doi.org/10.3390/BIOM13040692/S1

Ramesh, V., Bayam, E., Cernilogar, F. M., Bonapace, I. M., Schulze, M., Riemenschneider, M. J., Schotta, G., & Gotz, M. (2016). Loss of Uhrf1 in neural stem cells leads to activation of retroviral elements and delayed neurodegeneration. *Genes Dev*, *30*(19), 2199–2212. https://doi.org/10.1101/gad.284992.116

Ransom, B., Behar, T., & Nedergaard, M. (2003). New roles for astrocytes (stars at last). *Trends in Neurosciences*, *26*(10), 520–522. https://doi.org/10.1016/j.tins.2003.08.006

Rao, Z., Wang, R., Li, S., Shi, Y., Mo, L., Han, S., Yuan, J., Jing, N., & Cheng, L. (2021). Molecular Mechanisms Underlying Ascl1-Mediated Astrocyte-to-Neuron Conversion. *Stem Cell Reports*, *16*(3), 534–547. https://doi.org/10.1016/J.STEMCR.2021.01.006

Rhodes, K. E., Moon, L. D. F., & Fawcett, J. W. (2003). Inhibiting cell proliferation during formation of the glial scar: Effects on axon regeneration in the CNS. *Neuroscience*, *120*(1). https://doi.org/10.1016/S0306-4522(03)00285-9

Rio-Hortega, P. del. (1920). Estudios sobre la neuroglía. La microglía y su transformación en células en bastoncito y cuerpos granuloadiposos. *Trab. Lab. Invest. Biol. Univ. Madrid*, *18*, 37–82.

Rivetti Di Val Cervo, P., Romanov, R. A., Spigolon, G., Masini, D., Martín-Montañez, E., Toledo, E. M., La Manno, G., Feyder, M., Pifl, C., Ng, Y. H., Sánchez, S. P.,

Linnarsson, S., Wernig, M., Harkany, T., Fisone, G., & Arenas, E. (2017). Induction of functional dopamine neurons from human astrocytes in vitro and mouse astrocytes in a Parkinson's disease model. *Nature Biotechnology*, *35*(5), 444–452. https://doi.org/10.1038/NBT.3835

Robel, S., Berninger, B., & Götz, M. (2011). The stem cell potential of glia: lessons from reactive gliosis. *Nature Reviews. Neuroscience*, *12*(2), 88–104. https://doi.org/10.1038/NRN2978

Ronfani, L., Ferraguti, M., Croci, L., Ovitt, C. E., Schöler, H. R., Consalez, G. G., & Bianchi, M. E. (2001). Reduced fertility and spermatogenesis defects in mice lacking chromosomal protein Hmgb2. *Development (Cambridge, England)*, *128*(8), 1265–1273. https://doi.org/10.1242/DEV.128.8.1265

Salih, D. A. M., Rashid, A. J., Colas, D., de la Torre-Ubieta, L., Zhu, R. P., Morgan, A. A., Santo, E. E., Ucar, D., Devarajan, K., Cole, C. J., Madison, D. V., Shamloo, M., Butte, A. J., Bonni, A., Josselyn, S. A., & Brunet, A. (2012). FoxO6 regulates memory consolidation and synaptic function. *Genes & Development*, *26*(24), 2780–2801. https://doi.org/10.1101/GAD.208926.112

Sanchez-Gonzalez, R., Koupourtidou, C., Lepko, T., Zambusi, A., Novoselc, K. T., Durovic, T., Aschenbroich, S., Schwarz, V., Breunig, C. T., Straka, H., Huttner, H. B., Irmler, M., Beckers, J., Wurst, W., Zwergal, A., Schauer, T., Straub, T., Czopka, T., Trümbach, D., … Ninkovic, J. (2022). Innate Immune Pathways Promote Oligodendrocyte Progenitor Cell Recruitment to the Injury Site in Adult Zebrafish Brain. *Cells*, *11*(3), 520. https://doi.org/10.3390/cells11030520

Santopolo, G., Magnusson, J. P., Lindvall, O., Kokaia, Z., & Frisén, J. (2020). Blocking Notch-Signaling Increases Neurogenesis in the Striatum after Stroke. *Cells*, *9*(7). https://doi.org/10.3390/cells9071732

Sasaki, T., Hirabayashi, J., Manya, H., Kasai, K. I., & Endo, T. (2004). Galectin-1 induces astrocyte differentiation, which leads to production of brain-derived neurotrophic factor. *Glycobiology*, *14*(4), 357–363. https://doi.org/10.1093/GLYCOB/CWH043

Shchaslyvyi, A. Y., Antonenko, S. V., Tesliuk, M. G., & Telegeev, G. D. (2023). Current State of Human Gene Therapy: Approved Products and Vectors. *Pharmaceuticals 2023, Vol. 16, Page 1416*, *16*(10), 1416. https://doi.org/10.3390/PH16101416

Shi, W., Feng, Z., Zhang, J., Gonzalez-Suarez, I., Vanderwaal, R. P., Wu, X., Powell, S. N., Roti, J. L. R., Gonzalo, S., & Zhang, J. (2010). The role of RPA2 phosphorylation in homologous recombination in response to replication arrest. *Carcinogenesis*, *31*(6), 994. https://doi.org/10.1093/CARCIN/BGQ035

Shimada, I. S., LeComte, M. D., Granger, J. C., Quinlan, N. J., & Spees, J. L. (2012). Self-renewal and differentiation of reactive astrocyte-derived neural stem/progenitor cells isolated from the cortical peri-infarct area after stroke. *The Journal of Neuroscience : The Official Journal of the Society for Neuroscience*, *32*(23), 7926–7940. https://doi.org/10.1523/JNEUROSCI.4303-11.2012

Silver, J., & Miller, J. H. (2004). Regeneration beyond the glial scar. *Nature Reviews Neuroscience 2004 5:2*, *5*(2), 146–156. https://doi.org/10.1038/nrn1326

Simpson Ragdale, H., Clements, M., Tang, W., Deltcheva, E., Andreassi, C., Lai, A. G., Chang, W. H., Pandrea, M., Andrew, I., Game, L., Uddin, I., Ellis, M., Enver, T., Riccio, A., Marguerat, S., & Parrinello, S. (2023). Injury primes mutation-bearing astrocytes for dedifferentiation in later life. *Current Biology*, *33*(6), 1082-1098.e8. https://doi.org/10.1016/J.CUB.2023.02.013

Sirko, S., Behrendt, G., Johansson, P. A., Tripathi, P., Costa, M. R., Bek, S., Heinrich, C., Tiedt, S., Colak, D., Dichgans, M., Fischer, I. R., Plesnila, N., Staufenbiel, M., Haass, C., Snapyan, M., Saghatelyan, A., Tsai, L.-H., Fischer, A., Grobe, K., … Götz, M. (2013). Reactive Glia in the Injured Brain Acquire Stem Cell Properties in Response to Sonic Hedgehog. *Cell Stem Cell*, *12*(4), 426–439. https://doi.org/10.1016/j.stem.2013.01.019

Sirko, S., Schichor, C., Della Vecchia, P., Metzger, F., Sonsalla, G., Simon, T., Bürkle, M., Kalpazidou, S., Ninkovic, J., Masserdotti, G., Sauniere, J. F., Iacobelli, V., Iacobelli, S., Delbridge, C., Hauck, S. M., Tonn, J. C., & Götz, M. (2023). Injury-specific factors in the cerebrospinal fluid regulate astrocyte plasticity in the human brain. *Nature Medicine 2023 29:12*, *29*(12), 3149–3161. https://doi.org/10.1038/s41591-023-02644-6

Smith, D. K., Yang, J., Liu, M. L., & Zhang, C. L. (2016). Small Molecules Modulate Chromatin Accessibility to Promote NEUROG2-Mediated Fibroblast-to-Neuron Reprogramming. *Stem Cell Reports*, *7*(5). https://doi.org/10.1016/j.stemcr.2016.09.013

Sofroniew, M. V. (2005). Reactive astrocytes in neural repair and protection. *The Neuroscientist : A Review Journal Bringing Neurobiology, Neurology and Psychiatry*, *11*(5), 400–407. https://doi.org/10.1177/1073858405278321

Sofroniew, M. V. (2009). Molecular dissection of reactive astrogliosis and glial scar formation. *Trends in Neurosciences*, *32*(12), 638–647. https://doi.org/10.1016/J.TINS.2009.08.002

Sofroniew, M. V. (2015). Astrocyte barriers to neurotoxic inflammation. *Nature Reviews. Neuroscience*, *16*(5), 249–263. https://doi.org/10.1038/NRN3898

Sofroniew, M. V. (2020). Astrocyte Reactivity: Subtypes, States, and Functions in CNS Innate Immunity. *Trends in Immunology*, *41*(9), 758–770. https://doi.org/10.1016/J.IT.2020.07.004

Sofroniew, M. V., & Vinters, H. V. (2010). Astrocytes: biology and pathology. *Acta Neuropathologica*, *119*(1), 7–35. https://doi.org/10.1007/S00401-009-0619-8

Stadelmann, C., Timmler, S., Barrantes-Freer, A., & Simons, M. (2019). Myelin in the central nervous system: Structure, function, and pathology. *Physiological Reviews*, *99*(3), 1381–1431. https://doi.org/10.1152/PHYSREV.00031.2018/ASSET/IMAGES/LARGE/Z9J003192 9070008.JPEG

Starkova, T., Polyanichko, A., Tomilin, A. N., & Chikhirzhina, E. (2023). Structure and Functions of HMGB2 Protein. *International Journal of Molecular Sciences*, *24*(9). https://doi.org/10.3390/IJMS24098334

Stein, D. G., Geddes, R. I., & Sribnick, E. A. (2015). Recent developments in clinical trials for the treatment of traumatic brain injury. *Handbook of Clinical Neurology*, *127*, 433–451. https://doi.org/10.1016/B978-0-444-52892-6.00028-3

Suh, Y., Obernier, K., Hölzl-Wenig, G., Mandl, C., Herrmann, A., Wörner, K., Eckstein, V., & Ciccolini, F. (2009). Interaction between DLX2 and EGFR regulates proliferation and neurogenesis of SVZ precursors. *Molecular and Cellular Neuroscience*, *42*(4), 308–314. https://doi.org/10.1016/J.MCN.2009.08.003

Sun, D. (2014). The potential of endogenous neurogenesis for brain repair and regeneration following traumatic brain injury. *Neural Regeneration Research*, *9*(7), 688. https://doi.org/10.4103/1673-5374.131567

Sun, D., Bullock, M. R., McGinn, M. J., Zhou, Z., Altememi, N., Hagood, S., Hamm, R., & Colello, R. J. (2009). Basic fibroblast growth factor-enhanced neurogenesis contributes to cognitive recovery in rats following traumatic brain injury. *Experimental Neurology*, *216*(1). https://doi.org/10.1016/j.expneurol.2008.11.011

Sypecka, J., Janowska, J., Perez-Gianmarco, L., & Kukley, M. (2023). Understanding the Role of the Glial Scar through the Depletion of Glial Cells after Spinal Cord Injury. *Cells 2023, Vol. 12, Page 1842*, *12*(14), 1842. https://doi.org/10.3390/CELLS12141842

Szepesi, Z., Manouchehrian, O., Bachiller, S., & Deierborg, T. (2018). Bidirectional Microglia–Neuron Communication in Health and Disease. In *Frontiers in Cellular Neuroscience* (Vol. 12, p. 323). Frontiers Media S.A. https://doi.org/10.3389/fncel.2018.00323

Takahashi, K., & Yamanaka, S. (2006). Induction of pluripotent stem cells from mouse embryonic and adult fibroblast cultures by defined factors. *Cell*, *126*(4), 663–676. https://doi.org/10.1016/J.CELL.2006.07.024

Tarashansky, A. J., Musser, J. M., Khariton, M., Li, P., Arendt, D., Quake, S. R., & Wang, B. (2021). Mapping single-cell atlases throughout metazoa unravels cell type evolution. *ELife*, *10*. https://doi.org/10.7554/ELIFE.66747

Tasset, A., Bellamkonda, A., Wang, W., Pyatnitskiy, I., Ward, D., Peppas, N., & Wang, H. (2022). Overcoming barriers in non-viral gene delivery for neurological applications. *Nanoscale*, *14*(10), 3698–3719. https://doi.org/10.1039/D1NR06939J

Taupin, P., & Gage, F. H. (2002). Adult neurogenesis and neural stem cells of the central nervous system in mammals. *Journal of Neuroscience Research*, *69*(6), 745–749. https://doi.org/10.1002/JNR.10378

Than-Trong, E., & Bally-Cuif, L. (2015). Radial glia and neural progenitors in the adult zebrafish central nervous system. *Glia*, *63*(8), 1406–1428. https://doi.org/10.1002/GLIA.22856

Thomas, J. O., & Travers, A. A. (2001). HMG1 and 2, and related "architectural" DNA-binding proteins. In *Trends in Biochemical Sciences* (Vol. 26, Issue 3). https://doi.org/10.1016/S0968-0004(01)01801-1

Vasan, L., Park, E., David, L. A., Fleming, T., & Schuurmans, C. (2021). Direct Neuronal Reprogramming: Bridging the Gap Between Basic Science and Clinical Application. *Frontiers in Cell and Developmental Biology*, *9*, 681087. https://doi.org/10.3389/FCELL.2021.681087/BIBTEX

Verkhratsky, A., & Nedergaard, M. (2018). Physiology of Astroglia. *Physiological Reviews*, *98*(1), 239–389. https://doi.org/10.1152/physrev.00042.2016

Verkhratsky, A., Parpura, V., Li, B., & Scuderi, C. (2021). Astrocytes: The Housekeepers and Guardians of the CNS. *Advances in Neurobiology*, *26*, 21–53. https://doi.org/10.1007/978-3-030-77375-5_2

"Virchow, Rudolf: Die Cellularpathologie in ihrer Begründung auf physiologische und pathologische Gewebelehre", Bild 5 von 462 | MDZ. (n.d.). Retrieved March 11, 2024, from https://www.digitale-sammlungen.de/de/view/bsb10926743?page=5

Virchow, Rudolf: Gesammelte Abhandlungen zur wissenschaftlichen Medicin (1856) - Bayerische Staatsbibliothek. (n.d.). Retrieved March 11, 2024, from https://opacplus.bsb-muenchen.de/Vta2/bsb10086613/bsb:BV013341011?page=5

Waly, B. El, Macchi, M., Cayre, M., & Durbec, P. (2014). Oligodendrogenesis in the normal and pathological central nervous system. In *Frontiers in Neuroscience* (Vol. 8, Issue 8 JUN, p. 145). Frontiers Research Foundation. https://doi.org/10.3389/fnins.2014.00145

Wan, Y., & Ding, Y. (2023). Strategies and mechanisms of neuronal reprogramming. *Brain Research Bulletin*, *199*. https://doi.org/10.1016/J.BRAINRESBULL.2023.110661

Wang, D. D., & Bordey, A. (2008). The astrocyte odyssey. *Progress in Neurobiology*, *86*(4), 342–367. https://doi.org/10.1016/J.PNEUROBIO.2008.09.015

Wang, H., Song, G., Chuang, H., Chiu, C., Abdelmaksoud, A., Ye, Y., & Zhao, L. (2018). Portrait of glial scar in neurological diseases. *International Journal of Immunopathology and Pharmacology*, *31*, 1–6. https://doi.org/10.1177/2058738418801406

Wang, R., Rossomando, A., Sah, D. W. Y., Ossipov, M. H., King, T., & Porreca, F. (2014). Artemin induced functional recovery and reinnervation after partial nerve injury. *Pain*, *155*(3). https://doi.org/10.1016/j.pain.2013.11.007

Wanner, I. B., Anderson, M. A., Song, B., Levine, J., Fernandez, A., Gray-Thompson, Z., Ao, Y., & Sofroniew, M. V. (2013). Glial Scar Borders Are Formed by Newly Proliferated, Elongated Astrocytes That Interact to Corral Inflammatory and Fibrotic Cells via STAT3-Dependent Mechanisms after Spinal Cord Injury. *Journal of Neuroscience*, *33*(31), 12870–12886. https://doi.org/10.1523/JNEUROSCI.2121-13.2013

Wapinski, O. L., Lee, Q. Y., Chen, A. C., Li, R., Corces, M. R., Ang, C. E., Treutlein, B., Xiang, C., Baubet, V., Suchy, F. P., Sankar, V., Sim, S., Quake, S. R., Dahmane, N., Wernig, M., & Chang, H. Y. (2017). Rapid Chromatin Switch in the Direct Reprogramming of Fibroblasts to Neurons. *Cell Rep*, *20*(13), 3236–3247. https://doi.org/10.1016/j.celrep.2017.09.011

Wapinski, O. L., Vierbuchen, T., Qu, K., Lee, Q. Y., Chanda, S., Fuentes, D. R., Giresi, P. G., Ng, Y. H., Marro, S., Neff, N. F., Drechsel, D., Martynoga, B., Castro, D. S., Webb, A. E., Sudhof, T. C., Brunet, A., Guillemot, F., Chang, H. Y., & Wernig, M. (2013). Hierarchical mechanisms for direct reprogramming of fibroblasts to neurons. *Cell*, *155*(3), 621–635. https://doi.org/10.1016/j.cell.2013.09.028

Welch, J. D., Kozareva, V., Ferreira, A., Vanderburg, C., Martin, C., & Macosko, E. Z. (2019). Single-cell multi-omic integration compares and contrasts features of brain cell identity. *Cell*, *177*(7), 1873. https://doi.org/10.1016/J.CELL.2019.05.006

Westergard, T., & Rothstein, J. D. (2020). Astrocyte Diversity: Current Insights and Future Directions. *Neurochemical Research*, *45*(6), 1298–1305. https://doi.org/10.1007/s11064-020-02959-7

Wong, L. E., Gibson, M. E., Arnold, H. M., Pepinsky, B., & Frank, E. (2015). Artemin promotes functional long-distance axonal regeneration to the brainstem after dorsal root crush. *Proceedings of the National Academy of Sciences of the United States of America*, *112*(19), 6170–6175. https://doi.org/10.1073/PNAS.1502057112/SUPPL_FILE/PNAS.201502057SI.PDF

Wu, Y., Dissing-Olesen, L., MacVicar, B. A., & Stevens, B. (2015). Microglia: Dynamic Mediators of Synapse Development and Plasticity. In *Trends in Immunology* (Vol. 36, Issue 10, pp. 605–613). Elsevier Ltd. https://doi.org/10.1016/j.it.2015.08.008

Xue, Y., Ouyang, K., Huang, J., Zhou, Y., Ouyang, H., Li, H., Wang, G., Wu, Q., Wei, C., Bi, Y., Jiang, L., Cai, Z., Sun, H., Zhang, K., Zhang, Y., Chen, J., & Fu, X. D. (2013). Direct conversion of fibroblasts to neurons by reprogramming PTB-regulated microRNA circuits. *Cell*, *152*(1–2), 82–96. https://doi.org/10.1016/J.CELL.2012.11.045

y Cajal, S. R. (1920). *Una modificación del método de Bielschowsky para la impregnación de la neuroglia común y mesoglia y algunos consejos acerca de la técnica del oro-sublimado*. Imp. y lib. de Nicolás Moya.

Yang, T., Dai, Y. J., Chen, G., & Cui, S. Sen. (2020). Dissecting the Dual Role of the Glial Scar and Scar-Forming Astrocytes in Spinal Cord Injury. *Frontiers in Cellular Neuroscience*, *14*, 515129. https://doi.org/10.3389/FNCEL.2020.00078/BIBTEX

Yoo, A. S., Sun, A. X., Li, L., Shcheglovitov, A., Portmann, T., Li, Y., Lee-Messer, C., Dolmetsch, R. E., Tsien, R. W., & Crabtree, G. R. (2011). MicroRNA-mediated conversion of human fibroblasts to neurons. *Nature*, *476*(7359), 228–231. https://doi.org/nature10323 [pii] 10.1038/nature10323

Younsi, A., Unterberg, A., Marzi, I., Steudel, W. I., Uhl, E., Lemcke, J., Berg, F., Woschek, M., Friedrich, M., Clusmann, H., Hamou, H. A., Mauer, U. M., Scheer, M., Meixensberger, J., Lindner, D., Schmieder, K., Gierthmuehlen, M., Hoefer, C., Nienaber, U., … Bullinger, Y. (2023). Traumatic Brain Injury—Results From the Pilot Phase of a Database for the German-Speaking Countries. *Deutsches Arzteblatt International*, *120*(35–36), 599–600. https://doi.org/10.3238/ARZTEBL.M2023.0152

Yu, S., & He, J. (2019). Stochastic cell-cycle entry and cell-state-dependent fate outputs of injury-reactivated tectal radial glia in zebrafish. *ELife*, *8*. https://doi.org/10.7554/ELIFE.48660

Zamanian, J. L., Xu, L., Foo, L. C., Nouri, N., Zhou, L., Giffard, R. G., & Barres, B. A. (2012). Genomic analysis of reactive astrogliosis. *The Journal of Neuroscience : The Official Journal of the Society for Neuroscience*, *32*(18), 6391–6410. https://doi.org/10.1523/JNEUROSCI.6221-11.2012

Zamboni, M., Llorens-Bobadilla, E., Magnusson, J. P., & Frisén, J. (2020). A Widespread Neurogenic Potential of Neocortical Astrocytes Is Induced by Injury. *Cell Stem Cell*, *27*(4), 605-617.e5. https://doi.org/10.1016/j.stem.2020.07.006

Zambusi, A., & Ninkovic, J. (2020). Regeneration of the central nervous system-principles from brain regeneration in adult zebrafish. *World Journal of Stem Cells*, *12*(1), 8–24. https://doi.org/10.4252/WJSC.V12.I1.8

Zeisel, A., Hochgerner, H., Lönnerberg, P., Johnsson, A., Memic, F., van der Zwan, J., Häring, M., Braun, E., Borm, L. E., La Manno, G., Codeluppi, S., Furlan, A., Lee, K., Skene, N., Harris, K. D., Hjerling-Leffler, J., Arenas, E., Ernfors, P., Marklund, U., & Linnarsson, S. (2018). Molecular Architecture of the Mouse Nervous System. *Cell*, *174*(4), 999-1014.e22. https://doi.org/10.1016/J.CELL.2018.06.021

Zhang, Y., & Barres, B. A. (2010). Astrocyte heterogeneity: an underappreciated topic in neurobiology. *Current Opinion in Neurobiology*, *20*(5), 588–594. https://doi.org/10.1016/J.CONB.2010.06.005

Zheng, X., Boyer, L., Jin, M., Mertens, J., Kim, Y., Ma, L., Ma, L., Hamm, M., Gage, F. H., & Hunter, T. (2016). Metabolic reprogramming during neuronal differentiation from aerobic glycolysis to neuronal oxidative phosphorylation. *ELife*, *5*(JUN2016). https://doi.org/10.7554/ELIFE.13374

Zhou, L., & Luo, H. (2013). Replication Protein A Links Cell Cycle Progression and the Onset of Neurogenesis in Drosophila Optic Lobe Development. *The Journal of Neuroscience*, *33*(7), 2873. https://doi.org/10.1523/JNEUROSCI.3357-12.2013

Zhou, Q., & Anderson, D. J. (2002). The bHLH Transcription Factors OLIG2 and OLIG1 Couple Neuronal and Glial Subtype Specification. *Cell*, *109*(1), 61–73. http://www.sciencedirect.com/science/article/B6WSN-45KRP3V-9/2/4fded65ff8a508813de1225e384ba711

Zhu, Y. M., Gao, X., Ni, Y., Li, W., Kent, T. A., Qiao, S. G., Wang, C., Xu, X. X., & Zhang, H. L. (2017). Sevoflurane postconditioning attenuates reactive astrogliosis and glial scar formation after ischemia–reperfusion brain injury. *Neuroscience*, *356*. https://doi.org/10.1016/j.neuroscience.2017.05.004

Zweifel, S., Marcy, G., Lo Guidice, Q., Li, D., Heinrich, C., Azim, K., & Raineteau, O. (2018). HOPX Defines Heterogeneity of Postnatal Subventricular Zone Neural Stem Cells. *Stem Cell Reports*, *11*(3), 770. https://doi.org/10.1016/J.STEMCR.2018.08.006

5. Curriculum Vita

6. Publications

- **Priya Maddhesiya*,** Tjasa Lepko*, Andrea Steiner-Mezzardi, Veronika Schwarz, Juliane Merl-Pham, Finja Berger, Stefanie M. Hauck, Lorenza Ronfani, Marco Bianchi, Giacomo Masserdotti, Magdalena Götz, Jovica Ninkovic. **Hmgb2 improves astrocyte to neuron conversion by increasing the chromatin accessibility of genes associated with neuronal maturation in a proneuronal factor-dependent manner.** bioRxiv, Sep 2023. doi: 10.1101/2023.08.31.555708.

- **Priya Maddhesiya,** Finja Berger, Christina Koupourtidou, Alessandro Zambusi, Judith Fischer-Sternjak, Tatiana Simon, Jovica Ninkovic. **Stab wound injury induces transit amplifying phenotype-like phenotype in parenchymal astrocytes** *(in submission).*

- Bharat Prajapati, Mena Fatma, **Priya Maddhesiya**, Manjot Kour Sodhi, Mahar Fatima, Tanushri Dargar, Reshma Bhagat, Pankaj Seth & Subrata Sinha. **Identification and epigenetic analysis of divergent long non-coding RNAs in multilineage differentiation of human Neural Progenitor Cells.** RNA Biol., Nov 2018. doi: 10.1080/15476286.2018.1553482

- Bharat Prajapati, Mahar Fatima, Mena Fatma, **Priya Maddhesiya,** Himali Arora, Teesta Naskar, Subhashree Devasenapathy, Pankaj Seth & Subrata Sinha. **Temporal transcriptome analysis of neuronal commitment reveals the preeminent role of the divergent lncRNA biotype and a critical candidate gene during differentiation.** Cell Death Discov., April 2020. doi: 10.1038/s41420-020-0263-6

- Amit Talukdar, **Priya Maddhesiya**, Nima Dondu Namsa & Robin Doley. **Snake venom toxins targeting the central nervous system.** Toxin Reviews, May 2022. doi: 10.1080/15569543.2022.2084418

7. Eidesstattliche Versicherung/Affidavit

8. Declaration of author contributions

Publication 1: **Priya Maddhesiya**, Finja Berger, Christina Koupourtidou, Alessandro Zambusi, Klara Tereza Novoselc, Judith Fischer-Sternjak, Tatiana Simon, Sebastian Jessberger, Jovica Ninkovic**.** Stab wound injury induces transit amplifying progenitor-like phenotype in parenchymal astrocyte. Manuscript ready for submission.

The contribution of authors is as follows:

P.M, J.N., and F.B. conceived the project and designed bioinformatic experiments. C.K., A.Z., J.F.S. generated single cell sequencing data. P.M. performed the bioinformatic analyses. F.B. performed Immunohistochemical analyses. J.N, K.T.N, S.J, and T.S. performed neurosphere assay. P. M. and J.N. wrote the manuscript with input from all authors.

My contribution to this manuscript in detail:

I was responsible for all the bioinformatic analyses presented in the manuscript. This included conducting single-cell transcriptomic (scRNA-seq) analysis, integrating data from both mouse and zebrafish species, and correlating these findings with the neurogenic niches in the subventricular zone (SVZ). I used various tools and pipelines to process, integrate, and visualize the integrated datasets. Additionally, I actively participated in the writing and editing process of the manuscript.

Confirmation of author contributions:

Prof. Dr. Jovica Ninković Priya Maddhesiya

--- ---

Publication 2: **Priya Maddhesiya***, Tjasa Lepko Modic*, Andrea Steiner-Mezzardi, Veronika Schwarz, Juliane Merl-Pham, Finja Berger, Stefanie M. Hauck, Lorenza Ronfani, Marco Bianchi, Giacomo Masserdotti, Magdalena Götz, Jovica Ninkovic. Hmgb2 improves astrocyte to neuron conversion by increasing the chromatin accessibility of genes associated with neuronal maturation in a proneuronal factor-dependent manner. doi: https://doi.org/10.1101/2023.08.31.555708

The contribution of authors is as follows:

P.M., T.L.M. and J. N. conceived the project and designed experiments. T.L.M, A.S.M., V.S., F.B., and J.N. performed experiments. J.M.P. and S.M.H. analysed proteome. P.M. performed the bioinformatic analyses. L.R. and M.B. provided Hmgb2 KO animals. P.M. and J.N. wrote the manuscript with input from all authors.

My contribution to this publication in detail:

For the manuscript, I performed bioinformatic analyses of RNA-seq and ATAC-seq data to investigate the specific changes in gene expression and chromatin accessibility associated with efficient astrocyte-to-neuron conversion by Hmgb2 and Neurog2. I evaluated the effects of Hmgb2, Neurog2, and their combination under EGF+FGF2 and FGF2 culture conditions. I used different tools to visualize and perform downstream analysis. Furthermore, I contributed to the writing and editing of the manuscript.

Confirmation of author contributions:

Prof. Dr. Jovica Ninković	Dr. Tjasa Lepko Modic	Priya Maddhesiya
---	---	---

9. Acknowledgements

I would like to express my gratitude to my supervisor, Prof. Dr. Jovica Ninkovic, for entrusting me with projects that have significantly contributed to my professional growth and led to valuable discussions. I appreciate his guidance, expertise, and feedback throughout my PhD journey. His support has been instrumental in shaping my skills and fostering meaningful academic development. I am also thankful to Prof. Dr. Michael Kiebler for persuading me to come to Germany and embark on this career path. Looking back, I must say it was a decision that has profoundly impacted my academic and professional growth. I am grateful for his insightful suggestions, availability, and willingness to help, especially with bureaucratic aspects.

I extend my thanks to the members of my thesis committee, Dr. Maria Abad and Prof. Dr. Wolfgang Enard, for their valuable feedback and suggestions. I am also grateful to the Graduate School for Systemic Neurosciences (GSN) for useful courses, workshops and financial support during the final months of my PhD. I would also like to acknowledge the EpiSyStem training network for providing diverse opportunities to learn and present at different scientific forums.

I am also thankful to my colleagues for creating conducive working environment and adding humour to my work, making the journey enjoyable. I extend my thanks to the entire former and present Ninkovic group, including Tjasa, Tamara, Sven, Alessandro, Klara, Silvija, Christina, Veronika, Finja, Sofia, Xenia, Viviane, Buse, Julia, Marta, and Milos. Each of you has contributed in your own unique way, whether it was listening to me, offering suggestions, helping with reading German documents, steering me in selecting vegetarian food options, teaching me how to bake a cake, or simply sharing moments of laughter and camaraderie, and, most importantly, turning me from a lemonade drinker to a Munich mule enthusiast. You have all played a part in my personal and social growth.

I extend my thanks to my Munich friends (whole München Bharatham group) who always made this place feel like home, whether celebrating the colourful Holi festival, lighting Diwali, or going for a Bollywood DJ night. You all hold a special part of my journey, and I truly appreciate it.

My deepest acknowledgement goes to my family and friends for their unwavering love and encouragement throughout this process. I am especially grateful to my Mom, Dad and

Sisters, Pooja and Neha, who have always been there for me despite the distance and time.

I dedicate this PhD thesis to the loving memory of my childhood friend, Anamika, who passed away during my PhD journey. She inspired me to pursue science, and in her words, “whether you finish or I, it’s the same thing,” continue to resonate with me. Completing this thesis is my tribute to her unfinished PhD work. Her presence and friendship will forever be cherished and missed, and her belief in me has been a guiding force in my personal growth.

Last but not least, I extend my heartfelt gratitude to Rishabh, my steadfast school friend and life partner. I am certain I would not have reached the end without his ceaseless encouragement. His enduring support and unwavering belief, even from afar, has been my pillar of strength during challenging times.

In essence, I would like to conclude with a quote that encapsulates this journey: “*Alone we can do so little; together we can do so much*” - Helen Keller